Evaluation of Truck Shipment Transit Hazards in Kenya and the Effect of their Simulations on the Physical Quality of Bulk-Packed Black Tea as a Basis for Establishment of a Pre-shipment Testing Protocol for Packaged Goods to Optimize Packaging Designs.

A thesis submitted for the degree of Doctor of Philosophy in the

Department of Mechanical, Aerospace and Civil Engineering

By

Arthur Kirimi Rimberia

College of Engineering, Design and Physical Sciences

Brunel University

March 2015

DECLARATION

This thesis is my original work and has not been

presented for a degree award in any other

University

Arthur Kirimi Rimberia

This thesis has been submitted for examination

with our approval as University supervisors.

DR. Y.H. JOE AU

Signature ----------Dated ----------

Department of Mechanical, Aerospace and Civil Engineering

Brunel University

PROF. MICHAEL W. OKOTH

Signature ---------- Dated ----------

Department of Food Science, Nutrition and Technology

University of Nairobi

DEDICATION

To my beloved wife, Cathryn Kithiira Rimberia, for her love, encouragement and unreserved support during the whole period of this research. To my children Dennis Gitobu Rimberia and Caroline Karwitha Rimberia for their understanding and patience while away for extended periods in the course of carrying my research work.

Last and not least, to my father and mother John M'Rimberia and Tabitha Mukothuura M'Rimberia respectively for their sacrifice in taking me through education but unfortunately never lived long enough to see the outcome of this work.

ACKNOWLEDGEMENTS

I would wish to express my sincere gratitude to my supervisors of this work Dr. Joe Au and Prof. Michael W. Okoth who gave me invaluable support and encouragement to carry on even when it appeared un-surmountable. Special thanks go to Dr. Au who unreservedly supported the planning, design, execution and thesis writing as well as going an extra mile to ensure my safety and comfort while in the U.K. Further gratitude goes to Kenya Tea Development Agency Ltd (KTDA) for their support during the field data collection and Chai Trading Ltd who assisted in measurement equipment retrieval from the trucks at the end of the journey. The contributions of River Cross Ltd in availing their fleet management and tracking software cannot escape my appreciation. My gratitude also extends to Prof. Ibi Essat of Mechanical Engineering Department at Brunel University for allowing use of the dynamics laboratory and the simulation and allied equipment used during the laboratory work. Special gratitude is extended to both Keith Withers and Paul Szadorski of Mechanical and Civil engineering laboratories respectively for their assistance in availing vital laboratory equipment and accessories needed for this work. Many thanks to Keith Withers for his great support in the laboratory work especially the dynamics equipment set up and the fabrication of the rig apparatus. Many thanks to Dr David Shires of Packaging Industry Research Association (PIRA) who gave invaluable advice on the field data collection equipment set up. Further appreciation is extended to Mr Geoff Murphy of Data Physics Ltd for his assistance in availing the exciter programming operation data and for his quick repair support when the equipment malfunctioned during the simulation work.

Finally, I wish to thank all my fellow research students and staff in the manufacturing that in several ways played a vital role in ensuring I remained motivated and focused to complete this work.

ABSTRACT

Focused transit hazard evaluations of distribution environments have become increasingly important in the recent past. This is due to the realization by businesses such as those in China (Baird et.al.,2004) that pack design optimization can result in reduction of packaging and other related costs, ensuring safe delivery of products as well as enabling companies to comply with global statutory obligations that demand packaging waste reduction via optimal packaging of goods.

This work involved focused evaluation of the distribution hazards in truck transport within the bulk packed tea supply chain in Kenya as a basis for establishment of a pre-shipment protocol for packaged goods in order to optimize package designs and protect the physical quality of tea in transit. The parameters addressed included vibrations, shock, and environmental conditions of temperature and relative humidity. The research further examined how above transit conditions may affect important black tea physical quality parameters of density, particle size distribution, colour, and particle morphology. The work also formulated a new a pre-shipment testing protocol for tea (and other goods) moved within this supply channel thus allowing businesses to optimize their packaging designs. Furthermore, such pre-shipment protocols would help in predicting possible failure in transit.

The Lasmont's Saver model 3x90 transit data measuring unit mounted on the truck bed was used to collect transit data while a programmable electrodynamics vibration table was used to simulate the measured transit conditions. Using the specially fabricated rig apparatus for the experiment, analysis of changes of the tea physical properties of particle size distribution, bulk, tapped and compact densities as well as particle morphology and colour were investigated.

The results showed that truck transport transit conditions experienced in the Kenyan roads with a composite spectrum of 1.358 (Grms) for the routes measured are more severe than the test standards set by both American Standard Testing Methods (ASTM) and International Safe Transit Association (ISTA) for truck transport conditions of 0.242 and 0,519 (Grms) respectively. This shows Kenyan roads compared to those where both ASTM and ISTA data was derived from are poorer and further confirms that both ASTM and ISTA standard tests may not be appropriate for use in designing optimal packaging for the Kenyan distribution environment. In addition, vibration intensities experienced were relatively higher than

average recorded from other similar studies carried out in other parts of the world such as Brazil (0.628 Grms), USA(maximum 0.89 Grms), Spain (0.194Grms) and Indian highways (0.161 Grms). The work revealed how poor Kenyan roads are and that they would lead to damage of delicate physical qualities of tea including particle size distribution for each grade of tea, particle morphology and density unless the right packaging is used. This therefore underpins the importance of carrying out focused pre-shipment testing for a given distribution environment as general test procedures will not allow optimization of packaging designs.

Due to the prevailing poor road conditions in Kenya as shown earlier by relatively high vibration and shock impacts, results showed that these hazards together with load compression affected the tea particle integrity in transit leading to breakage of larger tea particles to give rise to smaller particles unless adequate protective distribution packaging has been given due consideration. Equally, particle density as well as the particle surface morphology was affected resulting in undesirable impact on tea physical quality. Consistency in density of tea is an important aspect for the blenders of bulk tea since packing machines often operate within defined density limits. Compressive forces within the pallet load led to the crushing of larger tea particles into smaller ones, thus undermining the desirable black colour tea leaving it greyish which is considered in the tea trade as poor tea quality. In addition, the results confirmed that the effect of compression load on the physical tea quality was more severe than the vibration/shock impact alone. Moreover, the change in physical quality was related to the transit time (vibration period) up to maximum equilibrium level. Density of tea increased with compression load up to a maximum of 350g. The same, however, declined at 400g static load due to resonance conditions of the simulation assembly. Tea morphology measurements indicated that the initial rounded shape of the tea particles gradually changed to an elongated shape with rugged surface. This had an effect of not only damaging the desired black colour but also altered the flow properties of the tea which is an important aspect for bulk tea buyers during their subsequent handling activities of blending and packaging. A new relationship called compact density and compact ratio was established that related elevated tea density in transit due to 'jamming' of tea particles upon application of static load pressure on the tea at the lower levels of the pallet load. In addition, a correlation of density against tea powder "stain" travel within the test container containing tea particles, further confirmed that force impulses from the static load on top of tea particles was being transmitted perpendicular down to the bottom of the pallet load. The correlation of

both the distance moved by the static load inside the tea container and tea powder “stain” column height on the test tube below the static load with the compact density of tea, brought out further empirical data that could be used by researchers to accurately predict the tea density from both the above parameters. The research further revealed that compressive forces on the tea particles at lower levels of the pallet load had more impact on the damage of tea particles compared to vibration/shock impacts. Finally, there is need for the existing packaging standards for bulk packed black tea to be revised in the light of the newly developed pre-shipment testing protocols from this research.

TABLE OF CONTENTS

LIST OF FIGURES

LIST OF TABLES

NOMENCLATURE

^{0}C - Degrees celcius.

A/D - Analogue to digital.

Adsorption - the adhesion in an extremely thin layer of molecules (as of gases, solutes, or liquids) to the surfaces of solid bodies or liquids with which they are in contact.

ASTM - American standard testing methods.

Athermal- Describing any process that does not involve either heat or a change in temperature.

Black tea leaf- Black colour denotes well-made tea and well-handled to avoid abrasion of tea particles at all stage.

Black tea- Type of tea that results from oxidation of tea catechins.

BP1 - Broken pekoe 1.

Brightness(tea) -Denotes tea liquor having a lively fresh tea with good keeping quality..

Briskness (tea) - Tea liquor with the most "live" characteristic that results from good manufacture of tea.

Bulk density- Mass of many particles of the material divided by the total volume.

Bulk packed tea- Tea packed in large transport packages meant for later blending and packing into retail packs.

cc or cm^3 - Cubic centimetre.

Clean tea- Leaf which is free from fibre, dust or any extraneous matter.

Compact density- A new term in this research denoting density measured after compression of granular matter.

Granular matter- Conglomerate of discrete solid, macroscopic particles.

Compression- Decrease in volume of any substance resulting from applied stress.

CTC - Cut, tear, and curl.

D - Dust.

D1 - Dust 1.

DDGS - Distillers dried grains soluble.

Desorption – A phenomenon whereby a substance is released from or through a surface.

EC - European Community.

ECD - Equivalent circle diameter.

ED - Electro-dynamic.

EU - European Union.

FFT - Fast Fourier transform.

FFV - Fresh fruits and vegetables.

Focused simulation- Mimic of transport conditions in the laboratory based on collected field data.

Ft – Feet.

FTA - Freight Transport Association.

g -Acceleration due to gravity ($9.81 m/s^2$).

GDP - Gross domestic product.

General simulation- mimic of transport conditions based on standardized conditions.

gm - Gramme.

Grey tea- denotes negative quality of tea caused by abrasion of tea grains during sorting or handling.

Grms - Root mean square acceleration.

G-Value - The highest deceleration level that does not cause product/package damage.

Hygroscopic- Readily taking up and retaining moisture.

Hz – Hertz.

ISO - International Standards Organization

ISTA - International Safe Transit Association.

kg – Kilogramme.

KTDA - Kenya Tea Development Agency.

lb – Pounds.

LTP - Lawrie tea processor.

m – Metre.

Mechanical shock- A sudden acceleration caused for example by impact, drop etc.

Mechanical vibration- Measurement of periodic process of oscillations with respect to an equilibrium point.

mm – Millimetre.

MUX – Multiplexer.

Non simulation tests- Testing based on standardized test procedures.

Organoleptic- Involving use of sense organs like taste.

PD - Pekoe dust.

PF1 - Pekoe Fanning 1.

PIRA- Packaging Industry Research Association.

Powdery tea- A negative quality of tea caused by presence of fine tea powder in tea.

PSD - Power spectral density.

Pycnometry- A procedure in which use a pycnometer as vessel for measuring the density or specific gravity of materials

Random Vibration- Motion which is non- deterministic or future behaviour cannot be precisely predicted

Reynolds' granular dilatancy- The tendency of a compacted granular material to dilate when under shear.

RSA- Random sequential adsorption.

RTG- Radio thermoelectrc generator.

Segregation- de-mixing of granular particles due to vibration or shaking.

SEM - Scanning electron microscope(micrograph).

SME - Small and medium enterprise.

Sorption isotherm- Represents the equilibrium of the sorption (adsorbed) material at a surface at constant temperature.

SRS - Shock response spectra.

Tan – Tangent.

Tapped density- Density obtained after mechanically tapping a measuring cylinder containing sample of granular matter.

UK - United Kingdom.

USA - United States of America.

Volumeter- An instrument used for measuring volumes 9 as of gases or liquids) or (as solids) by displacement of a liquid.

WHO - World Health Organization.

µP - Microprocessor.

1.0 Chapter 1

1.1 Background to research

Kenya is situated astride the Equator and enjoys a warm and wet climate that is suitable for agricultural activities including tea (Figure 1-1). Kenya is primarily an agricultural based economy and agriculture is the main source of livelihood for the majority of citizens. Over 2/3 of the country's population is employed in the agriculture sector. Agriculture and Forestry is the single largest contributor to the country's Gross Domestic Product. In 2013, Agriculture achieved a growth rate of 2.9 %. The sector contributed 24.6% and 25.3% the country's economic growth in 2012 and 2013 respectively. Agriculture accounts for about 70% of the total country's export earnings (Kenya economic survey, 2014).

Kenya is a key producer and exporter of tea globally. In 2012 and 2013 Kenya was recorded as the 3rd single largest tea producer in the world after China and India (Figure 1-2). During the period 2011 to 2013 the tea sector achieved a volume increase of 17 % from 369.4 million tons to 432.4 million tons. During this period Kenya was the largest single tea exporter in the world (Figure 1-3). Tea is an important cash crop for Kenya and is currently the leading foreign exchange earner for the country (Kenya economic survey, 2014).

Tea is grown in the cooler and rich well drained soils found in the Kenya highlands that are situated on both eastern and western slopes of the Great Rift Valley which runs through the middle of the country from North to South. Over 95 % of the tea is exported in bulk form packed in multi-walled paper sacks while the balance is packed in consumer packs for local consumption and for export (Kenya Economic Survey, 2010). Tea produced and packaged at the production factories situated in remote areas close to the tea gardens is transported in truck loads for shipment at the port of Mombasa. Mombasa port is the main entry and exit port for goods into and out of Kenya. The port also handles tea and other goods exports for the other landlocked neighbouring countries of Uganda, Rwanda, Burundi, Democratic Republic of Congo and the new Republic of Southern Sudan. Tea is also grown in all the above countries apart from South Sudan and is transported through Kenya for the weekly auction sales in Mombasa where it is also exported. Mombasa is one of the largest world tea auction centres.

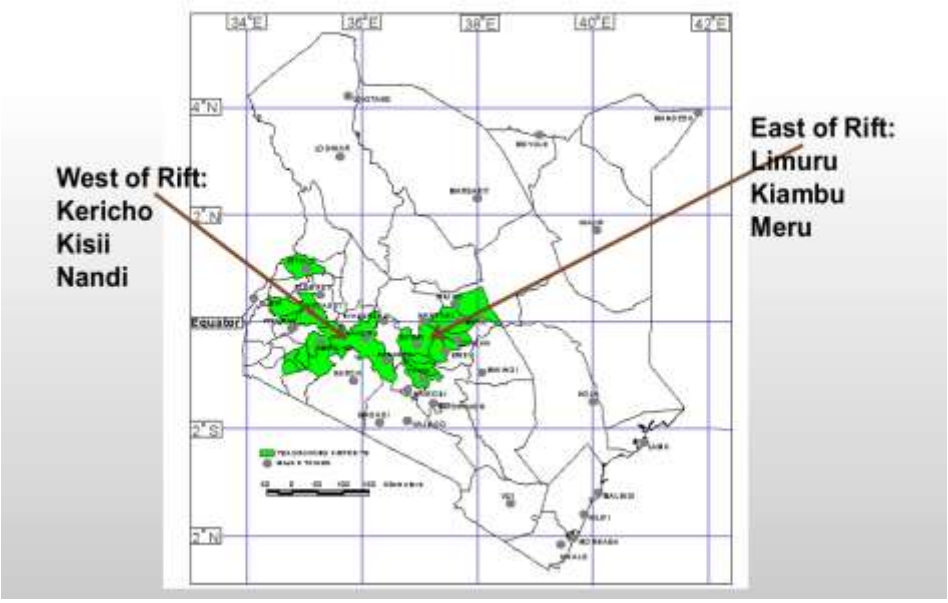

Figure 1- 1 Map of Tea producing regions in Kenya

(Kenya Tea Board, 2014)

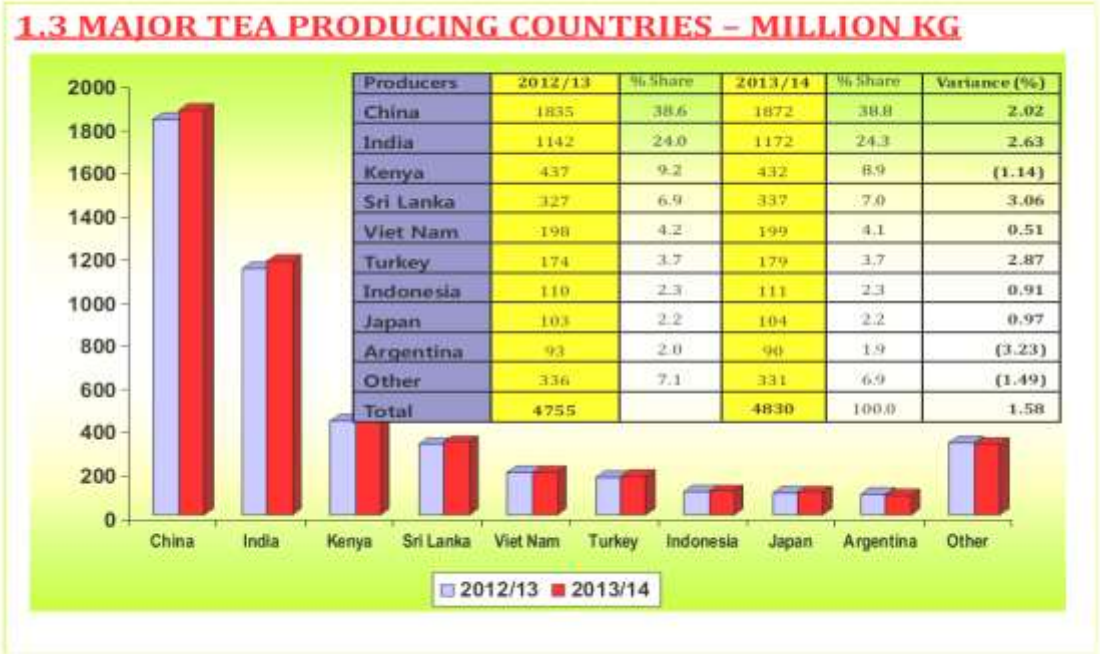

Producers	2012/13	%Share	2013/14	%Share	Variance (%)
China	1835	38.6	1872	38.8	2.02
India	1142	24.0	1172	24.3	2.63
Kenya	437	9.2	432	8.9	(1.14)
Sri Lanka	327	6.9	337	7.0	3.06
Viet Nam	198	4.2	199	4.1	0.51
Turkey	174	3.7	179	3.7	2.87
Indonesia	110	2.3	111	2.3	0.91
Japan	103	2.2	104	2.2	0.97
Argentina	93	2.0	90	1.9	(3.23)
Other	336	7.1	331	6.9	(1.49)
Total	4755		4830	100.0	1.58

Figure 1- 2 Global tea production 2012- 2014

(KTDA, 2014)

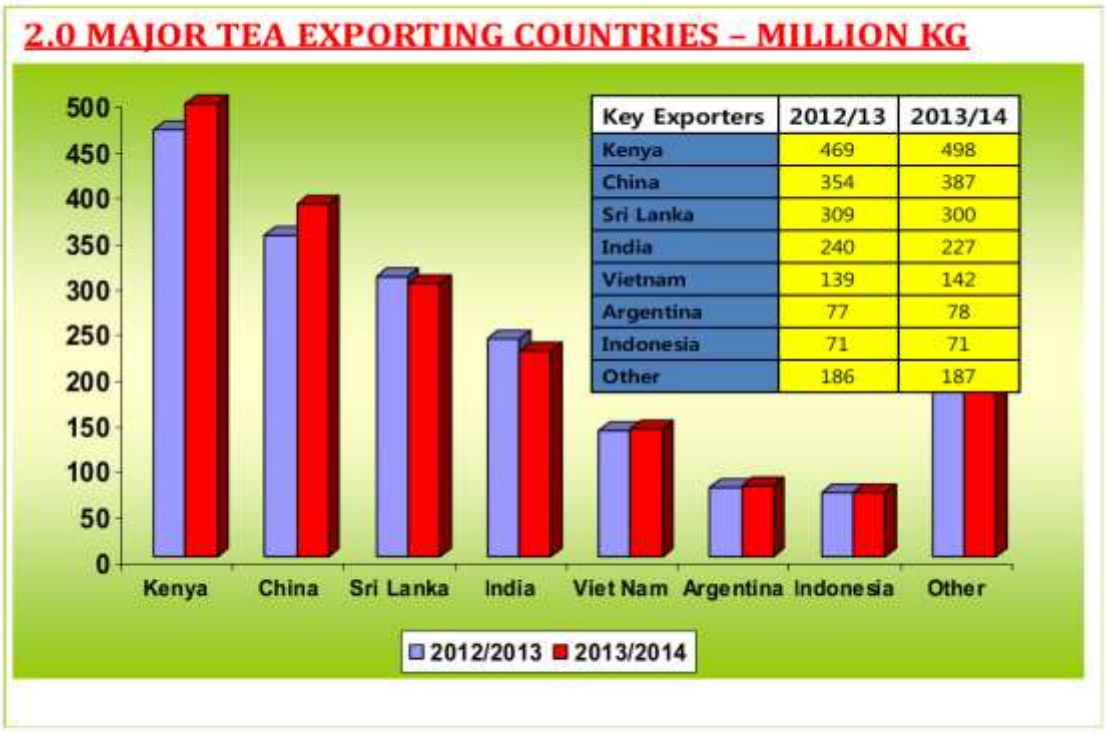

Key Exporters	2012/13	2013/14
Kenya	469	498
China	354	387
Sri Lanka	309	300
India	240	227
Vietnam	139	142
Argentina	77	78
Indonesia	71	71
Other	186	187

Figure 1- 3 Global tea exports 2012- 2014

(KTDA, 2014)

1.2.0 Goods distribution environment

During distribution from the production sites to the target markets, goods encounter various transit hazards that could affect both the product as well as package integrity. Transportation by road, rail, water and even air all present varied hazards to packaged goods in transit that may include vibration, shock, compression, temperature, humidity and even atmospheric pressure. If proper packaging (including distribution packaging) is not optimally provided by the shipper, serious damage to the product, package or both could undermine product acceptability by the ultimate buyer. Optimal distribution packaging (based on actual conditions of the distribution environment) will therefore avoid over-packaging while enabling products to survive transit physical hazards of transportation and distribution (Baird et.al, 2004; Young D., 1993). This ‘just right’ packaging will need to be designed and certified against ‘just right’

pre-shipment testing that adequately simulates the hazards of actual distribution environment (Rouilland and Sek, 2000; Baird and Young, 2004). In order to carry out meaningful focused transport package tests for a particular distribution environment, accurate conditions of the hazards must be known including their levels and even sequence (Chonhenchob and Singh, 2005). Increasing stringent demands in the world trade, varying transport and distributions conditions, international competition and packaging waste regulations, now demand that a more focused transit hazard analysis and evaluation be carried out within a defined distribution channel in order to achieve optimal package design (Bernad,et.al., 2011). Such focused hazard measurements within the distribution system have allowed companies to optimize their pack designs with significant cost reductions, compliance with environmental regulations of the target market and above all, safe delivery of their products to their customers. Distribution environment measurements often reveal the nature of one's own environment, the mechanism by which the various hazards produce damage to goods and the appropriate methods to overcome those challenges (Kipp,W., 2000). Furthermore, accurate distribution environment measurements, followed by laboratory packaging evaluation and improvement on product and/or package designs can effectively predict and control over-packaging and under-packaging leading to significant savings in packaging costs (Guo and Xu, 2010). Therefore, an optimum protective package consists of a product and a packaging of known ruggedness which together provide sufficient resistance to damage during distribution without over- packaging (Schueneman, 1996). Nevertheless, several companies have in the past reported higher than anticipated incidences of shipment damage even after a well-engineered package has been designed and tested against conventional test methods (Schueneman, 1996).This rather unusual dilemma of unexpected damage to products in transit can be explained to be due to the following possibilities:

(a) The potentially damaging effects of vibration which in the past had not been widely considered in package design process or in testing of package systems (Schueneman, 1996).

(b) Insufficient or inaccurate information on the severity of the distribution environment leading to inaccurate package design. This may have been due to use of inaccurate test equipment such as the older mechanical data loggers that were prone to errors (Baird, et al., 2004; L.A.B, 2006).

1.3.0 Advantages of transit hazard measurements

There are many possible benefits of carrying out a focused transport data measurements of a given distribution environment by a shipper. They include the following:

1. Help solve problems with existing packaging such as transit product damage or package failures.

2. Identify potential cost savings in packaging by establishing optimal packaging level for a given distribution environment.

3. Ensure the packaging conforms to regulatory guidelines such as those of the European Commission Packaging Directives on environment and therefore avoid possible penalties and trade barriers.

4. Predict, in a laboratory, the performance of a package during distribution and ensure acceptance by customers thus avoiding expensive in transit product losses or consumer rejections and possible loss of goodwill (Baird, et.al, 2004).

5. Provide a basis for technical communication with other bodies including designers, packaging material suppliers and even bodies involved in formulation of package tests such as International Safe Transit Association (ISTA) and American Standard Testing Methods (ASTM).

6. Decide if a new product development is on track and suitable for use for the anticipated distribution environment without incurring undue actual test expenses.

7. Decide if a new product development is on track and suitable for use for the anticipated distribution environment without incurring undue actual test expenses.

8. Establish a reliable overall statistical hazard property that are encountered for particular journey or distribution modes that could form a basis for laboratory physical simulation Protocol to validate package integrity
9. Provide a basis for evidence in legal proceedings: product liability, product claims, patents etc. thus protecting the business from undue losses from law suits (Rouillard et. al., 2007).

1.4.0 Importance of laboratory simulation in optimal package design

In recent times, the importance of accurate laboratory simulation has become embraced by designers in the packaging industry. This is due to both economic and environmental concerns that demand optimization of packaging designs (Bernad et. al., 2011; Aba et.al, 2012). Both ISTA and ASTM have come up with a series of package testing procedures that are aimed at assisting package designers to optimize their designs thus reducing packaging costs as well as solid waste obligations arising from packaging activities. Packaged goods manufacturers including the Kenya Tea Development Agency Ltd that hitherto were not using focused transit hazard data in their designs have realized that there are valuable advantages, not least, cost reduction when they optimize their packaging designs (Silvers, et.al.,1976;). Today, the general packaged goods testing methods are increasingly losing their popularity and are being replaced by focused test protocols. This is partly due to the packaging laboratories turning to the use of new electronic data collection loggers that allow high precision and accurate almost continuous measurements of the distribution environments compared to the older mechanical gadgets (Rouillard, et. al., 2007).

Furthermore, environmental concerns have become a global matter and many governments have today put in place strict packaging material minimization thresh-holds with which goods entering their trade frontiers must comply as a way of managing packaging waste. For instance, the EU Packaging Waste 94/62/EC directive and its revised versions set very strict waste management obligations to exporters to the EU region that dictate minimal use of packaging. In the UK this waste management strategy is implemented through the Producer Responsibility Obligations (Packaging Waste Regulations 1997 and its revised versions) and (Essential Requirements) Regulations of 1998 and its revised versions. These regulations dictate use of optimal packaging designs for all products which in turn can only be achieved by use of appropriate focused laboratory simulation methods.

1.5.0 Goods transportation in Kenya

There are two main modes of goods distribution in Kenya, namely road and rail. There are no navigable rivers in the country and the available water transport is limited to use of small ships and dhows over Lake Victoria and along the Indian Ocean coast line. Air transport is prohibitively expensive for most low value and non- perishable products including tea. Road transport is by far the most common means of transport in the country and in the region. The transport sector has been growing steadily contributing an average of 7.6percent annum to the

GDP between 2004 and 2007. This is envisaged to grow to an average of 10percent by 2030 (Kenya Economic survey, 2010).

1.5.1 Railway transport

Railway transport is the next common form of goods transport after road. The sector has been handicapped by many challenges that hinder its performance and efficiency. Railway networks remain undeveloped as there is only one main line linking the major towns of Mombasa and Kampala in Uganda leaving the vast agricultural productive areas in the eastern and central regions including those where tea is produced virtually without any railway services. The branch railway line from Nairobi through central Kenya to Nanyuki is now almost abandoned with most shippers preferring the faster road transport alternative. Locomotive availability is low, averaging only about 48percent for the main line and branch lines. This is below the international rolling stock availability average of approximately 80percent. Locomotive reliability is also low and is coupled with a high rate of locomotive failure and low availability of wagons due to long turnaround times (Irandu, 2000). Indeed, the railway system in Kenya has been characterized by problems that act as a disincentive to many potential shippers in the region. These include:

(a) The over century old Kenya – Uganda railway mainline has been neglected over the years leaving it in an obvious state of disrepair. It is plagued by safety concerns and prone to a high number of derailments of wagons.

(b) Kenya railways utilizes the narrow gauge track (1000mm or 3ft $3^{3/}_{8}$ in.) that is not capable of handling high speed trains needed for fast delivery schedules of goods and passengers. The maximum speed allowed is 30mph or 48.3 km/hr. Goods usually take an inordinately long time to reach their destinations compared to road haulage. There are now plans to build a standard gauge railway line to replace the current rather almost obsolete line.

(c) There is lack of sufficient wagons and locomotive engines to handle the available goods shipped within the country and those destined to neighbouring countries such as Uganda. (Current rail line covers only Kenya and Uganda). Only about 25percent of available locomotives are in good condition while about 30percent of the available wagons requiring major rehabilitation before they can be put to commercial use (Irandu, 2000). Rift Valley Railways who are currently responsible for railway management in the country are making

frantic efforts to raise funds to buy new locomotive engines in order to address the motive power problem.

(d) The network consists of a single-track main line from Mombasa to Malaba with important branch lines to Kisumu and Nanyuki and minor branch lines to Taveta, Nyahururu, Solai and Kitale. The current pattern of freight traffic heavily favours the main line route (Mombasa-Malaba-Kampala). The minor branch lines such as Nairobi-Nanyuki and Gilgil-Nyahururu are idle for most of the year because they have little freight traffic (Irandu, 2000). This leaves no railway services in the main productive areas of the country where the bulk of the export goods such as tea, horticultural produce and coffee originate, leaving truck transport as the only reliable and economical means of haulage from these areas.

(e) Railway transport is only cheap for large shipments and is therefore, out of reach to most small and medium enterprises (SMEs) although these altogether contribute the bulk of the cargo hauled on Kenyan transport network. Furthermore, SMEs often require fast delivery of their goods to their ultimate customers without the need for "last mile" road intervention as is mostly the case in rail transport. This is because most of their customers are located in far-fetched locations where railway services are lacking.

1.5.2 Road transport

Road transport is by far the most common means of transport in the country and in the region accounting for over 93percent of the total domestic freight and passenger traffic (Kenya Ministry of Transport Sessional Paper 2010). Truck transport alone accounts for over 80percent of goods haulage (Irandu, E., 1995; Bundi. J., 2003; Kenya Institute of Economic Affairs, 2008).

A twelve wheeler tractor unit joined to a tri-axle trailer is the common type used for bulk cargo shipments due to its economies of scale. Most bulk cargo and all tea are transported primarily via road using truck transport. Despite road being generally a more expensive mode for bulk shipments compared to rail, road transport remains the preferred mode of transport for most goods including bulk tea due to its convenience.

1.5.3 Kenyan road network

Despite the popularity of road transport in the country and especially truck transport, 86percent of the total classified road network (63,291km) is either gravel (43percent) or earth (43percent) leaving a mere 14percent of the total classified road network in the country under bitumen

surface. The bitumen road category includes International Trunk Roads-A (32.3percent), National Trunk Roads-B (16percent), Primary Roads-C (27.8percent), Secondary Roads-D, Minor Roads-E and Special Purpose Roads (23.9percent). A total of 133,800 km representing 67.9percent of the entire road network in the country is unclassified with bulk of this barely motor able (Table 1.1).

Table1. 1 Kenya roads network and classifications

A- Classified Road Network *(km)* *(km)* *(km)* *(km)*

Road Network	**Administering Agency**	**Bitumen**	**Gravel**	**Earth**	**Total**	**%**
International Trunk Roads-A	Roads Dept. of Min. of Roads and Public Works	2,886	717	152	3,755	6
National Trunk Roads-B		1,433	842	524	2,799	4
Primary Roads-C		2,487	3,209	1,972	7,668	12
Secondary Roads-D	District Roads Committees	1,167	6,484	3,565	11,216	18
Minor Roads-E		751	7,206	18,592	26,549	42
Special Purpose Roads		214	8,724	2,366	11,304	18
Totals		8,936	27,182	27,171	63,291	100
%		14	43	43	100	

***B-Unclassified Road Network**:*

Road Network	**Administering Agency**	**Road Type**	**km**	**%**
Urban Road Network	Municipal Authorities (City & Municipal Councils)	Adopted urban streets	7,000	5.2
Other Unclassified Roads	County Councils	Rural roads and tracks	110,000	82.2
Roads in National Parks & Reserves Roads in National Reserves (contracted from Local Authorities)	Kenya Wildlife Service	National Parks & Reserves Roads (contracted from Local Authorities)	6,000 2,800	6.6
Forest roads	Forest Department	Forest roads	8,000	6.0
Total unclassified road network			133,800	100

(Kenya Roads Board, 2012)

82.2percent of the unclassified roads consists of the rural roads networks where much of agricultural activities including tea are located. Indeed, it is the classified road network that can be considered suitable for large cargo haulage. Most rural road conditions could be expected to

present high transport hazards and challenges to the goods that are carried over them often leading to damages to packaged goods where appropriate packaging has not been provided.

1.6.0 Problem statement:

1.6.1 Research question

How do the truck shipment conditions in Kenya differ from those of other distribution environments and how would these conditions affect black tea physical quality in transit?

There is so far no documented distribution hazard measurements data for the Kenyan distribution environment on which pre-shipment testing of packs and goods could be based on. Road transport including truck transport presents the greatest vibration damage hazard compared to the other transport modes. Since truck transport often serves as a link to other transport modes, it can be argued that an effective laboratory random simulation using the actual road spectra data represents the worst case scenario of hazards goods are likely to experience within any supply chain (USA Department of agriculture, 1979; L.A.B, 2008).

Distribution hazard measurements carried out in other distribution environments such as the USA, Spain, Brazil, Japan and even India have revealed that standard industry recommendations for laboratory simulated tests may not be adequate to ensure goods protection as well as optimal pack designs for all destinations. Singh e.t al. (2006), suggested that in the presence of current more realistic transport spectra data from various parts of the world, the spectrum in ASTM D4169 may not be appropriate for use in all parts of the world. This is particularly so for those areas with poorer road conditions than those of developed world where much of the empirical data used in formulating the standards originated.

Industry-standard recommendations usually represent accelerated tests whose extrapolation to any given testing/simulation situation may not be suitable. When distribution systems are known to be significantly different from what has been previously studied but there is no quantifying data, the only recourse is a focused simulation testing (Martinez et. el., 2008). The team further concluded that often the best approach in such a case is to measure a number of shipments that are directly applicable to that particular environment and then compile data that can be used for simulation in the laboratory. A study commissioned by the European Commission on the distribution environment in Mexico concluded that both road and rail vibrations in Mexico are more severe than in the USA (Kipp et.al, 2008). Baird et. al. (2004) further concluded on the “China case study”, that distribution conditions in China were

sufficiently different so as to require not only new testing protocols, but new approaches to design of packages and in some cases even design of the products themselves. Singh et. el. (2007) investigated road and rail conditions in India and concluded that road conditions in India were significantly different and more severe than those of developed environments such as USA and Europe. There is therefore sufficient reason to believe road conditions in a developing country like Kenya may be quite different from those of a developed country like USA and Europe where most data (including that used to set test recommendations by both ISTA and ASTM) has been derived. Packaging design engineers in Kenya have therefore no credible road conditions data against which they could test their designs and have to adopt an overcautious approach to package design in order to guarantee no failure occurs in transit. This strategy, however, may be wasteful in resources and further may not meet the strict environmental thresholds such as the EU Packaging Directive and other packaging waste regulations in other countries that demand minimum packaging. Only focused simulation that target actual distribution environment as envisaged in this work, could gather information that would allow establishment of a credible testing protocol for goods in the Kenyan distribution environment.

In addition, most of the previously collected road data was done using spring/mass recorders and other equipment before the advent of more accurate data loggers. The former instruments have been shown not to accurately quantify package drop heights resulting in high in-accuracies even of the pack designs (Schueneman, 1996). More coordinated data collection of the distribution environments and application of uniform data reduction has been proposed in order to update the available literature. Furthermore, many of the previous transport distribution studies which were carried out for specific objectives such as defence using specialized vehicles have included data and information not considered applicable to the common carrier distribution environment (Schueneman, 1996). This new information for the Kenyan distribution environment will therefore add to the new knowledge on the levels of transit hazards and not the least from the less developed world where very limited distribution environment information is currently available. Attempts have been made to relate the levels of transit conditions such as vibration with possible damage to products such as fresh fruits and vegetables and various consumer products. No such documented information unfortunately covers damage to the physical quality of tea in transit.

1.7.0 Benefit to the Kenyan tea and other goods shippers

This work will allow actual data collection from the Kenyan distribution environment. This will then be used to compile a composite truck spectrum data which could be used in pre-shipment testing for goods for this distribution network. With such a pre-shipment testing protocol in place shippers would be able to optimize bulk tea and other goods packaging designs and save costs and minimize packaging waste creation to the environment.

The work will also shed light as to the extent the physical quality of tea may be undermined in transit in truck transport in order to design an appropriate packaging system to preserve tea quality during distribution.

1.8.0 Aims and objectives of the research

1.8.1 Aim

The aim of this project is to measure and analyse the distribution environment within the bulk tea supply environment in Kenya as a basis for establishment of a pre-shipment protocol for the packaged goods within this supply chain.

1.8.2 Broad objective

To evaluate the Kenyan bulk-packed tea truck transports transits conditions and later simulate them to find out their effect on the physical quality of CTC black tea.

1.8.3 Specific objectives

1. To establish vibrations/shock and load compression levels in truck shipments in the bulk-packed tea supply chains in Kenya and compare them with data from other parts of the world.

2. To develop a pre- shipment testing protocol based on the composite spectrum derived from all measured distribution routes that would allow shippers in Kenya to test their package designs in order to optimize them.

3. To evaluate the environmental conditions of temperature and relative humidity within the truck load in order to understand their levels and how they could affect tea quality.

4. To carry out laboratory simulations of the road conditions found on the Kenyan roads in order to understand how they could affect the tea quality parameters of particle size and its distribution, density, particle morphology, colour and flow characteristics.

1.9.0 Summary

Kenya is an important producer and exporter of black tea which is an important contributor to the country's GDP. Kenya tea exports are mainly in bulk packed form which is transported in trucks to the port of Mombasa from where it is exported. Most of the roads used for tea shipments are in relatively poorer conditions compared to those of other countries such Europe and USA but there is no data at the moment to support this view. Past studies indicated that Kenyan goods are over-packaged as there is no pre-shipment testing protocol to help shippers in this region to optimize packaging designs. Many distribution packaging researchers advocate use of focused pre-shipment procedures in order to achieve optimal packaging that guarantees safe delivery of goods without over-packaging. The research focuses on understanding the Kenyan bulk tea supply chain through evaluation of the truck load shipments in order to formulate a suitable pre-shipment protocol for packaged goods. The research will further explore how truck distribution environments could affect physical tea quality.

2.0 CHAPTER 2: LITERATURE REVIEW

2.1.0 Introduction

This chapter provides an account of the various attempts that have been made to measure and analyse the transport environments in various parts of the world. It further looks at various measuring instruments that have been employed in both transit data collection and in simulation of those environments. General behaviour of granular matter including tea and effect of simulation excitations on this behaviour was explored.

2.2.0 Distribution environment hazard measurements

In recent years, it has been realized that many products get damaged during transportation and handling. Vibration and shock forces that occur during transportation of goods are the most significant causes of damage to products in transit. Lately, there has been a lot of impetus to gather field road transport data from various destinations that included China, Brazil, Spain, India, USA, Nigeria , Japan and even Thailand in order to develop data to define a 'global distribution environment'. Data from such studies has been able to help define the actual distribution hazards of vibrations and shock by quantifying their intensities to enable comparison with data obtained in past work and that specified in various test protocols such as ISTA and ASTM. Distributions spectra for various modes of transport within a given environment such as those for developed world could be evaluated against conditions found in developing countries. Such new data has been used to review both ISTA and ASTM recommended transport tests. Needless to say, as data from hitherto relatively unknown parts of the globe becomes available, this will define the test parameters more precisely to embrace today's globalization. As international trade and globalization becomes the world commerce order, goods hitherto consumed in the neighbourhoods have now to be delivered to some of the remotest parts of the globe. In some of these new markets, (especially in the developing and underdeveloped countries), distribution systems are quite rudimentary and therefore their thorough knowledge is essential in order to optimize pack designs while ensuring safe delivery of goods. Arising from data already obtained from some developing countries such as India, ASTM and ISTA's current test recommendations may not be adequate to accurately simulate those conditions (Singh et. al., 2007). There is therefore a need for focused transit hazards evaluation for such environments in order to optimize package designs and ensure safe delivery of goods (Forest products; 1979, Allied, 2009).

2.3.0 Test protocols for goods

2.3.1 Pre-shipment testing

Laboratory pre-shipment testing of goods and packages is now a well-accepted and popular practice in many organizations. This is because it enables organizations to make product and pack designs that allow goods to be safely distributed at minimal possible packaging costs (Becker et.al., 1997). Such testing procedures when conducted under controlled conditions allow firms to predict how their goods would withstand transit hazards in actual conditions of distribution and hence avoid expensive failures. For such tests to be useful, however, the test protocols chosen must deliver the desired outcomes so that correct decisions may be arrived at on the appropriate packaging required (L.A.B, 2006). Several tests exist depending on the level of information required by the shipper.

2.3.2 Integrity testing (Non –simulation tests)

These tests aim at evaluating the strength or robustness of the product- package systems without necessarily trying to replicate the actual distribution environment. It is the most basic and simplest laboratory performance testing carried out for most goods. It is also a low- cost pre-shipment package evaluation method. Examples of integrity testing include:

(i) Free fall drops of product-package combination from a predetermined heights as well as face of contact with the target.

(ii) Compression tester designed to ascertain the amount of compressive force the product package system can endure before failure.

(iii) Horizontal and inclined plane test system that evaluates the extent the product- package can withstand distribution impacts.

(iv) Environmental chamber testing system that evaluates the effect of the distribution environmental conditions on the product-package combination.

(v) General hydraulic vibration system that attempts to evaluate the extent that the product-package can withstand vibrations in distributions.

Because general integrity tests are not based on any actual measured conditions of the distribution environment, the test parameters often tend to adopt an overcautious approach that ensure no failure takes place. Because of this approach, where these tests actually work, often tend to display a" worse case" scenario test intensities. Product-package designs based on integrity tests that successfully protect products in large scale shipments often exhibit over-

packaging and over- protection (Baird et.al, 2004).These tests are therefore not the focus of this research.

2.3.3 General simulation

This test method attempts to realistically model the damage-producing inputs of distribution in the laboratory. Broad based depictions of various parameters including intensities of various hazards, sequences and even test conditions are used. Usually the test protocols used are based on generalizations such as industry consensus, compilations from various sources, calculations and even own personal experience. The procedure involves for instance, using various impact tests, varying drop heights, impacting angles for drops, using simple shaped random vibration regimes to simulate actual distribution hazards, compression tests using generalized top loads and stack heights, controlled atmospheric test conditions as well as combinations of various hazards. Attempts are made as much as possible to tailor the tests to the actual distribution conditions including package types, various modes of distributions used and even having tests in the laboratory carried out in the sequence in which they occur in actual shipment.

General simulations requires the user to have a good idea about the character of the target distribution system albeit in broad terms; in order to determine the types of tests required, intensity, sequence and even combinations of tests as accurately as possible. Broadly, test intensities will depend on product value, hazards extremes and even shipping quantities (Kipp, 2001).

Obviously, the capital outlay requirements and complexity for general simulation is far much more than for general integrity tests. It should, however, be appreciated that the test works well when there is a good match between the actual distribution environment and the selected laboratory tests, intensities and sequences (Kipp, 2001). Examples of general simulation tests include American Society for Testing Materials (ASTM Practice D 4169), International Standards Organization (ISO Standard 4180) and the International Safe Transit Association (ISTA 3 – Series). These tests procedures have shown good correlation with actual field shipments in the USA, Western Europe and Canada. This may not be true though in other environments especially those from developing world such Thailand and Brazil (Singh et.el., 2007). This testing procedure is therefore not used in this research.

2.3.4 Focused simulation

Focused simulation is the most extreme type of laboratory pre-shipment method. It is usually used in situations where high correlation between the test and actual field conditions is required. This is particularly important where high value goods are distributed or for situations where a high level of diligence is required to preserve product quality or meet other regulatory threshold of target market. Although a comprehensive general simulation test may appear similar to a focused simulation, there are significant differences in the details such as vibration spectrums, number and magnitude of impacts, velocities, controlled environment parameters, etc. Indeed, for a successful focused simulation to be undertaken, actual shipments environments must be researched and implemented in order to obtain a near-perfect correlation to the actual transportation/distribution environment. This way data used for package designs will ensure pack optimization not only to address packaging costs but also environmental concerns including the European packaging Directive Waste 94/62/EC directive; and the revised version 2004/12/EU of 11th February, 2004 (The packaging professional, 2006). While a comprehensive general simulation test covers all envisaged hazards, a focused simulation links the characteristics of those hazards to a particular type or class of product-package system, and particular means and modes of distribution (Kipp, 2008).

In general, success of focused simulation will very much depend on understanding of the real world situation and how well the laboratory simulation conditions are organized to get a near perfect correlation to the real world conditions. This requires use of appropriate equipment, good positioning of the measuring equipment on the carrier or other hazard area, enough data to permit valid analysis and correct data analysis.

Accurate transit data measurements have been made possible due to availability of miniature self- contained electronic field data loggers that could be mounted unto the transport vehicles and other distribution modes. These recorders are able to record both static and dynamic information such as relative humidity, shock, vibration, pressure and even temperature. The implications of this is that pre-shipment testing in the laboratory can be tailored to mirror the actual field conditions in terms of types and levels of hazards experienced by the goods during their transportation. This approach is more likely to give to an optimal package design than the general simulation that is not based on any actual transit data. This is the approach that was employed in this research.

Random vibration profile data is usually graphically represented by a power spectral density (PSD) plot. The PSD plot has G_{rms} intensity (G^2/Hz) as one axis and the frequency (Hz) as the

other, both on power of 10 logarithmic scales. The log-log plot allows display of a wide range of values on a reasonably sized chart, although this could tend to make large differences appear small (L.A.B, 2006; (ASTM D4169 and ASTM D4728). PSD is done directly by the method called Fourier transformation. (Figure 2-1) represents a typical shape of the PSD plot. So the

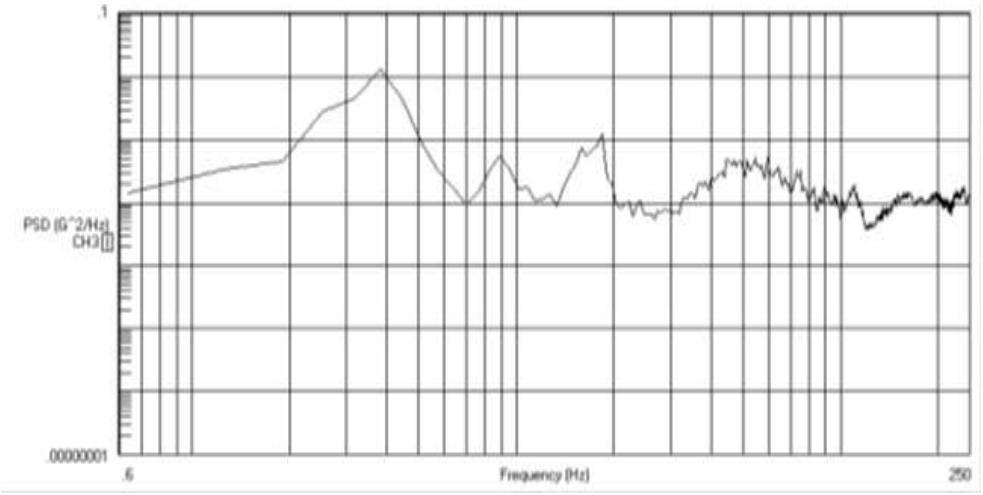

Figure 2- 1 A typical power spectral density (PSD) graph

(Kipp, 1998)

2.3.5 Comparison of Vibration for various transport modes

Steel leaf-spring truck-trailer vibration in developed regions show suspension, tyre and structural resonances in fairly defined frequency bands (Singh et. al. 2006; L.A.B.,2006) and overall intensities in the 0.20 to 0.35 G_{rms}. Figure 2-3 shows a standard ISTA simulation spectrum for a truck.

Air-ride truck trailers tend to exhibit lower frequency suspension resonances with roughly 50% lower overall intensities compared to steel-spring trucks of the same type. Rail vibration intensities are generally much like those of air-ride trucks while air transport vibrations are quite low. Ocean vibration intensities are extremely low too (L.A.B, 2006). Figure 2-3 shows a generalized comparison of vibrations for the various transport modes.

It appears therefore truck transport particularly with the leaf spring suspensions often presents the greatest vibration damage to goods (Figure 2.3). This is because the spectra have generally higher overall vibration intensities compared to rail, air, or ocean transport. Since truck transport typically serves as a link to the other modes, it could be argued that an effective

laboratory random vibration programme might be performed with only truck spectra (L.A.B., 2006).

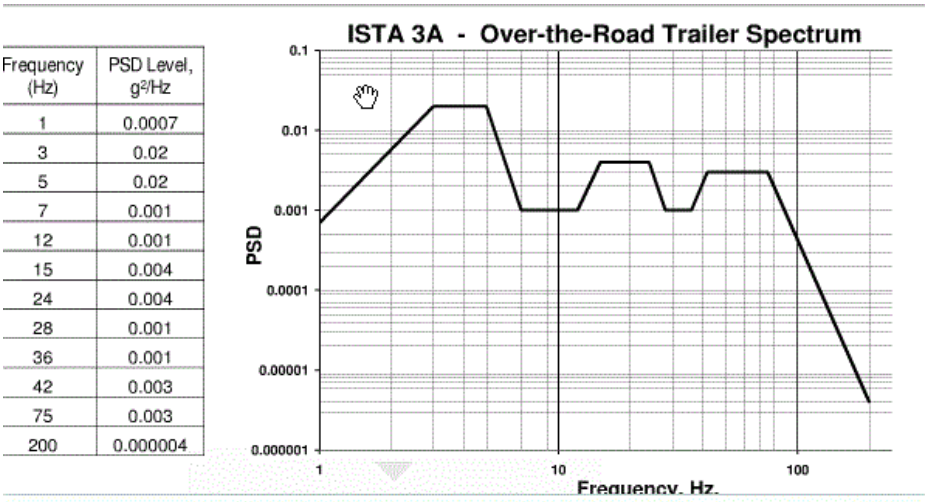

Frequency (Hz)	PSD Level, g²/Hz
1	0.0007
3	0.02
5	0.02
7	0.001
12	0.001
15	0.004
24	0.004
28	0.001
36	0.001
42	0.003
75	0.003
200	0.000004

Figure 2- 2 Industry-standard random vibration PSD plot for simulating truck transport

(ISTA, 2008)

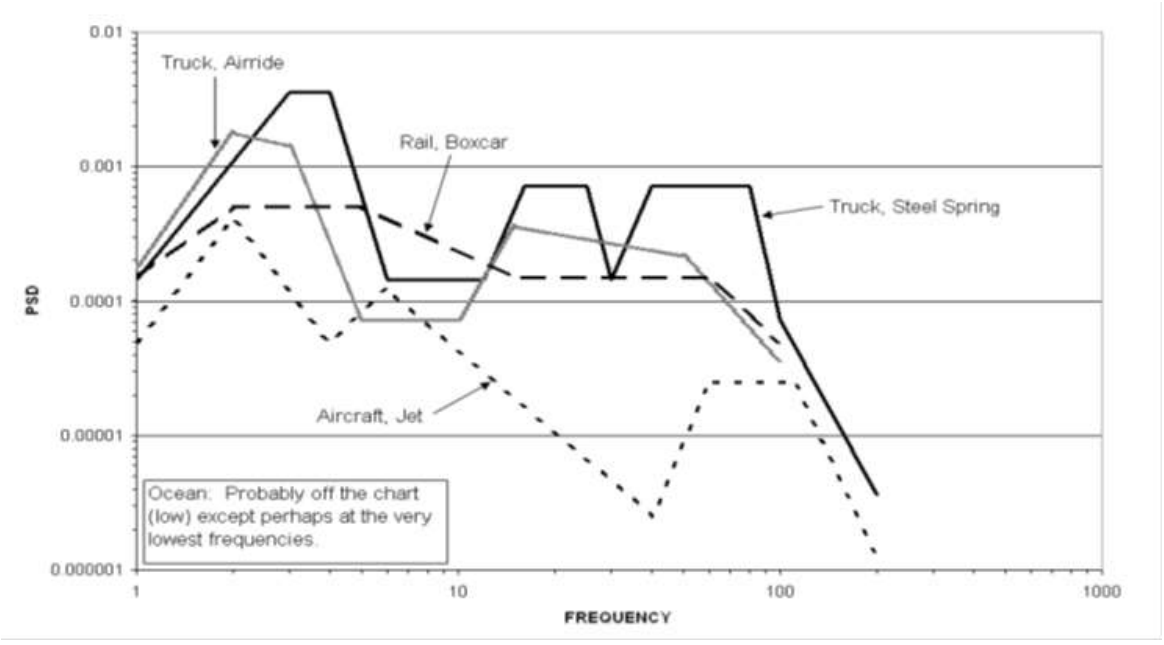

Figure 2- 3 Comparison of PSD plots for common transport modes

(L.A.B., 2006)

2.4.0 Transit hazard simulation methods

There are three main approaches employed in road simulation tests that include:

2.4.1. Laboratory simulation

This is carried out using various types of vibrating tables/shakers that are programmed to simulate various conditions experienced during real shipment. Inputs signals of vibration and shock such as amplitudes, accelerations, frequency are varied in such a way that they reflect the cargo load dynamics. This method of simulation has several advantages that include:

(a) Reduced test times compared to actual road transport tests. Laboratory simulations are a practical and convenient way to investigate distribution performance in real time. Through real time video the root cause of a problem can be identified and corrected before shipment.
(b) Repeatability within same laboratory and reproducibility between different laboratories is possible in laboratory conditions. This means that the test can be repeated or reproduced in another laboratory with modified samples. Simulation can also be carried out in a defined and controlled condition such as temperature and humidity.
(c) Great cost savings are realized as hidden costs of vehicle operations associated with actual shipments are eliminated. In addition, real shipment failure or lack of it due to over-packaging may be expensive to business.
(d) Laboratory testing offers increased safety standards particularly when dealing with dangerous cargo that could pose risks to the handlers in case of failure. Some very large cargo may not, however, be possible to test in laboratory conditions.

There are three main categories of laboratory simulated tests for packages, which are explained in this section.

2.4.2 Repetitive shock or “bounce” or “fixed- displacement

This method (specified in ASTM D 999 Method 1) has the specimen placed on table of the machine that is set to move in a vertical motion with a constant displacement of 25mm in the vertical direction. The test is conducted at a fixed frequency of 4.5 Hz. The specimen is observed to intermittently leave the table surface and “bounce” thus the test tends to impact shock on the specimen rather than true vibration motion. This test cannot, therefore, be said to simulate the actual transport conditions in a carrier as although there is observed cargo bouncing in actual transport, the frequency and amplitude are not constant but quite random in nature. There could be instances where repetitive shock tests are shown to produce same

damage or performance observed in actual shipment. This can only apply to a particular package- products system for a given transport mode and distance as there exists a very close correlation and the results cannot be extended and generalized to cover all product/ package and transport situations (Bernad, et.al.,2011).

2.4.3 Sinusoidal test

The second type of laboratory vibration test is that as specified in ASTM D 999 Methods B and C and in other similar tests such as those of ISTA. This is a sinusoidal or sine test where the vibration table moves in smooth sinusoidal motion with variable and controllable frequency and amplitude. Variants of the test can be that of dwell tests (both frequency and amplitude kept constant) or that of Sweep tests in which the frequency is slowly varied to cover a wide frequency range. While sweep tests are useful to identify the natural frequencies of the product/package systems and dwell tests to assess the damage those natural frequencies may have on the material, they cannot, however, be said to represent the actual truck transport conditions that are usually random and not sinusoidal vibrations (Lu, et.al.,2010).

2.4.4 Random vibration test

The third laboratory transport vibration simulation category is that specified in ASTM D 4728. This is the most reliable road transport simulation test that nearly mirrors the actual road transport conditions. In this test, the vibration table moves with a constantly- changing complex mixture of frequencies and amplitudes. Consequently, the vibrations produced by this test nearly simulate the actual conditions experienced by goods in the transport environment. This is much more so if actual transit conditions have been measured and the same spectrum fed into the vibrating table so as to simulate the actual field random conditions. Different transport vehicles and haulage conditions will produce different vibration spectra (Power Spectra Density) shapes and amplitudes (Singh et.al, 2006). Random vibration tests can therefore be said to be the ones that realistically closely represent the actual transport conditions and that can be used in the laboratory for evaluation of product/package systems. This is because normal truck vibrations and shock are difficult to predict and therefore random due to road surface irregularities (Ostrem, 1965; Rouillard et. al., 2007).

2.4.5 Test tracks

Arising from sometimes difficulties of establishing the ‘‘worst case” road conditions; standard test tracks are often used in evaluating the shipment conditions and their effects on packaged

goods. This involves use of suitable standard test tracks which are expected to be as close as possible to the conditions encountered in real life shipment conditions. A wide range of test tracks are available but not all are suitable for road transport simulation. Great care is therefore needed in selecting suitable surfaces that are representative of the actual shipment environment. Use of test tracks though, has some advantages in certain circumstances that include:

(a) They permit standard road surfaces to be travelled at constant speed significantly reducing non stationary component of dynamic responses.
(b) Test tracks may sometimes reduce occurrence of transients within responses.

The major disadvantage of this method is the difficulties in being able to mirror actual shipment conditions often leading to unusually high amplitude and bounce that could be induced at a rate of occurrence many orders above the normal pay road responses (USA Department of Agriculture, 1979). Such conditions could induce modes of failure which are unlikely to occur in practice. As there are variants in the distributions environments, there is great difficulty in choosing the track that mirrors the actual road conditions in each situation. This test method was not used in this research.

2.4.6 Road trials

Simulation using standard test tracks and real life shipment is convenient for large and rather awkward pay roads that are not possible to scale down and therefore not practical to handle in the laboratory set up. This is true especially where the payload interacts significantly with the dynamics of the carrier. As real road condition may depend on such factors as speed and manoeuvring that are influenced by traffic flow, it is not therefore practical to control such variables in actual shipment situations. The major disadvantage of road trials as already pointed out in 2.4.2 for track trials is the high costs associated with the transport activity and product losses in case of failure. Masking of over-packaging is normally the case in case of non-failure. As it is not possible to accurately control test conditions in road trials, such test procedures are characterized by a high degree of variance making achievement of optimal packaging using this test method unrealistic, time consuming and therefore uneconomic. This method was therefore not a focus on this research as the laboratory test procedures were preferable.

2.5.0 Goods transport modes and their variables

There are four main transport modes that are commonly used in the world to distribute goods from the point of production to the target market. They include road, rail ocean/water and air. Within each of these modes of transport there are legions of variables that can be encountered. There are therefore almost infinite numbers of variations that can be reproduced for each transport mode making the use of general test standards unrealistic for accurate evaluation of transit conditions especially for optimal distribution packaging design work.

2.5.1. Road transport variables

In road transportation, there may be variations on the carrier types, speed, road surface, type of suspensions, and amount of load carried and even moving and stopping regimes.

2.5.2. Air transport variables

In air transport, the type of carrier, transit conditions such as turbulence, take-off and landing manoeuvres will affect the vibrations and shock levels in the carriage and hence the safety of cargo.

2.5.3 Rail transport variables

The type of locomotive used, track conditions, speed, shunting etc. will affect shock and vibration levels transmitted to goods by rail.

2.5.4 Ship transport variables

In the case of transportation over water, sea transient conditions such as sea currents and even engine vibrations will affect goods in ships.

2.6.0 The Importance of road transport in Goods distribution

Road transport remains the most popular mode of transport in the world. The American Trucking Associations reported that in 2012, trucks moved 9.4 billion tons of freight or about 68.5percent of all freight tonnage transported domestically. Freight transport is the backbone of many countries commerce having to cope with ever increasing imports and exports. Reliable land transportation is essential for robust economy of a country (Steyn, et al. 2012). In the USA, highways are the primary means of transporting people and freight (Lambert, 2003; Steyn, 2012). In most developing countries, road and especially truck transport is the predominant mode for goods distribution.

The trucking industry is a crucial part of the transport modal mix, particularly with trucks typically acting as the" last mile" service provider, bringing goods directly to consumers (FTA, 2008; Steyn et. al.,2012).The USA transport system serves seven million businesses that depend on it to move goods to target markets, mainly using trucks (American truck, 2012). The agricultural sector accounts for nearly 30% of all freight transportation services in the USA, making it the largest single user of freight transportation in the USA (FTA, 2008).

In Kenya, road transport accounts for over 80percent of goods haulage (Irandu, E., 1995; Bundi. J., 2003; Kenya Institute of Economic Affairs, 2008). This is because road is the most developed and convenient mode of haulage in the country compared to the other modes such as rail, water and air. Despite this scenario, 86percent of the total classified road network (63,291km) is either gravel or earth leaving a mere 14percent of the total classified road network in the whole country under bitumen surface. As mentioned earlier in 1.4.2.1, the bulk of the entire road network is unclassified and hardly motor able (Table 1.1). Indeed, it is the classified road network that can be considered suitable for large cargo haulage. Such road conditions could be expected to present high mechanical hazards to the goods that could result in damages if appropriate packaging is not used.

2.7.0. Types of vibrating testing equipment

Vibration testing is an important tool that allows the product designer to evaluate the product in the laboratory before its shipment in order to evaluate its possible behaviour and safely in transit. A vibration table is used to determine the resonant frequencies at which a product is mostly likely to suffer breakage during transportation or accelerated degradation during its lifespan (Miller, 2012). There are several types of vibrating table systems that can be used to carry out vibration tests in the laboratory. They include: electro-dynamic shakers, hydraulic shaker and mechanical shakers.

2.7.1. Electro-dynamic (ED) shakers

These are designed around an electromagnet driven armature. The armature is wrapped in coils and placed inside a permanent magnet. When the coils are energized the armature and the test assembly are forced upwards at the desired rate. This type of shaker allows the system to run through a wide range of testing profiles often ranging from 0 to 3000Hz. This makes the ED shaker ideal for testing specific vibration profiles especially for items less than 45kg. Since this shaker is capable of reaching much higher frequencies than the hydraulic and or mechanical

shaker, it is ideal for accurate determination of resonant frequencies of electronic components and boards (Miller, 2012).

2.7.2 Hydraulic shakers

These shakers are designed around a hydraulic piston. They are designed to handle basic frequencies necessary for prediction testing. They have a much higher force potential than ED shakers making them quite ideal to test items up to hundreds of kilograms. However, since these units are basically designed to test relatively higher payloads, they cannot reach higher frequencies (above 300-500Hz) necessary to test small appliances and electronics.

2.7.3. Mechanical shakers

Mechanical shakers are usually used to test integrity of various components and even the whole device. These tests are basically expected to measure the "robustness" of an item and thus provide a comparison to an established baseline or comparing several design concepts side by side. The shaker is composed of ridged test platform suspended over the frame and fitted with isolation shock absorbers at the corners. The system is powered by a motor (rotary, pneumatic, or hydraulic) that is usually controlled by a variable speed controller. Indeed, computer controlled or customizable test profiles are very rare (Miller, 2012).

Although mechanical shakers offer a very economical testing approach, the system is incapable of running a specific test profile across a broad band of frequencies and accelerations as the ED and Hydraulic shakers can perform. Figure 2-4 shows the force and frequency ranges of the various shaker types discussed so far and the type of devices they are more suited to test.

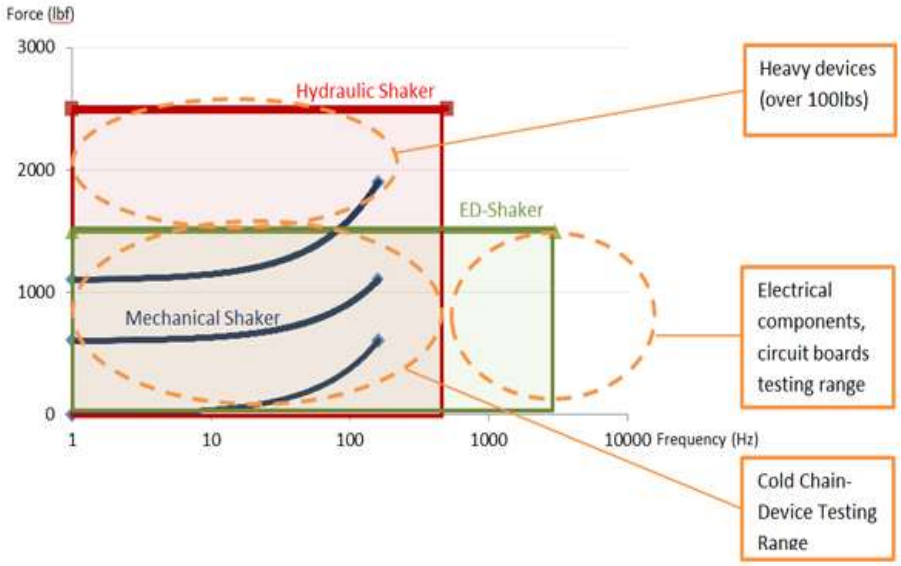

Figure 2- 4 Force and frequency ranges for hydraulic, electro-dynamic and mechanical shakers

(Miller, 2012)

2.8.0. Research on transit hazards

2.8.1. Transit environment measurement and analysis

In the recent past, transportation transit hazards of vibration and shock has received a lot of attention from several researchers in various countries. This is due to the realization by many shippers that only focused transport studies can address accurately mechanical and other hazards experienced by packaged goods in various environments. Road transportation between the manufacturing points and warehouse bases and retail distribution outlets can subject goods to mechanical and even environmental hazards that could damage those products while in transit. Road transportation produces a composite of continuous vibration (Gaussian) and transient random (shock) motions (O'Brien, 1973). Distribution environment road conditions in many countries are so diverse that it is exceedingly difficult to optimally address in- transit product damage concerns without accurate measurement of transit environment.

What Happens between Manufacturer and Consumer?

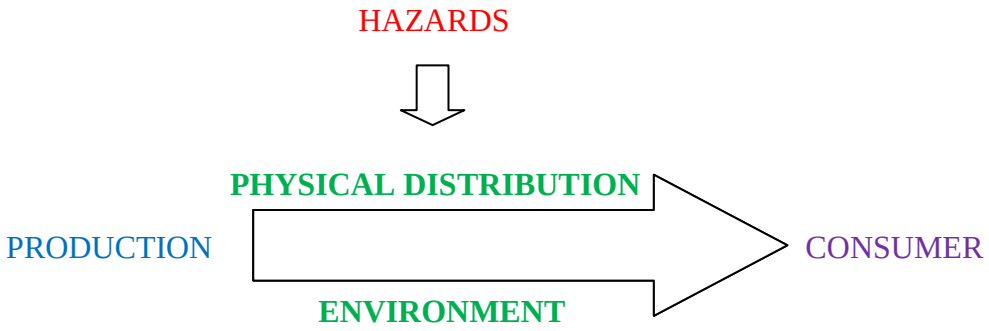

Figure 2- 5 Physical distribution

(Seroka, 1996)

Sharpe et. al. (1973) reported vibrations from scheduled common motor semi-trailers. Three fully loaded trailers with loads of 19 776kg (43 507lb), 2 727.3kg. (6 000lb), 4 090.9kg (9 000lb) and trailer lengths of 13.72m.(45 ft.), 12.20m (40ft) and 12.20m (40ft.) respectively were studied. A fourth trailer 9.15m. (30ft.) long and starting with a load of 2 227.3kg (4 900lb.) was used for local deliveries (the load decreased as deliveries were made). The data for all trailers showed the rear vertical vibrations to be the severest. The front vertical vibration levels were between those recorded in the rear and middle of trailer. Generally lateral vibrations were smaller by a factor of two or more. Trailers with light cargo were reported to have a lower level of vibrations independent of speed. The report further indicated that levels of vibration increased with speed in all cases.

Silvers et. al. (1976) and Forest Products Laboratory (1979) reports on studies carried out at Westinghouse Electric Company focused on vibrations in tractor trailers. The studies aimed at determining the effect of various suspension systems (convectional leaf spring, rubber isolator, damped coil springs, and air bags), amount of load, rear wheel position, road type and driver on vibration levels. The worst ride was experienced at high speed on interstate highways. On the load weight and location, the worst ride was reported experienced at the rear axle for a lightly loaded trailer. The report further noted individual drivers had little effect on vibration levels.

Rissi, et. al. (2008) examined truck transport environment in Brazil for various road types (asphalt, concrete, stone and dirt). Various vehicle types were used for long distance (haulage trucks) as well as short distance (metropolitan delivery vans). The team concluded that road conditions in Brazil showed wide regional variations and that metropolitan distribution had lower vibration levels. The study further concluded that accelerations increased with lighter loads, bad road conditions and vehicle speeds.

Singh, et. al. (2006 a) investigated vibrations caused by leaf spring and air ride suspensions on USA roads as a basis for development laboratory spectra to simulate those conditions. The study noted that air ride suspensions resulted in lower vibrations intensities created compared to leaf spring. This explains why vehicles fitted with air ride suspensions are often preferable as they are less likely to damage goods carried in them compared to vehicles with leaf spring suspensions. Further work by Martinez, et. al. (2008) confirmed Singh et. al.(2006a) conclusions that air ride suspensions exhibited significantly lower RMS (G) levels than those of leaf spring suspensions. They further held the opinion that the loaded truck showed higher Grms (G) levels compared to unloaded for both air ride suspensions and leaf spring suspensions. Martinez (2008) observed that the predominant suspension frequency for air ride trailers was measured between 1.5 to 2.0 Hz while that for leaf spring ranged between 4 to5 Hz. Martinez further discovered that the vibrations levels measured in Spain were lower than those found in the US and that the vibration levels on Spanish roads were significantly lower than ASTM, ISTA and ISO test levels. Martinez (2008) concluded that the recommended test levels from above agencies were therefore not suitable for optimizing pack designs and there was need for alternative test parameters for this environment to be developed using actual road environment data.

Singh et. al. (2006) compared lateral (across the vehicle chassis on horizontal plane) and longitudinal (along the vehicle chassis on the horizontal plane) vibration levels to vertical (vertical plane from the chassis) levels in same truck trailer travelling on an average USA highway. Of the 4 trucks used in the measurement two had light loads while two had heavy load. Singh (2006) observed from the Power density spectra plots that below the frequencies of 20 Hz, lateral and longitudinal vibration levels were generally much lower than vertical levels but at frequencies above 20Hz, all three vibration levels were similar. The more heavily loaded trucks showed higher lateral and longitudinal vibration compared to lightly loaded trucks.

Singh et. al. (2007) carried out truck and rail transport environment measurements in India and concluded that both rail and road vertical vibration levels in India were severer than the intensities indicated in ASTM and ISTA existing test methods. The research further revealed that higher vibration intensities were found in the Indian environment compared to those from North America and Europe confirming that there is often a marked difference between various distribution environments not the least those in developing countries (where road conditions are poorer) compared to those in developed economies. The study underscored the importance of actual environmental measurement and analysis in order to achieve optimal packaging designs since distribution environments are quite different.

Interesting work reported by Nei et. al. (2008) involved analysis by wavelet algorithm of shocks and vibrations during transportation. Continuous wavelet transform was effective for detecting the non- stationary nature of vibration data. Nei (2008) observed that a wide range of frequency components are present during shocks. They then suggested that continuous wavelet transform is useful for time-frequency analysis, because wavelet basis functions are local in both frequency and time axis, while Fourier basis functions are local only in frequency. They further proposed that the frequency of shocks is dependent on shock direction, and the frequency of horizontal shock tends to be lower than that of the vertical. Upon investigating the wavelet analysis using various coefficients, they finally proposed a method of laboratory shock generation that seems to reflect the actual shock profiles but hastened to caution that further studies are required to be able to simulate shocks and accurately reflect transportation environments.

Lu, et. al.(2010) on the other hand investigated the effect of vehicle speed on shock and vibration levels in commercial truck transport. They used an unloaded 14ton payload Mitsubishi Fuso Truck with front leaf spring suspension and rear air ride suspension. The team monitored vibration and shock events over a distance of 850 km. with 400 km being highway while the rest was on normal delivery routes. Their results indicated that the effect of truck speed on root mean square acceleration (Grms) including shock and vibration was strong at lower speeds but only slightly at higher speeds. Lu et. al. found out that the highest Grms including shock and vibration was at 45- 59.9 km/h on local roads and this was higher than that experienced in highway driving. They further reported that at speeds below 45 km/h. the peak power spectra density (PSD) of acceleration including shock and vibration increased as the truck speed increased while at vehicle speeds above 45km/h - there were no significant

changes in the peak PSD noted with changes in vehicle speed. In addition, Lu et. al. noted that the higher the vehicle speed, the higher the Grms and peak PSD values of vibration in both the vertical and lateral directions. As regards shocks, Lu and his team concluded that they were caused by road roughness, metal joints, difference in levels on the asphalt surface road, pedestrian and railway crossings, road curves, vehicle turns, manholes and other sporadic non Gaussian events. The team further concluded that transport shock increases damage probability on packaged goods and for the food products such as fresh fruits and vegetables (FFV) was responsible for shortening the shelf life due to enhanced microbial and biochemical changes on damaged produce. In tea transport, shocks increase damage probability to the tea particles through attrition, and further encourage segregation which negatively affects both physical and organoleptic qualities.

Becker et. al. (1997) carried out extensive road transport vibration and shock measurements on over-the- road testing of Radio Thermoelectric Generators (RTG) used in power generation. This work obtained real time recordings of accelerations of an air-ride suspensions system trailer floor, packaging and support structure. The results showed that the shock response spectra (SRS) analysis in the frequency range of 5 to 200Hz had a maximum response of 3.2 t0 3.5 g in the 16 to 20Hz range of the converter support ring and package mounting system. They further reported that all other Shock Response Spectra (SRS) plots showed maximum response values of less than 2g. Furthermore, Power Spectra Density (PSD) analysis (for all the accelerometers at various locations that were used in this work) showed maximum values of less than $0.01g^2$/Hz for frequencies less than 20 Hz and less than 0.0001 g^2/ Hz for frequencies of 20 Hz to 1000 Hz. Becker et. al. further demonstrated that air ride trailer suspension systems effectively filter out vibration motion at frequencies above 20 Hz. They further concluded that input shock spectrum excites a response of transportation system at frequencies below 20 Hz and that the packaging responds as a highly damped system with only a few response frequencies. It is evident that special vehicles used in this research had unique suspensions that led to highly damped vibrations in order to protect the delicate equipment. However, for vehicles used in the commercial cargo haulage, much higher damaging shocks are inevitable especially for those vehicles fitted with leaf spring suspensions and being driven on poor roads.

2.8.2. Effect of transit hazards on packaged goods

Several research works have been done on the effect of vibration and shock on the product quality. On the food sector these have mainly targeted the fresh fruits and vegetables (FFV). Some research has been done on non-food products including defence equipment and electrical appliances. However, no related work appears to have been carried on black tea to understand how vibrations may affect its physical properties and quality.

Chonhenchob and Singh (2005) investigated effect of road transit hazards of vibration and shock on quality of Papaya fruit during its distribution in Thailand, and effect of various cushioning materials in reducing the damage. Their research indicated that mechanical damage on fruits due to vibration and shock was responsible for high post-harvest losses of the fruit. With appropriate distribution packaging using various cushion materials, the problem was contained. The appropriate level of cushioning was determined after measurement of actual distribution conditions followed by laboratory simulations of those transit conditions with fruits packaged in various test materials.

A similar study carried out later in Thailand using fresh pineapples (Chonhenchob et. al., 2008) further confirmed that vibration and shock hazards in vehicles were the major causes of fruit bruising in transit. The work demonstrated that the problem could be overcome by using appropriate cushioning such as paperboard partitions and foam-net which isolated the product from the in-transit vibration and shock waves.

Aba, et. al. (2012) carried out a laboratory simulated transport study for Nigeria's tomato distribution routes conditions in order to compare performance of traditional natural fibre basket packaging against a plastic carriage container. The team developed a vibrating table which was used to excite vibrations over a 4 hour period and thus impact on packaged fruits in both containers according to the ASTM D 4169-08 International Standard Assurance Level II. The vibration table was designed using actual field data of pothole depths, bump heights and elevation profiles of major roads used for fresh tomato shipments in order to obtain typical road shipment conditions in Nigeria. Results by Aba et. al. (2012) indicated higher fruit damage from the top fruits in both baskets compared to those fruits at the bottom and middle of the containers. Furthermore, there was more fruit damage from the traditional baskets compared to the plastic ones. While the work by Aba and his group gave useful information on the suitability of the plastic container compared to the traditional basket, a simulation regime

using actual distribution environment testing protocol fed into a programmable vibrating table would probably have yielded more realistic field conditions. Use of ASTM and even ISTA test spectra may not be representative of haulage conditions in a developing country (like Nigeria) where road conditions are mostly likely worse than what is found in developed countries (Young, et.al.1993;Singh et. al., 2006).

Although tea is not within the FFV category, the vibrations/ shock and compression hazards experienced during FFV transportation resulting to the fruit damage due to abrasion and subsequent skin damage are also likely to cause damage to the delicate tea particle integrity through attrition. Such damage could lead to change in particle size that alters the tea density as well as leading to segregation, all of which affect negatively the quality of tea. This will be investigated in this research.

2.9.0. Common hazards in distribution

2.9.1. Mechanical shock

Shock is an impact, characterized by a sudden and substantial change in velocity (Seroka, 1996). It may be characterized by a rapid increase in acceleration followed by a rapid decrease in a limited time period. Packaged goods may experience shock while in transit over road due to a variety of vehicle impacts. These may include sudden vehicle turns, starting and stopping, rail-crossing, jolting, hitting road potholes**,** uneven road surfaces, road speed bumps and other moderately violent actions. The shock wave arises because in each instance the package tends to suffer an impact with another object such as truck bed, pallet, bulkhead of another package etc. This impact results in mechanical shock to both objects in contact. In addition to shock due to transportation, goods may encounter shocks in the wider distribution environment from several sources that may include:

1. Sudden arrests on the conveyors.
2. Drops from conveyors, machinery and chutes.
3. Accidental falls of goods from pallet loads.
4. Deliberate or accidental falls during manual handling
5. Impacts due to railway wagon shunting and wagon coupling at the marshalling yards
6. Transient experienced in planes during landing and take off
7. Transients experienced in sea cargo as a result of strong sea waves etc.
   (Seroka, 1996).

Mechanical shocks to packages, however brief they may be, could cause considerable damage to products. By knowing their acceleration magnitude as well as the shock duration one can estimate the potential damage a given shock may cause. Mechanical shock is defined by magnitude in g's, peak acceleration and the duration.

2.9.2 Shock on free falling package

During handling (especially for light goods) packages may suffer shock due to accidental or deliberate drops. Depending on the nature of the item as well as conditions, such impacts could lead to product or package damage.

The time ***t*** taken and impact velocity $\boldsymbol{v_I}$ by a free falling object dropping from a height ***h*** can be estimated:

$$t = \sqrt{2h/g} \tag{2.1}$$

$$v_I = \sqrt{2gh} \tag{2.2}$$

where: g = 9.81m/s^2

A package thus dropped will rebound and the extent of this rebound will depend on the nature of the package and the surface it hits. For such an object the rebound velocity $\mathbf{v_R}$ can be estimated as:

$$v_R = ev_I \tag{2.3}$$

where: v_R is the rebound velocity; e is the coefficient of restitution and v_I the impact velocity. The coefficient of restitution ***e***, describes the rebound velocity as a function of the impact velocity. The coefficient e takes values between 0 and 1.

The total velocity change Δv, for an impact is therefore the sum of absolute values of the impact and rebound velocities.

$$\Delta v = \left| v_I \right| + \left| v_R \right| \tag{2.4}$$

Since '0≤ e ≤ 1 we may estimate that the total velocity change due to drop impact will be between the impact velocity and twice that value. Numerically, velocity change is equal to the

area beneath the shock pulse (Figure 2-6). Hence mechanical shock damage of a package is related to peak acceleration, velocity change involved and the duration.

When the critical velocity change $\boldsymbol{V_c}$ is known (by experiment) the equivalent free fall drop range (EFFDR) $\boldsymbol{h}$ for a shock can be calculated:

$$h = \left(\frac{v_c^2}{1-e}\right)\frac{1}{2g} \qquad (2.5)$$

when $0 \leq e \leq 1$

realistic range $0.25 \leq e \leq 0.75$

where: V_c the critical velocity below which no damage occurs; e is the coefficient of restitution and g acceleration due gravity.

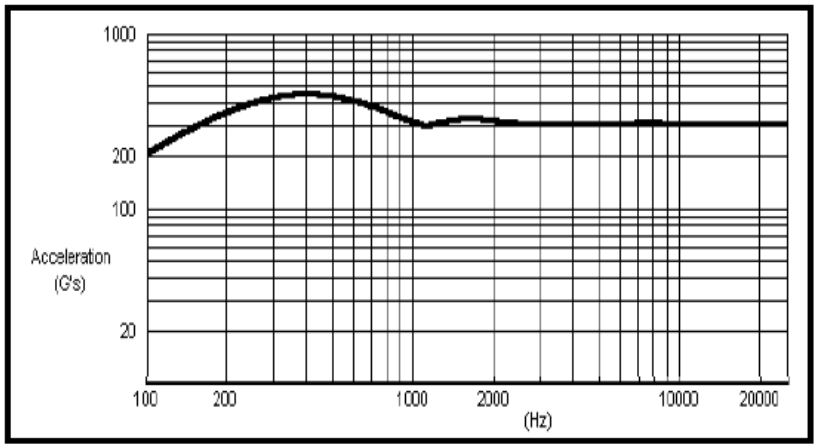

Figure 2- 6 A general shape of shock graph

(Kipp, 1998)

2.9.3 Product fragility

Product fragility refers to maximum shock that an article can withstand without suffering damage. Ideally, the fragility of a product is determined in the laboratory by use of a shock machine. The procedure subjects the test item to a series of gradually more severe shocks (decelerations or negative accelerations) in order to determine the lowest impact that will damage the product. The highest deceleration level which does not cause any damage is the G-Value or Factor of the product. The lower the G-value of a product, the more fragile the

product is and therefore the less the G's it can withstand. (Table 2.1) lists the fragility index figures for various commercial items.

$$G=\frac{Observed\ acceleration}{Acceleration\ of\ gravity} \qquad (2.6)$$

Depending on the number of orientations a particular item is shipped, it is necessary to determine its fragility levels in the various orientations as it is not uncommon for a product to exhibit greater strength in one direction compared to others.

Table2. 1 Approximate fragility of typical packaged articles

Type of Fragility	**Examples of items**	**Fragility factor (g)**
1. Extremely Fragile,	**Aircraft altimeters, gyroscopes, items with delicate mechanical alignment,**	**15-25**
2. Very Delicate,	**Medical diagnostics apparatus, X-ray equipment**	**25-40**
3. Delicate,	**Display terminals, printers, test instruments, hard disk drives,**	**40-60**
4. Moderately, Delicate	**Stereo and television receivers, floppy disk drives**	**60-85**
5. Moderately Rugged	**Household appliances, furniture,**	**85-115**
6. Rugged,	**Household appliances, furniture,**	**115+**

(Seroka, 1996)

While it is not uncommon for the fragility levels of a product to be estimated, it is strongly recommended that the fragility level is defined through test data. This is because the major

benefits derived from optimal package design could be lost when designers use estimated G-values. If the G-value of a product is over-estimated and a large G-Value is used, the product is under-designed and unable to survive the anticipated shock levels during shipment. On the other hand, using a too low an estimated G-value means the product can actually withstand higher shocks levels than anticipated and the product can be said to over-designed leading to unnecessary use of materials/resources, increased cost and more impact on the environment (Brandenburg, et. al., 1985).

2.9.4. Mechanical vibration

Mechanical vibration refers to an oscillation or motion about a fixed reference point. The maximum distance moved by the mass from the reference point is the amplitude and the number oscillations or cycles occurring within a specified unit of time (per second) are the frequency, usually expressed as Hertz.

$$Frequency\ (cycles/second) = \frac{1}{Period(seconds)} = \frac{1}{T} \qquad (2.7)$$

The period is the time required for one complete cycle

T= period in seconds

All modes of transport are associated with some vibration but each mode has its characteristic frequencies and amplitudes at which damage may occur to products carried. (Table 2.2) shows various common modes of carriers and their typical vibration frequency range.

Table2. 2 Typical vibration frequencies for the most common modes of transportation

Carrier	Conditions / source of vibration	**Frequency Range (Hz)**
Truck	Normal highway travel:	
	- suspension	2-10
	- tires	15-20
	- structural (e.g. chassis…)	20-70
Railroad	Normal freight car:	
	- suspension	2-7
	- structural	50-70
	- rail joints	30-300
Ship	- engine/propeller revs	2-7
	- ship movement (waves)	0,06-0,12

	- bulkheads - weather changes	2-200 very low
Aircraft	- landing bump - structural - cargo floor - (fix mounted equipment)	2 1-10 2-200 <2000

(Brandenburg et. al., 1985)

2.9.5 Compression

Compression is a compressive load mainly associated with goods/packages during storage and pallet load transportation. Compression usually causes consolidation especially in granular solid matter leading to increase in bulk density. This is also true for tea when stacked in a pallet during its transportation or storage in warehouses leading to compression of tea particles and increase in density. Unfortunately this may cause breakage of tea particles thus altering the tea quality. However, for fragile items compression could lead to damage or breakage thus requiring an appropriate cushioning on such items depending on their fragility factor.

2.9.6 Static compression

Stacking is an effective way to optimize the available space in storage or even cargo space. The stacking duration, stack height, transport time and ambient conditions all affect the strength of packaging material to resist compression and hence staking capability. Static compression is a force experienced by goods/packages within a static environment such as a warehouse by virtue of slow rate load or force applied on them. Static compression tests are usually conducted using dead-load stacking tests to determine the maximum load that can be applied for a given period within specified environment conditions before stack failure. Static compression can be readily considered during package design and/or testing once the prevailing conditions at warehouse (ceiling height, equipment, stacking procedure) have been established. Tea is usually stored stacked in pallets each having 10 bags of tea. Sometimes two or three pallet loads are placed on top of each other exposing the bottom tea particles to a lot of static compression.

2.9.7 Dynamic compression

Dynamic compression involves application of compressive load/force to a system in a rapid rate. Such dynamic conditions are experienced by cargo during freight transportation, rail

shunting and normal transit conditions. Dynamic compression loads resulting from transportation are more difficult to establish compared to static compression. Load amplification can occur due to vibrations at critical resonance frequencies. Amplification factors of up 6 have been reported for corrugated cases (Godshall et.al., 1971; USA department of Agriculture, 1979) and amplification factors of 4 for fruit in cartons (O'Brien et.al., 1973). Such amplification factors when applied to the static compressive load can result in extremely high dynamic loads at the bottom of the consignment. Compression forces are known to damage dry brittle products such as tea and breakfast cereals due to crushing (Malave, 1985). The forces could also result in package fatigue failure.

Most standard laboratory compression tests are dynamic in nature where apparent compression strength could be affected by load application rate. For instance when viscoelastic materials are tested under rapid load application, the apparent strength value is higher than when the material is loaded slowly (Seroka, et al. 1996 page 373). To ensure that comparable data is obtained among laboratories, loading rates have been standardized to 10 $\pm$ 3mm. per minute (Seroka e.t al., 1996; BS EN 22872).

2.9.8 Environmental conditions

Regardless of the type of haulage used, the product and package will be subjected to the prevailing environmental conditions that could affect their performance. Key to the environmental factors that could adversely affect products and packaging materials is temperature, humidity and in some instances pressure. While the effects of climatic conditions of temperature and humidity may appear relatively less important to containers made of wood and steel, they are an important consideration for paper and paper board as well as plastic containers. Both temperature and humidity can be directly observed or monitored in transit using appropriate measuring instruments. However, both temperature and humidity conditions encountered by general cargo in typical distribution cycles are difficult to summarize because of the many factors which influence not only the ambient conditions but cargo response as well (USA department of Agriculture , 1979). There is need to be aware of how the temperature and humidity data was obtained before making an assumption that these conditions will be manifested within the cargo. This is because there are several factors that may influence cargo response to climatic inputs which include cargo weight, cargo specific heat, thermal conductivity, configuration, emissivity, surface absorption and even ventilation or wind.

2.9.9 Effect of humidity

Humidity affects many product- package systems leading to product damage and failure in transit. For instance, both the paper sack used to pack bulk tea and dry tea are hygroscopic and therefore are susceptible to changes in moisture and relative humidity of the atmosphere they are exposed to. Depending on the surrounding atmospheric conditions, moisture content of paper range from around 3percent to over 20percent. A change in relative humidity from 40percent to 90percent could result in a loss of about 50percent of corrugated container stacking strength (Seroka, 1996). In freight containers where the moisture content may be relatively fixed, rapid external changes in ambient temperature can result in condensation on the cargo or walls of the transport unit. Ambient relative humidity has a significant effect on the load-carrying capability of such material as corrugated boxes particularly in respect to the stacking strength. The relative ambient relative humidity is the driving force that determines the moisture content of the corrugated box. Tea is particularly hygroscopic and leads to moisture uptake that also affects its bulk density.

2.9.10 Effect of temperature

Temperature changes for instance could affect certain plastics making them softer or even brittle greatly undermining their potential transit strength. On the other hand, changes in temperature and related moisture content will affect the physical quality of dry materials such as density and its ability to resist compressive forces. Temperature data will need to be interpreted with great caution depending on prevailing conditions. Data have shown for instance that the cargo temperature could lag behind ambient temperature fluctuations due to thermal inertia of the cargo, or could exceed the ambient temperature because of direct solar radiation on the vehicle (USA department of Agriculture, 1979). The temperature of the cargo inside a container parked in the sun for long periods would be expected to be much higher than the ambient temperature. On the other hand, cargo inside a moving truck would usually record lower cabin temperature for hot days due to motion or higher internal temperatures than ambient during winter. This therefore implies that although representative temperature data may be available for specific situations, this could only act as a guide to estimating cargo temperature due to the many variables that affect cargo response. Precise cargo temperature can, however, be obtained using commercially available temperature recorders.

2.10.0 Transit environment measuring recorders

It is only from 1970's or so has technology been able to adequately satisfy the need for transport environment measuring recorders which provide adequately useful and accurate information at an affordable price (Bernad, 2011). Earlier transport environment measurements yielded results that were often inaccurate and difficult to objectively compare them. Various technologies were used to measure similar transit inputs and results displayed in varied forms.

2.10.1 Simplest and least expensive recorders

The earliest transport measuring instruments were fairly basic, simple and least expensive devices. They involved those that change colour or configuration when a transit hazard event takes place. This could be a change in colour of a chemical indicator when a certain temperature is attained or a ball being dislodged from its spring holder due to impact or even a magnetic attraction being overcome at a given acceleration level. While these devices may appear cleverly designed using various physical, chemical and even material properties, they are limited in that they record a one 'trip point' of a measured parameter and have no capability to indicate, time, date and even location where the event took place.

2.10.2 Mechanical impact recorders

Mechanical impact or vibration recorders incorporated spring- mass systems that tend to respond to input motion with and connected to a pen system that writes the impact of the input signal unto a paper chart. The accuracy of such systems is generally undermined by the fact that spring-mass systems could have their own resonance within the frequency band width that they are trying to measure leading to erroneous results. Many mechanical systems accuracy may be affected by environmental factors if not appropriately isolated.

2.10.3 Electronic "transportation recorders"

These are the modern transport recorders used in many recent transport environment measurements. They are self-contained, miniature units incorporating sensors, analogue and digital circuits, batteries and high capacity data storage and readout. They are capable of measuring both static and dynamic parameters such as humidity, temperature at regular intervals of time.

2.10.4 Full- waveform recorders

These units are today the most sophisticated of the modern transport data recorders. They measure and store entire acceleration versus time waveforms of shocks and vibrations that take place during transportation. They also measure other parameters such as temperature, humidity, drop heights, pressure and others. The specific circuits and features of various full-waveform recorders are known to vary between manufacturers but they tend to share a basic concept and measurement approach. Figure 2-7 shows a generic diagram of full wave recorders showing major elements common to all such instruments.

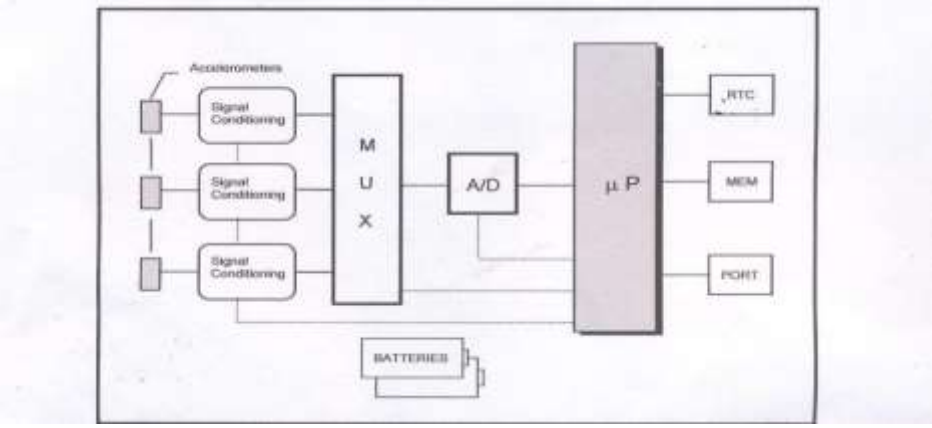

Figure 2- 7 A generic block diagram of a waveform recorder

(Kipp, 1998)

The vibration and shock sensors are typically three accelerometers (or tri-axial accelerometers) that can measure in the X, Y and Z axes. This allows a 3D vector to be calculated hence resulting in omni-directional measurement capability. Following the accelerometers is the circuitry that amplifies and filters their signals so as to make them suitable for recording and prevent aliases. The conditioned signals are then connected to a multiplexer (MUX) and the MUX output is connected to an Analogue- to- Digital (A/D) converter. The MUX thus acts like a switch which alternately switches the multiple inputs unto a single output so that only one A/D convertor is required. This arrangement thus removes the need of an A/D converter for each channel. This saves space, power consumption and even cost. The A/D is finally connected to a microprocessor (µP) which both handles the data as well as controlling the entire instrument operation. The instrument also has a digital memory for real time data storage, a real- time clock (that allows data time and date stamping) and the computer communication port. The instrument is powered from batteries via a power supply

circuitry. Data can be analysed in both frequency and time domains and even statistical analysis can be carried out. Because the instruments are computer based and have their own internal microprocessors they are able to link to an external computer running their companion software programme for equipment set up and retrieval of information, file exports, data analysis and even report generation. Figure 2-8 shows various types of transit measuring instruments that have been used in collecting transit data in various locations.

Figure 2- 8 Types of transit data collecting recorders

(Kipp, 1998)

2.11.0 Accelerated simulation testing:

Due to the time the actual shipment may take, especially for long transport destinations, there have been attempts to shorten the actual test time in relation to the actual shipment time. Attempts have been made to relate the actual testing period to actual distances covered during shipment. Fackler et. al. (1972) proposed a method for compressing vibration tests in relation to actual shipment tests. Young et. al. (1993) further proposed a formula for calculating the amount of acceleration increase corresponding to a test time reduction as follows:

$$I_T = I_o\sqrt{T_o/T_t} \qquad (2.8)$$

where:

I_T = the test intensity in Grms (overall intensity of the PSD profile)

I_0 = the original intensity (overall Grms of the original profile)

T_o = time duration of the original profile

T_t = the test time

Grms (root-mean- square acceleration) is a mathematical process by which the time-average intensities are calculated by taking the square of a waveform function, then averaging resultant over time and taking the square root of the resulting function (Kipp, 2001). Graphically this is equivalent to the area under a PSD curve.

Kipp et. al. (2008) further proposed a time compression ratio of not greater than 5:1 for T_0:Tt for actual journey and the laboratory simulation period in order to preserve validity. This meant that for the actual transport period T_0 the laboratory pre-shipment test period Tt would be a fifth of the actual transport period. Nevertheless, he pointed out that while this formula may be true for USA and Western Europe where the standard of their roads is relatively high, it may not apply in places with poorer road conditions and that more work needs to be carried out to confirm the validity of the formula. In addition, the formula would hold for the type of vehicles used in his research. Furthermore, the formula only focuses on Grms levels ignoring the spectra shapes which could have great effect on test results.

Shires, (2011) observed that many broad random vibration tests are time compressed by using the Basquin model of cyclic fatigue. Using the model, therefore, the test time can be compressed by increasing test intensity. In the Basquin model, the assumed (assumed because for packaging testing the applicability of fatigue models has not been proven) relationship between actual and test duration is:

$$\frac{t_j}{t_t} = \left(\frac{a_t}{a_j} \right)^k \qquad (2.9)$$

where:

t_t= test duration

t_j= actual journey duration

a_t= test intensity (G_{rms})

a_j= actual journey intensity (G_{rms})

k is a constant whose value depends on the material/product in question

Shires D. (2011) further suggested that in packaging testing $\frac{tj}{tt}$ is typically limited to $5^{2.3}$ and therefore time compression is commonly expressed as multiple (for example, "x5") and the *k=2* value is commonly used in packaging. For *k=2* the test equation is usually expressed as:

$$a_t = a_j\left(\frac{tj}{tt}\right)^{0.5} \qquad (2.10)$$

Shires finally concluded that use of Basquin model above may not always be accurate in testing packaging materials because:

1. Many failure modes seen in packaging product distribution are not as a result of fatigue.

2. Transmission of vibration through an assembly of packages may not be linear with input amplitude (especially near structural resonances).

3. While Basquin model is widely used in metals, many packaging materials are non- metallic.

4. Some failure mechanisms (such as surface scuffing or closure back off) may have an endurance limit, that means there will be a magnitude of stress cycle below which failure will not occur regardless of the number of stress cycles experienced.

Furthermore, packaging test and performance standards (as also noted by Shires, 2011) differ in their approach to time compression procedures.

ASTM D4169 vibration schedules and International Safe Transit Association (ISTA) general simulation procedures 3A and 3F appear (from duration and intensity data) to use time compression though there is no mention of this.

ASTM D4728 indicates that test levels are often increased over the actual field data to shorten test period. Uses of such 'equivalence' techniques tend to assume linearity of specimen response to the test input which is unlikely for most packaging systems.

ISTA procedures 3E and 3H on the other hand give a relationship between test time and journey distance instead of intensity as follows:

$$t_t = \frac{dj}{8} \quad (2.11)$$

where:

$t_t =$ test time in minutes

$d_j =$ journey distance in kilometres.

The European Union funded project (SRETS) uses time compression but with value of k=5 in Basquin equation.

From the above reports, there appears at the moment to be no uniform or reliable methodology for carrying out an accelerated packaging transport vibration to allow designers to test their current and future packaging for a specified distribution environment. The actual journey measurement appears at the moment a more common and reliable method for laboratory simulation especially for short duration journeys as this method gives designers a far more accurate indication of how the field journey may affect the packaged goods and the package. There is therefore a gap in knowledge in this area and needs further research. The full journey test method was therefore adopted in this research.

2.12.0 General granular matter characteristics and behaviour

2.12.1 Granular media general characteristics

Granular materials are an assembly of discrete solid particles dispersed in an interstitial fluid and interact with each other in normal and tangential directions through energy dissipating contact forces (Tai et. al., 2010; Majid et. al., 2009). “Substances known as "granular media" include anything that is made up of many distinct grains including common materials as diverse as sand, rice, tea, sugar, ball bearings, and even flour. If the particles are non-cohesive, then the forces between them are basically of repulsive nature such that the shape of the material is largely determined by gravity and external boundaries with surrounding particles. For dry materials any interstitial fluid such as air can in many cases be ignored. Granular media flows and handling have a wide application in several industries such as food industries, chemical industries, ceramics, and pharmaceuticals. In these industries, proper selection of the shape, size and distribution of powder and particulate materials is a critical element as this has a major bearing in their subsequent transportation, handling and processing. This also applies to tea especially at the blending and packing plants where small variations in particle

characteristics could lead to process holdups and delays as equipment operates within narrow density tolerances. Yet despite their apparent simplicity, granular material such as sand and powder exhibit complex behaviour when subjected to external energy during their handling, processing and transportation (Ben-Naim et. al., 1998). Many of the unusual static and dynamic properties of granular media are as result of partial stability of a large number of particle configurations (states) at steady state macroscopic densities (Jaeger et. al, 1996; Nowak et. al., 1998). It should further be noted that granular matter consist of "grains" that are generally too large to respond to any thermal motion. Their thermal energies are so small compared to their gravitational and elastic energies that principally govern their behaviour. Due to the large size of the particles, granular media tend to have so many degrees of freedom which generally enable them to have very inelastic collisions. The particles when moved around by an external shear settle rather quickly and have no time to find their configurations that offer them the lowest energy level to acquire equilibrium (Ben-Naim, et. al., 1998).

2.12.2 Granular matter behaviour versus fluids

One quite unique characteristic of granular matter is the ability to sustain shear forces better than fluids. It is therefore possible to walk over granular bed such as sandy beach without sinking. This is because the weight of the object is transmitted through a network of contacts within the granular structure to the underlying base or the walls of the container. In this case, the Archimedes buoyancy does not occur. The up-thrust experienced by a body submerged or partially submerged is not equal to the mass of the material displaced.

Another major difference of granular matter compared to fluids is the fact that there no linear increase in pressure with depth of the media. Indeed the pressure stabilizes after a short distance such that the rate of discharge of a free flowing granular matter in a hopper or silo can be said to be substantially constant. The rate of discharge M for a free flowing powder can be calculated by the following equation:

$$M = \frac{\pi}{4} \rho_b \sqrt{gB^5}\ 2\ tan\ \beta_H \qquad (2.12)$$

where:

$\rho_b =$ material bulk density

$\beta_H =$ hopper half angle

B = opening hopper diameter

g= gravitation acceleration 9.81m/s^2

2.13.0 Granular matter characterization

There are a large number of materials encountered in industry that are in powder and granular form. These include both food and non- food products. These materials often tend to have a highly irregular shape and size. There is therefore a need for accurate information about their physical properties in order to understand their handling and processing characteristics. For many granular media and powders understanding of their physical properties such as particle size, bulk density, moisture content and even particle size distribution in a sample is an important aspect in industry and not the least the food industry. Several methods have been employed to describe granular media majority of which have often irregularly shaped particles. Such descriptions and measurements are important for calculations and even trade communications. The proper selection of the shape, size and particle size distribution of particulate and powder materials is a critical element in many industries dealing in granular matter processing and handling. For instance, tea is commercially graded by size and even shape of the tea particles. The distribution of various sizes of particles in a blend will not only determine its physical properties but also the liquor organoleptic properties such as briskness, brightness and even thickness as evaluated by experienced tea tasters. Thus any subsequent damage of tea particles which may occur during transportation and handling undermines the grade integrity that is principally determined by the particle size and even shape distribution.

A lot of interest has in the recent times been generated by researchers in trying to understand the physical characteristics of bulk solids. Such information has been used to understand how granular media could behave under various conditions. Moreover, physical properties of granular solids play an important role in their resulting storage and flow behaviour. Understanding of granular media physical characteristics is therefore essential in order to design appropriate, efficient and economic handling and storage equipment and other related structures (Ganesan et al, 2008). Flow ability (ability of granular materials and powders to flow) which is an important aspect in material handling and processing will to a large extent depend on material physical properties.

2.13.1 Particle size characterization

2.13.2 Particle size analysis

There are several different types of equipment employed to measure particle size of irregular granular material (Table 2.4). The different measuring equipment all typically provide equivalent spherical diameters based either on projected area (microscope), mesh size (sieve), particle chord length (length), volume (coulter counter), Fraunhofer diffraction (area-light scattering properties).

2.13.3 Equivalent spherical diameter

One method often used in particle size characterization of an irregular granular matter is use of the concept of equivalent spherical diameter where some physical property of the particle could be related to a sphere that has the same property such as volume. One such way to quantify shape of a granular material is use of Waddell's sphericity (*β)* defined as:

$$\beta = \frac{surface\ area\ of\ sphere\ of equal\ volume\ to\ the\ particle}{surface\ area\ of\ the\ particle} \qquad (2.13)$$

Table 2.3 shows various common industrial materials shapes and their Wadell's sphericity equivalents.

Table2. 3 Wadell's sphericity equivalents for some industrial materials

Descriptor	Wadell's sphericity	Example
spherical	1.000	glass-beads, calibration latex
rounded	0.82	water worn solids, atomized drops
cubic	0.806	Sugar, calcite
angular	0.66	crushed minerals
flakey	0.54	gypsum, talc
platelet	0.22	clays, kaolin, mica, graphite

(Escubed Ltd, 2006)

2.13.4 Particle size determination using sieve analysis

This is probably the commonest method for granular particle analysis available today and at a reasonable cost. This is also the equipment used to analyse particle size distribution in this work. Today standardized sieves are available covering a range of sizes. These sieves are

generally round and designed to sit on top of each other in a stack so that materials falls through smaller and smaller meshes until it reaches a mesh which is too small for it to pass through. The stack of sieves is normally mechanically agitated or tapped to promote the passage of the particles through the pores of the various sieves. The finest particles are finally retained on the pore-less bottom pan at the bottom of the stack. The fraction between two pairs of meshes is determined by weighing the fraction collected on each sieve. There is a need to maintain a standard method in all the analysis to ensure results are comparable. The sieving results will very much depend on the period and manner of agitation.

Table2. 4 Common particle size analysis equipment and type of measurements

Name	Equivalent spherical Diameter
microscope	Projected area
Sieve	Mesh size
Lasentec™ (particle chord length FBRM)	Length
Malvern ™ (fraunhofer diffraction)	(Area- light scattering Properties
Coulter Counter™ (electric zone sensing)	Volume
Sedigraph ™ and Andreasen pipette	Sedimentation

(Escubed Ltd, 2006)

2.13.5 Granular matter density

2.13.6 Bulk density

Bulk density of powders and bulk solids is an important parameter in industry to characterize storage, flow ability and other aspects of handling during processing. It is particularly useful in determining the volume of transport vehicles and planning for storage vessels in industry. The bulk density of a powder or granular solid is the ratio of mass of untapped powder samples to its volume including that of inter-particle void volume. It can thus be argued that the bulk density of a granular material represents the situation at which the grains are constrained and have no time to find a configuration of the lowest energy level. Bulk density therefore, will depend on both the powder particles density and their spatial arrangement of the particles within the powder bed (WHO, 2012). Bulk density is usually expressed in grams per millilitre

(g/ml) but the internationally (kg/m^3). Often the measurements are done using measuring cylinders and are expressed in grams per cubic centimetre (g/cm^3). Bulk density indicates how a bulk material will compact under various applied stresses and also of its flow. Bulk density of materials having fine grains will very much depend on its consolidation strength. Thus, coarse materials such as dry sand are difficult to compress and have relatively lower bulk density while fine powder such as ground sugar will show a noticeable compression due to the fine particles filling the voids. Bulk density can thus be a reasonable assessment of how materials are likely to be by the time they are received by the customer especially due to the effect of handling such as transportation. The bulking properties of granular matter are not static and very much depend on its storage, handling and even its preparation. Particles can pack to have a range of bulk densities. Furthermore, any slight disturbance of the granular bed could end up with a different bulk density. Thus bulk density of a powder is often very difficult to measure with good reproducibility and, in reporting the results, it is essential to specify how the determination was made (WHO, 2012).

Bulk density will mainly depend on the particle size, moisture and chemical composition as well as the handling and processing operations (Ganesan et. al., 2008). Bulk density of foods and other organic matter has been known to decrease with increase in particle size as well as with an increase in equilibrium relative humidity (Yan and Barbosa-canovas, 1997; Ganesan et. al., 2008).

The other granular matter physical property related to bulk density is the porosity. It is often expressed as a percentage of voids in a bulk solid.

$$P = \left[\frac{V - Vp}{V}\right] 100 \qquad (2.14)$$

where:

P = porosity (%)

V = bulk volume of the bulk (cm^3)

Vp= particle volume of the bulk (cm^3)

The porosity P is affected by the flow of the granular materials. Thus the porosity decreases, as the bulk density of the material increases (Sjollema, 1963)

2.13.7 Tapped Density

Tapped density is an important characteristic of granular matter. It is an enhanced bulk density obtained after manually or mechanically tapping the container of the granular or powder sample. Tap density is therefore the maximum packing configuration of a powder or granular solid media (or their blends) achieved under the influence of a well-defined, externally applied forces. The minimum packed volume thus achieved will depend on several factors including particle shape, particle size distribution and particle cohesiveness due to surface forces including moisture and particle true density (Ganesan et. al., 2008). Tap density of a material can therefore be used to predict its flow properties and compressibility. In industry several methods are applied such as agitation, vibration and other consolidation methods to improve bulk solid material density in order to reduce its volume. This also reduces storage space and even transports volume. Tap density determination is quick and easy in that upon observing the initial powder volume or mass (bulk density) the graduated cylinder containing the powder is then mechanically tapped (or manually tapped) usually by raising it through to a given distance and allowing it to drop under its own weight.

$$Tapped\ density = \frac{Mass\ of\ the\ powder}{Tapped\ volume\ of\ the\ same\ powder} \qquad (2.15)$$

2.13.8 Pycnometry

A pycnometer is used to measure the skeletal (or true) density of solids (and some liquids). This is carried out by measuring changes in pressure with gas displacement. Helium gas is usually used because of its small and inert molecules that easily permeate the small voids and open pores to displace the gas (but does not permeate any closed porosity). Pycnometry therefore remains the best technique to measure granular matter true density. In Appendix 5 is represented a pycnometer used to measure granular matter's true density.

2.13.9 Compressibility (Carr's) index and Hausner ratio

Inter-particle interactions influencing the bulking characteristics of granular and powder materials also tend to affect their flow ability. Comparison of bulk and tapped densities will thus indicate the relative importance of inter-particulate interactions in a given material. Such comparisons indicate the ability of the powder to flow and are often used as an index of flow properties of a powder/granular matter. Both compressibility index (often referred as Carr's index) and Hausner ratio are measures of propensity of a powder to be compressed. Table 2.5 shows the relationship of above flow parameters and propensity of the material to flow. They

are indeed, measures for the powder's ability to settle and permit an assessment of relative importance of inter-particulate interactions (WHO, 2012; Apeji, et al, 2010). Hausner ratio is often used as an internal friction index in cohesive powders (Guo et. al., 1985; Malave e.t al., 1985; Ganesan et. al., 2008). Free flowing powders have less significant inter-particulate interactions and their bulk and tapped density values will be close. Table2.6 gives the densities and flow characteristic (Carr's index and Hausner ratio) for common household granular materials. On the other hand, in poorly flowing powders, there are usually greater inter-particulate affinities and greater differences between their bulk and tapped densities manifested which are in turn reflected in their compressibility index and Hausner ratio.

$$\textit{Compressibility index or Carr's index} = \frac{100\,(V0-Vf)}{Vo} \equiv 100*(D_f - D_0)/D_f \qquad (2.16)$$

$$\textit{Hausner Ratio} = V_0 / V_f \equiv \quad D_f/D_0 \qquad (2.17)$$

where:

V_0 is unsettled apparent volume of the material (bulk density)

V_f is final tapped volume of the material

D_0 is the unsettled density of the material

D_f is the final tapped density of the material

Table2. 5 Scale of granular material flow ability

Compressibility index (%) or Carr's index	**Material Flow character**	**Hausner Ratio**
≤ 10	Excellent	1.00-1.11
11-15	Good	1.12- 1.18
16-20	Fair	1.19- 1.25
21-25	Passable	1.26- 1.34
26-31	Poor	1.35- 1.45
32-37	Very poor	1.46- 1.59
≥ 38	Extremely poor	1.60

(Escubed Ltd, 2006)

Table2. 6 Typical density and flow ability characteristics for common household products

Material	Bulk density	Tapped density	Hausner ratio	Carr's index
Blue bath salts	1.10	1.175	1.068	6.383
Peach bath salts	0.713	0.723	1.014	1.351
Brand talc	0.585	0.843	1.440	30.556
Own brand Talc (Tesco)	0.673	0.886	1.316	24.000
washing powder	0.666	0.730	1.097	8.824

(Escubed Ltd, 2006)

2.14.0 Granular matter dilatancy

Dilatancy is a property that granular matter and powders have which is not found in liquids. This phenomenon arises due to the fact that in a granular media particles rest on each other so that for such plane to move horizontally, a shear plane of particles must rise vertically. Such vertical movement therefore unlocks the granular particle arrangement so that they are able to slide over each other. As a consequence of the planes moving apart from each other during shear, the porosity increases. The porosity at which the granular matter can shear is thus referred to as "critical porosity". Dilatancy is therefore an important characteristic in granular media flowing in chutes where expansion boxes are provided to enable powder to change direction and therefore allow the granular matter to dilate or expand to ensure continued flow.

2.15.0 Granular matter density determination

Usually the bulk density of powder/granular matter is determined using several methods:

2.15.1 Measuring the volume of known mass

Measuring the volume V_0 of a known mass M of a sample that may have been sieved into a graduated cylinder and the volume read off.

$$D = M/V_0 \qquad (2.18)$$

2.15.2 Measuring the mass of known volume

Measuring the mass M of known volume V_0 of powder/granule, which has been passed through a volumeter into a cup.

$D = M/V_{0.}$

Figure 2.9 shows a diagram of a volumeter used in determination of granular matter volume.

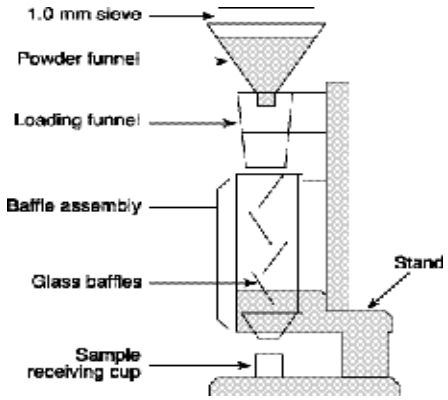

Figure 2- 9 Volumeter used for granular powder density determination

(WHO, 2012)

2.15.3 Measuring the mass of powder from a standard measuring cup

Measuring the mass *M* of powder, that has been collected from 100ml measuring standard cup. D= M/100. Figure 2.10 shows a standard measuring vessel used in density determination.

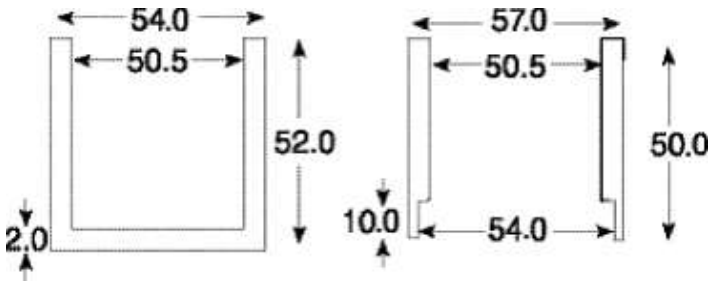

Figure 2- 10 Density determination standard measuring vessel (left) and cap (right)

-dimensions in mm and vessels round; (WHO, 2012)

2.16.0 Granular media behaviour under external agitation

Although quite extensive research has been carried out and documented for mechanical vibrations of rigid and elastic bodies, machines and structures, in comparison the area of granular solids and powders vibration has received less attention. This may be attributed largely to the extreme difficulty of accurately modelling and theoretically analysing such materials under dynamic conditions (Roberts, 1997). The complexities inherent in such parameters as shape and particle size distribution, moisture, temperature, relative humidity, consolidation and even loading conditions have meant that much of the research to-date has

relied heavily on experimental investigation. Thus most of the published results in this area can be considered rather empirical (Roberts, 1997).

Bulk solids behave differently from solids or liquids on very many occasions. Granular materials exposed to even small agitation tend to lose their macroscopic rigidity and form (Majid et. al., 2009). The main characteristic is that porosity depends strongly on mechanical forces such as compression, vibration, impact and shaking (Runge et. al., 1989; Linemann et. al., 2004). The emergence of fluctuating forces makes particle re-arrangements and flow possible even at very small stresses (Tai et. al., 2010; Jaeger et. al., 1992). The behaviour of granular media when subjected to motion due to external forces remains astonishingly a barely understood phenomenon (Farady, 1831; Walker, 1982a; Gallas et. al., 1992; Majid et. al., 2009). Examples of such encounters include the so- called "brazil nut" segregation (Williams.1976; Haff et. al., 1986; Gallas et. al., 1992; Mobius et.al, 2001), heap formation under vibration (Walker, 1982a; Baxter et. al., 1989) and density waves emission (Walker 1982b; Gallas et. al., 1992). The above behaviour may partly be explained by the ability of the granular material to form a hybrid state between a solid and a fluid (Gallas et al 1992). Granular media tend to change bulk density during agitation as a result of particle re-arrangements. When the density exceeds a certain critical level, it behaves like a solid and is resistant to shear. Below this critical density, the material is fluidized.

Attempts have been made to understand the complex rheology of granular matter as a basis of accounting for their complex behaviour. They include continuum equations of motion (Jaeger, 1992), cellular automation (WHO , 2012) and random walk theory (Roberts, 1997). Despite the above studies, it is only in rare cases that it has been possible to have a quantitative prediction that satisfies experimental data (Gallas et. al., 1992). Thus much basic understanding of the mechanisms that tend to govern behaviour of granular materials when subjected to various treatments is still rudimentary.

2.16.1 Theoretical models explaining granular solids behaviour under mechanical stress

Several researchers have put forward various mechanisms to account for behaviour of solid particulate and powder media under agitation based on experimental and theoretical data. A number of models have been proposed mainly to try and account for the experimental findings.

Such mechanisms include adsorption-desorption, convection, particle segregation, granular compaction, void space filling and even jamming.

2.16.2 Compaction of granular solids materials due to vibration and shocks.

Bulk or granular solid materials compatibility and density changes during processing, handling, transport and storage is of great importance in industries as it has a major influence on their effective and efficient performance. Indeed, such material changes in density due to compaction during processing have a major influence on machinery and equipment design. While compression by normal stress can be reproduced and mathematically described, the influence of shocks and vibrations remains very poorly understood (Linemann et. al., 2004). In addition, Linemann et. al. (2004) while quoting Runge et. al. (1989), reported that compression of a packing by uniaxial pressure can be physically reproduced, and the density curve dependent on normal stress can be described by approximately 25 different mathematical equations. Depending on the physical characteristics of a bulk material both vibration and shock could result in degradation of the material and changes in particle size distribution.

Edwards et. al. (1994) introduced a statistical mechanics of granular media behaviour under the influence of an external force or excitations such as vibrations. The group used a mixture of elongated rods and spheres (both mono and poly disperse).Edward et. al. (1994) hypothesized that the granular system would be characterized by a small number of parameters (analogous to temperature etc.) and that the granular system has properties which are reproducible given the same set of operations on it. Operations here are acting upon the whole system rather than upon individual grains. The group averaged over all the possible configurations of the grains in real space using configurationally statistical mechanics theory to describe the random packing of the grains. They further assumed that the systems may be characterized as a population of rigid grains with different distributions of shapes (configuration). The group then argued that there is an analogy that can be drawn between the energy of a thermal system and the volume *V* occupied by a granular matter. The "effective temperature" for a powder also called the compactivity index *X* is a measure of the packing of grains and can be defined as:

$$X=\frac{\delta v}{\delta s} \qquad (2.19)$$

where *v* is the volume occupied by the powder

and *s* is the entropy of the powder defined by the logarithm of the number of available configurations.

The significance of this so called effective temperature or compactivity is that it permits characterization of a static granular media system. Compactivity is therefore a measure of "fluffiness" in the powder (Nowak et. al., 1998). Thus when the powder $X = 0$ it is in the most compact state whereas when $X = \infty$ the powder is least dense.

Granular compaction therefore involves the evolution from an initial low density packing state to one of higher final density status (Nowak et. al., 1998). The phase space for a granular matter is not determined by fluctuations induced by ordinary temperature but by external noise sources such as vibration, shock, dead- weight application etc.

Molerus et. al. (1975) derived a relationship between the external compressive load and the resulting normal load. The equation for this is:

$$\left(\frac{1-e}{e}\right)\frac{N}{d^2} = \frac{V}{A} \qquad (2.20)$$

where

e= void ratio

A= area of the plane of interest (equivalent to area of the shear cell)

V= compressive force acting on the plane of interest (equivalent to the normal force acting on shear cell)

d= particle diameter

N= resulting normal load

The void ratio will depend on the degree of consolidation of the bulk material. During consolidation the particle contact tends to receive deformations which are responsible for cohesive forces in bulk materials (Roberts, 1997).

2.16.3 Adsorption- desorption model

Several researchers have explained the density fluctuations of granular media after attainment of steady state level or upon maximum density attainment on the basis of adsorption-desorption model.

Nowak et. al. (1998) monitored power spectrum of density fluctuations around a steady state for various values of tapping strength. They observed a two- step spectrum that was characterized by two frequencies that both increased with increasing tapping strength. The group accounted for the slow kinetics of compaction on the existence of a "reversible" steady state. They further went on to explain that the fluctuations on power spectrum were due to simple adsorption- desorption mechanism or "parking lot" model.

Talbot et. al. (1999) investigated both analytically and by numerical simulations the kinetics of microscopic adsorption of hard rods on a linear substrate. The team argued that when a trail particle does not overwrap with a previously adsorbed particle, it is accepted and the rate of adsorption is k_+. On the other hand, all the adsorbed particles are subject to removal (desorption) at random with a constant rate of k_-. The properties of the adsorption-desorption model were found to depend on the ratio $K= k_+/k_-$ such that for a large value of K this would correspond to a small desorption rate.

When time is expressed in units of k_+^- the densification kinetics is given by:

$$\frac{d\rho}{dt} = \varphi(t) - \frac{\rho}{K} \qquad (2.21)$$

where $\varphi(t)$ the insertion probability is the fraction of the substrate that is available for the insertion of a new particle.

$\frac{d\rho}{dt}$ is the time rate of change in granular media density

ρ is the granular media density.

k_+ is the rate of adsorption

$k-$ is the rate of desorption

$K = \frac{k+}{k-}$

Talbot et. al. (1999) thus concluded that the presences of a relaxation mechanism or competing desorption and adsorption with an equilibrium *K*, implies that the system eventually reaches a steady state.

When $k_+ = 0$, starting with any configuration of particle, one would obtain a solution for this uniform desorption (Van Tassel et al., 1997; Talbot et al., 1999). The limit $k- \rightarrow 0^+$ allows a small but non-zero possibility of rearrangement of the granular particles leading to a final density of equal to 1. Indeed as $k- \rightarrow 0^+$ the process cleanly divides into two sub processes; with the initial phase consisting of an irreversible adsorption loop followed by an infinite sequence of desorption - adsorption. During this later phase the rods detaches from the surface and the gap that is created is immediately filled up by one or two new rods (Talbot et al., 1999).When the system reaches k- = 0 a jamming limit is achieved and particle grains are "locked up". At this level, adsorption is totally irreversible and the process mirrors a Random Sequential Adsorption (RSA) (Evans, 1993). Figure 2.11 represents the adsorption–desorption mechanism. While the final density is independent of the initial configuration of the granular media on the line, the jamming limit for RSA depends strongly on the initial state of the line. Talbot et. al. (1999) finally concluded that for a small, but finite desorption rate, the system reaches the equilibrium state very slowly. In addition, the long term kinetics displayed three successive regimes:

1. An algebraic regime where the density varies with the reciprocal of time.
$$\rho \propto \frac{1}{t} \qquad (2.22)$$

2. A logarithmic regime where density varies inversely with the logarithm of time.
$$\rho \propto \frac{1}{ln(t)} \qquad (2.23)$$

3. An exponential terminal decay.

where $\rho = density$

t = time

Talbot and his group while were able to fully explain the actual granular material behaviour mechanisms involved in the first two steps of their granular model, they however, failed to predict the relaxation rate associated with the last step of the exponential terminal decay. This is a knowledge gap that needs further research. During its transportation, tea is subjected to compressive forces in the pallet load as well as due to vibration/shock. Such "granular temperature" will lead to the consolidation of tea particles with time and therefore growth in

density and it will be of interest to find out whether or not upon attainment of its maximum density there is any further change in density and if there is any resemblance with Nowak's adsorption- desorption behaviour model. This would allow tea handling equipment designers at the receiving end to anticipate this fact in their designs.

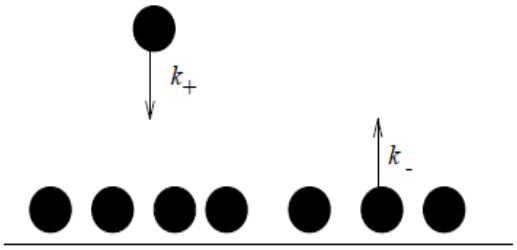

Figure 2- 11 Adsorption-desorption process

(Ben-Naim, 1999)

2.16.4 Convection model

Granular convection phenomenon takes place where granular material is subjected to shaking or vibrations forcing them to exhibit circulation patterns similar to fluid convection. The phenomenon is sometimes referred to as the "Brazil nut effect" when the largest particles of a granular mixture of various sized end up at the surface of the container (Rosato et. al., 1987; Majid et. al., 2009) The name is derived from the general observation that in a typical container of mixed nuts, the larger Brazil nuts end up at the top after vibration. A similar effect is observed in a packet containing muesli breakfast cereals of different sizes but similar density. A granular convection phenomenon is likely to occur in tea when transit hazards result in particle degradation with differing particle size distribution regime as well as density. Under truck shipment conditions involving vibration and shock inputs, granular convection currents involving tea particles would take place. This ultimately affects even distribution of tea particles as "powdery" tea particles migrate to the bottom of the package.

Just as in liquids and gases where convection currents exist due to thermal energy gradients, granular materials convections take place often resulting in segregation or de-mixing of granular particles (Gallas et. al, 1992; Enrichs et. al, 1995; Grossman, 1997; Hsiau et. al, 2002; Lu et. al., 2008; Majid et. al., 2009). This convection movement, unlike that in solids and liquids is due to a "granular temperature" gradient such as that is due to agitation or tapping of the container as happens in shakers and other mixers. The smaller granular particles tend to move upward in the vibrated container centre and travel downwards in a boundary along the walls of the container. The larger particles on their part move upward with the convective

smaller particles flowing towards the free surface close to the walls (Knight et.al., 1993; Tai et. al., 2010).

Figure 2-12 gives a diagrammatic representation of the particle convection mechanism.

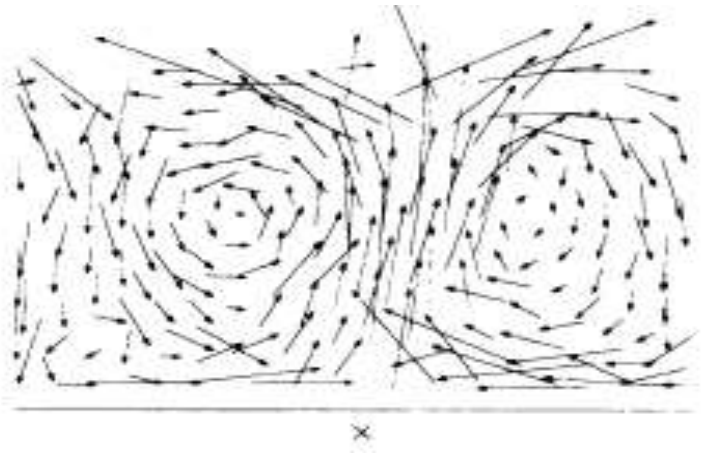

Figure 2- 12 Granular convection cells representation

(Gallas et al., 1992**)**

Knight, et. al. (1997) postulated that the convection phenomenon was due to the effect of granular material undergoing a transition from a dense (solid-like) state to a dilute (liquid like state). During the particle bed expansion process larger "voids" are created during this re-organization period allowing smaller particles to fall through to the bottom (Tai et. al., 2010; Hsiau et. al., 1997). Tai et. al. (2010) further explained that this re-organization mechanism quickly disappears at low vibration accelerations since there are not enough relative movements for larger enough voids to be formed. When vibration accelerations are too high, the void are too large to allow even the larger particles to fall through resulting in no segregation conditions within the granular bed.

2.16.5 Particle segregation model

Segregation is a process in which a homogeneous bulk solid composed of various constituents or species becomes spatially non-uniform due to relative movement within the material (Lance et al., 1996; Rosato and Blackmore, 2000; Rosato et. al., 2002).

Solid mixing is an important aspect in the processing operations in many industries including the pharmaceutical, ceramic, and food and chemical industries. This often involves formulations where active ingredients may be present in very small amounts and whose

uniform presence in the entire batch is critical. Segregation therefore needs to be avoided after mixing as this would result in uneven distribution of critical ingredients within the batch. For instance, in pharmaceutical formulations higher limits could be toxic while lower limits could result in under dose. In food formulations, critical fortification ingredients such as vitamins and essential minerals have to be within recommended nutritional limits since excessive use could lead to complications in their metabolism and possible ill-health. Furthermore, many of the food additives are normally costly and use of the correct amounts in the formulations is a major commercial concern (Bates, 1997; Rosato et. al., 2002). Occurrence of segregation in industrial sector during processing, handling and even transportation of bulk solids is therefore of universal concern. In the tea industry, segregation is undesirable especially for flavoured tea production where small flavouring ingredients are added in small amounts into the batches and their even distribution in the entire tea is an important quality aspect. On the other side, segregation is desirable in tea grading at the processing factory to enable separation of tea into the various grades based on their size and morphology.

Many effects cause the segregation of granular materials and these include, differences in the particle sizes, the particle density, the shear of granular flow, the angle-of-repose of the materials and the granular temperature gradient (Rippie, 1967; Williams, 1976; Savage, 1987; Tai et. al., 2010). When a mixture of granular matter in a container receives a vertical vibration the larger granules rise up and settle on top of the small granules (Williams, 1976; Rosato et. al., 1987; Mobius et. al., 2001; Fang et. al., 2007). While mixing of free flowing mono-size solid ingredients is relatively easy, mixing of non-uniform ingredients results in segregation due to physical differences such as size, density, humidity and even rotational inertia differences etc. (Williams, 1963; Anjani, et. al, 2010). Segregations occur when a system containing particles is subjected to motion such as vibrations that can cause particles to preferentially accumulate into one area over another' (Rippie, 1964; Holdich, 2002). An example of segregation is the presence of large particles at the top of a breakfast cereal or loose tea pack while the fines are confined to the bottom. Failure to achieve a uniform mix of solid bulk media throughout its processing history often affects the final quality of the product (Goodwill, 1986). Segregation can therefore be mitigated, if not eliminated, by clearly understanding the factors contributing towards segregation in a particular system (Johanson, 1978; Anjani et al, 2010). Segregation has however, some useful application in several industries including the food industries. For instance it has been widely used in the sorting and

grading of teas where separation of particles by density and particle size is at the core of various tea grades and blends. So in this particular case segregation is a positive attribute.

Williams (1963) carried out one of the first qualitative experiments on vibration segregation using a large sphere in the sand bed that was vertically vibrated. He observed an upward trajectory movement of the sphere that he attributed to the "locking" effect of the overburden pressure that it exerts on the column of materials directly beneath it (force chains are transmitted to the bed floor) thereby preventing it from moving down. As the large particles so experience an upward thrust during the vibration, the smaller particles tend to move beneath it and become locked. In his subsequent work, Williams (1976) reported that segregation is mainly promoted by particle size, density, shape and even elasticity. He further reported three main types of segregation that included percolation of fines, trajectory segregation and the rise of larger materials due to vibration. Later other mechanisms were identified including that of convection segregation (Knight et. al., 1993; Tai et. al., 2010). Knight et. al., (1993) specifically investigated flow paths of larger granular particles inside a vibrating granular bed of many small particles. They noted that the smaller particles moved upward in the container centre and then moved downward in a boundary layer along the side walls of the container. The larger particles on the other hand moved upward with convective small particles flowing towards the free surface close to the container walls. This is similar to the convection granular flow due to "granular temperature" noted earlier in 2.16.1.4 (Gallas, et.al., 1992). It should be noted that while the smaller grains move up at the middle and later go down along the container walls, the larger particles (such as brazil nuts) remain at the top because the spaces created at the container sides due to the migration of particles to the middle of container, are not large enough to accommodate the large grains. It can be postulated that tea particles of varying grades and therefore sizes if they undergo some vibration especially during transportation are likely to experience "brazil nut effect" leading to migration of powdery teas to the bottom of the container while the larger tea particles migrate to the top. This is part of the investigation in this research.

Figure 2- 13 Brazil nut effect where larger nuts migrate to the top on vibration/agitation

(Rosato,et. al.,1987)

Figure 2-13 shows a classical example of the segregation commonly referred to as "Brazilian nut effect".

Yang et. al., 2006 investigated segregation on mixing binary mixtures of steel and glass beads of the same size but different density with particles subjected to a vertical oscillatory excitation. Observation of time evolution patterns reviewed that heavy particles first moved towards the container bed centre before concentrating near the centres of the two convection cells of the vibrated bed. In total, thirteen segregation mechanisms have been reported and out of those segregation types, percolation segregation is the most dominant during granular media mixing, conveying and storage.

Rosato et. al. (2002) in his research on segregation concluded that a crucial aspect of the phenomenon of segregation is that often it is governed by a combination of mechanisms, which themselves depend on the nature of flow, particle properties, and environmental conditions. The group further pointed out that the particle features that influence segregation behaviour include: particle sizes and distribution, shape, morphology, contact friction, elasticity, brittleness, density, chemical affinities, ability to absorb moisture and magnetic properties.

Segregation of bulk tea in transit especially after particle damage is undesirable since this interferes with the blending formula at the receiving factory where homogeneity in each consignment is important. Since as pointed out by Rosato and his team that particle size and its distribution, shape, and density are among features that influence segregation behaviour in

granular matter, investigation into these aspects in tea as proposed in this research will improve on current knowledge of tea granular behaviour.

2.16.6 Void space filling model (Percolation)

Predicting microscopic dynamics or behaviour in granular matter is generally more difficult than in gases. This difficulty has been partly attributed to the lack of appreciable thermal impetus on the part of granular matter. Such negligible thermal effects means the system is far from thermal equilibrium. At room temperature granules are rather static and, without external excitation, cannot explore any "void" space unlike gas molecules. Thus a column of loosely packed granules (having large gaps or voids between neighbouring granules) will not spontaneously fill the voids available to form a compact column due to absence of thermal motion common in gases. This is despite the fact that a compact state has a lower centre of gravity and hence lower potential energy and better stability. Gently tapping of the vessel containing the column, however, gives the granular media a small amount of kinetic energy with which to rearrange and achieve a next lower energy level. Percolation in a granular mixture requires dynamic conditions such as those induced by shear forces or vibration (Vallance et. al., 2000; Anjani et. al., 2010). Vallance et. al. (2000) further reported that size and density are the two most important parameters influencing segregation of fertilizers and other granular materials via percolation leading to small granules and powder at the bottom of the bags. Percolation is thus a type of segregation mechanism that occurs in granular materials during conveying, storage, and mixing. Percolation segregation depends on several factors including particle shape, density, intensity of movement, particle size and relative humidity (Jha et. al., 2011).

2.16.7 Jamming mechanism in granular media

Granular matter is composed of many distinct solid particles that interact only via their contact forces. In such a granular pile, the strain resulting from grains weight combines with their randomness within the granular mass to hinder any motion of individual grains. This 'frustration' in grain mobility leads to what is referred to as jammed state. It is this frustration state that makes the dynamics of granular matter surprisingly quite different from that of fluids.

Cates et. al. (1998) hypothesized that in granular media a network of force chains (or "granular skeletons") evolves until it can just support the applied load, at which point it comes to rest. They further argued that such chains then remain intact so long as no incompatible load is

applied on it (Figure 2-14). Majmudar et. al. (2005) further found out that in response to applied stress, dry granular matter and other athermal systems tend to form a chain network in which large forces are distributed none homogeneously into linear chain like structures. Jaeger et al. (1996) used carbon paper studies to quantify force chains.

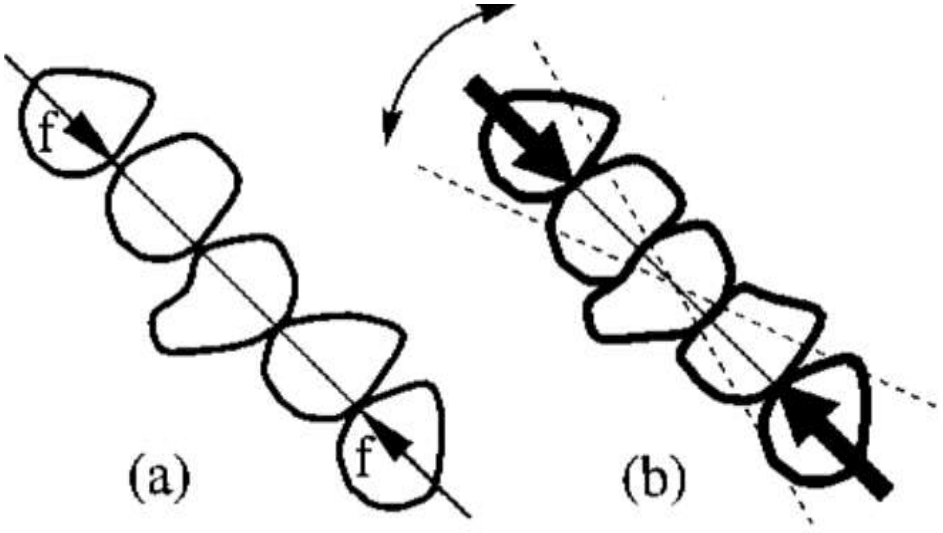

Figure 2- 14 Force chains mechanism that account for jamming in granular media

(Cates et. al., 1998)

Jamming granular matter represents a transition from a flowing state to a solid like state in disorder. It is usually manifested by dynamic seizure, an infinite increase in viscosity and emergence of mechanical stability with a finite resistance to external loading (Goncu, 2012). Jamming is not limited to granular matter and is known to occur in thermal as well as athermal systems, foams and even colloids. This similarity in behaviour between otherwise quite different systems as above led to Liu and Nagel (1998) to propose a phase diagram to explain general behaviour of granular matter.

Figure 2-15 shows a phase diagram that can be used to explain granular matter behaviour due to various external forces. The phase diagram is represented by three control variables, of temperature T, inverse of volume fraction 1/v and shear stress ϭ that represent its axes, and the surface separating jammed phase and unjammed phase. Due to lack of thermal impetus in granular as well as other athermal systems the temperature axis here is inapplicable and therefore the transition in a granular matter is rather solely determined by its density and applied stress.

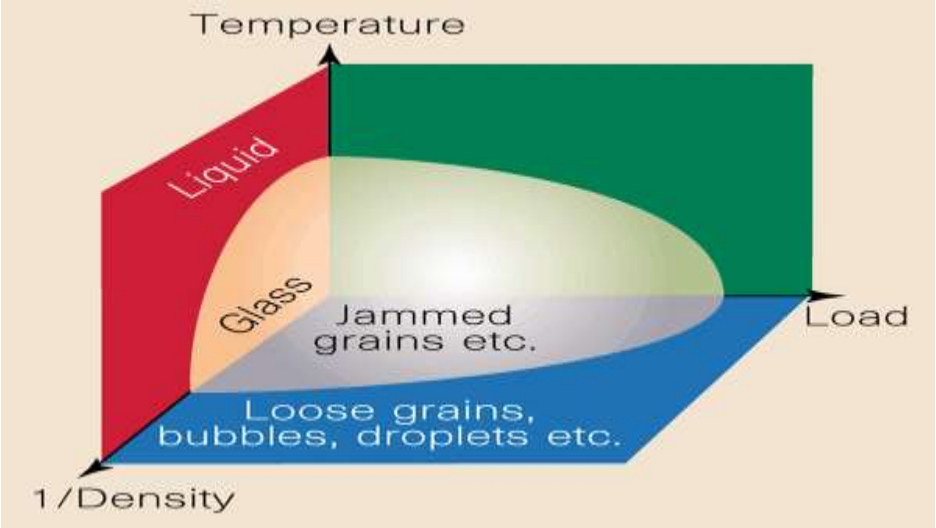

Figure 2- 15 Granular phase diagram

(Liu et.el., 1998)

2.17.0 Past research on effect of vibration on density of granular media

Several researchers have in the past carried out work to understand the effect of vibration input on the overall density of non-cohesive granular media.

Yang (2006) investigated the density effect of mixing and segregation process in a vibrated binary granular media. The mixture consisted of steel and glass beads with identical sizes but different densities. The particles were subjected to a vertically oscillatory excitation using an electrodynamics shaker. The simulation model used in mixing during his work was Discrete Element Method (DEM) as proposed by (Cundull and Strack, 1979). Yang (2006) observed that the time evolution of pattern formations that the heavy particles first move towards the centre of the bed and then concentrate near the centre of the two convection cells.

Yang concluded that the governing equations of the motions for the particle i are as follows:

$$m_i \frac{dvi}{dt} = Fgi + \sum F_{cij} + F_{lij} \qquad (2.24)$$

and

$$I_i \frac{d\omega i}{dt} = \sum R_{ij} \times F_{cij} \qquad (2.25)$$

where: $_i$ is the particle in motion.

m_i is the particle mass.

I_i is the particle moment of inertia.

v_i is the particle translation velocity.

ω_i is the particle rotational velocity.

F_{gi} gravitational body force of particle.

F_{cij} is the contact force of particle i due to particle j.

F_{lij} is the liquid bridge force between particles i and j.

R_i vector directed from the centre of the particle i to the contact point between particles *i and j.*

Although the bead size used by Young and his team were much larger than black C.T.C tea particles, the general principles of granular mechanics will also apply to the smaller tea particles as in larger beads. The only differences would be their respective required "granular temperatures".

Yang et. al. (2006) simulation experiment results concluded that the granular temperatures of heavy particles are higher than those of light particles. This implies that the granular temperatures do not equilibrate for the mixture. The team further found out that the segregation intensity indicates the mixing rate increased with vibration strength, but decreased with initial heights of the mixture.

This explains why mixing tea of different grades and therefore varying densities could lead to an undesirable segregation situation arising from vibrations in truck load transport.

Nowak et. al. (1998) carried out systematic density measurements for granular media under vibration using mono-disperse spherical beads confined to a cylindrical container. A series of external excitations consisting of discrete vertical shakes or taps each consisting of one complete cycle of a 30 Hz sine wave were applied to the container. The team observed that under vibrations, the density of the pile slowly reached a final steady-state about which the density fluctuates. The spectrum of density fluctuations around the steady state value provides a probe of the internal relaxation dynamics of the system. They noted that the process of compaction due to taps was quite slow and as the density approached its final steady state value approximately logarithmically in the number of taps applied (Figure 2-16).

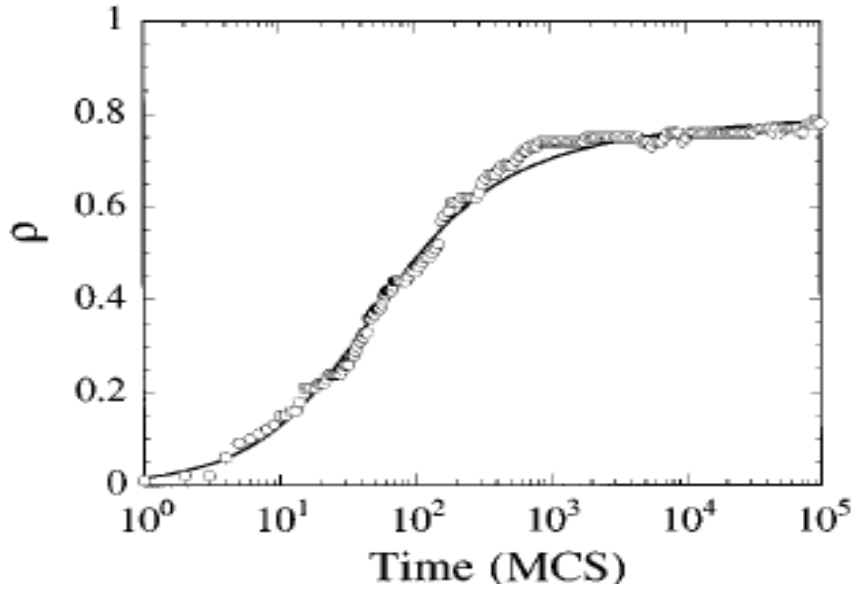

Figure 2- 16 Granular matter density evolution with agitation period

(Nowak, et. al., 1998)

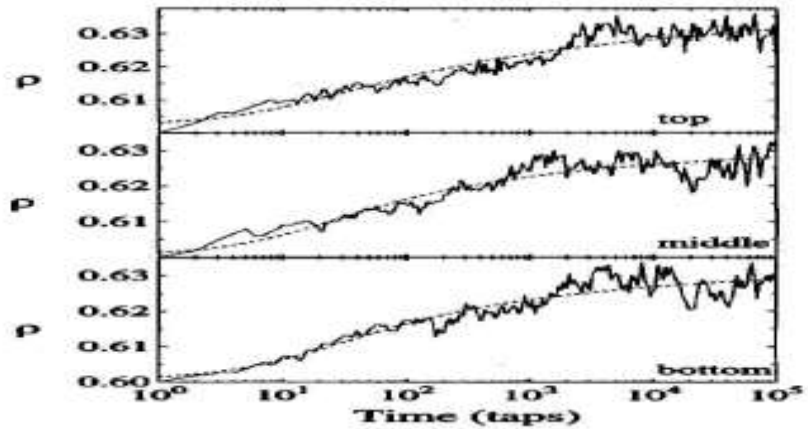

Figure 2- 17 Effect of tapping/ vibration time on the granular matter density at various depths (Nowak, et. el. 1998**)**

This scenario was noted to hold even at varying depths within the granular matter container (Figure 2-17).

The research further revealed that once the steady state density value is attained any further taps would cause only slight changes in density either higher or lower than it was before (Figure 2-18).

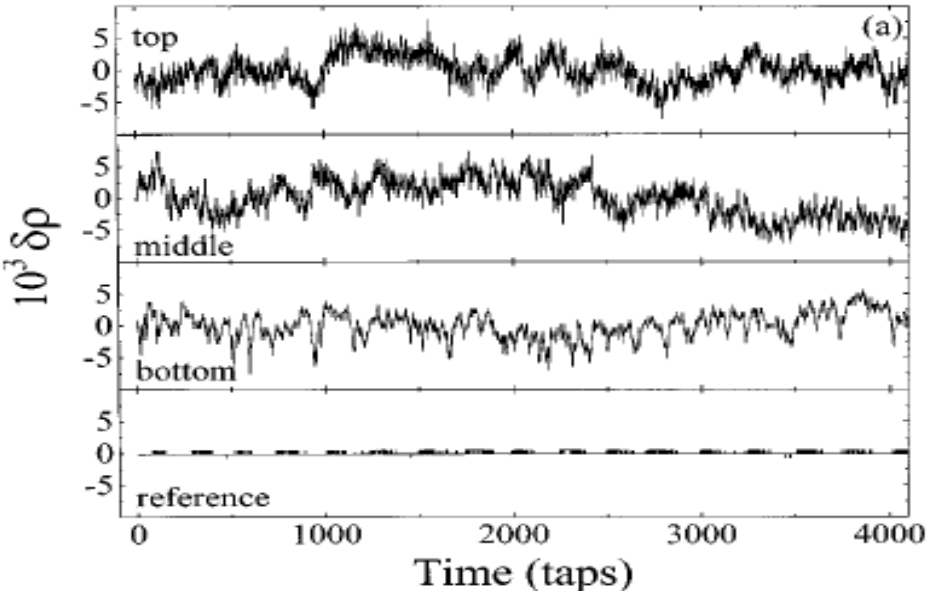

Figure 2- 18 Small fluctuations of density around steady state with increased excitation

(Nowak et. al. 1998)

The team concluded that the spectrum of density fluctuations around the steady state value is a probe of the internal relaxation dynamics of the system. Furthermore, such fluctuations are reminiscent of thermal fluctuations about an equilibrium state. This position by Nowak and his team appears true in view of the fact that once steady state density is attained there is not much void spaces left in the system small enough to fit even the smallest granules within the agitated matter. This will apply for any granular model used in explaining the position on non-cohesive granular matter (that includes tea) where the main forces acting on the particles are mainly due to gravity and surrounding granular mass members (Evans, 1967; Edward, 1994). This position may not hold for cohesive granular matter where the other inter-particular forces come into play and influence the effect of external agitation.

In this research, the density growth of tea during road conditions simulations will be observed in order to reveal the exact behaviour of tea particles density with agitation time and how one could predict the density of tea based on its vibration spectrum and period of vibration. At the commercial level where bulk tea is normally vibrated to achieve a target density needed to fill

the paper sack, the vibration period required to achieve the target density can be set for each packing unit without the need to periodically evaluate the density.

In a granular system, fluctuations of density from the steady state represent the various dilations that result in different volume configurations accessible to the particles subject to the external excitation. There is therefore an analogy between the role the vibrations play in athermal system such as granular media and the role played by temperature in thermal systems.

Nowak and team also investigated the frequency dependence and amplitude of the fluctuations as a function of vibration intensity *T*.

$$T = A/g \qquad (2.26)$$

where:

A= peak acceleration during a single tap.

g= gravitational acceleration =9.8m/s^2

2.18.0 Flow properties of granular media.

With ever increasing quantity and variety of granular materials produced and handled in industries today, there is a need for information about their handling and processing characteristics (Guo, 1985; Schubert, 1975; Teunou et. al., 1999). Granular materials often exhibit different physical properties that dictate their flow properties and other behaviour during processing. Measurement of various physical properties for any granular matter is important because such information can help in predicting the behaviour of the material during storage, processing and handling.

One such important physical characteristic is the granular matter flow behaviour under varying conditions of pressure, humidity and temperature (Tennou, et. al., 1999). While a lot is known about how to characterize and specify fluid system, knowledge of how to handle and store granular matter is limited. This is despite the considerable attention directed to this in recent times. The problem of granular matter flow in silos, chutes, hoppers and conveyors is not limited only to lack of desired flow. There are many instances of process difficulties arising from sudden surge or easy flow of materials leading to overflow of process vessels often

referred to as “powder flooding”. The optimal process conditions normally desired is to have a controlled and predictable flow of material into the process equipment.

2.18.0 Flow properties of granular media

2.18.1 Granular matter flow measurements

Flow properties of tea are an important aspect during the handling and packaging activities at the blending plants. Both the handling and packaging activities are normally carried out using equipment which often is designed to handle tea of particular consistency within narrow density range. Large fluctuations in tea density could affect smooth conveyance of tea within the plant as well as interfering with set filling limits of the packaging line.

2.18.2 Indirect flow measurements

Tea is a dry granular material. At the tea packaging factories, tea needs to be conveyed through the various processing lines from the receiving and storage hoppers, blending equipment and even the package filling lines. As these processes normally take place at high speeds, tea needs to flow easily to avoid any holds up that would disrupt smooth operations. The flow characteristic of tea that depend on such factors as particle shape or morphology, surface interactions and even its moisture content are very important as these also determine the design of the equipment used.

2.18.3 The angle of repose

Angle of repose has been used in many industries to characterize the flow of granular solids particularly when designing handling and processing equipment to be used. The angle of repose is the constant three dimensional angle (relative to the horizontal base) assumed by a cone like pile of material dropped from some designated elevation (Ganesan et. al., 2008). It is the angle that a hopper needs to exceed in order to assure powder flow. Typically, the lower the measured angles of repose of dry material, the better is the flow ability and vice versa (Carr, 1965a; Ganesan et. al., 2008). For many free flowing powders the angle of 30^0-40^0 is normally acceptable barring any tendency of the particle to form cohesive structure based on their past history. On the other hand higher angles (50^0-60^0) indicate material with difficult flow (Ganesan et. al, 2008).

Table 2-7 gives flow characteristic corresponding to various angles of repose.

Table2. 7 Ranges of angle of repose and their type of flow

Angle of repose in degrees	**Type of flow**
< 25	Excellent
25- 30	Good
30-40	Passable
> 40	Very poor

(Aulton, 2000)

The angle of repose is therefore related to the inter-particulate friction or resistance to movement between various particles in contact. The more irregular the surfaces of the particles are the higher the inter-particle resistance to movement and the angle of repose. Thus the tangent of the angle of repose is equal to the coefficient of friction between the granular matter particles.

$$Tan\ \theta = \mu \qquad (2.27)$$

where:

θ = angle of repose

μ = coefficient of friction

Flow characteristics of tea are an important commercial consideration as this will inform the design of the tea handling and storage machinery and equipment both at the primary processing factory as well as at the blending and packaging unit.

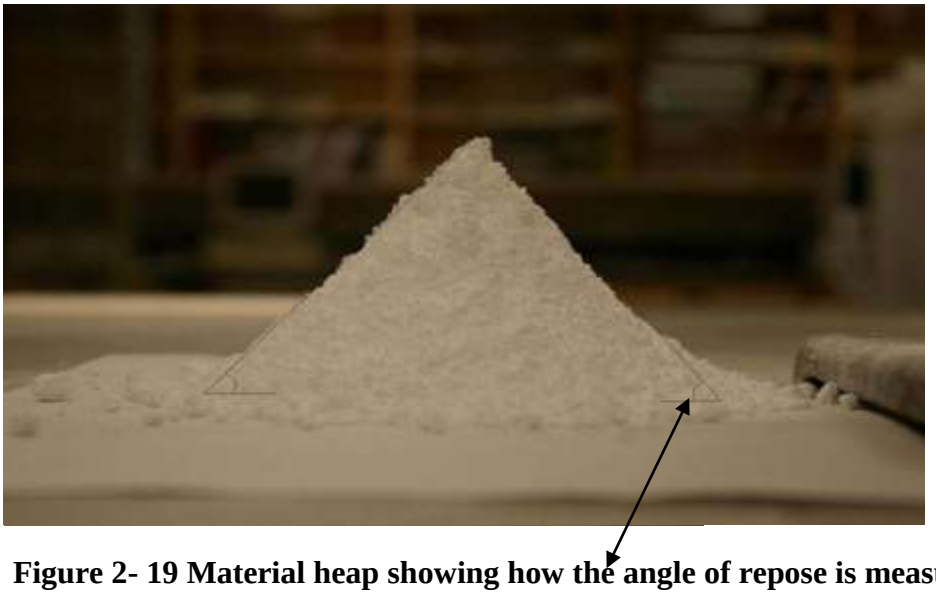

Figure 2- 19 Material heap showing how the angle of repose is measured

(Bodhmage, 2006)

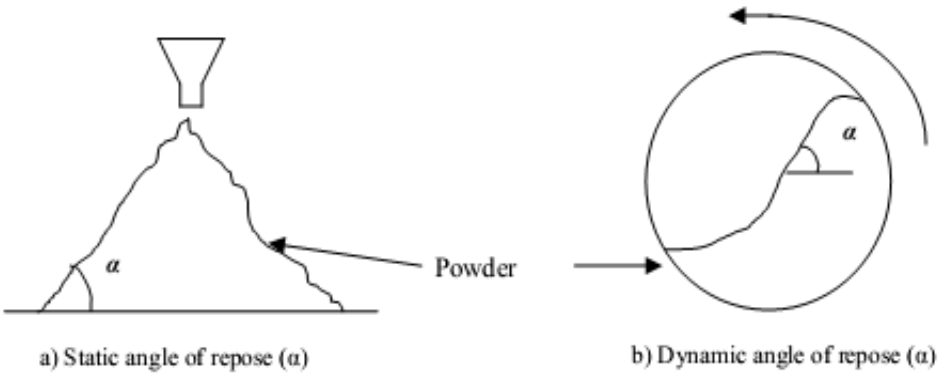

Figure 2- 20 Sample image used to determine the static and dynamic angle of repose

(Bodhmage, 2006)

A simple way to determine experimentally the angle of repose of a granular media is to pour the material into an upside down funnel and then carefully removing the funnel to leave the heap (Figure 2-19 and Figure 2-20). The height and diameter of the resulting cone are measured. Using the following equation the angle of repose ϱ can be calculated as follows:

$$Tan\ \ddot{\eta} = 2\ H/\ D \qquad (2.28)$$

where

H is the height of granular cone

D is the diameter of the granular cone.

Despite the fact that it has been reported that the angle of repose measurements tend to differ depending on the method used, usage of such measurements are nevertheless quite common in many industries. This is because such measurements have been found very helpful in predicting the behaviour of granular matter during its processing, handling and storage. Angle of repose cannot, however, be considered to be an intrinsic property of a granular matter as it is very much dependent on the method used in forming the granular cone and this could account for the bulk of measurement differences earlier reported. Craik and Miller (1958) and Ganesan et. al. (2008) both reported that within a specified method, the angle of repose measurements give reproducible results thus explaining the reasons why it is a popular method in assessment of flow properties of dry solid granular media in many industries. The particle size distribution has a complex effect on angle of repose. A graph of the angle of repose plotted against the percentage of fines present usually shows a minimum.

2.18.4 Direct flow measurements

The simplest method to measure granular solid matter or powder flow ability is to measure its flow rate from a hopper or flow tube. A shutter is placed over the hopper or flow tube outlet and the vessel is filled with granular matter. The shutter is removed to allow material discharge under gravity. The time taken for the material to discharge completely is noted. The flow rate is then calculated by dividing the mass of the discharged material by the time taken to discharge it.

2.19.0 Factors affecting flow properties of solid granular media

Many factors including combination of material physical properties, environmental conditions and even equipment used in their handling affect granular matter flow properties. Dry food products such as tea, break-fast cereals and even coffee powders often have flow characteristics affected by such factors as moisture content, particle size, humidity, and pressure.

2.19.1 Effect of moisture content

Moisture content of most dry food products will not only affect its keeping quality (moisture strongly influences microbial growth) but will also affect the flow properties and even physical properties such as bulk density. Most organic matter and dry food products are hygroscopic in nature and they will lose or gain moisture depending on the surrounding humidity. Generally, moisture sorption leads to increased cohesiveness in a material due to formation of inter-particle liquid bridges (Teunou et al., 1999); Ganesan et al, 2008). Moisture content of a granular media tends to affect its cohesiveness (Walker, 1982a) and both caking and arching abilities (Johanson, 1978). As the moisture content of granular media increases so are the adhesive forces (Craik and Miller, 1958) as well as cohesive ones (Moreyra and Peleg, 1981; Teunou et. al., 1999).

Teunou et. al. (1999) investigated the flow properties of four food powders (flour, skim- milk whey- permeate and tea) due to water sorption. Water content (wet basis) was determined by weighing a quantity of sample before and after drying in an oven at 105 ^{0}C for 3days. Water sorption isotherms were measured by placing a known weight of oven dry samples in jars with different relative humidifies controlled by saturated salts at a given temperature. The weight of each sample was recorded until an equilibrium was attained (that is two successive weighing of a sample yielded a difference of less than 0.002g). The equilibrium moisture contents for each relative humidity at 20 ^{0}C were measured and recorded. The water sorption isotherm is a quantitative evaluation of the effect of relative humidity on the water content of powder. This is important because of the effect of water content of powder on its flow ability. The group noted that the uptake of moisture by all the powders affected reduced their flow characteristics. The tea powder was the most hygroscopic and took most water with increasing relative humidity. Upon scrutiny of flow indices of the four powders they concluded that the flow ability was a function of moisture and particle size of the materials under the low consolidation stresses of less than 100 kPa that were used.

Ganesan et. al. (2008) conducted an experiment to characterize flow properties of Distillers Dried Grains with Solubles (DDGS) and found out that their flow ability significantly reduced with increase in moisture content as measured by the material angle of repose.

(Jenike et.al. (1969) and Walker et. al. (1967) reported that flow ability of powder decreases with increase of moisture content up to a critical water content above which it increase. They

further concluded that the rate of decrease of flow ability as well as the critical water content depends on particular powder behaviour in presence of water. The flow properties of moist insoluble bulk solid materials depend mainly on particle size distribution as well as moisture content (Tomas 2001). The influence of moisture granular is obvious considering the strong adhesive bridges formed by water molecules and the dry matter particles.

2.19.2 Particle size

Both Particle sizes and particle size distribution are some of the most important physical properties of solid granular matter that affect its flow and other properties. Even a small change in particle size can lead to a significant alteration of flow ability of a solid granular matter. It is generally considered that powders with particle sizes larger than 200 microns are freely flowing while fine powders are subject to cohesion and their flow ability is more difficult (Teunou et al, 1999). Furthermore, reduction in particle size often tends to decrease the flow ability of a given solid granular matter due to the increased surface area per unit mass (Fitzpatrick et. al., 2004 a,b; Ganesan et. al., 2008).

Farey and Valentin (1967/68) investigated the effect of particle size distribution on bulk powder properties and concluded that particle size was a significant factor affecting the structure of a powder compact. Particle size and its distribution affect granular matter compressibility. Thus an increase in particle size generally leads to a reduction in volume and therefore material compressibility (Yan and Barbosa- Canovas, 1997). Bodhmage et. al. (2006) while investigating effect of particle size on granular matter flow concluded that "Particle size was found to be the most reliable indicator of powder flow ability, with decreasing particle size corresponding to lower flow ability; however, other parameters such as particle elongation and irregular shape were also found to have an influence on powder flow ability". Indeed, while agreeing with the above researchers on the influence of particle size on the flow ability of granular matter, the author believes it is the particle shape and surface configurations that tend to influence more the particle flow especially those with elongated shape and rugged surface thus increasing coefficient of friction.

2.19.3 Pressure

Compacting pressure is an important factor that affects flow properties of solid granular media. Such compaction on the bulk material may be due to vibration during transportation or processing operations in the factory. It may arise from impacts from falling stream of particles (such as filling of hoppers, silos) or could be due to load stacking pressure at the warehouse or even on pallets during transportation on a carrier. The effect of pressure is that it leads to a larger number of contact points between particles, thus causing more inter-particle adhesion (Irani et al., 1959). It also leads to a significant increase in critical dimensions that encourage arching (Ganesan et al. 2008). Pressure may further break down particles, more so if they are dry and brittle such as breakfast cereals and other foods thus changing particle size distribution and hence its flow parameters as well.

2.19.4 Humidity

Relative humidity of the air and interstitial spaces is related to the moisture content of the granular matter. Exposure to high relative humidity of certain granular materials including pharmaceuticals, chemicals and even dry foods could lead to several problems (Teunou et. al., 1999). This is because many dry granular and powder products tend to be hygroscopic and readily absorb moisture from humid environments increasing their moisture content. This could lead to an increase in angle of repose (Ganesan et. al., 2008) as well as increase in bulk strength of the material (Marinelli and Carson, 1992). As the angle of repose increases flow ability of material is reduced. Several researches have demonstrated that higher humidifies affect the flow properties and cohesiveness of granular material (Johanson, 1978; Stanford and Corte, 2002; Fitzpatrick et. al., 2004b; Ganesan et. al., 2008). Table 2.8 shows the various granular matter properties and how they affect their flow ability.

Table2. 8 Some granular properties and how they affect flow

Property	**Free flowing**	**Difficult flowing**
Size	> 400microns	< 100 microns
Range	Narrow	Wide
Shape	Spheres	**N**eedles
Moisture	Not too low	High and none
Internal friction	Low	High

(Holdich, 2002)

2.20.0 Particle shape (morphology) descriptors

A variety of methods have been used to quantify granule/powder shape. Bodhmage (2006) quoting Ulusoy et. al.(2003) concluded that there is no universally accepted shape factor. "Each factor will be sensitive to a specific attribute of shape depending on the parameters selected for its calculation".

2.20.1 The aspect ratio (φAR)

This is one of the earliest known and common shape factors. It is the ratio of the length of the minor axis to the length of the major axis (Figure 2-21).

$$\alpha AR = b/l \qquad (2.29)$$

where:

αAR is aspect ratio

b = the length of minor axis

l = the length of major axis.

From (2.29) small values of the aspect ratio represent elongated particles. Unfortunately, the aspect ratio is limited since it only reflects the elongation of the particle.

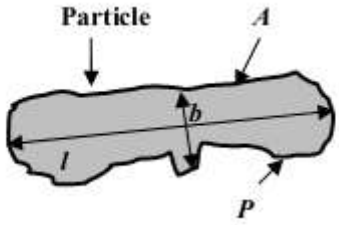

Figure 2- 21 Dimensions to calculate flow characteristic of an irregular particle

(Bodhmage 2006)

2.20.2 Roundness or circularity

Hill and Cox, (2002) as also reported by Li et. al., (2002) and Bodhmage, (2006) proposed circularity ($W_{circularity}$) or roundness R based on the projected area A of the particle and the overall perimeter of the projection P as follows:

$$R = 4\pi A/P^2 \qquad (2.30)$$

where:

R is the particle roundness

A is the particle projected area

P is the overall perimeter of the projection

For a perfectly spherical particle both the values of aspect ratio and roundness approach unity but approach zero for an extremely elongated particle.

2.20.3 Irregularity factor (I)

Another important particle shape descriptor is the irregularity factor which is the ratio of the projected perimeter of the particle to that of the major axis.

$$I = P/L \tag{2.31}$$

where:

I is the irregularity factor

P is the projected perimeter of the particle

L is the particle length of the major axis.

Both Podczeck, (1997) and Bodhmage, (2006) pointed out that elongation will cause the value of this ratio to decrease whereas irregularities tend to increase it.

2.20.4 Equivalent circle diameter

Liu et. al. (2002) proposed that particle size and size distribution could be obtained from image analysis by using the equivalent circle diameter (*ECD*). This is the diameter of a circle that has equal area to the area of the particle.

$$ECD = 2\sqrt{\frac{A}{\pi}} \tag{2.32}$$

where:

ECD = the equivalent circle diameter

A = projected area of the particle

2.20.5 Other shape factors

Several other shape factors have been reported in the literatures to characterize granular particles. They include:

1. Concavity *CA* based on the area *A* of the particle.

$$CA = \frac{A' - A}{A'} \tag{2.33}$$

2. Concavity (CP) based on the perimeter P

$$CP = \frac{P - P'}{P'} \tag{2.34}$$

3. Irregularity parameter *IP* which the ratio of diameter of maximum inscribed circle *D* to diameter of the minimum subscribed circle *d*. (Figure 2-22) illustrates these aspects.

$$IP = \frac{D}{d} \tag{2.35}$$

where

CA = the area based concavity
CP = the perimeter based concavity
IP = the Irregularity parameter
A = projected area of the particle
A' = area of maximum inscribed circle
P = projected particle perimeter
P' = perimeter of the maximum inscribed circle
D = diameter of the maximum inscribed circle
d = diameter of the minimum circumscribed circle

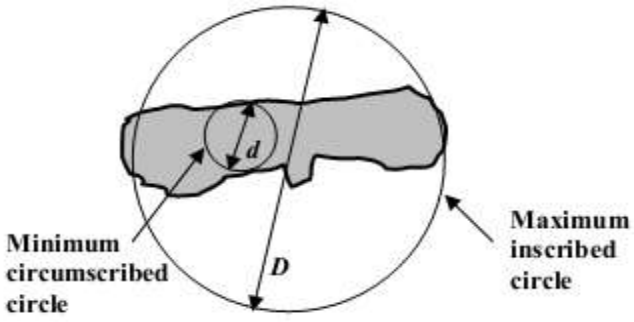

Figure 2- 22 Maximum and minimum inscribed circle diameters of irregular particle

(Bodhmage 2006)

2.21.0 Black tea processing

Black tea is usually made from the top leaves and the terminal bud of the tea plant commonly known as Camellia sinensis. The process involves maceration of leaf to rupture the cell walls in order to allow oxidation of tea the catechins followed by drying, sorting and grading operations.

2.21.1 Black tea processing methods.

There are four main processes in black tea manufacture. They include Roller orthodox, Rotorvane orthodox, CTC (Cut, Tear, Curl) and LTP (Lawrie Tea Processor), or combinations of these. These processing methods result in different types of leaf makes and grades with the latter two producing relatively finer and more uniform and denser teas (Jose 2001; Harris and Ellis, 1981). In addition, grade percentage and outturn have a major impact on the production economics as different sized grades could have substantially variable market values. CTC and LTP processes besides generally having higher outturns produce also denser fine grain teas.(Hampton, 1992; Jose, 2000) .

2.21.2 Black tea processing steps

The process involves 8 steps as shown in Figure 2-23.

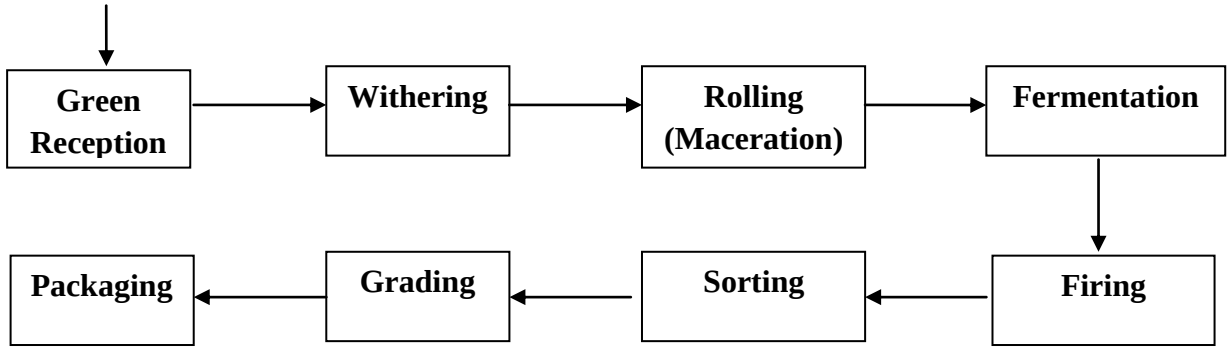

Figure 2- 23 Black CTC tea process flow chart

Step 1 Green leaf reception:

This is the first handling stage at the factory where fresh green leaf is received at the factory from the field. At this stage, quality inspection is usually carried out to assess the quality of leaf delivered against the agreed factory standard. The leaf may also be weighed (if not already

done at the field) or as a check against any transit losses that may have taken place before the leaf arrives at the processing plant and to guard against possible fraud.

Step 2 Withering

This involves application of heated air or normal air leading to partial dehydration of green leaf to remove water in the leaf. This also softens the leaf to ease subsequent maceration during the rolling process. During this period there is a concentration of cell sap which also later aids enzymatic polyphenols oxidation after disruption of cells during the rolling. Furthermore, there is obvious formation of aroma that is an important quality criterion for tea. Withering leads to reduced moisture content of tea to around 50-70% depending on the type of processing being used.

Step 3 Rolling (maceration)

During this stage of processing, the cell walls and cell membranes are disrupted resulting in the mixing of contents of cell cytoplasm and the vacuole. This leads to enzymatic oxidation of tea catechins by atmospheric oxygen which is carried out in subsequent "fermentation" process. There are several equipment for the commercial rolling process that include orthodox roller, CTC, rotorvane and Lawrie Tea Processor originally used in tobacco industry.

Step 4 Fermentation

This is the process of catechin oxidation by polyphenol oxidase and other enzymes naturally present in leaf cells. Fermentation cannot take place in an intact leaf since the substrates and the enzymes are separated by cell membranes. During fermentation as the process is usually referred, the enzymatic polyphenol oxidation leads to the formation of the main compounds of theaflavins and thearubigins which are the main tea quality ingredients that determine the briskness and brightness and tea colour respectively. Thus the green leaf turns from green to – yellow- brownish as the process progresses. The process is terminated after the desired colour and aroma have been achieved.

Step 5 Firing (drying)

The aspect of tea drying is often referred to as 'firing'. This involves drying by removal of moisture of fermented leaf to 2-3% moisture content using oil or steam fired stoves. The main reason of drying is to arrest fermentation once the desired quality level of fermentation has

been achieved (extended fermentation leads to loss of tea quality). Drying also reduces the bulk density of tea as well as improving on its keeping quality. It is during the firing process that black tea assumes its characteristic colour due to formation of mellanoids during the high drying temperatures.

Step 6 Sorting

Tea leaving the drier mouth is heterogeneous and requires some sorting and cleaning before it is graded. This involves extraction of tea fibres and stalk, removal of any metallic contaminants and other extraneous matter that may have come into contact with tea during processing.

Step 7 Grading

Tea Grading involves separating the now sorted tea into its various commercial sizes using sieves. The grade is determined by the sieve size through which it passes and the sieve size on which it is retained. Grading is normally done on motor driven vibratory shakers fitted with wire meshes or reciprocating crank driven systems with trays having meshes.

Step 8 Packaging

The final step in in tea processing is the packaging that is desired to ensure safe delivery of the product to the ultimate buyer/consumer is a sound condition at a competitive cost. Bulk tea for export is usually packaged in aluminium lined multiwall paper sacks. Tea is hygroscopic in nature and the packaging needs to prevent any moisture ingress into the tea. The product has also a delicate aroma that needs a good aroma/gas barrier to preserve the product quality.

2.22.0 Black tea density.

Density is normally defined as mass per unit volume:

$$Density = \frac{Mass}{Volume} \tag{2.36}$$

However, in the tea industry, the standard test "density" usually refers to the volume over a specific mass (usually 100g).

$$\text{"}Density\text{"} = \frac{Volume\ (cm3)}{100g} \tag{2.37}$$

Thus in tea terminology the volume measure for the mass of 100g of tea is usually referred to as “density”. The normal density can then be obtained by dividing 100g into this read off volume.

Black made tea just like other food products requires responding to constantly changing market requirements and consumer tastes as well as technological advancements. The onset of CTC (cut, tear, curl) machines as well as LTP (Lawrie tea processor) was as a result of such market demands for higher density and finer tea particles that were suited to the tea bag market (Hampton,1992). Furthermore, tea buyers who have hitherto been placing much emphasis on tea liquor qualities such briskness, strength and colour; have now turned attention to the tea grain characteristics that include particle size and density and particle morphology (Jose, 2001). The dominance of tea bags market in many developed world markets such as Britain has fuelled the change from large leaf orthodox teas (suited for loose tea packet) to smaller grain and more rounded tea particles such as those of the CTC technology. For instance, tea bags account for 89 per cent tea sales in U.K. (Jose, 2001).

Generally a tea bag has specific volume to contain a certain weight of made tea (usually around 2-3g). Manufacturers/ tea packers need tea blends within a specific density range in order to correctly fill the bags and even packets. Indeed, if the made tea is outside the specified density limits for the grade, then this is likely to cause bag sealing difficulties as well as possible marketing problem. This requires that the grading operation (size separation using specified meshes) is done accurately and that such tea requires to be delivered to the packer with minimal particle damage for ease of packing. Tea bag machines are programmed to fill to a certain weight so that the density is within the set limits otherwise the machines do not function properly (Jose, 2000)

2.22.1 Factors affecting density of made tea

Several factors are known to affect the density of made tea. These include particle size distribution, the moisture content, presence of fibre in tea, plucking standard, moisture content of withered leaf, type of tea clone used, agronomic conditions such nitrogen supply and even the time of the year.

2.22.2 Effect of Particle size distribution.

Smaller tea particle as found in such grades as the dusts and Pekoe Fanning (PF) have a higher bulk density compared to larger ones. For instance PD (Pekoe dust) density is in the range of

230-260 cm^3/100g or 43-0.38 g/cc while that of PF (Pekoe fanning) is around 260-300 cm^3/100g or 0.38-0.33 g/cc. Conversely a grade such as BP1 comprising of large particles (330-350 cm^3/100g or 0.30- 0.29 g/cc has a large volume for 100g made tea sample and therefore low density (Mitchell, 2001; Jose, 2001).

During tea grading, smaller sieve sizes collect dust grades which have lower volume for the 100g while compared to larger sieve sizes where particles occupy a larger volume for a similar 100g weight (Figure 2-24). Similarly during commercial tea grading using meshes with various sieve sizes, the bulk of teas collected over the various sieves will dictate the density of the tea (Table 2.9). For instance the bulk of the teas (95.5%) collected over mesh 14 are of 1mm size and this is the size that will majorly determine the overall density of this grade. Similarly, teas over mesh 16 consist mainly of particles around 1 mm size (83.7%) and particles around 0.7 mm (15.2%). It is clear therefore the density of teas over mesh 14 will be lower than that of mesh 16 teas (Table 2.9). Using this argument it clear why tea particles collected over mesh 24(PF1), 30 (PD) and 40 (Dust) have correspondingly higher densities (Tables 20.10 and 20.11).

Thus particle size distribution within a tea has a major impact on the overall density of the tea as well as the packaging, other market considerations and handling (Tables 2.5, 2.7 and 2.8).

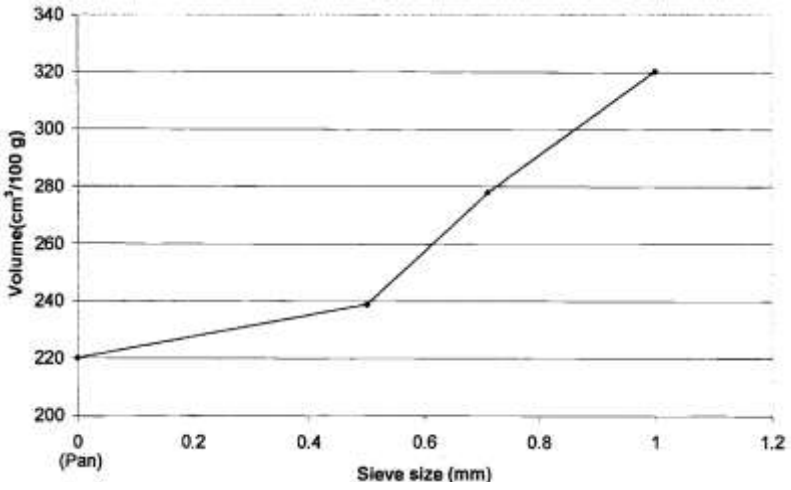

Figure 2- 24 Relationship between particle size and tapped volume/100g

(Jose, 2000)

Table2. 9 Distribution (%) of particles on the different meshes

Mesh size #	Sieve size (mm)				
	Pan*	0.50	0.71	1.00	1.40
14	0.7	0.3	0.9	95.5	2.6
16	0.4	0.7	15.2	83.7	
24	0.9	3.7	95.2	0.2	
30	0.5	13.2	86.3		
40	22.6	77.4			

(Jose, 2000)

Table2. 10 Distribution (%) of particles in different main grades

Grade	Sieve size (mm)				
	Pan*	0.50	0.71	1.00	1.40
D1	11.8	88.2			
PD	5.4	94.4	0.2		
PF1	2.5	16.6	74.9	6.0	
BP1		2.21	2.79	17.40	77.60

Pan*= Particles $< 0.50mm$.

(Jose, 2000)

2.22.3 Effect of particle shape (morphology)

The shape of the tea particles also influence the density of made tea in the sense that small and spherical (grainy) particles occupy less space and tend to pack tightly compared to large, irregular and flakey ones with open packing structure (Jose, 2000). Flakey particles are flat or curled in shape and therefore difficult to pack tightly. Very often, large particles are formed as a result of coalescing of small particles during processing or handling .In particular lack of ball breaking and aeration during fermentation, high moisture contents during maceration and poorly meshed rolling rollers and possible case hardening during the drying all enhances formation of large irregular particles of made tea. The particle shape has a bearing on its flow properties such that large rounded smooth surfaced particles tend to flow more easily than small elongated rough surfaced particles. (Table 2.8)

2.22.4 Effect of moisture content and relative humidity.

The moisture content of tea will affect its density. If teas are dried below the usual standard of 3% moisture content, the volume/100g would be increased as some of the dry matter would be lost through the resultant burning action. Conversely, if the moisture of tea rises above expectation via adsorption of moisture by tea particle from the surroundings, there is a fall in Volume/100g ratio or increased density (Jose, 2000). The ability of a powder to adsorb moisture from the atmosphere depends also on its composition. Materials such as sugar, salt and even tea that contain readily moisture adsorbing materials tend to be hygroscopic in nature. Moisture will also affect the flow properties of tea with higher moisture contents reducing its flow to cohesion of tea particles. Teunou et. al., (1999) investigated the effect of relative humidity on flow properties of tea powder. The research reported a decrease in powder flow ability with increasing relative humidity and temperature. At high relative humidity, the tea powder tended to adsorb water transforming it into a sluggish, rubbery material. They further noted the effect of relative humidity and temperature on tea particles flow properties was determined by the time of exposure and the dimensions of the powder bed.

2.22.5 Effect of presence of fibre

Presence of fibre in tea is usually as a result of poor leaf plucking standard resulting in delivery of coarse leaf for processing. Such leaf will undoubtedly have higher amounts fibre found in tea after their processing. Such fibre needs to be carefully separated from tea although not all can be removed and the amount left will depend on the effectiveness of the fibre cleaning system employed. In addition, some fibres remain imbedded within the tea particle and are difficult to remove without damage of the tea granules leading to degradation of aesthetic tea quality attributes. Fibres tend to have lower dry matter content and therefore their presence will tend to lower the mass per unit volume and therefore the tea density.

2.22.6 Effect of plucking standard

While fine plucking (usually two leaves and bud) commonly practiced in Kenya results in made tea of higher primary grades and lower fibre content, coarse plucking of up four leaves and twigs results in highly lignified and fibrous material in the made tea. Such tea will therefore have low amount of dry matter and hence lower density. Besides, coarse plucking affects grade outturn and tends to promote more secondary grades including BMF and Fanning all of which contribute low density teas in larger proportion than expectation. With the bulk of

tea produced being of larger particle sizes and increased fibre content, the resulting tea significantly decreases in density.

2.22.7 Effect of moisture content of withered leaf

Jose (2001) investigated the effect of withered leaf moisture content on made tea density. He used five levels of moisture content of withered leaf (66, 68, 70, 72, and 74) and used 3 leaves and a bud plucking standard. The leaf was rolled (macerated) using a triplex CTC machine and fermentation of 50 min at 25^{oc} and a drying period of 10minutes. (Jose (2001) concluded that densities increased with increase in physical wither. A similar trend had also been observed in Kenya (Owour, 1993). This appears to contradict earlier observation that during withering in addition to the loss of moisture the leaf losses 3-4% of soluble dry weight on account of loss of carbohydrates due to respiration (Hampton, 1992; Jose (2001) further noted that low wither moisture contents gave higher proportion of the particles in the 1mm category compared to high wither moisture content.

Table2. 11 Relationship between tapped and bulk densities of various tea grades

Grade	Bulk density	Tapped density
BP1	0.271	0.287
PF1	0.326	0.356
PD	0.381	0.418
D1	0.417	0.467

Jose, 2000)

2.23.0 Gap analysis

The following knowledge gaps were identified from the literature review:

1. Despite Kenya being the top exporter of tea in the world, there is no road distribution data on transit hazards and their levels (including for roads used for bulk tea shipments that would allow comparison of Kenya's distribution networks with those from the other regions. This research is expected to generate road hazard data that is representative of the conditions on the Kenyan roads in order to be able to compare these with other similar distribution environments in other parts of the world.

2. There are nowadays specific local pre-shipment testing protocols for goods in a number of regions where the general ISTA and ASTM test procedures have been found to be unsuitable because they do not represent the prevailing transit conditions of those regions. Areas that have developed their own local goods testing procedures include

Spain, Brazil, Mexico, India, and Thailand. Although Kenyan distribution conditions are believed to be poorer than those where general test methods have worked, there is currently no pre-shipment testing protocols for this region to allow shippers to test their packaged goods. The research will therefore focus on developing one such a protocol suitable for testing goods within the Kenyan distribution environment.

3. Tea particle size is an important physical quality of tea that defines its density, grade and its morphology. Tea pricing is based on tea grades that are defined by their particle size, shape, density, colour, and particle size distribution within each grade. Any damage to the tea particle integrity in transit due to compression, vibration/shock affects both the physical and organoleptic tea of quality. There is currently no data to show how such transit hazards of vibration/shock or compression could affect those important physical qualities of tea. The research will find out effects of truck shipment environment on tea quality.

4. Despite attempts by a number of researchers to formulate an accelerated simulation testing protocol that would reduce pre-shipment testing period in the laboratory thereby saving on testing time, there is so far no accepted procedure for accelerated testing. Full journey tests are still a common feature. There exists a knowledge gap in this area that requires further research to come up with an acceptable accelerated testing procedure to reduce pre-shipment test period. This area is not covered in this research due to time and resource constraints and is therefore recommended for further work.

5. A lot of useful information has been generated in recent times to explain the complex behaviour of granular matter under the influence of "granular temperature". Although many of the behaviour models have successfully been experimented on in the laboratory, there are still challenges in a number of occasions of formulating equations that could predict their behaviour under varying conditions. There is no data for example to show how tea particles would behave under influences of vibration/shock at different external conditions such as moisture, relative humidity. This is not covered in this work and is recommended for further work.

6. Attempts have been made to formulate equations to explain the fluctuations in density of a granular matter under external vibration upon its attainment of the maximum density using the adsorption-desorption model. While the equations explaining the first

two regimes have been formulated, the behaviour in the third exponential terminal decay is not well understood and there is need for further research in this area. This has however, not been addressed in this work.

2.24.0 Summary

Today's effects of globalization and international trade have made the world of trade a global village. Goods hitherto produced in far and isolated remote parts and consumed in the neighbourhood, now have to be sold in far off cities of the world where they are required. In order to address large diversities in road conditions found in various parts of the world, researchers in area of distribution packaging have advocated for data to be collected from various regions and analysed into PSDs plots that allow comparison of road conditions found in different parts of the world. The advent of miniature self-contained electronic transit data loggers have made this possible as they continuously capture transit data that can be fed directly into the pre-shipment test program that allows optimization of packaging designs for that distribution environment. Researchers have therefore further faulted the use of the general ISTA and ASTM test procedures for transit conditions for all distribution environments because in some cases they have been found not to represent actual transit conditions for those areas. Road conditions data from various regions such as USA, Brazil, Mexico, Spain, India and Thailand show material differences in vibration and shocks impacts. Since environmental concerns are now a global matter, many governments have put in place very strict packaging material reduction thresholds with which goods entering their trade frontiers must comply.

Various testing methods and equipment that could be used in the pre-shipment testing of packaged goods have been reviewed to show their capabilities and also their limitations. Research from different sources and distribution environments was reviewed and indicated significant diversity in road conditions in various parts of the world and how such environments could impact on the quality of goods in transit. At the moment, however, there appears to be no data available for the Kenyan distribution environment that would allow shippers to carry out pre-shipmen tests for their goods, to optimize designs. This is the focus of this research.

Research carried out by different researchers on granular matter behaviour showed that irrespective of the size and material, when given some external impetus, it in many instances obeyed the general granular matter mechanics. From the granular matter phase diagram,

granular matter is athermal and often does not respond to changes in temperature but to load and density. Granular material thus responds to external excitations such as vibration, shock and compression. Several studies on granular matter behaviour under external excitation have revealed its complex nature that is dependent on several factors that may include shape, size, brittleness, surface morphology, particle size, density, elasticity, contact friction, chemical affinities, ability to absorb moisture and magnetic properties. Indeed, it is these factors that define the behaviour model the specific granular matter will exhibit during its handling, conveyance, processing, and transportation. A number of granular behaviour models have been put forward by various researchers in this field to try and explain the complex responses of granular matter to athermal situations.

Tea is granular matter with several factors that define its physical quality; key to them that includes density, particle size and its distribution, particle shape and colour. These quality attributes are important not only for the commercial purposes such as pricing and overall quality, but also dictate the handling practices and equipment design at the blending and packaging factories. Any changes during transportation and handling in the above quality attributes for tea will negatively affect its quality and value. Truck transport is a common mode of tea haulage from the factories to the port of export. There appears to be no data at the moment on how truck transit conditions may affect the above mentioned tea physical quality attributes. Knowledge of extent of transit damage of tea quality will assist packaging designers in improving their designs in order to protect tea quality in transit. This is the focus of this research.

3.0CHAPTER 3: RESEARCH DESIGN AND METHODOLOGY

The actual steps of the methodology used in the research are shown below (Figure 3-1).

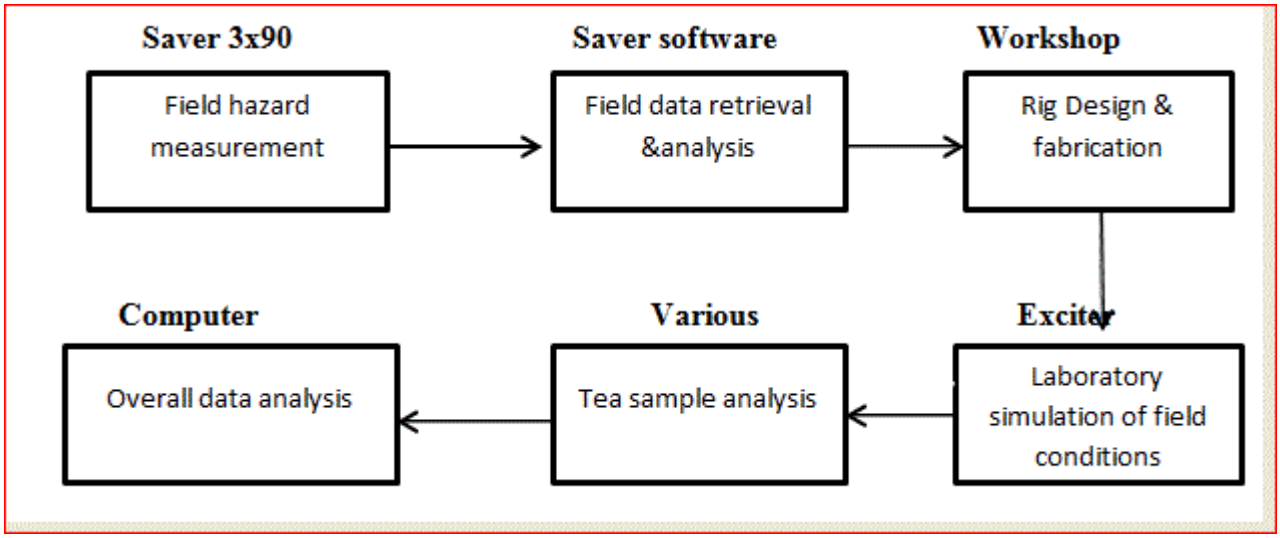

Figure3- 1 Research methodology flow diagram

The methodology adopted in the research involved collection of the truck transit environmental conditions of vibrations, shock, temperature and relative humidity for the entire truck journey for each of the four test routes used. This strategy ensured that the laboratory simulations that followed were as close as possible to the actual road conditions by programming the exciter unit using the actual journey spectrums. The transit measurements were carried out using the Saver data loggers. The logger data was downloaded into the computer at the end of every journey for analysis and resulting PSD was used to program the vibrating table. A suitable simulation rig was designed using granular matter mechanics and fabricated in the workshop and used in the simulation of the measured field conditions using a programmable vibration table. Tea samples were drawn at intervals during the simulation exercise and the same were analysed in order to understand how the field conditions could affect the physical quality of tea during its transportation. These tests included density, particle size distribution, particle morphology, moisture content, aspect ratio and angle of repose. This methodology has been found by researchers to be more efficient and cost effective for achieving optimal designs compared to the general simulation methods or actual road trials. Furthermore, it allowed collection of useful data for empirical investigation of various physical relationships of transit

conditions with tea quality parameters such as density, particle size distribution, particle morphology, colour, and flow characteristics.

3.1.0 Transit hazard measurements

3.1.1 Materials, methods and equipment

Transit data was measured using Lansmont Saver unit model 3x90 from Lansmont Corporation, Monterey, Cal. USA (Figure 3-2). The data loggers were firmly mounted inside the trailer bed on the left side at the rear axle in each truck (Figure3-7). For the two routes viz. Kambaa to Mombasa and Michimikuru to Mombasa the Saver data loggers were fixed on both the right and left rear sides on the truck beds. The left side near the rear axle instrument mounting position was chosen as it had been noted that the left side of the road for right hand drive vehicles tend to be more uneven compared to the right hand side. Furthermore, the roads in Kenya are characterized by worn out and uneven "shoulders" that tend to present much more severe surface compared to the rest of the road (Figure 3-11). The positioning of the instruments at the rear of the truck was also chosen because initial trials before the actual work tended to indicate this while previous studies had shown that the highest vibrations that could cause goods damage in a truck environment are experienced at the rear (Singh, et al., 2006).

The self-powered Saver data recorders had capability to measure vibration and shock in both time and signal triggered modes and relative humidity and temperature throughout the journey. They also had inbuilt tri-directional accelerometers that allowed measurement of vibration and shock outputs in the vertical, lateral and longitudinal directions at every 2 minute interval. In addition, the data recorders had memory, data transmission and download capabilities that allowed download of data into a computer at the end of the journey for subsequent analysis. A complete tri-directional vibration/shock data set for the Nyamache to Mombasa route is presented in Appendix 2. In addition, gadgets for fleet tracking were fitted into every truck used that enabled tracking the trucks in real time (report received every 2 minutes) from the computer. The system besides provided vehicle speeds at each location. A summary is presented for the Nyamache to Mombasa route under Appendix 8.

The following instrument settings were used during the transit data measurements:

Signal triggered settings:

1. Minimum time triggered sampling: 2 min
2. Minimum sampling rate:1000 samples per second
3. Sample size:1024
4. Trigger threshold level: 0.25g
5. Data retention mode: overwrite
6. Temperature humidity sampling intervals: same as the vibration sampling.

These settings were chosen after several field tests were done to find out at what levels all the Kenyan road conditions were captured by the measured data. A Similar approach had been used by other researchers in other parts of the world using similar equipment and further, these are the settings recommended by equipment manufacturers for poor road conditions.

Figure3- 2 Saver 3x90 measuring unit used in road hazard measurement

3.1.2 Routes and trucks used

Four Mercedes Benz tractor units fitted with tri-axle trailer trailers were used one for each of the four routes used in this work. Kambaa and Michimikuru routes were served by the same truck. Chebut-Mombasa route trucks had air-ride springs fitted at the rear (Figure 3-5) while others had leaf spring suspensions (Figure3-6). Figure3-4 shows one of the vehicles used in the experiment while Figure 3-7 shows the saver transit data collecting unit fitted inside a loaded vehicle. Table 3.1 gives details of the vehicles used in each route while Figure 3-3 gives the map of the four routes used by the trucks. The routes chosen were the key transport routes for the bulk tea transport although they also happen to be the main routes for haulage of bulk of

the goods for export in Kenya. The road surfaces for the routes used included dirt, gravel and tarmac (Figures 3-8, 3-9, and 3-10, 3-11) respectively.

Figure3- 3 Map showing transportation routes used during the investigation

Key: --- Kambaa to Mombasa Route

--- Michimikuru to Mombasa Route

--- Nyamache to Mombasa Route

--- Chebut to Mombasa

Table3. 1 Trucks used in the road transport hazard measurement

Vehicles	Trip details	Tractor				Trailer		
		Make	Type	Year of manufacture	Engine H.P	Type	Make	Year of manufacture
1	KBA-MSA ,&MCI-MSA,	Mercedes Benz	Actros 2546,	2006	460	Tri-axle	Doll	2010
2	NME-MSA,	Mercedes	Axor 2540,	2004	460	Tri-axle	Elite	2009
3	CBT-MSA,	Mercedes	Axor 2540,	2002	460	Tri-axle	Bachu	2009

Key: KBA-MSA- Kambaa to Mombasa trip -542km

MCI- MSA- Michimikuru to Mombasa trip -726km

NME-MSA- Nyamache to Mombasa trip -763km

CBT- MSA- Chebut to Mombasa trip -881km

Figure3- 4 One of the trucks used in the transit hazard measurement experiment (Chebut to Mombasa route)

Trucks used were all Mercedes Benz tractor unit fitted with a tri-axle trailer with payload capacity of 25-30tons.

Figure3- 5 Air ride springs on the rear axle for the truck used in Chebut to Mombasa route

The truck used in Chebut to Mombasa route had the rear truck unit fitted with above shown air-ride suspension assembly.

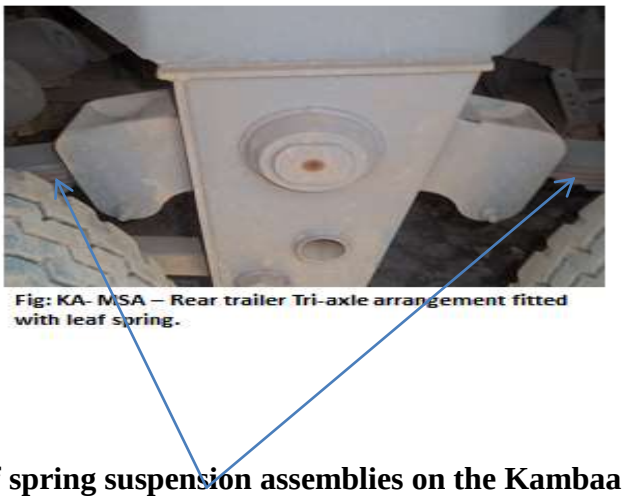

Figure3- 6 Tri-axle leaf spring suspension assemblies on the Kambaa to Mombasa trailer

Trucks used in all other routes apart from Chebut to Mombasa route were fitted with leaf spring suspension assemblies.

Figure3- 7 Loaded truck fitted with Saver 3x90 measuring units at rear axle

Brick-like formed tea sacks were arranged on a square wooden pallet containing 20bags and pallets loaded into the truck as shown above.

Figure3- 8 A section of the dirt road used during the road hazard measurement (Michimikuru to Mombasa route)

The dirt roads had several potholes especially due to delays in grading them and also became very slippery and impassable during the wet seasons. These roads are found near the tea processing factories. They fall under the county governments and are usually poorly maintained compared to the main highways that are managed by the central government.

Figure3- 9 A section of the gravel road used in the road hazard measurement (Michimikuru to Mombasa route)

Gravel roads were passable throughout the year but had quite rough leading to high vibration and shock impacts from the trucks. These are found near the tea factories where road networks are poorly developed and maintained by the respective county governments.

Figure3- 10 A section of the tarmac road with unmarked speed control bump (Michimikuru to Mombasa route

An unmarked road bump

Both Michimikuru and Nyamache to Mombasa routes had several unmarked speed control pumps near the schools, market centres, cattle dips and hospitals meant to avoid accidents. Lack of signs to warn drivers of their presence led to high shock and vibration impacts.

Figure3- 11 Section of narrow road (Chebut to Mombasa) with worn out “shoulders”

Several sections of the route used by trucks had steep worn out road “shoulders” that would register high shock impacts when the trucks are pulling down on the road side.

3.2.0. Laboratory Simulation Experiments

3.2.1 Materials, methods and equipment

3.2.2 Black tea

Commercial black tea was obtained from a U. K. supermarket. The tea was sieved using hand sieves and the fraction passing through a 2 mm sieve pore but retained on top of a 1 mm sieve was used as the mother batch for all focused simulation experiments. The 1 mm size sample was preferred because it represented the larger particles of CTC manufacture composed mainly of BP1 commercial grade. The tea fraction with particles larger than the 2mm sieve pore was discarded as it represented a very small amount of BP grade that may have accidentally found its way into BP1 grade. The BP1 particles were chosen as they had lower bulk density and were also more likely to undergo most degradation arising from transit hazards in a truck transportation system and even handling.

3.2.3 Fabrication of simulation rig

Justification of the rig design is first presented. Majmudar and Behringer (2005) while working with an assembly of photo elastic disks concluded that when a shear deformation is applied to

an assembly of particles, the contact forces aligned with the direction of shear. Tordesillas (2007) further reported that even in case of isotropic compression, the forces align in the direction of the major principal stress.

Langroudi et. al. (2010) compared the normal stress applied to the top surface of the particle assembly with stresses recorded by the normal stress sensors on the bottom and noted that stresses in a granular bed travelled mainly in the direction of the force application. Goncu (2012) quoting Majmudar and Behringer (2005) reported that force networks show strong directional anisotropy depending on the nature of external loading. Roberts et. al. (1997) while quoting Scarlett and Eastman (who studied propagation of shock waves through a bed of granular materials in a vertical cylinder filled with granular material) reported that the intensity of disturbance from the bottom reaching the surface was strongest vertically above the energy source and decreased along inclined lines until no disturbance was detected outside a 45^0 cone emanating from the energy source. The velocity through the bed was independent of the height of the bed and the size fraction of the sand used, but was at maximum in the vertical direction while decreasing for lines along increasing angle to the vertical.

Applying the above fundamental principles of powder mechanics to this work, multiwall paper sacks normally used for bulk tea packaging have filled dimensions such that the sack length (1100 mm) and width (560mm) are relatively large compared to its depth (205mm). From this scenario, it can be assumed that when such sacks are stacked on top of each other in a pallet pile with the 205mm side as the height, the dominant static load force propagation will be projected vertically along the bag depth to the bottom sack on the pallet pile. In other words, an anisotropic force is applied in the vertical direction downwards by overlaying static load and gravity to the pile bottom, and only negligible force stresses may be propelled perpendicular to the force direction to the bag sides which are more or less rigid after the sack has been filled under vibration inside a rigid metallic forming box that ensures the sack assumes a solid brick form. This understanding of force transmission within a granular bed in relation to applied static load therefore formed the basis of the truck transit conditions simulation rig design.

Circular rigid Perspex tubes were used to represent brick-like tea sacks with rigid sides. The whole rig assembly consisted of Perspex tubes having 25.4mm internal diameter that were firmly fixed on an aluminium 330mmx150mmx10mm base plate with threaded screws. The size of the base plate chosen was that which was convenient to mount on the exciter without much overhang. (Figure 3-12) shows the arrangement of tubes on the plate. The size of the

tubes was chosen such that two rows of tubes could fit on the base plate (Figure3-12). It should be noted that the size of the tubes used did not very much matter provided they matched the circular metal rods that needed to be inserted loosely into them as well as ensuring the size of the metal static load gave the desired compression (force/unit area) inside the tube representing pressure exerted on tea particles at a given point on the pallet load. In this experiment, both the Perspex tubes and round metal rods were readily available in the stores and therefore did not need to buy more for the experiment. The base plate was in turn fixed to the exciter using two centre screws.

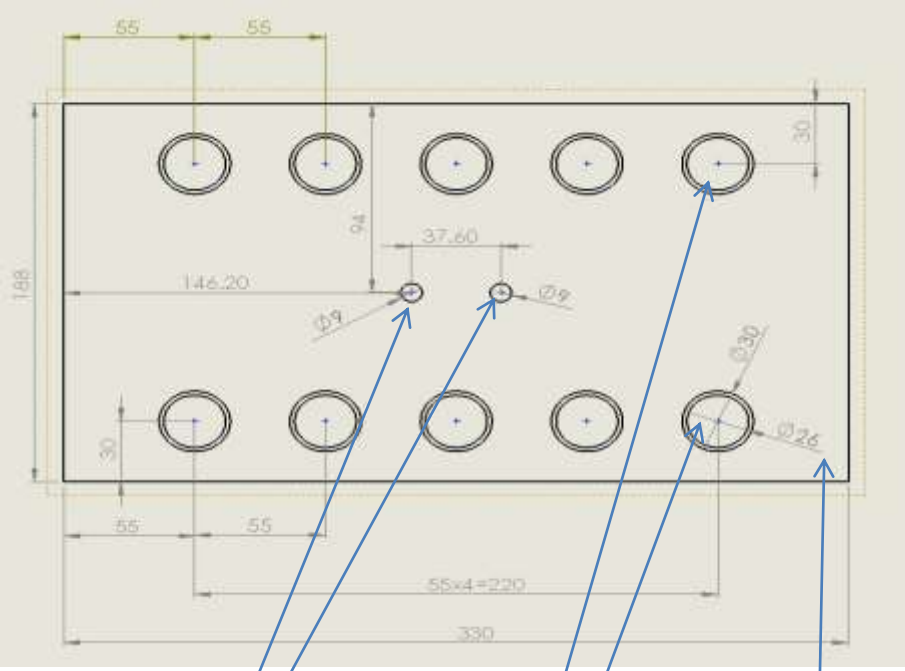

Figure3- 12 Rig design showing Perspex glass tubes firmly fixed on aluminium carrier plate (dimensions in millimetres)

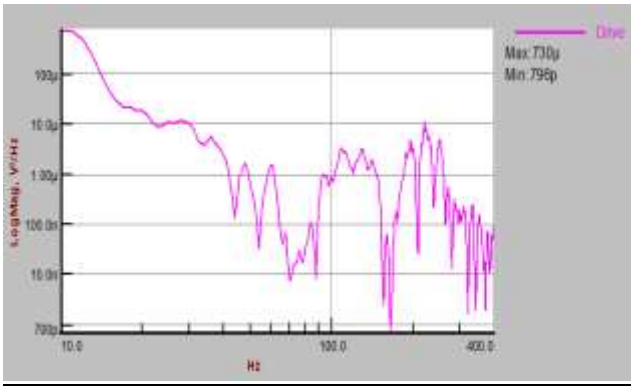

Figure3- 13 Actual road spectrum input into the shaker drive programme

Various tubes representing chosen levels of tea bags on pallet were filled with a known weight and volume of sieved mother tea as described earlier. Approximately the same volume and mass of tea was filled in each tube to minimize any possible variations due to differing tea column heights. Loosely fitting round bars of known mass representing static loads on the predetermined levels on the tea pallet were placed on top of the tea inside the tube. (Figure 3-14). The static loads used on the tubes were 89.06g, 178.86g, 278 g, 356.56g and 447.10g representing tea particles at various randomly chosen levels on the pallet from top to bottom. Appendix 6 gives details of the design parameters used in the rig apparatus. One of the tubes did not have any static load and was, therefore, under the effect of shock and vibration alone. The control tube was not mounted unto the rig assembly for vibration and therefore did not have any treatment. The whole assembly (tubes, steel weights and base plate) was fixed to a programmable vibration table (Figure 3-15) that had been programmed using the vertical transit vibration shock data obtained from the actual field measurements for each journey (Figure 3-13 and Appendix 2). Vertical vibrations were chosen because they represented the highest vibrations experienced by goods in a truck environment compared to both longitudinal and lateral vibrations. The programmed vibratory table produced shaped random vibrations that simulated nearly the actual road travel conditions for each journey (Figure 3-13).

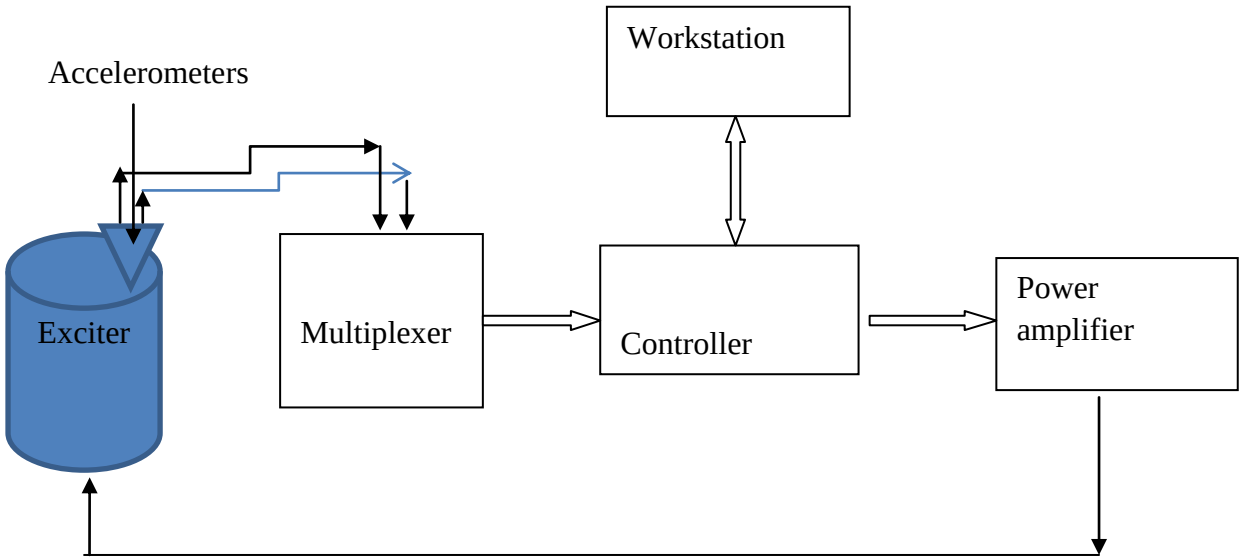

Figure3- 14 Block diagram of a laboratory vibration test system

Bulk, compact and tapped densities were monitored during the simulation experiment. In addition, changes in particle shape were analysed during the experiment using Scanning Electron Microscope (SEM) measurements.

Figure 3-14 shows the diagrammatic representation of the simulation apparatus while Figure 3-17 gives the complete focused simulation set up used in the experiment. Table 3.2 shows the exciter machine settings.

Table3. 2 Details of the shaker used for the focused simulation

Model	**Derritron VP 85**
Displacement	+/_ 13mm
Acceleration	550m/s^2 peak
Frequency range	1.0- 5000Hz
Maximum load	38.5kg.
Maximum Thrust (random)	4560N
Maximum Acceleration	94g

(Manufactured by Data Physics Ltd, Michigan USA)

Appendix 1 gives the detailed shaker set up parameters used in this experiment.

Figure3- 15 Focused simulation rig assembly mounted onto the exciter machine

3.3.0 Particle physical quality determination

Particle size distribution analysis was carried out at various intervals during the simulation and at the end of a complete truck journey using stainless steel hand held sieves.

A set of five hand sieves of rectangular pore sizes 1mm, 500 microns, 250 microns, 125 microns and 63 microns were used to determine the particle size distribution at various intervals up to the end of the simulation period. The above sieve sizes were chosen because these are the same sizes used in commercial tea grading in factories. The contents of each tube were emptied into the top sieve with the largest pore size of the sieve assembly. The entire sieve pack assembly was arranged such that the largest pore size mesh was at the top and smallest at the bottom of the pile (Figure3-16).

Figure3- 16 A set of stainless steel sieves assembly used in particle size analysis

The whole sieve assembly was gently shaken by hand in a gyrating manner for about 5 minutes to ensure complete separation of the various particle fractions in the mixture. The content of each sieve was then weighed using a laboratory analytical balance and a percentage of each size fraction to the total tube contents calculated. This was repeated for all measurements made at various intervals during the vibration. The volume of each fraction was determined using a graduated measuring cylinder. The rig assembly was mounted to a programmable electromagnetic shaker used in simulation. The shaker was connected to the signal synthesizer, the control panel and the computer into which the required vibration spectrum programme is fed.

Figure 3-17 shows the actual set up of the simulation apparatus in the laboratory. The controller was programmed with the field spectrum for each route and the shaker vibrations more or less traced the field spectrum.

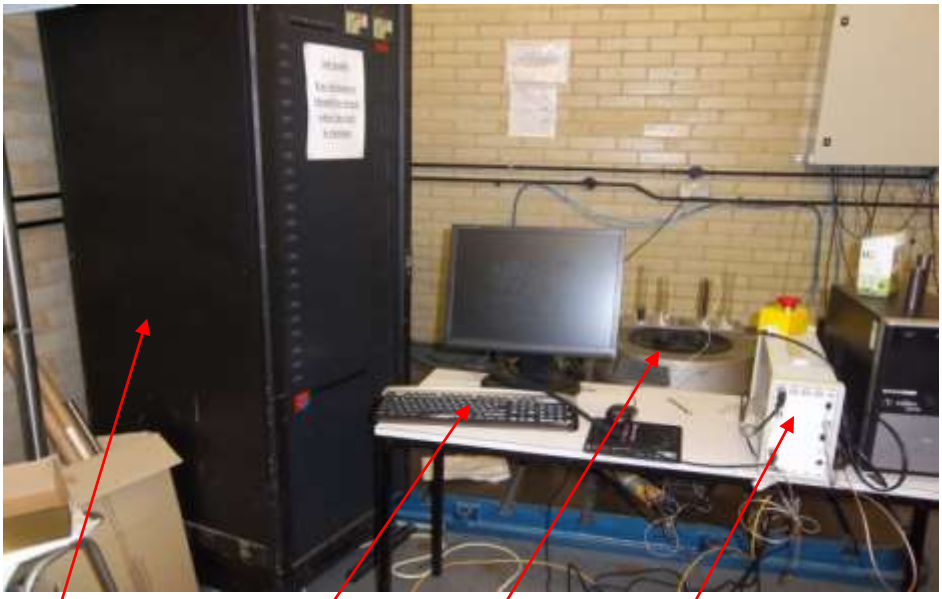

Figure3- 17 Complete laboratory equipment used in the simulation experiment

Power amplifier unit Work station shaker Controller

3.3.1 Tea density determinations

The graduated measuring cylinder method was used to determine the volume. Sufficient amount of tea was passed through a sieve of apertures equal to 2mm. Any agglomerate that may have formed during storage was broken to avoid changing the nature of the material. Approximately 100g of the test material (m) was weighed using a laboratory scale with 0.1% accuracy. The weighed quantity was gently introduced into a 250ml graduated cylinder (readable to 2ml) avoiding any compacting. The tea was carefully levelled out without compacting and the unsettled volume (V_o) read out to the nearest graduated unit. The bulk density was calculated using the formula:

$$\text{Bulk density} = m / V_o \qquad (3.1)$$

For the smaller tea fractions below 100g the actual weight was determined and density calculated as above.

3.3.2 Free flow (bulk) density determination

After each period of vibration in the shaker, the contents of each tube were carefully weighed in grams using analytical balance to the nearest 10 milligrams before being poured into a measuring cylinder and the volume recorded. The bulk density was calculated by dividing the mass of tea by the volume (Equation 3.1).

3.3.3 Tapped density determination

Tapped density was determined using a modified measurement method similar to that used in the commercial tea industry where the measuring cylinder having already weighed tea is subjected to drops using a stepwise wooden apparatus. The apparatus consists of a wooden plank with three steps each 32mm and placed in a fitting wooden enclosure. The measuring cylinder which is permanently attached to a wooden base is placed on the highest step of the wooden plank. The plank is slowly drawn away from the housing subjecting the tea cylinder two three stepwise drops. The exercise of drops is repeated before the final volume is read from the measuring cylinder. In the absence of above apparatus the measuring cylinder with the weighed material was manually subjected to similar drop heights as those normally used in measuring tea density. The test tube containing tea to be tested was tapped by dropping it gently on the table from a distance of 32 mm six times and the final volume recorded. This is the same drop height used in tea tapped density determination in commercial tea test laboratories where 100g of tea in a measuring cylinder have the volume read of after 6 times stepwise drop.

3.3.4 Compact density determination

The compact density of the tea was determined by measuring the volume of compacted granular mass in each sample tube after the simulation period (without disturbing the compact mass at all) and taking the mass in grams of the same. The density was calculated the density using Equation 3.1 above.

3.3.5 Determination of moisture content of made tea

A sample of tea between 3- 5gm. was accurately weighed to the nearest milligram on a dry sample watch glass of known weight. The glass and contents was placed in a controlled temperature oven with temperature controlled at 103±1 ^{0}C overnight. The final weight of the sample was taken when the two consecutive weighing's yielded insignificant difference.

The moisture content is the amount of water in the tea and is regarded as the ratio of the loss of mass of test material when dried as stated above to its initial mass and is normally expressed as a percentage.

The moisture content is calculated using the following formula:

$$\text{Moisture content \% (MC)} = \frac{B-C}{B-A}100 \qquad (3.2)$$

where:

A is the weight of empty glass dish

B is weight of the dish and tea before drying in oven

C is the weight of dish and tea after drying

3.3.6 Particle shape (morphology) determination

Particle shape of tea particles was determined using Scanning Electron Microscope (SEM) .The system comprised an evacuated column containing an 'electron source' or 'gun'(tungsten, electron lenses and scan coils, a specimen stage and signal detectors for electron and X –rays).

The essential features of the SEM are:

(a) An electron source such as tungsten filaments or field emission tips able to generate high energy electron beams or accelerating voltages.
(b) Electron lenses, electrostatic or electromagnetic, to de-magnify and focus the electron beam on to the sample.
(c) A scanning system to translate electron beam in a regular array of parallel lines over a selected area of the specimen.
(d) Detectors to collect and amplify the emitted signals from specimen and also control image contrast.
(e) A display and recording system to view the image and store information.
(f) A vacuum system maintained by oil filled rotary pump capable of maintaining a low pressure in the electron source and optical column.

Fractions collected from various sieves depicting various particle sizes were analysed and SE micrographs produced were analysed for any surface morphology changes during simulation. The SEM was used instead of the optical microscope because it allowed high resolutions necessary to observe detailed particle surface structure to understand how tea particles interacted with each other in order to predict their coefficient of friction and flow behaviour.

3.4.0 Summary

The research methodology involved first collection of the transit data from the truck load shipments of bulk tea from each of the four transport routes used. This ensured actual distribution transit conditions were captured to be used in subsequent simulation exercise that needed to mirror as much as possible the actual distribution hazards encountered during truck transportation. Designing and fabricating of a simulation rig using granular matter mechanics such that the effects of the simulated inputs are accurately measured. Carrying out simulated transit conditions on a programmable exciter for each route using its respective spectrum (PSD) obtained after field data analysis. In order to find out how the truck transit conditions affected the physical quality of tea, quality attributes of particle size and its distribution, densities, morphology, colour and flow characteristics were carried out on the tea at regular intervals during the simulation exercise.

4.0 CHAPTER 4: EXPERIMENTAL RESULTS AND DISCUSSIONS

4.1.0 Introduction

This chapter describes the experimental results of the transit hazard measurements conducted on packaged tea in transit on four main Kenyan transport routes. It provides the measurements of vibration, shock, relative humidity and temperature experienced within a truck environment during tea shipment from various manufacturing sites in Kenya to Mombasa port for storage and subsequent shipment. The vibration/shock transit data is presented as Power Spectra Density (PSD) plots that indicate the vibration intensity and are easy to compare with similar measurements from other parts of the world. Results of laboratory simulations carried out using spectra obtained from the field measurements are presented to gauge how such transit hazards could affect the physical quality of tea that includes particle size distribution, colour, shape, and density. The chapter also includes detailed investigations on how vibration time in transit as well as dynamic conditions of vibrations and shock inputs on the static load within the tea pallet load inside a truck could affect the tea density and tea particles in transit.

4.2.0 Vibration/shock transit Measurements

Vibration data obtained from field data recorders for each of the routes was analyzed to determine the power density (PD) levels of vibration associated with each frequency (G^2/Hz). Appendix 2 gives a complete set of tri-axial whole journey measurement results for the Nyamache to Mombasa route. By plotting the PD values against the associated frequencies (Hz) Power Spectra Density (PSD) plots for vertical, longitudinal and lateral directions in the timer (trigger time space) and signal (above set trigger level) modes respectively for each trip were produced. The PSDs were obtained by subjecting vibration accelerations records to fast Fourier transform (FFT). The PSD function therefore represents the strength of energy as a function of frequency. This is because in real truck load shipment acceleration amplitudes occur in a random manner over a range of frequencies (Singh et. al., 2007; Martinez et. al., 2008; Lu et. al., 2008). The truck PSDs will indicate the intensity of vibration energy at each frequency band. Thus the amount of energy within specific frequency range can be obtained by integrating PSD within the frequency range. The average power density (PD) within a given band of frequencies is calculated using the equation:

$$PD=\frac{1}{BW}\sum_{i=1}^{n}(RMS\ G_i^2)/n \quad (4.1)$$

where:

G_i is a sampled acceleration value measured in g's within a bandwidth (BW) of frequencies.

n is the number of samples.

BW is the bandwidth of frequencies.

RMS is the root mean square acceleration.

The corresponding power density (PD) was then plotted against its centre frequency of the bandwidth to obtain density spectra for the analysed data using the supplied data logger software that was installed in the computer.

The root mean square acceleration (Grms) for each trip and orientation (vertical, longitudinal, lateral) was calculated using this Saver software. Grms is indeed the square root of the area under the power spectral density plot and represents the intensity of vibration (energy) across all frequencies. The analysed spectra as per above method can be used to compare levels of vibration and frequencies for different trucks, payloads, geographical regions and logistical systems (Rissi et. al., 2008). The PDS results from these truck environment measurements for the four key routes are presented under Figures 4-1 to 4-14.

4.2.1 Kambaa to Mombasa route

The Kambaa to Mombasa route was characterized by an initial short distance of earth/ murram road followed by a short distance of highly worn out and potholed section and the rest of the journey was made of bitumen surface. The route covered a total of 542 km.

The results of analysis of data from this route clearly show that the vertical direction average vibration was the highest (0.401Grms) followed by the lateral vibrations (0.230Grms) while the longitudinal vibration (0.225Grms) exhibited the least vibration intensity (Figure 4-1). A similar scenario was observed from the timer generated readings (Figure 4-2). The timer generated PSD's were lower than the signal generated spectra with average vertical, lateral and longitudinal vibration Grms of 0.091, 0.050 and 0.037 respectively. This variance in signal and timer generated PSDs may be explained by the fact that unlike the signal generated data that

recorded vibrations above a set threshold, the timer data included data from even very low vibrations with the result that when this was averaged out, the resultant Grms were relatively lower than those from signal generated data. Furthermore, timer recordings by their very nature are likely to miss out some vibrations of significant magnitude that may be outside the equipment timings.

The shock response spectrum for this route shows a similar trend with the highest acceleration figures recorded for the vertical direction and the least accelerations for the longitudinal direction (Figure 4-4). The highest vertical shocks of 10G were recorded between 400 to 700 Hz. These shocks could be attributed to uneven road conditions, due to potholes, railway crossings, unmarked speed pumps and even corrugations on murram and dirt sections of the road.

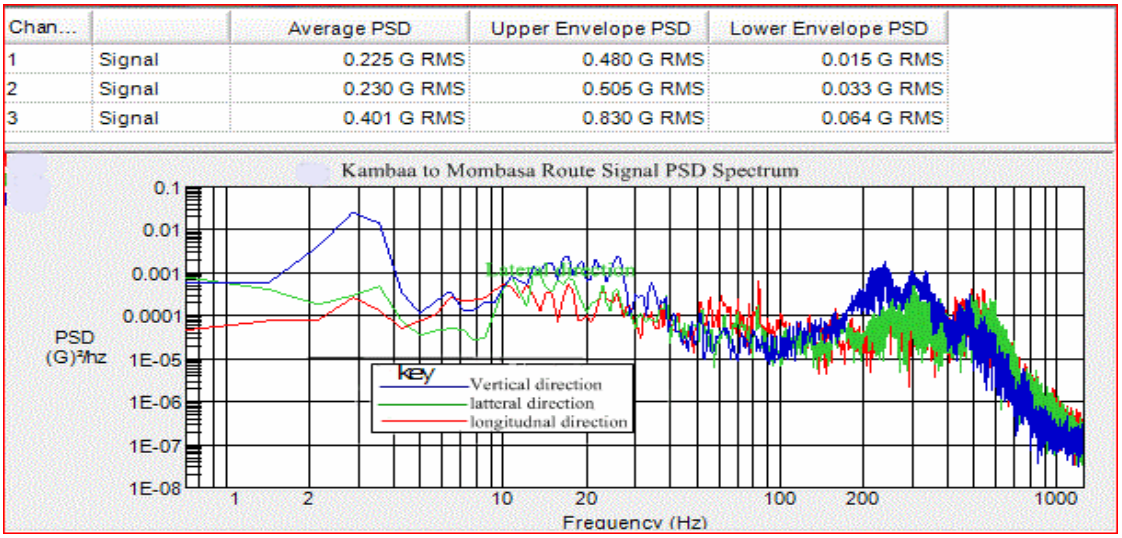

Figure 4- 1 Kambaa to Mombasa route signal generated power spectra density (PSD) - left side

Another important observation is that there is a significant variance between vibration magnitudes in the upper and lower PSD envelopes for both timer and signal generated data (Figure 4-2 and 4.3) respectively. For instance, the signal generated vibrations along the vertical plane (Figure 4-3) for the higher envelope is 0.830Grms compared to only 0.064 Grms for the lower envelope. A similar trend was obtained for the timer generated spectra where for the vertical direction, higher and lower envelope Grms are 0.636 and 0.001 respectively. The highest vibrations were experienced at the frequency around 2 to 4 Hz. moderately high levels of vibration were also experienced at frequencies around 12 to 30 Hz and still lower at 250Hz.

(Figure4-1). The highest vibrations for this route are higher than both ISTA and ASTM maximum truck laboratory simulation recommended figures of 0.242 and 0.519 respectively. Clearly this implies that both ISTA and ASTM testing methods may not be adequate for pre-testing goods destined to this environment to guarantee no or minimal transit damage of the packaged goods.

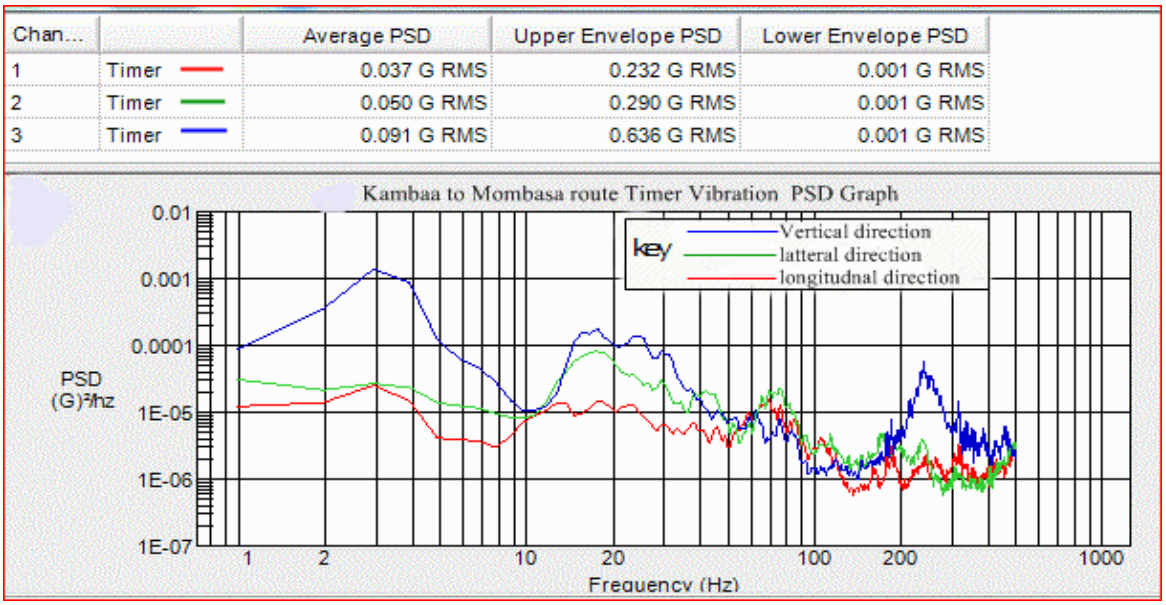

Figure 4- 2 Kambaa to Mombasa route timer generated PSD

Another observation for signal generated spectrum for this route Figure4-1 is that below the frequencies of 30Hz both lateral and longitudinal vibrations levels are lower than those of vertical direction. Above this frequency the vibrations on all three directions are similar. This contradicts the results of Singh et. al.(2006) who proposed 20Hz as the dividing line for the variance.

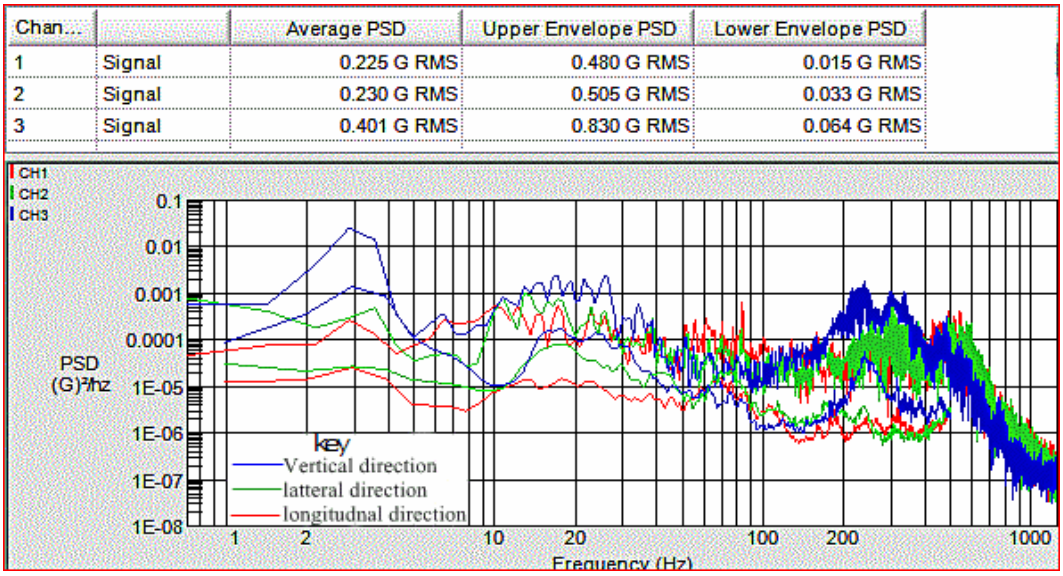

Figure 4- 3 Kambaa to Mombasa route signal generated PSD showing upper and lower envelope.

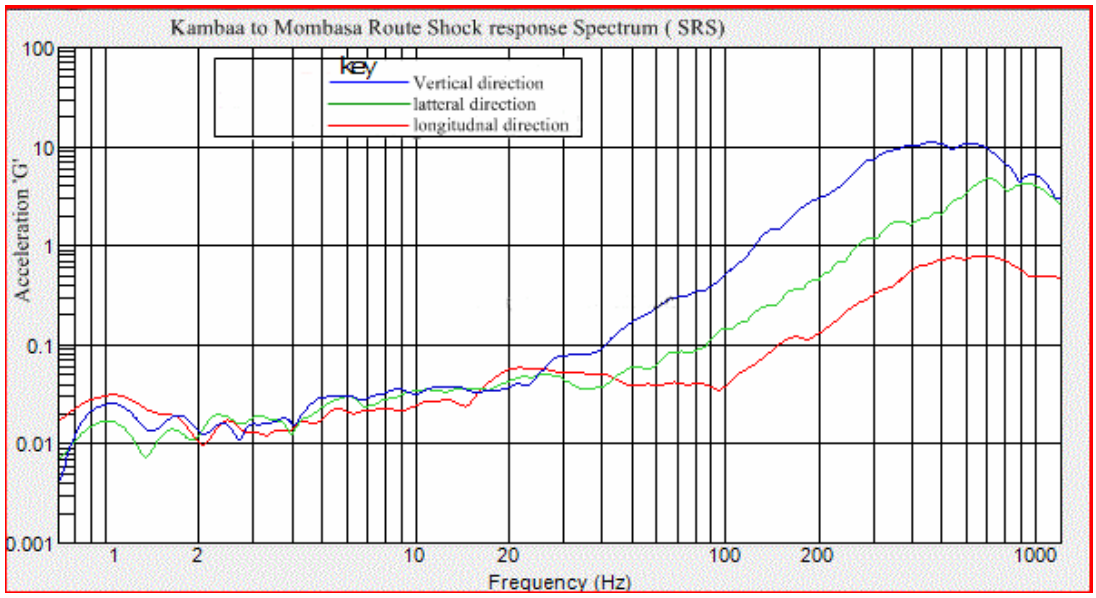

Figure 4- 4 Kambaa to Mombasa route Shock response spectrum (SRS)

Shock response spectrum levels for this route (Figure 4-4) are relatively high at maximum 10G compared for instance to the Chebut route at below 1G (due to low shock levels for air-ride suspensions) but only slightly lower than Nyamache route that registered shocks slightly more than 10G.

4.2.2 Michimikuru to Mombasa route

The route was characterised by dirt, gravel and stony section for 10km Figure 3-5 and 3-6 and the rest, tarmac road to Mombasa. The route had many unmarked speed control bumps between Michimikuru and Nairobi that clearly could result in high shocks. The truck was fitted with two measurement instruments, one on the right and the other on the left rear sides. This was basically to establish if there was any significant difference in vibrations on both sides of the truck. The results indicated that just as in the previous route of Kambaa to Mombasa, thye vertical direction recorded the highest vibration while the longitudinal direction showed the lowest vibration impacts.

Another important observation on this route is the fact that the vibration levels were significantly higher than those of the Kambaa to Mombasa route even though the same truck and driver was used in both routes. While the Kambaa to Mombasa route had the higher envelope power spectral density of 0.830 Grms and the average at 0.401Grms (Figure4-3), that of Michimikuru route recorded 2.110 Grms and 0.842 Grms respectively. It is therefore reasonable to conclude that the Michimikuru to Mombasa route subjected the cargo to relatively much higher vibration impacts compared to the Kambaa route. In other words, goods carried on this route were more likely to be damaged if adequate protection was not provided. Furthermore, the average vertical direction Grms of 0.842 is significantly higher than the recommended truck transport test levels by both ISTA and ASTM of 0.242 and 0.519 Grms respectively. It is therefore reasonable to conclude that both ISTA and ASTM's truck transport pre-shipment testing levels may not be adequate to guarantee in transit goods safety for this distribution environment. The only way to overcome this is by use of the focused environmental data for pre-shipment testing of goods as generated from this research.

The signal generated power spectral density (PSD) plots for both the right and left sides are shown under Figures 4-5 and 4-6. A comparative spectrum plot for the left and right side indicates that the left side vibrations are higher than those of the right side for similar location on the truck rear position.

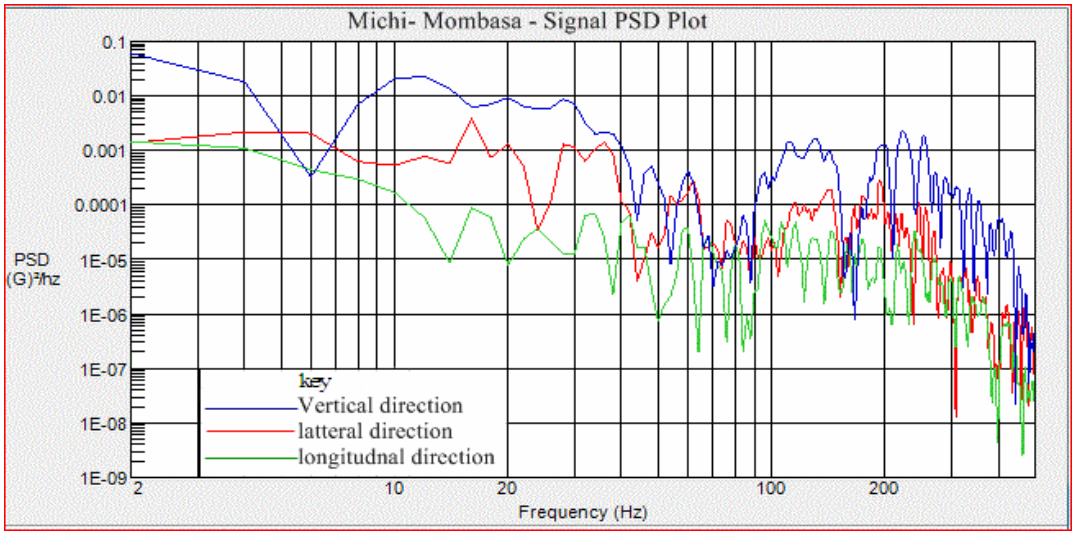

Figure 4- 5 Michimikuru to Mombasa route signal generated PSD (right hand side)

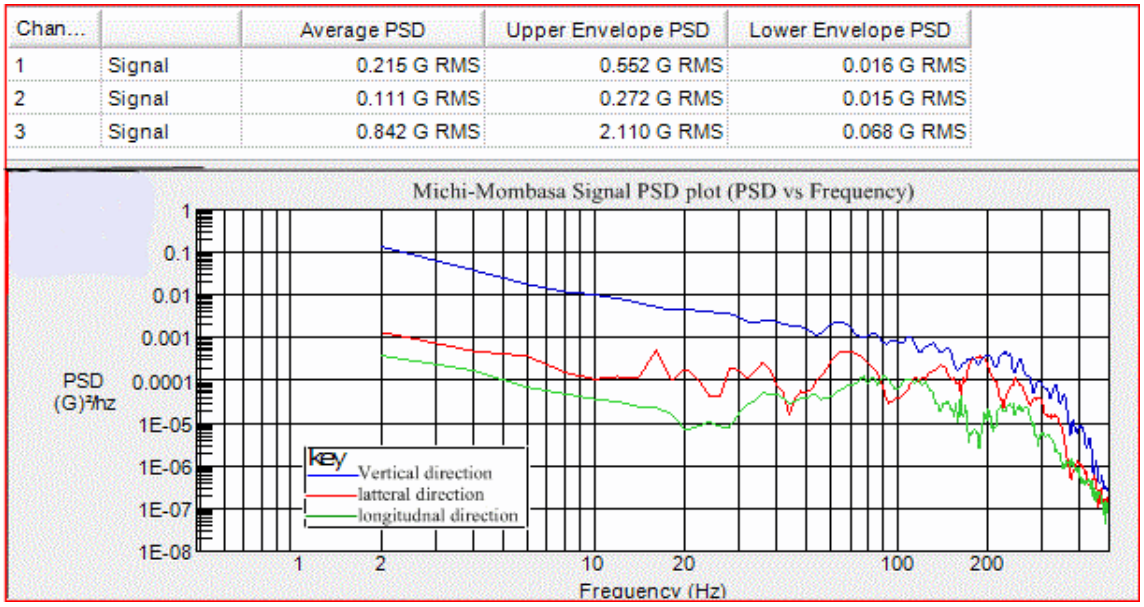

Figure 4- 6 Michimikuru to Mombasa route signal generated PSD (left side)

This scenario may be explained by the fact that the left side of the road was often more rugged and (lower than the right side) because of camber, leading to higher vibrations experienced by the truck on this side. A rather remote but possible explanation for this variance could be due to the difference in vehicle spring mass behaviour with left spring mass exhibiting a relatively higher excitation output for a similar input signal. Nevertheless, the higher vibrations on the left side have been mentioned (though no actual figures shown) by Singh et. al.(2006) .

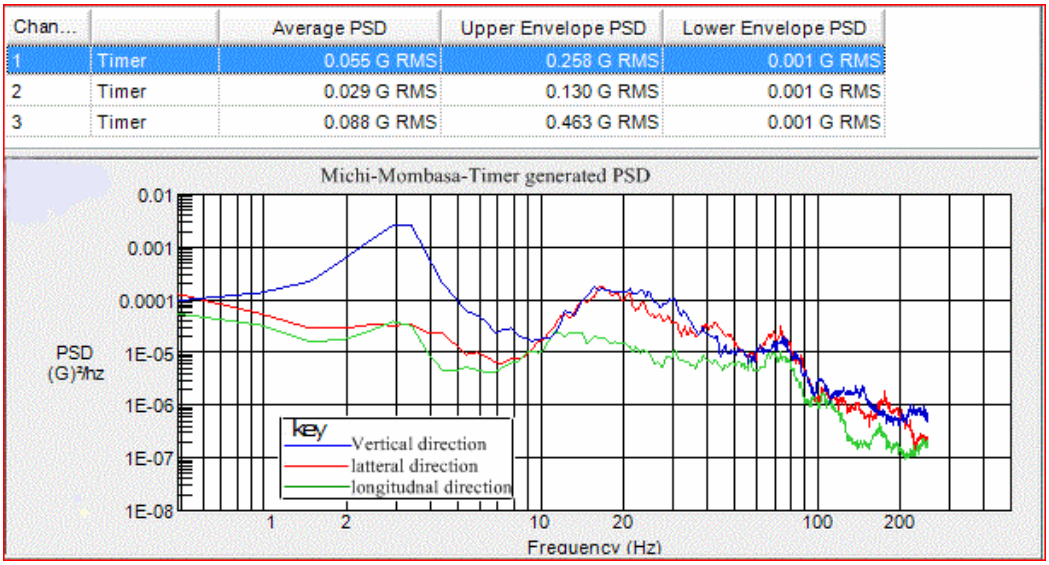

Figure 4- 7 Michimikuru to Mombasa route average timer generated PSD

Similar to the Kambaa to Mombasa route results and other previous studies carried out

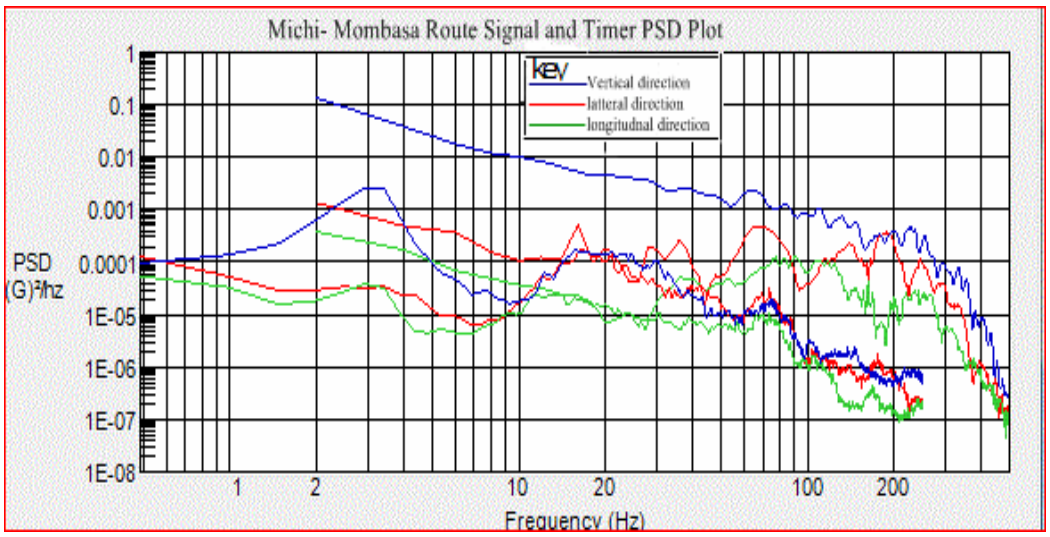

Figure 4- 8 **Michimikuru to Mombasa route signal and timer comparative power spectral density PSDs**

elsewhere (Singh et. al.2006; 2007), the signal generated vibration levels was higher than the timer generated one (Figures 4-7 and 4-8) for the same reasons as earlier advanced for the Kambaa situation.

4.2.3 Nyamache to Mombasa route

Nyamache Mombasa route Figure 3-2 had some earth road sections and the rest tarmac with several unmarked speed control road bumps. Appendix 7, shows the speed and locational data for this route while Appendix 8 gives the trip summary.

The spectra plots for this route indicate high vibrations around 1 to 2 Hz frequencies. As in the previous routes the vertical direction had the highest vibration/shock readings while the longitudinal direction had the lowest vibration impacts. Figures 4-9 shows the signal generated PSD for the route. Strangely, the vertical vibration remained higher than vibrations in the other directions throughout all the frequencies. Both ISTA and ASTM recommended truck testing levels are significantly lower than this route's average vertical direction Grms of 0.981. The upper envelope Grms for this route stands at 1.891.This again proves that both ISTA (0.242) and ASTM (0.519) test parameters may not be appropriate for use by packaging designers to obtain optimal designs for this distribution channel.

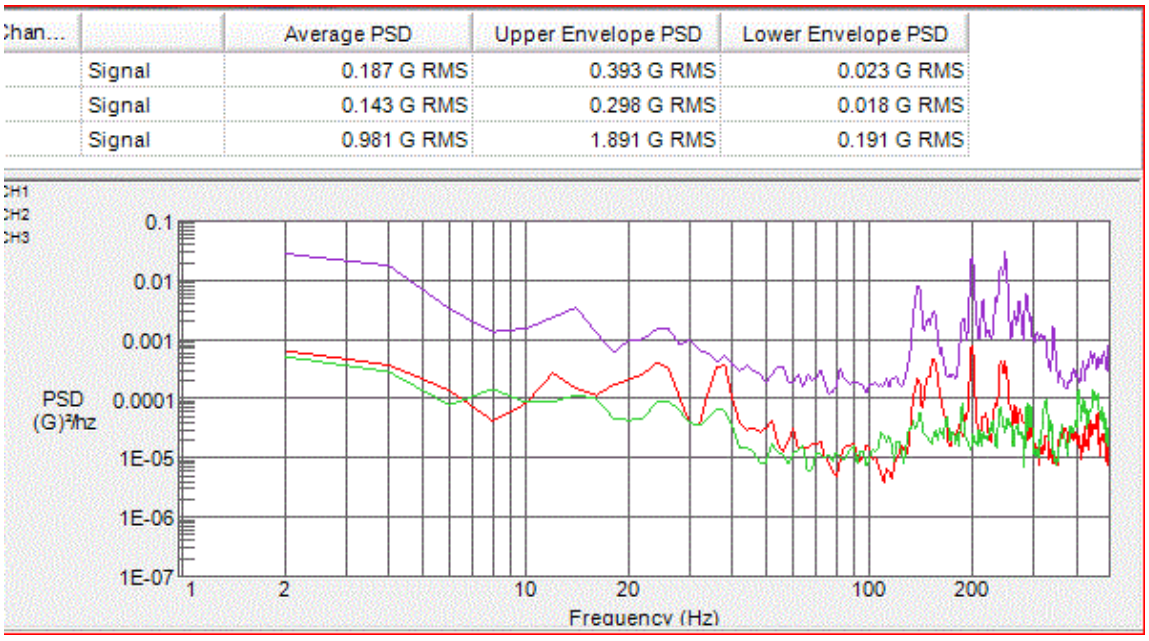

Figure 4- 9 Nyamache to Mombasa route signal PSD

Just like in the previous two routes, the signal generated power spectral density plots have higher readings compared to the corresponding timer generated spectra (Figure 4-10).

Chan...		Average PSD	Upper Envelope PSD	Lower Envelope PSD
1	Timer	0.033 G RMS	0.213 G RMS	0.000 G RMS
2	Timer	0.024 G RMS	0.211 G RMS	0.001 G RMS
3	Timer	0.084 G RMS	0.610 G RMS	0.000 G RMS

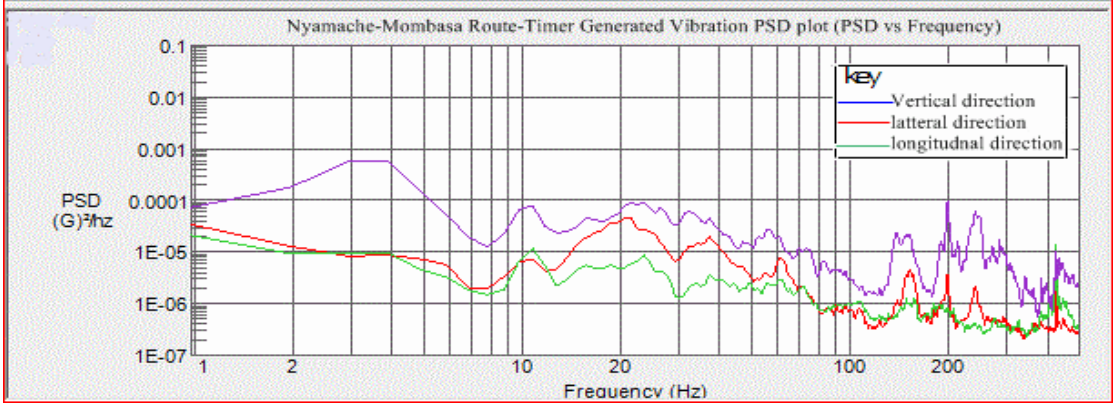

Figure 4- 10 Nyamache to Mombasa route timer generated PSD

Figure 4-11 shows the shock response spectrum for this route with highest level above 10G which is higher than that of Kambaa route. This may have been due to the many unmarked road bumps on this route similar those found on the Michimikuru route.

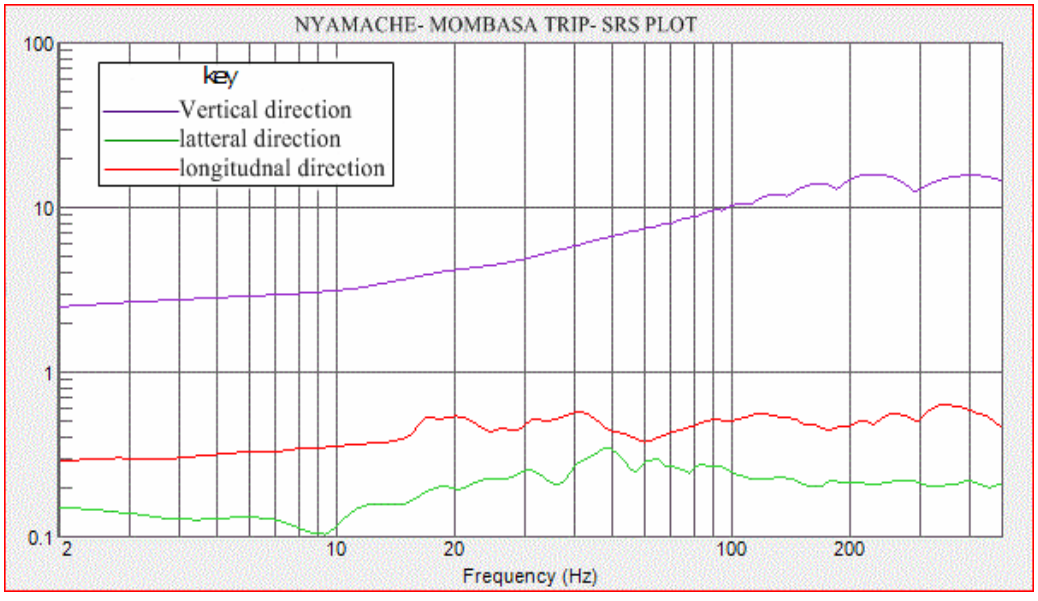

Figure 4- 11 Nyamache to Mombasa route SRS

Both ISTA and ASTM recommended truck testing levels are significantly lower than this route's average vertical direction Grms of 0.981. The upper envelope Grms for this route stands at 1.891.This again proves that both ISTA (0.242) and ASTM (0.519) test parameters may not be appropriate for use by packaging designers to obtain optimal designs for this distribution channel. Carrying out pre-shipment tests for packages using the developed protocol from this research is preferable in order to optimize pack designs.

4.2.4 Chebut to Mombasa route

This route had bitumen surface throughout. The truck for this route was fitted with a leaf spring suspension on the front axle and an air-ride suspension at the rear. This is unlike the trucks used in the previous three routes that had leaf spring suspensions on both the front and rear axles. Power density spectra for this route indicate that the vertical direction had the highest vibration impacts followed by the longitudinal direction while the lateral direction had the least. This differs from the rest of the routes where the lateral vibrations are second in vibration magnitude to the vertical vibrations. The higher longitudinal vibrations may have been due to space left between the cargo and vehicle body that allowed cargo to slide against each other and the vehicle body due to truck accelerations. The highest Grms were recorded at a frequency of 2 to 3 Hz. in all directions for both signal and timer generated spectra (Figure 4-12).

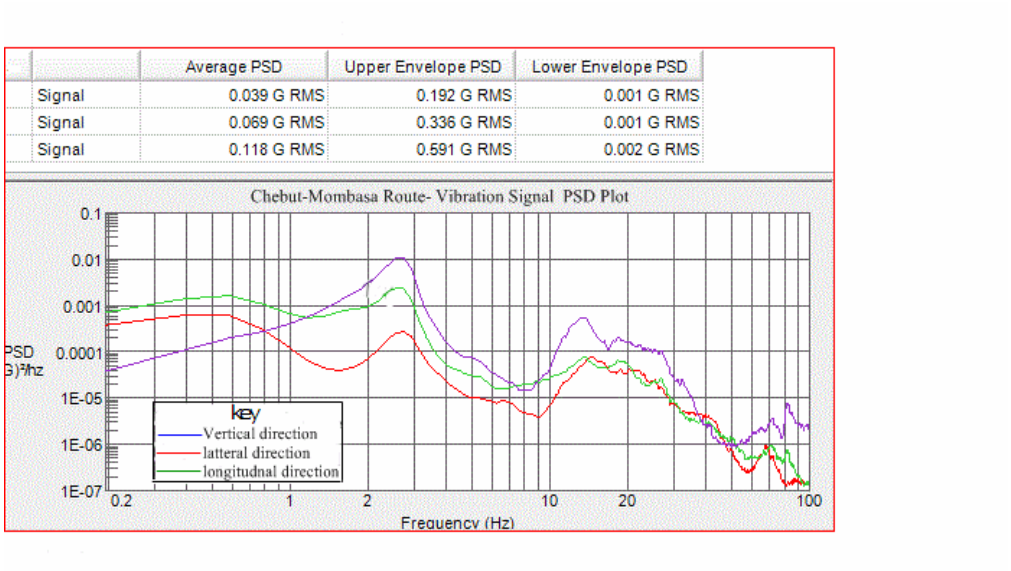

Figure 4- 12 Chebut to Mombasa signal generated PSD

The highest recorded average signal generated vertical spectrum was 0.118 Grms and the upper envelope spectrum stood at 0.591Grms.

The comparative timer generated average vibration was 0.059Grms and the upper envelope vibration stood at 0.29 (Figure 4-13). This indicates that this route had the lowest vibration outputs compared to the other three routes which recorded relatively higher vibration levels.

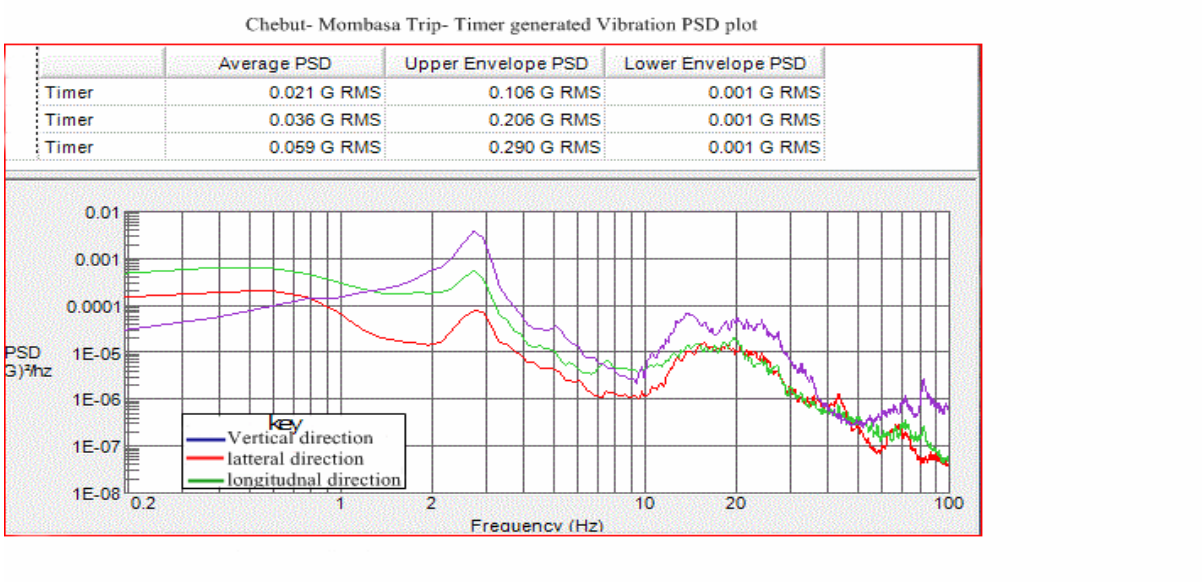

Figure 4- 13 Chebut to Mombasa route timer generated PSD

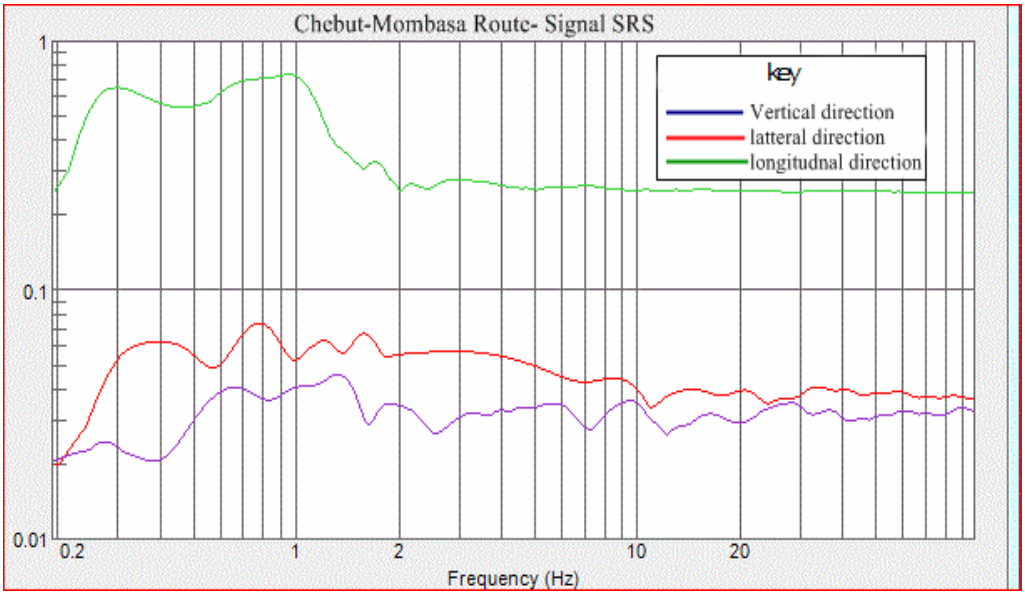

Figure 4- 14 Chebut to Mombasa route shock response spectrum

The highest Shock Response Spectra (SRS) recorded for this route is again below 1G (Figure 4-14). Martinez et. al. (2008) reported that air-ride suspensions tended to have significantly lower vibration impacts or Grms compared to leaf spring suspensions. The results in this case agree with the observations of Martinez et.al.(2008). This implies that air-ride suspensions are likely to transmit relatively less damaging vibration impacts on the carried cargo. However, leaf springs are known to be more versatile for rough terrains hence their suitability in those areas where road surfaces have either earth or gravel finish as in the other three routes investigated in this experiment. The Chebut to Mombasa route happened to be the only route of the four with an all bitumen surface and for this reason the air-ride suspensions were indeed more appropriate. Accelerations for this route also show a fairly even trend (Figure 4-15).

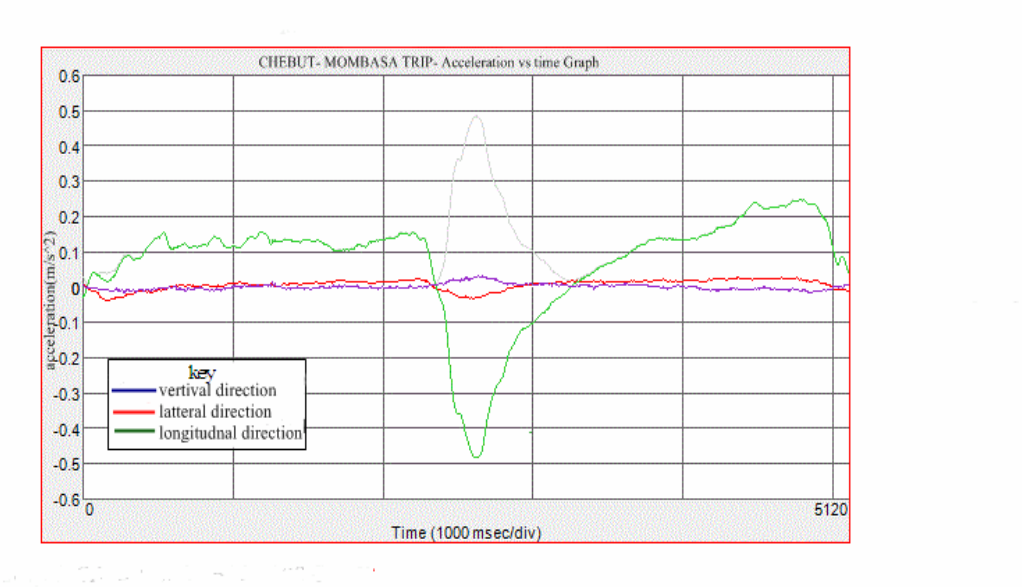

Figure 4- 15 Chebut to Mombasa route acceleration graph

From the measured road spectra on the four routes a composite upper envelope spectrum was worked out which is the mean value of the four vertical spectra of the routes used (Table 4.1).

Table4. 1 Composite of upper envelope Spectra (Grms) for all routes used

Route	**Vertical direction**	**Lateral direction**	**Longitudinal direction**
Kambaa- Mombasa	0.830	0.505	0.481
Michi- Mombasa	2.110	0.552	0.272
Nyamache- Mombasa	1.891	0.298	0.393
Chebut- Mombasa	0.600	0.199	0.373
Composite Grms	**1.358**	**0.389**	**0.634**

These represent events that have the highest impacts and could be responsible for package/ product failure if the same are not considered during package design process. The spectra indicate the vertical direction had the highest impacts on goods in transit (1.358 Grm**s),** followed by the longitudinal direction (0.634 Grms) while the lateral impacts had the least effect on goods in transit (0.389 Grms). In addition, the Michimikuru route had the worst vertical impacts, followed by Nyamache route while the Chebut route had the least damaging impacts on goods. The worst lateral impacts were experienced in Kambaa and Michimikuru routes at 0.505 Grms and 0.552 Grms respectively. The highest longitudinal impacts were within the Kambaa route at 0.481 Grms while Michimikuru route had the lowest longitudinal impacts at 0.272Grms.

In general vertical impacts may be attributed to vibrations due to vehicle structures, tyres and suspensions. The last two will very much depend on the nature of road surface with uneven road surfaces especially those noted on both the Michimikuru and Nyamache routes particularly on the earth road sections. Both routes had also many unmarked speed control bumps that contributed to high shock impacts. On the other hand, the Chebut route was mainly highways with smooth surface that offered fewer impacts to the cargo especially and further the truck used on this route was fitted with air-ride suspensions that resulted in lower vibration and shock impacts.

Longitudinal impacts were mainly caused by the movement of goods during accelerations and decelerations and depend very much on the driving habits of the truck driver. These impacts were more severe where the cargo arrangement would not assume a cubic profile and had spaces that allowed goods to slide along during vehicle accelerations. Lateral impacts was mainly due to vehicle swings and sudden turns which may be to some extent due to the driving habit and the nature of the roads especially on the Michimikuru and Kambaa routes that had very sharp bends.

Based on the signal generated PSD plots for the four routes used, an average composite simulation spectrum (Table 4.2) was developed that could be used for pre-shipment testing of goods within this distribution environment. Appendix 3 gives further details of how this average composite was derived from the signal generated vertical power densities (G^2/Hz) obtained at various frequencies for the four routes. Appendix 3 gives the calculations of the average GRMs four the four routes used.

Table4. 2 Composite simulation spectrum for Kenya (vertical direction)

Spectrum #	**Frequency(Hz)**	**Power density (G^2/Hz)**
1	1	0.009
2	2	0.03
3	3	0.03
4	4	0.01
5	7	0.0002
6	20	0.0004
7	100	0.00002

From the focused transit measurement of the Kenyan distribution system, it is quite clear that the general pre-testing protocols from both ISTA (0.242 Grms) and ASTM (0.519Grms) are far too low from the actual road conditions in Kenya and will not allow packaging designers from this region to optimize their designs in order to avoid load failure in transit. The newly developed pre-shipment spectrum for the Kenyan distribution environment (Table 4.2) from this research will allow packaging designers in this part of the world to optimize their designs and avoid over-packaging and save costs as well as ensuring the packages meet the current packaging minimum requirements of the various target markets.

Figure 4-16 shows the actual road spectrum for one of the routes used in this work against the actual spectrum generated by the exciter unit. Apart from a few low impact vibrations at the frequencies of 45 to100 Hz, the actual road spectrum was almost reproduced during the simulation exercise.

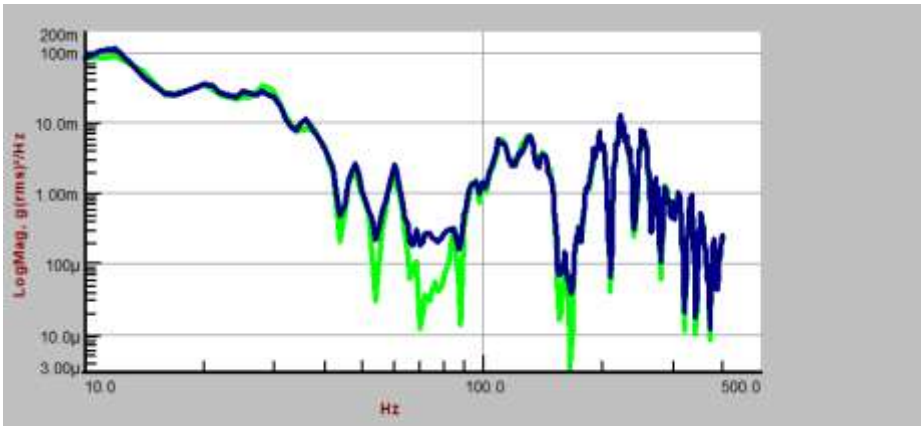

Figure 4- 16 Laboratory simulation Shaker spectrum output versus actual road

(Actual road spectrum (green) and the shaker unit spectrum (blue)

4.3.0 Effect of laboratory truck transport simulation on tea physical quality

4.3.1 Introduction

Tea physical qualities such as particle size distribution, bulk and tapped density, particle morphology or surface characteristics are important tea quality parameters that are also linked to its market value. Changes in any of the above mentioned tea physical parameters in transit will undermine its quality and it is therefore important that all efforts are made to preserve them. Transportation including road transport involves such hazards as vibration and shock whose effect is not well understood and if appropriate protection is not provided, they would affect the integrity of tea particles in transit. Such protection can be optimally provided only when the level and effect of the hazards is well understood. While compression by normal stress can be reproduced and mathematically described, the influence of shocks and vibrations remains poorly understood (Linemann et. al., 2004).

4.3.2 Effect on tea particle size distribution

Tea particle size is an important quality aspect in the tea trade. This is because tea is commercially graded by size and this also has a bearing on the monetary value attached to the tea. Changes in the particle size during transit are undesirable as this would ultimately alter the 'intended quality' of the product. Understanding how transit hazards such as vibration/shock or compression may affect the particle size of tea would inform the package designer on the appropriate packaging/cushioning to use in a given distribution environment in order to preserve the product integrity.

During the actual transit hazards simulation in the laboratory under different treatments, the changes in particle size distribution was closely monitored. Particle size analysis for each treatment was carried out using sieves and the fractions on each sieve weighed. The general observation was that although the mother batch used consisted of tea particles of uniform size range of 2mm-1mm only, there was continual reduction in the proportion of these particles as the simulation progressed that gave rise to the build-up of the proportion of small particle fractions over the sieve meshes 500, 250, 125 and 63 microns (Figure 4-17).

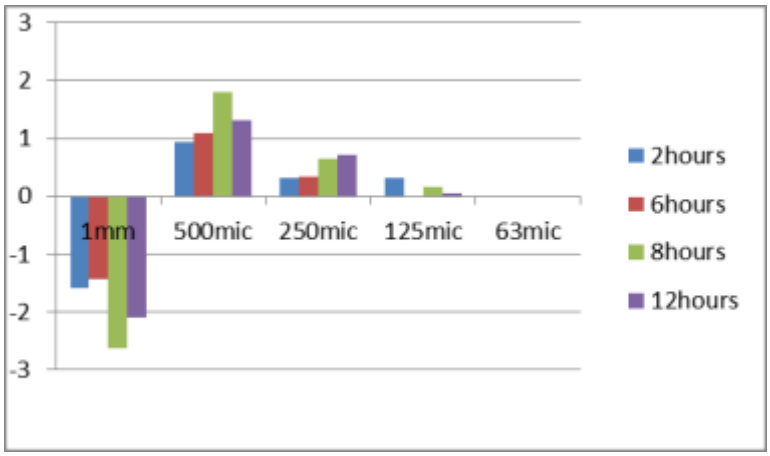

Figure 4- 17 Changes in particle size proportions during the simulation

There was a gradual reduction in proportion of 2-1mm particles with the highest proportion loss attained after 8 hours of simulation. A similar but converse trend was observed on the build-up of smaller tea fraction collected over the 500 micron sieve that peaked after 8 hours of treatment. On the other hand, the proportion of tea fraction collected over the 250 micron sieve continued to build up over the entire period while the fraction over 125 micron had the highest proportion of accumulation in the initial period of treatment and continued to diminish as the

treatment progressed. The logical general explanation for this behaviour is that in the initial stages of the simulation exercise the larger 2-1mm particles dominated the degradation process with the 500micron mesh being the main net beneficiary of this loss up to the peak at 8hours. After the peak the 500 micron sieve appeared to be the main donor of particles downstream with only limited amount originating from other meshes. The 63 micron sieve collected mainly fluffy material which though contributed negligibly in terms of mass proportion, had a major impact on part of quality agenda.

The average mean particle size distribution for all the simulated routes showed a similar trend. There was a general reduction of mean particle size distribution from 1.5mm at the start up or mother batch for the various static loads up to 350gm which had the lowest average mean size of tea particles at 1.38mm (Figure 4.18).

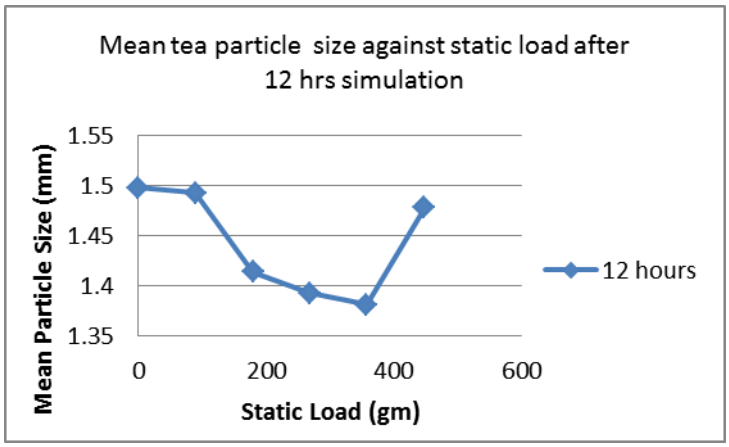

Figure 4- 18 Graph of mean tea particle size versus static load after 12hrs of simulation

This lowest mean size increased at higher static load above 350gm to arrive at average mean particle size of 1.48mm at static load of 447gm which was our highest test load equivalent to the static load at the bottom of the tea pallet load.

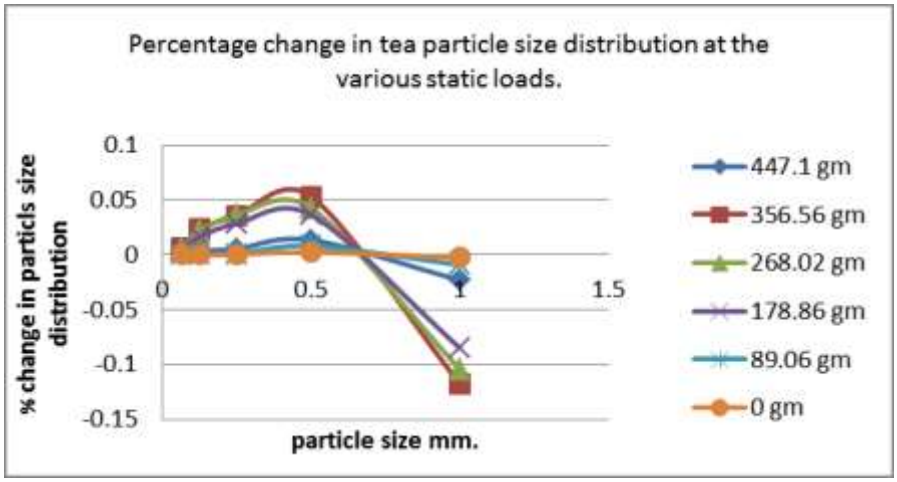

Figure 4- 19 Graph of percentage change in tea particle size proportion at the various static loads after 12 hr simulation period

Percentage change in particle size distribution for each static load (Figure 4-19) shows two distinct clusters at various static loads with the 356gm, 268gm and 178gm loads exhibiting a positive distribution for all particle size below 0.5mm with the peak at 0.25mm. The highest percentage changes in particle size distribution were recorded at 0.035%, 0.036% and 0.028% for static loads of 356gm, 268gm, and 178gm respectively. The other cluster group of percentage particle size distribution was observed at static loads of 447gm (0.0054%), 89gm (0.00073%) and the tea without static load on but experienced the simulation vibrations showing a very small percentage change in particle size distribution of 0.0001% at the corresponding peak level. The 447gm static load (representing the tea particle at the bottom of the pallet load) had an un-expectedly low particle size change consistent with its higher comparative mean particle size (Figure 4-18).

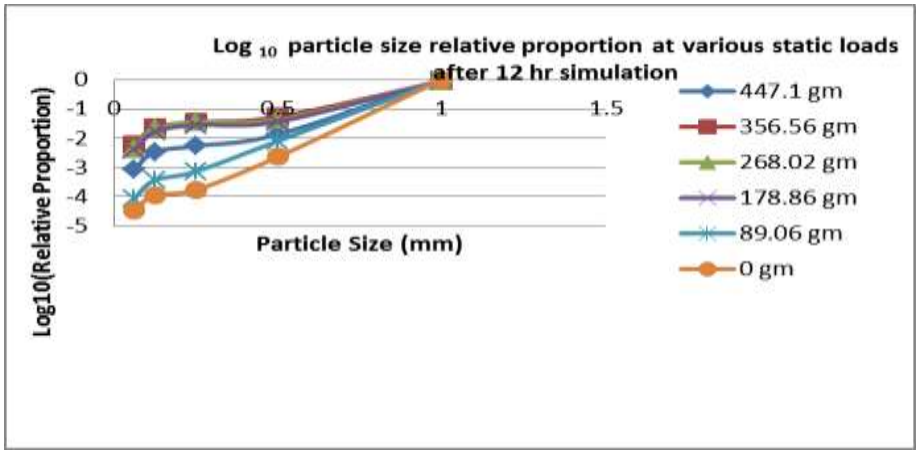

Figure 4- 20 Graph of Log_{10} of tea particle size relative proportion against static loads after 12 hr simulation period

A plot of the common logarithm ($\log_{10}$) of the relative particle size against static load Figure 4-20 shows a decreasing scenario more or less similar to the percentage change in particle size

distribution (Figure 4-19). Both cases segregate the results into two distinct groups. Figure 4-20 further indicates the proportion of each particle size fraction from1mm. to 0.063mm for each static load after the 12 hour simulation period.

4.3.3 Effect on tea density

Density of tea is an important parameter since the product is relatively bulky and its density could change with external excitation that may cause re-arrangement of the particles. As tea receives vibration input during transportation its bulk density may change due to "settling down" of the tea particles due to vibration/shock output from the carrier. The "tapped" density (due to in transit excitations) could therefore be higher than its original bulk density. If the tea further undergoes compression due to stacking load resting on it in the pallet load, its density is likely to be further increased (compact density). This work therefore reports how tea density may change in transit due to vibration/shock and compression simulated inputs and to transit time.

Density dictates the design of the package especially the retail package dimensions. Higher densities than anticipated will lead to packages having a large void space. While this is legally in order, customers could be alarmed. On the hand, low density teas tend to cause problems of fitting the expected weight into the package resulting to hold ups at the filling unit.

4.3.4 Effect of simulation time on density

The average density of tea for all treatments (static loads) including zero loading increased with simulation period. The simulation period between 0 to 2 hours showed a sharp density increase (steep gradient) while the density gradient between 2 and12 hours was much lower and this graph section exhibited gradual increase. This initial relatively high increase in density can be explained by the fact that at the initial stages there are several void spaces in the tea granular matter which are easily occupied by smaller tea particles as a result of their re-arrangement due to simulation impetus. These results in reduced volume and hence increase in density in a very similar manner to tapping, which increases the bulk density of most granular matter. As the amount of available void space for tea particles to occupy within the granular matter continues to diminish with simulation time, (after two hours or so of treatment) the rate of volume reduction is equally reduced and hence density. Eventually the density growth tails off and the maximum possible density or steady state was achieved after 8-10hrs of simulation for all the treatments. This phenomenon agrees well with observation made by Talbot et. al. (1999) on the long term granular matter kinetics of density changes with time due to vibration

input with initial algebraic growth, followed by logarithmic growth changes and finally exponential terminal decay. Perhaps what Talbot et.al, did not realize is that the final decay state is characterised by small density fluctuations around the steady state as observed by Nowak et.al (1998) which also agrees with the findings of this research.

Figure 4-21 shows the density growth with simulation time at the various static loads.

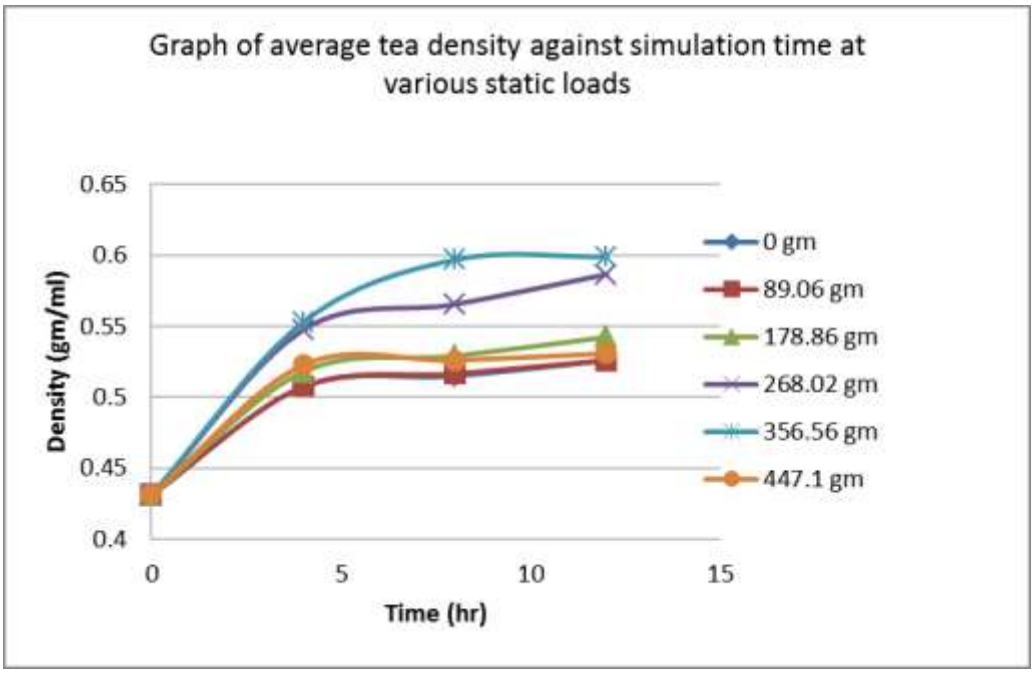

Figure 4- 21 Graph of average tea density against simulation time at various static loads

4.3.5 Effect of static load on tea density

A closer observation of the changes of tea density with the simulation time for various static loads revealed the following:

At all the treatment levels density growth curves had a similar general shape with initial steep gradient followed by a slow growth period before tailing off where the density curve appeared to flatten out at around the 10hr mark. After this point, barely any changes in density are observed and it can be argued that at this point the tea had attained its maximum density under the test conditions (Figure 4-21). The highest density growth was recorded by tea with the static load of 356.56gm while the 268.2gm had the second highest density growth curve. The third and fourth highest density growth curves were those at static loads of 178.86gm and 447.10gm respectively. The lowest density growth curve understandably was that of the

control (zero load) followed by that of tea having 89.06gm static load placed on it. It was observed that while vibration and shock inputs (control) had some effect on tea density growth in transit, the effect of compressive forces arising from "dead weight" on tea particles tended to have more prominence in determining the overall growth in tea density. In general, however, the density growth curve over time followed the magnitude of the static load applied on the tea except for that of the 447.10gm load that appeared to deviate from the norm and therefore begs some explanation.

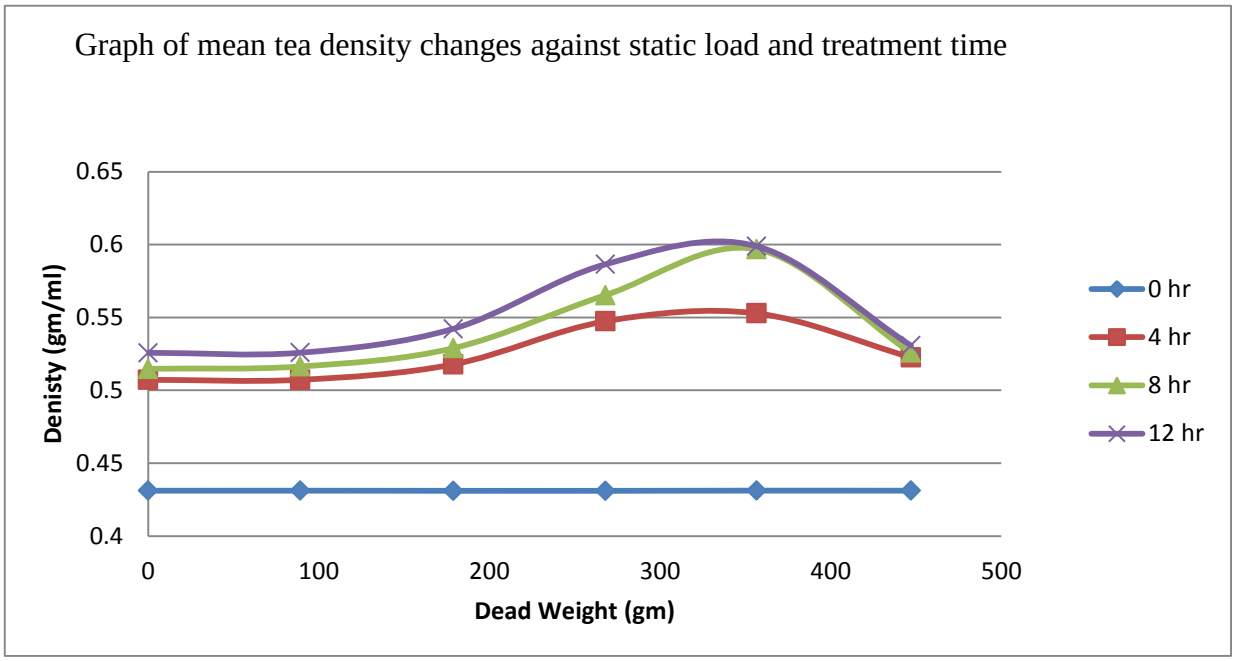

Figure 4- 22 Graph of mean tea density changes against static load for various treatment periods

When the average density levels were plotted against various static loadings for various simulation periods Figure 4-22, it was observed that the maximum densities were recorded at around 350 gm. loads after which the density sharply declined. The reason for this sudden decline in density between 356.56gm and 447.10gm static loads was most probably that at this loading the simulation system experienced a resonance such that the static load was literally "floating" and did not offer much of the expected compressive forces on tea particles below it to compact them. At this point, density increment was attributed to mainly vibration/shock dynamic forces and less to 'dead weight' static compressive forces. Effect of vibration time and static load on average tea bulk density Figure 4.22 showed the density curve was highest at 12hrs of treatment time while the 8hrs of treatment followed and the 4hrs of treatment

produced a density curve lower than the first two. The control which received no treatment remained more or less the same and the minimal density changes noted could be attributed to tea moisture content variations due to changes in relative humidity during the experiment.

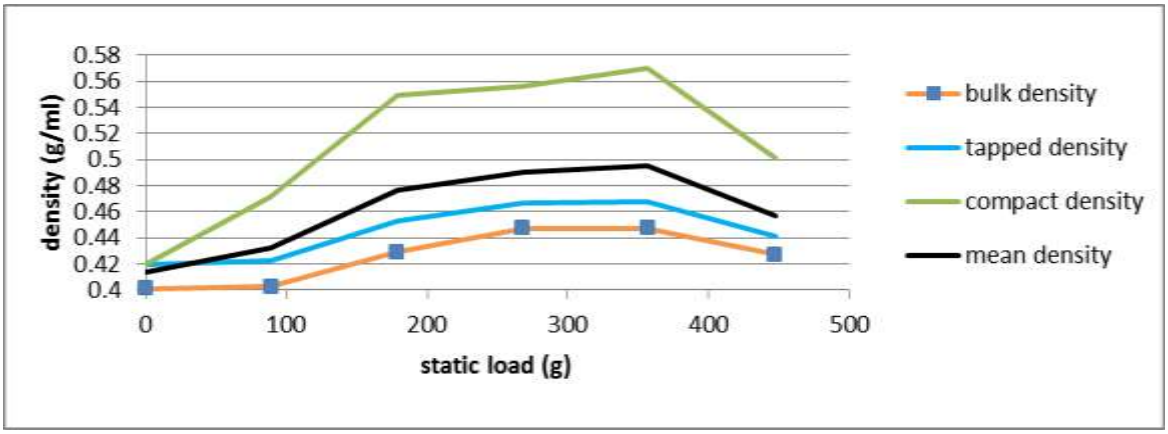

Figure 4- 23 Comparative graphs of tea densities against static load over the 12hr simulation period

Comparisons of the bulk density, tapped density and compact density Figure 4-23, showed as predicted that the compact density curve was higher than both bulk and tapped density. The compact density was achieved due to the action of static loads on tea particles that were compacted during the simulation to assume a state of minimum volume at the jamming state. At the compact density conditions, the tea particles were literally 'locked' together and restricted any inter-particle mobility. This was manifested at the macro level by reluctance of flow of tea from the test tubes even when the containers were turned upside down and therefore required some reasonable external agitation to force the tea out of the containers at the end of the experiment. It was further noted that at the "jamming" condition, the tea particles farther away from the static load pistons were shielded from the damaging or attrition forces in that the tea particles a few centimetres below the static load in the container were intact and had not received any appreciable degradation compared to the tea particles proximal to the static load.

The graphs of tea density against static load (Figure 4-22) and (Figure 4-23) almost mimic the shape of the graph for density against time (Figure 4-21) in that they all have relatively initial fast growth (steep gradient) followed by an inflection with a low gradient but rising to a maxima at the 350gm mark before experiencing a sharp decline (negative gradient). Various

densities plotted on the same axes (Figure 4-23) for bulk density, tapped density, compact density and mean density all depicted the above general graph shape with great similarity only differing in their magnitudes.

4.3.6 Tea powder "stain" column height correlation with tea compact density

During the simulation, the action of vibration and more specifically of 'dead weights" moving up and down inside the test tubes generated fine tea powder inside the tubes. This powder was transmitted downwards inside the tube following the force lines or impulses that were transmitted to the bottom of the tubes from the static loads as they moved up and down following the shaker vibrations. During this downward movement of force lines carrying with them very fine tea particles, a tea dust "stain" was left adhering to the test tube sides which was clearly visible below each static load in the test tubes except the control which did not have any load on top of the tea (Figure 4-24). The height of this powder stain column from the piston was measured as well as the distance moved by the static load pistons inside the tube from the start conditions.

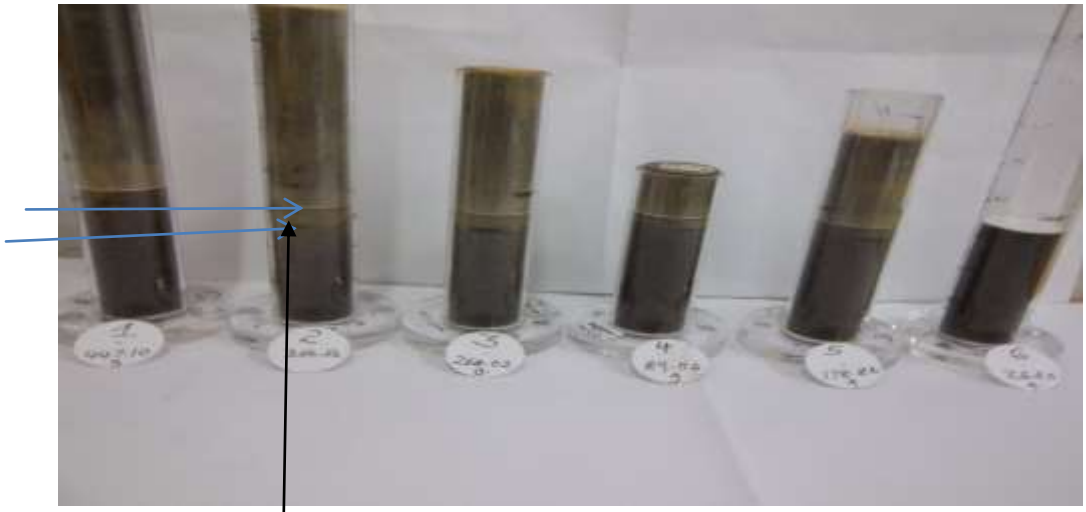

Figure 4- 24 Defined tea powder "stain" observations inside the test tubes below the static loads

(*Distance between the two arrows shows the visible tea powder "stain" column height*)

It was further observed that the graph of tea powder "stain" height inside the test tubes against the respective static loads (Figure 4-25) had a familiar sigmoid shape very similar to that of graph of density against static load (Figure 4-26).

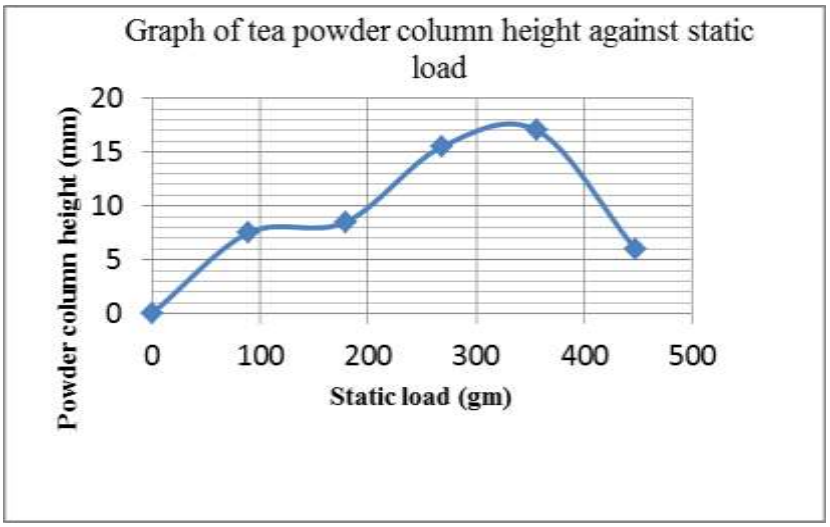

Figure 4- 25 Graph of tea powder column height against the load

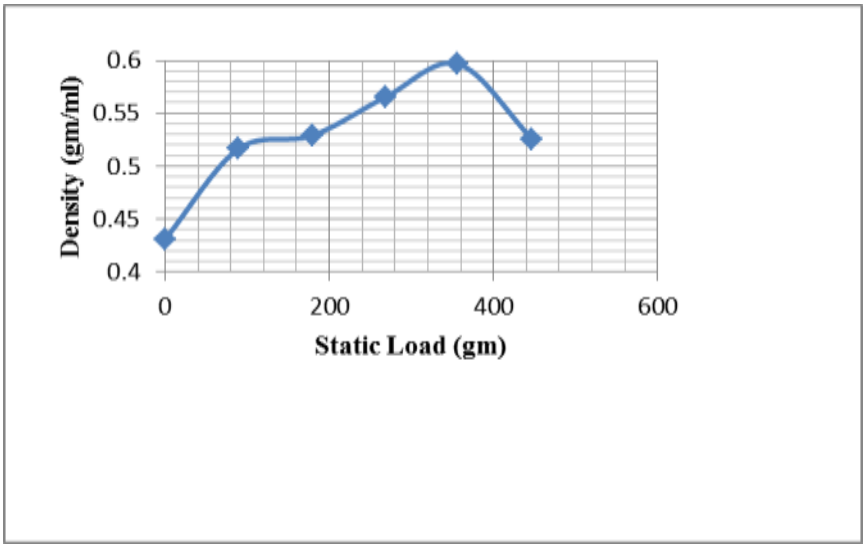

Figure 4- 26 Graph of static load against compact tea density

When a plot of powder height against its respective compact density was made (Figure 4-27), it showed an interesting correlation of 0.92. From this scenario it means that one could predict fairly accurately the compact density of tea from measurements of the powder column height inside the test tube using their linear relationship y= 0.0085x +0.4502

where:

y represents compact tea density in gm/cc

x represents the powder column height in mm

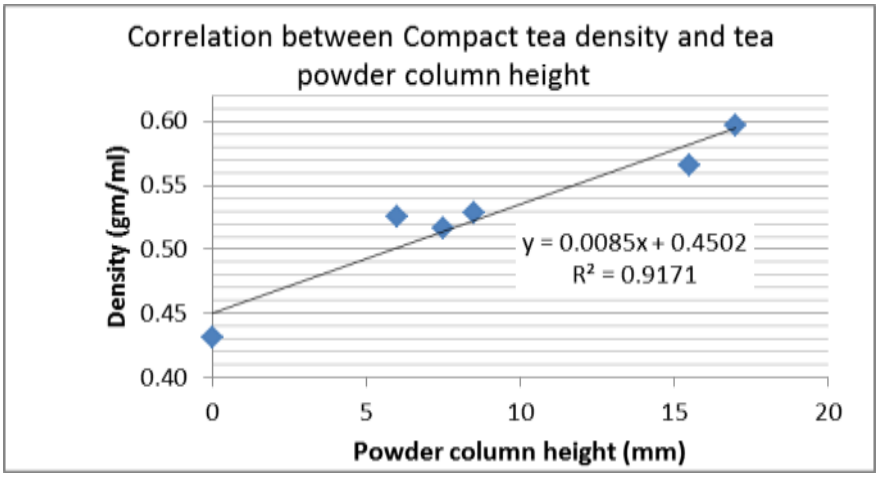

Figure 4- 27 Correlation between compact tea density and tea powder "stain" column height at various intervals of simulation

4.3.7 Static load piston travel distance correlation with tea density

During the laboratory simulation, as a result of vibration input by the shaker as well as the compression impact of the load piston, the tea volume shrunk. This ultimately resulted in the piston downward movement to occupy the void space thus created as tea particles within the test tube consolidated.

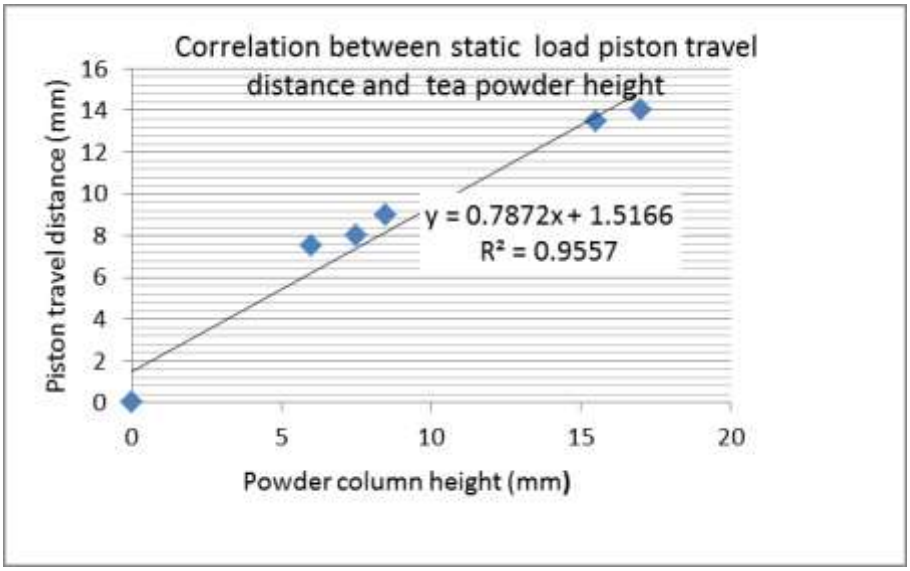

Figure 4- 28 Correlation between static load piston travel distance and tea powder "stain" column height

The distance moved by the piston from the start conditions to the end of the experiment was measured at various intervals and was plotted against the height of the tea powder 'stain" below it (Figure 4-28). There was a high correlation between both these values with factor of 0.96. This means that the distance moved by piston inside the test tube could fairly accurately be used to predict the height of tea powder "stain" below it using the linear equation y= 0.7872x+1.5166.

where:

y represents total distance travelled by the static load piston inside the test tube in mm

x is the tea powder "stain" column height below the static load in mm

The fact that tea powder dust column height inside the test tubes had a high correlation with tea density (Figure 4-27) and distances moved by the static load pistons also had reasonably high correlation to the powder height (Figure 4-28), implies that the distance moved by the "dead weight" piston is equally correlated to the tea powder density. This assumption may be summarized by the variation equations as follows:

If $P \alpha H$ (4.2)

then $P=k H$ (4.3)

and if $H\alpha D$ (4.4)

then $H=cD$ (4.5)

therefore $P= K HD$ (4.6)

where:

P is distance in mm moved by the piston inside the tube

H is the powder "stain" column height in mm below each static load in test tube.

D is the tea compact density (gm/cc) in the test tube

k is the constant for variation of piston distance against powder column

c is the constant for variation of powder height and tea density

K is the joint variation constant for both variation equations (4.3) and (4.5).

One can therefore argue that it is possible to predict the compact density of tea by measuring the distance moved by the piston within the sample tube or by measuring height of the tea powder "stain" adhering to the inside of the sample tube below the static load by using the respective equations above. This clearly implies that both the tea powder "stain" height and distance moved by piston inside the sample tube are related to the force impulses generated by the static load pistons inside the tubes. This close correlation further proves that the bulk of these force impulses generated by the static load on top of the tea inside the test tubes were transmitted vertically downwards to the bottom of the tubes as earlier assumed during the rig apparatus design. The validity of the assumptions made using the variation equations (4.2) to (4.6) was further tested experimentally.

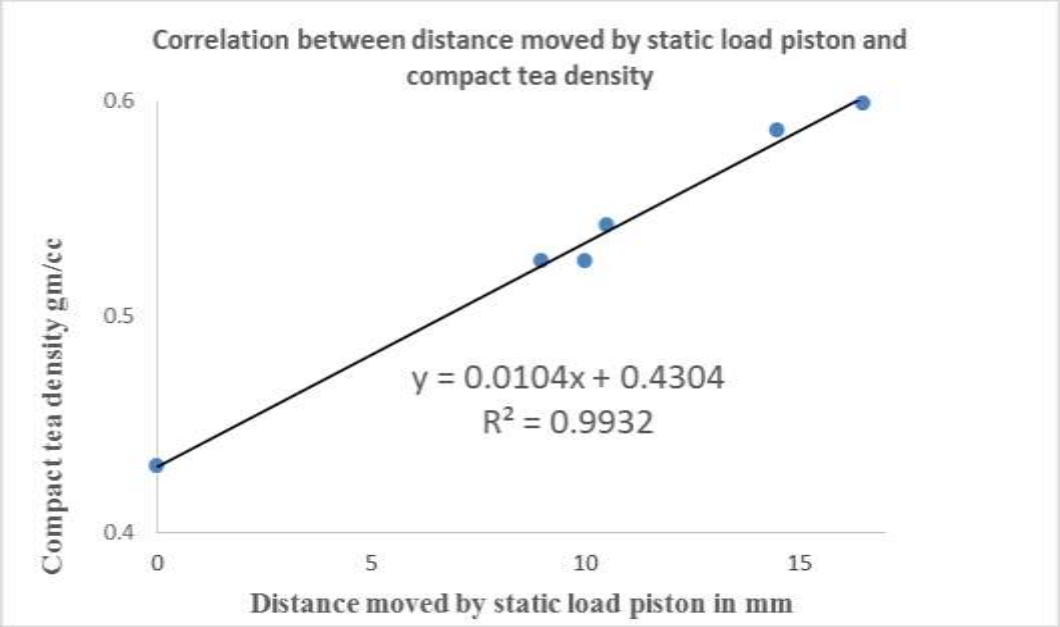

Figure 4- 29 Correlation between total distance moved by "dead weight" piston inside the tube and tea compact density

Figure 4-29 shows a correlation graph between distance moved by the static load piston and the compact density of tea in the tube during the experiment. This correlation with factor of 0.99 validates the assumption made earlier in equation (4.6). Appendix 10 gives the regression analysis of this relationship. The equation of the relationship is y= 0.0104x +0.4304

where :

y is compact density tea in gm/cc after simulation

x is the distance in mm moved by the static load piston during simulation

4.3.8 Effect vibration/shock/compression on tea particle morphology

The size and surface shape of granular matter has a major effect on its flow characteristics during its handling or processing. In general, smaller granular materials such as powders have better flow properties compared to their larger cousins. The shape of granular matter determines how various particles relate with each other and any changes on the granular matter morphology will therefore affect its flow properties. Such changes could for instance lead to particle surfaces interlocking thus resisting its flow during processing or handling. Elongated particle shape will resist flow compared to rounded granules while rough and non- rounded shaped particles are known to be more likely to offer resistance to flow than their smooth counterparts. Understanding changes in tea particle morphology as a result of transit vibration,

shock or compression will therefore allow tea packers to predict its flow behaviour while designing handling equipment such as storage and discharge hoppers and even conveyance machines. Changes in tea particle surface due to attrition in transit will lead to new surfaces created that also may affect the colour of the consignment.

The morphology changes of tea particles was monitored using Scanning Electron Microscope (SEM) for each size fraction and the micrographs were then compared for any differences in particle size and shape during the simulation exercise. The various micrographs are represented in Figures 4-30 to 4-34.

Figure 4-30 represents tea particles that passed through a 2mm pore screen and collected over a 1 mm pore screen (mother batch). Closer observation shows these particles are fairly rounded. The particle surface has visible several external voids and a fairly rugged surface. The average particle size was approximately 1.5mm. These particles due to their rounded nature will appear to promote particle flow during conveyance and storage but impeded by particle surface ruggedness. Since this is the true size of the BP1 grade any damage to the particle size will affect not only its physical and liquoring characteristics but possibly its flow ability as well. Such a situation could lead to disruption of its smooth conveyance and packaging operations.

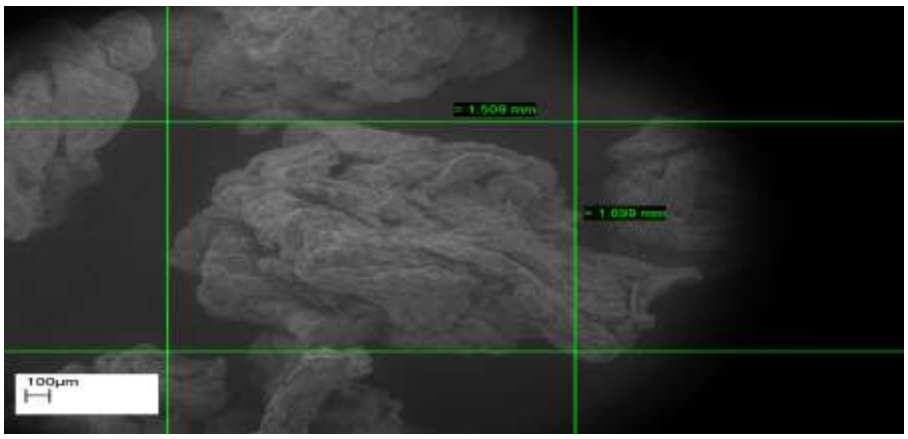

Figure 4- 30 Scanning electron micrograph of tea particle through 2mm and over 1mm sieve pore (x100 magnification)

Upon undergoing actual journey simulation treatment using an electrodynamics shaker, the tea particles (2-1mm) underwent gradual breakdown over time and there was reduction in the 2-1mm particles while tea fractions collected over meshes 500 microns, 250microns, 125 microns and 63 microns gradually increased.

Figure 4.31 shows SE micrograph of particles collected over 500 micron pore size screen but which were smaller than 1mm pore size. While the surface of the particles still remained rugged after their breakdown due to simulation action, their shape assumed a slightly less round profile compared to those of the mother batch. They still maintained uneven surface and their average size was around 750 microns.

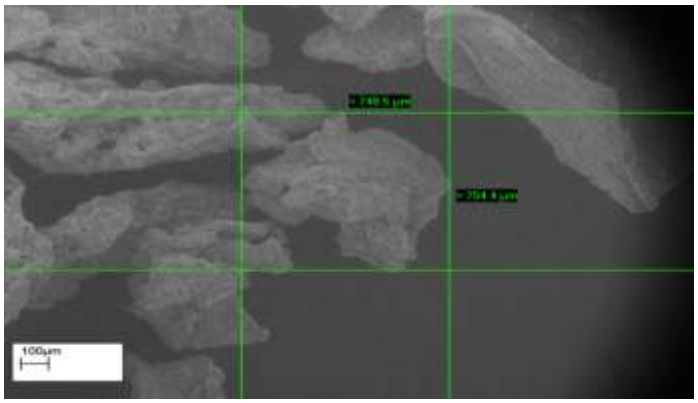

Figure 4- 31 Scanning electron micrograph of tea particle through 1mm and over 500 microns pore screen (x150 magnification)

Tea particles collected over the 250 microns pore size but which had passed through 500 micron pore size still had rugged surface but were more elongated in shape compared to the mother batch (Figure 4-32a and b).

(a)

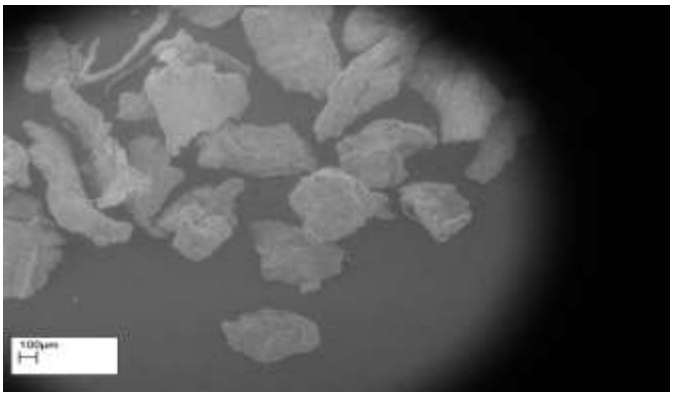

(b)

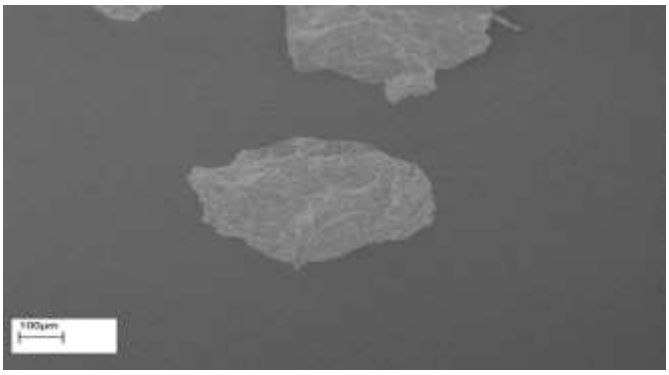

Figure 4- 32 SE micrographs of tea particle (a) over 250 and (b) through 500 microns pore size (x250 magnification)-Actual size 498 x 388microns

Both tea particles collected over the 125 and 63 microns pore size but which were smaller than 250 microns and 125 microns pore size respectively showed uneven surface and majority had elongated needle-like shape (Figures 4-33 and 4-34).

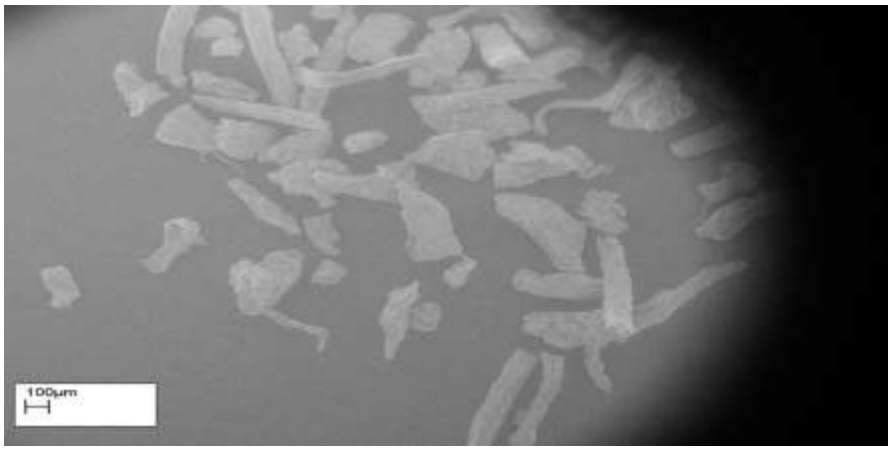

Figure 4- 33 **SE micrograph of tea particle over 125 and through 250 microns sieve size (x150 magnification)**

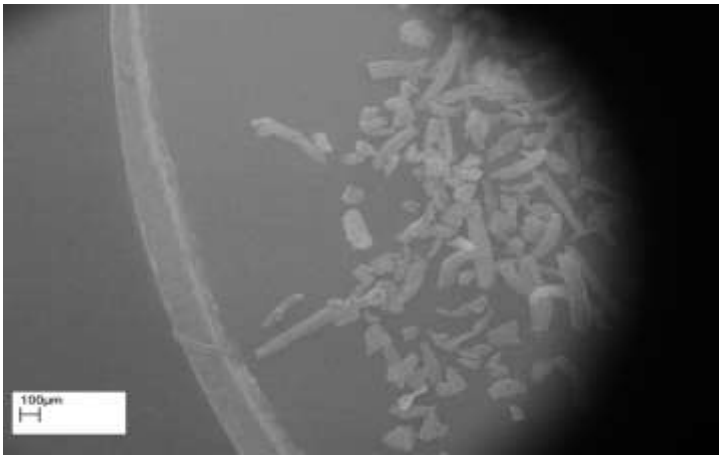

Figure 4- 34 **SE micrograph of tea particles over 63 and through 125 microns sieve size (x100 magnification)**

Close observations of Figures 4-30 to 4-34 revealed that vibration simulation tended to wear tea particles unevenly with the resultant smaller particles having an elongated shape rather than the original more or less spherical shape of the mother batch. This may be due to the presence of imbedded tea fibres within the tea particles which are difficult to break through by the compressive and attrition forces during the simulation. As the imbedded cellulose fibres have a thread structure which is relatively difficult to break through, during simulation the tea particle fracture lines will tend to run more or less along these fibres leaving behind an elongated breakdown fraction. The aspect ratio decreased as the particle size decreased and became more elongated. The aspect ratio is a measure of flow and this shows that the broken fractions were more likely to resist flow than the more rounded mother batch. The particle fraction 125- 63 microns and those less than 63 microns were fibrous and had a needle-like shape with aspect ratios of 0.44 and 0.33 respectively that represent high resistant to flow compared to the reasonably rounded mother batch size of 2mm-1mm with the aspect ratio of 0.88. Generally, granular matter of size less than 100 microns is difficult to flow (Holdich, 2002). The angle of repose figures reduced for the smaller tea fractions. Although all fractions had angle of repose less than 40^0 that would suggest fair flow (Aulton, 2000), the elongated nature of the particles undermined their potential mobility. The 1-2mm tea particles at an angle of repose of 27.8^0 have a better flow ability compared to 125-63 micron tea particles with higher angle of repose of 34.9 signifying poorer flow ability. Indeed, neither angle of repose or aspect ratio alone is an enough criterion to fully characterize flow properties of granular matter. The practical effect of this changed particle morphology to the tea packer is that as the particles become smaller and

more elongated; their flow ability is equally reduced. This could significantly affect both the installed handling and packaging processes that may have been designed to handle teas of better flow characteristics. There is therefore a need to ensure that the particle integrity of the tea is preserved in transit via appropriate distribution package design that protects the tea from quantified transit hazards.

Table4. 3 Flow data for various tea particle fractions

Particle fraction	**Actual size**	**shape**	**Aspect ratio**	**Angle of repose (^{0})**
2-1mm	1.699x 1.509mm	Spherical	0.88	27.8
1mm500microns	0.71x0.50mm	Oblong	0.70	29.3
500-250 microns	402x599 microns	Slightly elongated	0.67	31.3
250-125 microns	243x158 microns	Elongated	0.65	34.2
125-63 microns	114x257 microns	Needle-like	0.44	34.9
Less 63 microns	62.5x187.5 microns	Needle-like	0.33	No data

Appendix 4 shows the detailed calculation to determine the angle of repose for various tea particles analysed in the experiment while Appendix 9 gives the analysis of the angle of repose for the various black CTC commercial grades. Table 4.3 shows the size, shape and flow data of aspect ratio and angle of repose for the various tea size obtained during the simulation exercise.

Figure 4- 35 Tea particles at the start of simulation exercise

Another notable aspect of changes with respect to particle physical quality is that of the colour change from black at the start (mother batch) to a greyish shade at the end of simulation as shown in Figures 4-35 and 4-36 respectively.

Figure 4- 36 Greyish tea particles after the simulation period

The greyish teas were a result of crushing and attrition action on the tea particles. The colour change was due to the fact that a tea particle after drying is black mainly on the surface while the inside is greyish. As the tea is broken down to smaller fractions due to vibration and compression activity, this in turn exposes the grey surfaces and hence the general greyish shades of the whole batch. The commercial importance of this colour change is that greyish tea is considered inferior in quality in the black tea market where the black colour commands a

premium price. Since bulk tea is normally sold to packers/blenders that are quite conversant with tea trade quality requirements, any deviation of colour from the expected black standard for black tea is considered unacceptable.

4.4.0 Transit temperature and relative humidity measurements

4.4.1 Introduction

Temperature and relative humidity (R.H.) are important parameters during distribution as their changes could affect both the product and even the packaging. Tea is hygroscopic in nature and would be affected by changes in humidity leading to high moisture absorption and subsequent loss of quality such as "briskness" and strength. In addition, bulk tea is normally packed in multiwall paper sacks that are also prone to humidity changes undermining its strength properties and leading to package failure in transit. Paper unless treated is particularly sensitive to high and low relative humidity. During distribution, changes in the relative humidity and temperature within the truck load were monitored.

4.4.2 Environmental conditions for Michimikuru to Mombasa route.

The highest relative humidity (R.H.) recorded on this route during the experiment was 76% while the lowest R.H. was 58%. The route's lowest temperature was recorded at 17^0C and the highest at 28^0C (Figure 4-37). Both the highest temperature and relative humidity were recorded in the coastal region which was characterised by hot and humid conditions.

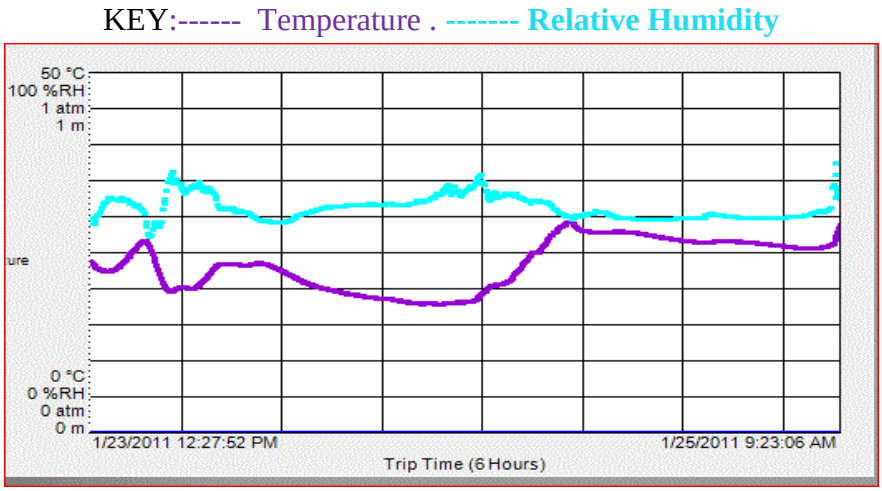

Figure 4- 37 Graph of temperature and relative humidity for Michimikuru to Mombasa trip.

4.4.3 Environmental conditions for Chebut-Mombasa route

This route recorded relative humidity ranging from 22% to 79%. The temperature for the route ranged between 18^0C and 39^0C (Figure 4-38).

4.4.4 Environmental conditions for Nyamache- Mombasa route

The relative humidity conditions for this route ranged between 42% to 81% and the temperature range was 17^0C to 32^0C (Figure 4-39)

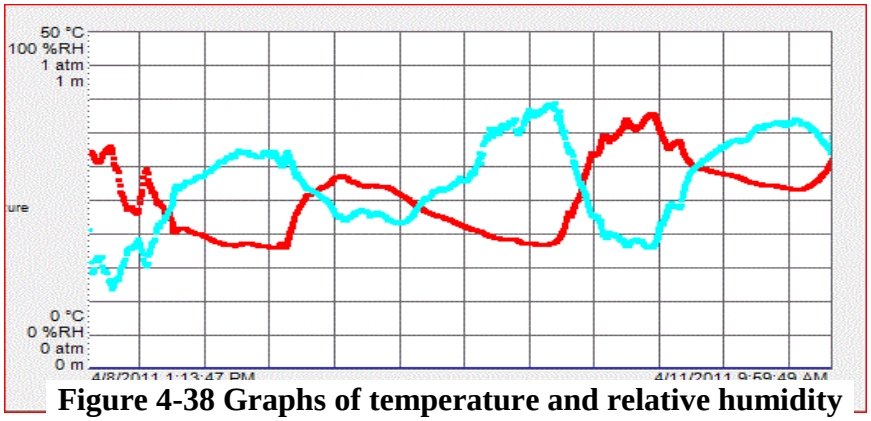

Figure 4-38 Graphs of temperature and relative humidity for Chebut to Mombasa route

KEY: ___ Temperature ____ Relative Humidity

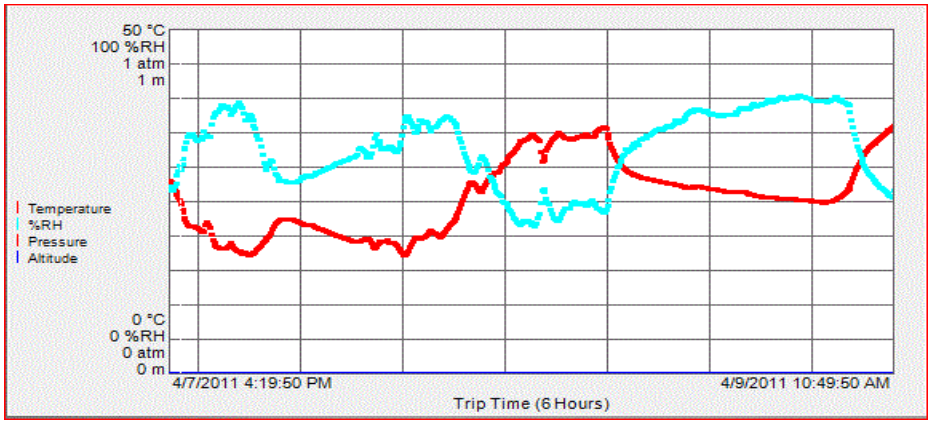

Figure 4- 39 Graphs of temperature and relative humidity for Nyamache to Mombasa route

From the Figures 4.37 to 4.39 that indicate the environmental transit condition within the truck, it is quite clear that there were large variations in both temperature (17 to 39^{0C}) and relative humidity (22 to 81%). This represents measurements made during the season of this work. From weather records of the areas covered by the trucks both temperature and relative

humidity maximum and minimum values could be higher and lower respectively. From recorded weather conditions during the experiment, quality of tea could be affected if appropriate packaging to keep off moisture was not provided. Nevertheless, it should be realized that many times conditions within the truck are different from those outside the container such that on a very hot day and for a stationary truck, temperature levels inside the cabin will be higher than those in the external environment. Conversely, during cold periods the temperature inside the truck will be slightly higher than ambient. It is therefore important that temperature and relative humidity measurements need to be taken on the inside of the truck (as done in this work) as these are the environmental conditions that are in equilibrium with the goods inside the carriage.

4.5.0 Summary

In this chapter results of the various investigations and tests are presented. They include the road measurement and analysis data of vibration and shock for the four routes that were used in this research. There are variations in vibration and shock impacts between the routes used which are consistent with the varying road conditions found in those areas. These are presented as power spectral density and shock response spectra plots for vibration and shock respectively. Environmental conditions of temperature and humidity during the shipment for each of the four routes is presented as time/temperature/ relative humidity graphs. They depict significant variance of temperature and relative humidity for the entire route. Percentage change in particle size proportion distribution for each sieve size during the simulation exercise is given as a bar graph while the mean tea particle size at each static load after the 12hr simulation period has been presented as a line graph. A line graphs of $\log_{10}$ against relative proportion of particle size at various static loads and that of percentage change in particle size proportion against same static loads have been shown. Line graphs of mean density changes against simulation time at various static loads are presented in addition to that of static loads against various types of densities. The general trend is that particle size changed during simulation due to the attrition effect on tea particles. This also affected the tea density leading to increase in density to a maximum level for each treatment. Pictorial presentation of tea powder "stain" column height seen adhering to test tube inside surface below the static load is presented. Graphs of tea powder "stain" column heights and compact densities against various static load have been given. Correlations graphs of compact tea density against tea powder "stain" height, tea powder "stain" column height against load piston travel distance, compact

density against load piston travel distance have been presented including their respective equations. Scanning electron microgrphs of the various tea particle sizes collected over the various sieves during simulation show that breakdown fractions ot the tea particles tend to assume an elongated shape from its original roundish shape. Pictorial presentations of tea particles at the start and end of the simulation exercise indicate loss of black tea colour quality during the simulations.

5.0.0 CONCLUSIONS AND RECOMMENDATIONS

5.1.0 Introduction

This chapter provides the main conclusions on the measurements and analysis of truck transit conditions in the major bulk tea distribution roads in Kenya. It also lists conclusions on how the Kenyan distribution environment compares with other environments in other parts of the world. The chapter further gives conclusions on how the above measured transit conditions may affect the physical quality of tea in transit when those conditions are simulated in the laboratory. In addition, several recommendations have been put forward that businesses in Kenya could adopt in order to optimize their package designs and also reduce on their packaging costs. Contributions to knowledge from this work are explained as well as recommendations for further work on areas that could not be carried out under this work programme.

5.2.0 Conclusions

The following conclusions were arrived at in this work:

1. The Kenyan distribution environment is quite different from many other recently studied distribution environments in that the measured vibration/ shock impacts on the goods were higher than those experienced in other parts including the USA, South America, India, Thailand and Europe. The vibrations/shocks are also more severe than those stipulated for the existing ASTM and ISTA test methods for truck transportation. Use of these test methods may not therefore allow packaging designers to optimize packaging designs for the Kenyan distribution environment.
2. There is a major diversity in the Kenyan road conditions such that while some roads have lower impacts on transit goods, others (especially those in the rural areas) are in very poor condition that subject goods to high vibration/shock impacts that can cause goods failure in transit unless the appropriate packaging was provided.
3. Measured vertical direction impacts are higher than both longitudinal and lateral impacts. The left side vibration/shock impacts are higher than those from the right hand side of the truck confirming that it is better to fix measuring data loggers on the rear left side in order to capture the highest impacts experienced by the goods in transit.

4. There are large variations in environmental conditions of temperature and relative humidity experienced by goods while in transit within Kenya. Such conditions could affect both tea quality and packaging in transit if appropriate preventive measures are not employed.
5. The existing levels of truck transport transit conditions can affect the physical tea quality of density, particle size distribution, particle morphology and even grain colour. These parameters are important quality attributes of tea.
6. Tea densities (bulk, tapped and compact) increased with simulation time up to a maximum level upon where there are only minimal fluctuations in density around the steady state with continued simulation.
7. There is a general increase in density with the amount of static load applied up to 350-400gm level where resonance conditions set in and the effect of static load on tea particles became less significant.
8. There is a general correlation of tea density with tea powder "stain" height on the test tubes below the static load as well as the total distance moved by the dead weight during the simulation exercise.
9. There is change in particle size distribution with simulation time such that the larger 1 mm particles of the mother batch undergo attrition over time and their proportion decreases during the simulation experiment. On the other hand, the smaller particle fractions collected in the 500, 250,125 and 63 micron sieves increases during simulation.
10. The smaller particle size fractions produced during the simulation experiment assume a rather elongated shape from the original rounded shape of the mother batch particles. This new shape alters the flow characteristics of angle of repose and aspect ratio and even changes the original colour of tea particles from black to a greyish shade at the end of the simulation exercise thus undermining the required quality attribute of black tea.
11. A new composite spectrum has been developed which will allow packaging design engineers to optimize their packaging designs.

5.3.0 Recommendation and Future work

The following recommendations and future work have been made from this research:

1. This work established actual truck transit hazard levels of vibration that may be experienced by goods moving within the Kenyan roads and finally the proposed pre-testing spectrum that may be used to test goods in this distribution environment. Packaging

designers can now use the improved testing protocol developed from this research to optimize their packaging designs and avoid costly over-packaging problem.

2. It is further recommended that in order to reduce the damaging effects in transit of static load on palletized tea, the pallet load should be secured tightly to reduce any "bouncing" effects of the cargo within the pallet. This may be achieved by strapping together the pallet load in addition to the use of stretch wrap film that mainly protects cargo from external hazards such rain and dust.
3. Tea greying in transit was found to be due to particle size degradation that was mainly on account of static compression on tea particles within the pallet load. This degradation could be reduced by subjecting tea sacks to adequate gentle vibrating input during the filling exercise such that the sack assumes a brick-like structure that resists external pressure. In this state, most tea particles are in a "jammed state" and are able to resist substantial external compressive forces that are exerted on the sack.
4. Despite its additional overall costs, use of appropriate cushioning material such as foam between the current sack layers especially on the bottom tiers could reduce the impact of damaging shocks and compression on tea in transit.
5. Use of vacuum packed sacks as an alternative not only ensures the tea particles resist any external compression (tea particles are "jammed") but further protects the delicate quality of tea and guarantees freshness of tea at the destination.
6. Alternatively, the tea could be packed in a giant one tonne sack under vibration to form a single brick pallet load that also resists external compressive forces. There is no "cargo bouncing" in this case and this protects the tea inside the bag.
7. Another alternative but that could be less popular, is having racking for individual tea sacks within the transport truck. This calls for dedicated specialised transport which may not be cost effective.
8. Investigate how transit hazards in truck shipments may affect safe delivery of other packaged products that are transported through the same environment by using the developed pre-shipment testing protocol.
9. Cost benefit analysis will need to be undertaken for each of the above recommendations in order to establish their economic viability before implementation.
10. Further research is required in order to come up with an acceptable accelerated testing procedure to reduce pre-shipment testing period from current actual journey simulation period

11. A lot of useful information has been generated in recent times to explain the complex behaviour of granular matter under the influence of "granular temperature". There is no data on how tea granular matter would behave upon application of external excitation at various conditions such as relative humidity. This area requires more research as it would inform better ways of handling tea during its transportation and processing.
12. Attempts have been made to formulate equations to explain the fluctuations in density of a granular matter under external vibration upon its attainment of the maximum density using the adsorption-desorption model. While the equations explaining the first two regimes have been formulated, the behaviour in the third exponential terminal decay is not well understood and there is need for further research in this area including one involving tea.

5.4.0 Contribution to knowledge

The author considers the following to be the contributions to knowledge from this research:

5.4.1 Production of composite road spectrum for the Kenyan distribution environment

The research established the actual prevailing truck transport transit conditions within the Kenyan distribution environment. This will make it possible to compare road conditions in Kenya with the data from other areas. The results indicate that road conditions in Kenya are poorer than those of other distributions environments such as Europe, USA, India, Thailand and Brazil where similar road measurements have been carried out. Kenyan road conditions data further shows that transit conditions are worse than those from where both ISTA and ASTM test recommendations are derived. Kenyan distribution environment therefore requires its own pre-shipment test protocol for the packaged goods that will allow packaging design engineers and shippers to optimize their packaging designs.

5.4.2 Establishment of a pre-shipment laboratory protocol for the Kenyan environment

Data collected from the Kenyan roads shows that vibration/shock levels are much more severe than those reported by other researchers from other parts of the world such as Brazil, the USA, Spain, Thailand and India. The transit hazard levels in the country are also found to be higher than both the recommended ISTA and ASTM test levels, making their test procedures inappropriate for pre-shipment testing of goods destined to the Kenyan distribution environment. A new laboratory pre-shipment testing protocol that is considered suitable for the

Kenyan environment has been developed which will allow Kenyan packaging designers to optimize their designs. From this research the composite road spectrum from the road data was developed that accurately characterizes road conditions in Kenya and used to formulate a pre-shipment protocol that will allow shippers in this region optimize packaging designs in order to save costs as well as meeting the current packaging waste management obligations as currently required by the target markets.

5.4.3 Establishment of the relationship between tea powder "stain" column height below the static load and compact density of tea

A linear relationship was established between the tea powder 'stain' column height on the test tube below the static load and the tea compact density. This relationship enables one to predict compact density of tea from the tea column height 'stain' independent of the static load on top of the tea. This implies that a static load under dynamic conditions as those found in road transport when it leads to the damage of granular matter into powder, the transmitted load impulses carry with it the fine particles such that their distance of travel can be used to predict the compact density of the whole granular matter using a correlation equation. This is an important insight into granular matter behaviour involving tea particles and that could also be true for other similar matter under dynamic conditions as specified in this research. The research brings new dimension that allows one to determine the density of tea using the correlation equation developed linking it to the powder stain height on the test tube irrespective of the static load on the tea.

5.4.4 Establishment of the relationship between the static load piston travel distance and tea powder column height

A novel relationship was established between the total distance travelled by the static load piston within the test tube containing tea during the simulation experiment and the tea powder "stain" column height below it within the test tube. This relationship was true for any static load applied thus was independent of the static load. The implication of this finding is that the distance the static load travels due to the consolidation of granular matter by its compressive forces is related to distance travelled by the granular matter powder as a result of static load force impulses projected perpendicular from it. The relationship can therefore be explained using a correlation equation as derived from this research. This empirical data is important for researchers involved in granular matter behaviour since the high correlation between the two properties enables one to predict the value of the other using the correlation equation

developed in this work. This could also apply to other similar granular matter with similar characteristics as those of tea. This relationship further implies that the force impulses emanating from the respective load was vertically transmitted downwards to the bottom of the tube and in so doing pushing down tea powder dust that adhered to the Perspex tube sides due to electrostatic charges created on its surface.

5.4.5 Establishment of the relationship between total distance moved by the static load and the tea compact density

An interesting correlation between compact densities of tea was inferred from 5.3.2 and 5.33 using joint variation equation. This was further validated by experiment to be a reliable method to predict the compact density of tea when the distance moved by the static load in the test tube was known. This is an important relationship for researchers in granular matter since using the distance the static load moved one can predict the density of granular matter over which the static mass is resting on. The static load led to the compression of tea particles thus reducing their volume and therefore growth in the tea density. Density is an important parameter for the tea blenders and packers since many packaging machines for tea use volumetric filling systems and the accurate density is very important to ensure attainment of the required package weight. Compression load can therefore be related to the respective tea compact density using the derived correlation equation from this research.

5.4.6 Production of data on the flow parameters of CTC black tea

This research further generated flow data of angle of repose and the aspect ratio for the various tea particle sizes encountered during this experiment. In addition, angle repose data was generated for the main CTC black tea commercial grades. This data is quite useful to the tea handling and conveyance equipment design engineers to allow them predict the flow behaviour of the various grades of tea during its blending and packaging operations. The average moisture content of tea at the start conditions was 5.5% and increased to 7.8%. This is because tea is hygroscopic and tends to absorb moisture from the environment. This moisture uptake increased its relative humidity which reduced its flow ability due to formation of water bridges between adjacent tea particles. This situation is expected to reduce the flow ability of the tea. Flow ability is function of moisture content and particle size (Teunou et. al., 1999). As the 1mm tea particle size at the start conditions was broken down to smaller particles the angle of repose for the resultant tea fractions increased from 27.8^0 at the start to 34.9^0. The particle shape changed from the rounded shape of the BP1 to the needle-like for the smaller dust

grades. Increased angle of repose for the breakdown fractions signifies poor flow ability of tea particles that could also lead to clogging of packaging machines (due arching) if this was not anticipated in their designs. The aspect ratio values for the small fractions teas also reduced from 0.88 to 0.33. Small values of the aspect ratio represent elongated particles that have poor flow ability. Impairment of free flowing ability of elongated particles was due to the increase of cohesive forces of the tea particles. Furthermore, smaller size tea particles had increased surface area per unit mass and this hinders their flow ability. Simulated conditions further led to the increased irregular surface configurations that resulted in higher coefficient of friction of tea particles thus reducing their flow capability. The static load pressure on the tea particles was responsible for compacting of tea particles into a chain-like structure leading to the "jamming" conditions proximal to the load due to particle adhesion.

5.50 Summary

This chapter gives the main conclusions arrived at from the results of this research that include transit hazard in the Kenyan bulk- packed tea distribution environment and their effect on physical quality of tea if adequate packaging is not provided.In addition, the chapter further suggests ways that bulk tea shippers could use in order to protect the physical tea quality in transit. Areas requiring further research have also been identified and contributions to new knowledge from this reasearch has been pointed out and explained.

5.6.0 REFERENCES

Aba,I., Gana,Y., Ogbonnaya,C., and Morenikeji, O., "Simulated Transport Damage Study on Fresh Tomato (Lycopersicon Esculentum) fruits".Agricul. Eng. International (CIGR Journal) **14** (2) (2012)1-14. (http://www.Cigrjournal.org/index.php/Ejournal/ar) Accessed on 4/2/2013.

Allied Environmental Conditions and Test Publication, AECTP-240 (edition1) July 2009.

American Society for Testing and Materials International. ASTM Standards, Vol 15.09: Packaging. ican 100 Barr Harbor Dr., West Conshohocken, PA 2002.

American Trucking Association report, 2012.

Anjani, L.J., and Virendra, M. P., "Percolation segregation of multi-size and multi- component particulate materials", Powder Technology **197** (2010) 274-282.

Apeji,Y.E., Oyi, A. R., and Musa, H., "Evaluation of the powder and compaction properties of microcrystalline starch derived from cassava (manihot esculenta crantz) by enzymatic hydrolysis". JPRHC **2** (4) (2010) 314-319.

Aulton. M.E. "Pharmaceuticals: the science of dosage form design. Edinburgh;Churchill Livingstone, 2000.

Baird T, Young D. The China Project: "An assessment of china shipping and handling environments", ISTA PST Newsletter, 2004.

Baxter, G.W., Behringer, R.P. and Johnson, G.A. Phys. Rev. Letters **62**,(1989) 2825.

Bates, L. "User Guide to Segregation". Bucks: British Materials Handling Board, (1997).

Becker, D, L., McCoy, J.C. "Over- the- Road Shock and Vibration Testing of the Radioisotope Thermoelectric Generator (RTG) Transportation system".- Project Hanford Management contractor for the U.S. Department of Energy, (1997).

Ben-Naim, E., Knight, J.B., and Nowak, E.R. "Slow relaxation in granular compaction" Physica D**123**(1998) 380-385.Found on:

http://www.physics.udel.edu/~nowak/publications/granular_materials/Ben-Naim_PhysD_123_380.pdf

Bernad, C., Laspalas, A., Conzalez, D., Nunez, J., L., and Buil, F., "Transport vibration laboratory simulation: on the necessity of multi-axis testing" Pack. Tech. Sci. **24** (2011**)** 1-14.

Bodhmage, A. Correlation between physical properties and flow ability indicators for fine powder" M.Sc. thesis, University of Saskatchewan (2006).

Brandenburg, R.K., Ling Lee J. J. 1985. "Fundamentals of Packaging Dynamics", 2nd Edition. MTS Systems Corporation, Minneapolis, USA.

BS EN 22872 "Complete filled transport package: Method of determination of resistance to compression" 1993.

Bundi, J., M., "Rural transportation problems: A case study of tea roads in southern tea growing region of Meru, Kenya." Master of Arts dissertation; University of Nairobi, 2003.

Carr, L.,' Evaluating flow properties of solids'. Chemical Engineering, 72(3), (1965a) 163–168.

Cates, E., Wittmer,P., Bouchaud,P.,and Claudia, P., "Jamming force chains and fragile matter" Phys. Rev. Lett. 81 (1998) 1841.

Chonhenchob, V., and Singh, P., "Packaging Performance Comparison for Distribution and Export of Papaya Fruit". Packag. Techno. Sci. **18** (2005**)** 125-131. Published online 7 March 2005 in Wiley InterScience (www.interscience.wiley.com) DOI: 10.1002/pts.681. Accessed on 6/5/2010.

Chonhenchob, V., Kamhahangwong, D., and Singh, P., "Comparison of Reusable and Single-use Plastic and Paper Shipping Containers for Distribution of Fresh Pineapples". Packag. Techno. Sci. 2008; **21**: 73-83. Published on line 25 May 2007 in Wiley InterScience (www.interscience.wiley.com) DOI: 10.1002/pts.780.

Craik , J., Miller F., "The flow properties of powders under humid conditions". Journal of Pharmacy and Pharmacology, **10** (1958) 136–144.

Cundull, A.,Stack, L., "A Discrete numerical model for granular assemblies" Geotechnique **29** (1979) 47-65.

Edward, S.F., and Mounfield, C.C., "The statistical mechanics of granular systems composed of spheres and elongated grains", Physica A **210** (1994), 290-300.

Edwards, S. F. "Granular matter, an interdisciplinary approach", edited by A. Mehta (Springer-Verlag, New York, (1994).

Ehrichs, E. E., Jaeger, H.M., Karczmar, G.S., Knight, J.B., Kuperman, S. R., and Nagel, S. R., "Granular convection observed by magnetic resonance imaging" Science, **267** (1995), 1632-1634.

Escubed Limited, "Analytical equipment bulletin 2006". Leeds Innovative Centre, Leeds LS2 9DF UK. http://www.escubed.co.uk/ accessed on 13/08/2013.

Evans, J.W., "Random and cooperative sequential adsorptions". Rev. Mod. Phys. **65** (4) (1993) 1281-1329.

Evans, P.E. and Millman, R. S. "Perspectives in powder Metallurgy" vol. 2: Vibratory Compacting (N.Y: Plenum) 1967.

Fackler, W. C., Equivalence techniques for vibration testing" Collins Radio Company,1972.

Fang, X., and Tang, J., "A Numerical study of the segregation phenomenon in Granular Motion'', J. of vibration and Control. **13**, (2007) 711

Farady, M., "On a peculiar class of acoustical figures, and on certain forms assumed by groups of particles upon vibrating elastic surfaces, Philos. Trans. R. Soc. London **52**, (1831) 299-345

Farey R., and Valentin F. H. H., "Effect of particle size upon strength of powders". Powder Technology, **1** (1967/68) 344-354.

Fitzpatrick J. J., Barringer, S. A., and Iqbal, T., "Flow property measurement of food powders and sensitivity of Jenike's hopper design methodology to the measured values". Journal of Food Engineering, **61** (3) (2004a) 399-405.

Fitzpatrick J. J., Iqbal, T., Delancy, C., Twomey, T., and Keogh, M. K., "Effect of powder properties and storage conditions on the flow ability of milk powders with different fat contents". Journal of Food Engineering, **64** (4) (2004b) 435-44

Forest Products Laboratory, Forest Service, U. S. Department of Agriculture, General Technical Report FPL22, *"*An Assessment of the Common Carrier Shipping Environment*"*, Madison, WI, 1979.

FTA (Freight Transport and Agriculture), "America's freight is America's future" 2008. Available at :http//:www.tradecorridors.org/factsfigures.html (Accessed on 10 September 2010).

Gallas, J.A.C., Herrmann, H. J., and Sokolowski, S., "Convection cells in vibrating granular media", Physical Review Letters **69** (9) (1992) 1371-1374.

Ganesan, V., Rosentrater, K.A., and Muthukumarappan, K., "Flow ability and handling characteristics of bulk solids and powders- a review with implications for distillers dried grains with solubles" Biosystems Engineering **101** (2008) 425-435.

Godshall. W. "Frequency response, damping and transmissibility characteristics of top-loaded corrugated cases. USDA For. Serv. Res. Paper FPL 160. Forest products Laboratory, Madison Wiscon, 1971.

Goncu, F., "Mechanics of granular materials: constitutive behaviour and pattern transformation" M.Sc. thesis Ecole Normale Superieure de Cachan, France, 2012.

Goodwill, J., "Understanding and eliminating particulate segregation mechanisms" proc. of European conference on the mixing, (1986) 139-144.

Grossman, E.L., "Effects of container geometry on granular convection", Physical Review E, **56** (1997), 3290-3300.

Guo, A., Beddow, J. K. and Vetter, A. F., "A simple relationship between particle shape effects and density, flow rate and Hausner ratio". Powder Technology, **43** (1985) 279-284.

Guo, Y. and Xu, W., "Study on design and evaluation method for transport packaging protection", 3rd. International conference on multi- functional materials and structures, MFMS , Jeonju, 2010.

Haff, P.K., and Werner, B. T., "Computer simulation of the mechanical sorting of grains" Powder Technol. **48**, 3 (1986) 239-245

Hampton, M. G., "Production of black tea: In Tea Cultivation to Consumption" pp.459-511 Chapman and Hall, London (1992) pp.459-511

Harris, N., and Ellis, R.T. "Black tea Manufacture: Effects on leaf structure of different processing systems." Annals of Applied Biology 99 (1981) 359-366

Head, D. A., and Rodgers, G. J., "A coarse-grained model for granular compaction and relaxation" J. Phys. A: Math. Gen. **31** (1998) 107-122.

Holdich, R., "Fundamentals of particle technology", Midland Information Technology & publishing, Leicestershire, U.K.(2002)ISBBN-0-9543881-0-0. Available on line at: http://www.particles.org.uk/particle_technology_book/particle_book.htm(accessedon 24/5/2014).

Hsiau, S. S. and Yu, H. Y., "Segregation phenomena in a shaker", Powder Technol. **93** (1997) 83-88

Hsiau, S.S., Wang, P.C., and Tai, C.H., "Convection cells and segregation in a vibrated granular bed", AICHE Journal, **48** (2002), 1430-1438

http://www.osti.gov/bridge/servlets/purl/10154458/10154458.pdf Accessed on 11/02/2013.

http://www3.nd.edu/~granular/ (Cited 10/10/2012)

Irandu, E., M., "Air transport in Kenya: analysis of Domestic and International Airline networks". PhD thesis, University of Nairobi, 1995.

Irandu, E. M., "Improving railway transport in Kenya" Policy options and achievements to-date, USAID/REDSO/ESA's Strategic objectives no 623-002-01, (2000).

Ipskamp Drukkers, Enschede, The Netherlands. ISBN: 978-94-6191-341-8.

Irani R R; Callis C F; Liu T., "Flow conditioning and anticaking agents". Industrial and Engineering Chemistry, **51**(10) (1959)1285–1288

Jaeger, H. M. and Nagel, S.R. Physics of the granular state Science **255,** (1992)1523-1531.

Jaeger, H. M., Nager, S. R., Behringer, R. P., "Granular solids, liquids and glasses", Rev Mod. Phys **68,** (1996b) 1259

Jenike,A.W, Johanson, J.R. "On the theory of bin loads" J. of Engrg. for industry, ASME, **91** (2) (1969) 339-344

Jha, A.K. and Puri, V. M.," Modeling and Validation of Percolation Segregation of Fines from Coarse Mixtures during Shear Motion" Kona powder & particle journal **29** (2011) 81-95

Johanson, J.R., "Particle segregation and what to do about it", Chem. Eng. (1978) 9-17.

Jose, M. S.F., "Made tea density" Tea Research Foundation (Central Africa) Quarterly Newsletter **138**, (2000) 10-11

Jose, M.S.F.," Factors that influence density of made tea". Tea Research Foundation (Central Africa). Quarterly Newsletter **143** (2001) 25- 33

Kenya Government, Ministry of planning economic survey report, 2010.

Kenya Government, Ministry of economic planning report, 2014.

Kenya Government, Institute of Economic Affairs report, 2008

Kenya Roads Board report, 2014 -found on http://www.krb.go.ke/road-network/road-network.html (accessed 11/10/2014)

Kenya Tea Board report, 2014- found on: http://www.kenyaembassy.com/pdfs/teaboardpresentation.pdf (accessed 23/5/2014)

Kipp, W. "Shock, Drop and Impact Testing Equivalence". Paper presented at Dimensions .01 meeting, Orlando, Florida March,1 2001.

Kipp,W. "Understanding today's Transport environment measuring recorders". Paper presented at the ISA 44th International Instrumentation symposium, 1998.

Kipp, W., "Vibration Testing Equivalence". Paper originally presented at Safe Transit association meeting in 2000. Paper revised and updated in 2008.

Knight, J. B., "External boundaries and internal shear bands in a granular convection", Phys. Rev. E **55** (1997) 6016-6023

Knight, J.B. and Jaeger, S.R., "Vibrated- induced size separation in granular media": the convection connection. Phys. Rev. Lett. **70** (1993) 3728-3731.

Knight, J.B., Fandrich, C. G., Lau, C. N., Jaeger, H. M., and Nagel, S. R., "------" Phys. Rev. E 51 (1995) 3957.

KTDA Ltd Marketing report, 2014.

L.A.B Equipment, Inc. "Vibration data collection": A road worth travelling?" 2006.

Lambert, B. "The FAF as a policy and systems analysis tool. Federal highway administration, office of freight management and operations", Washington D.C.: US department of transportation 2003.

Lance, G. E. N., Theory of fertilizer blending, The Fertilizer Society, proc, (1996) pp. 387. Cambridge, UK.

Langroudi, M. K., Sun, J., Sundaresan, S., and Tordos, G. I. "Transmission of stresses in static and sheared granular beds: The influence of particle size, shearing rate, layer thickness and sensor size". Powder Technology **203** (2010) 23-32

Linemann, R., Runge, J., Sommerfeld, M. and WeiBguttel, U. "Compaction of powders due to Vibrations and Shocks". Part. Charact. **21**(2004) 261-267

Liu, A. J. and Nagel, S. R., "Nonlinear dynamics - Jamming is not just cool anymore." Nature **396** (1998), 21-22

Liu, E., S. R. Tod, andX. Y. Li, "Effects of stress and pore fluid pressure

on seismic anisotropy in cracked rock". CSEGRecorder (2002) 92–98

Lu, F., Ishikawa, Y., Kitazawa, H., and Satake, T., "Effect of vehicle Speed on Shock and Vibration Levels in Truck Transport". Packag. Techno. Sci.**23** (2010) 101- 109. Published on line 4 February, 2010 in WileyInterScience (www.interscience.wiley.com) DOI: 10.1002/pts.882. Accessed on 6/2/2013.

Lu, L.S., Hsiau, S.S., "Mixing in a vibrated granular bed: diffusive and convection effects", Powder Technology, **184** (2008), 31-43

Majid, M. and Walzel, P.," Convection and segregation in vertically vibrated granular beds", Powder Technology **192**, (2009) 311- 317

Majmudar, T.S., and Behringer "Contact force measurements and stress-induced anisotropy in granular materials" Nature 435 (7045) 2005: 1097-1082.

Malave, J., Barbosa-Canovas, G. V. and Peleg, M., "Comparison of compaction characteristics of selected food powders by vibration, tapping and mechanical compression". Journal of Food Science, **50** (1985) 1473- 1476.

Marinelli, J., Carson, J.W., "Solve solids flow problems in bins, hoppers and feeders." Chemical Engineering Progress, **88** (5) (1992) 22-28

Martinez, M., Singh, P., Ballester, V., "Measurement and Analysis of Vibration Levels for Truck Transport in Spain as a Function of Payload, Suspension and Speed". Packag. Techno. Sci.**21**(2008)439-451.Published online 19 November 2007in Wiley InterScience (www.interscience.com). DOI 10.1002/pts.798

Miller, K., "Vibrating testing", (2012) http://www.file:///C:/vibrating%20Testing%20table%20Types.htm(accessed on 20/3/2013)

Mitchell, N.,"Tea tasting Course. Tea Research Foundation (Central Africa) and Tea Brokers (Central Africa) Ltd. Course Manual". (2001)

Mobius, M. E., Lauderdale, B.E., Nagel, S.R., and Jaeger, H. M, "Brazil –nut effect: size separation of granular particles," Nature **414** (2001) 270.

Molerus, O., "Theory of yield of cohesive powders", Powder Technology **12** (1975) 259-275. Moreyra,R. Peleg, M. "Effect of equilibrium water activity on the bulk properties of selected food powders". Journal of FoodScience,**46**, (1981) 1918–1922.

Nei, D., Nakamura, N., Roy, P., Orikasa, T., Ishikawa, Y., Kitazawa, H., and Shiina, T., "Wavelet Analysis of Shock and Vibration on the Truck Bed". Packag.Techno. Sci. **21** (8) (2008) 491-499.

Nowak, E. R., Knight, J. B., Ben-Naim, E., Jaeger, H.M. and Nagel, S. R., "Density fluctuations in vibrated granular materials". Physical Review E **57** (2) (1998) 1971.

O'Brien, M., Claypool, L., and Leonard, S., "Effect of mechanical Vibration on fruit damage during transportation.'' Food Technol. 17, 14 (1973).

Ostrem F. E and Rumerman M. L. (1965). "Shock and Vibration Transportation Environment Criteria"- A Report by General American Research Division, for National Aeronautics and Space Administration.

Owour, P. Tea Research Foundation (Kenya) Annual Report (1993)

Podczeck, F., Miah, Y., "The influence of particle size and shape on the angle of internal

friction and the flow factor of un-lubricated and lubricated powders", Int. J. Pharm., **144** (2)

(1996)187-194

Rippie, E. G., Faiman. M.D. and Pramoda, M. K., "Segregation kinetics of particulate solids systems IV: Effect of particle shape on energy requirements. Journal of Pharmaceutical Sciences, **56** (11), (1967) 1523-1525.

Rippie, E. G., Olsen, J.L., and Faiman, M.D. "segregation kinetics of particulate solids systems II: particle density -size interactions and wall effects". Journal of Pharmaceutical Sciences, **53** (11), (1964) 1360-1363.

Rissi, G., Singh, P., Burgess, G., Singh, J., "Measurement and Analysis of Truck Transport Environment in Brazil" Packaging Technol. Sci. **21**(2008) 231-246. Published on line 26 October 2007 in Wiley InterScience (www.interscience.wiley.com) DOI: 10.1002/pts.797 (accessed on 30/4/2010)

Roberts, A. W., "Vibration of fine Powders and its applications", Chapter 5. Handbook of Powder Science and Technology (1997) Chapman and Hall, New York. Available at http://link.springer.com/chapter/10.1007%2F978-1-4615-6373-0_5#page-1 (accessed on 24/5/2014)

Rosato, A.D., and Blackmore, D. L., (Eds.). IUTAM symposium on segregation in granular flows. "Solid mechanics and its applications", Dordrecht, Netherlands. Dordrecht: Kluwer academic publishers (2002).

Rosato, A.D., Blackmore, D.L., Zhang, N. and Lan, Y., "A perspective on vibration- induced size segregation of granular materials". Chemical Engineering Science **57** (2002) 265-275

Rosato, A.D., Strandburg, K. J., Prinz, F.B., and Swendsen, R. H., "Why the Brazil nuts are on top: size segregation of particulate matter by shaking", Phys. Rev. Lett. **58**, (1987) 1038-1041.

Rouillard, V., and Richmond, R., "A Novel Approach to Analysing and Simulating Railcar Shock and Vibrations", Packag. Techno. Sci.**20 (2007)** 17-26. Published on line 3rd May 2006 in Wiley InterScience (www.interscience.wiley.com) DOI 10.1002/pts. 739. Accessed on 1/5/2010.

Rouillard, V. and Sek, M. “Monitoring and simulating non-stationary vibrations for package optimization". Packaging Technology and Science **13** (2000) 149-156.

Runge, J. and weiBguttel U. Ein Beitrag zur Beschreibung der Verdichtbarkeit von schuttgutern bei Normalspannungen bis zu 30 kPa. Aufbereitungs- Technik **30** (1989) 138-143.

Savage, S. B., “Inter particle percolation and segregation in granular materials”: A review, in: A.P.S. Selvadurai (ed.) Development in Engineering Mechanics, Amsterdam, Elsevier (1987) 347- 363.

Schubert, H., Herrmann, W., and Rumpf, H., “Deformation behaviour of agglomerates under tensile stress” Powder Technol. **11**(1975)121.

Schueneman, H., “Measuring the Distribution Environment”, Conference proceedings held at Westpak, Inc., San Jose, CA, July (1996).

Seroka, W., “Fundamentals of Packaging Technology”. Iop, Rev. U.K edition (1996). pp. 335-380

Sharpe, W.N., and Kusza, T.J., 1973. “Preliminary Measurements and Analysis of Vibration environment of Common Motor Carriers”, Michigan State University, School of Packaging, Tech. Rep. No **22** (1973).

Shires, D., 2011 “On the time compression (Test Acceleration) of broadband random Vibration” Packag. Techno. and Sci.**24** (2) (2011) 75-87. Accessed on Google scholar on 10/10/2013.

Silvers, W., Caruso, H., “Advances in Shipping Damage Prevention”: The shock and Vibration. Bull. No **4 (**4) (1976) 41-48.

Singh, P.A. and Burgess, G., “Comparison between Lateral, Longitudinal and Vertical Vibration Levels in Commercial Truck Shipments”. Packag. Techn. Sci. **5** (2) (2006) 71-75. Published online on 28 April, 2006 in Wiley InterScience. DOI:10.1002/pts.277. http://onlinelibrary.wiley.com/doi/10.1002/pts.2770050205/abtract Accessed on 5/2/2013.

Singh, P., Jarimopass B., and Saengnil W." Measurement and analysis of vibration levels in commercial truck shipments in Thailand and its impact on packaged produce". Packaging Technology and Science, **18** (2005) 179-188.

Singh, P., Joneson, E., and Singh, J., "Measurement and Analysis of U.S. Truck Vibration for Leaf Spring and Air Ride Suspensions, and Development of Tests to Simulate these Conditions". Int. J. Packag. Technol. Sci.**19**(6) (2006b)309-320.

Singh, P., Sandhu, A., and Joneson, E., 'Measurement and Analysis of Truck and Rail Shipping Environment in India'. Packag. Techno. Sci. **20** (2007) 381-392. Published on line 9 January 2007 in Wiley InterScience (www.interscience.wiley.com) DOI: 10.1002/Pts.764. Accessed on 30/4/2010.

Sjollema, A., "Some investigations on the free flowing properties and porosity of milk powders". Netherlands Milk and dairy Journal **17** (1963) 245-259.

Stanford M K; Corte C D "Effects of humidity on the flow characteristics of PS304 plasma spray feedstock powder blend"NASA/TM-2002-211549. Ohio 2002.

Steyn, W., Monismith, C.,Nokes, W.,Harvey, J.,Holland, T., Burmas, N., "Challenges confronting road freight transport and the use of vehicle-pavement interaction analysis in addressing these challenges". Journal of the South African Institution of Civil Engineering, **54**(1) (2012) 14-21 found on: http://www.scielo.org.za/scielo.php?script=sci_arttext&pid=S1021-20192012000100002 (Accessed 8/05/2014

Tai, C.H., Hsiau, S.S., and Kruelle, C.A. 'Density segregation in a vertically vibrated granular bed' Powder technology **204** (2010) 255-262

Talbot,J., Tarjus, G., and Viot,P., "sluggish kinetics in parking lot model" Journal of Physics A Mathematical and General **32 (**16) (1999) 2997-3003.

Teunou, E., and Fitzpatrick.J.," Effect of relative humidity and temperature on food powder flowability". *J.Food Eng*., **42**(2) (1999)109–116.

The packaging Professional magazine, **29** (5) (2006).

Tomas J (2001b). "Assessment of mechanical properties of cohesive particulate solids". Part 2: powder flow criteria. Particulate Science and Technology, **19**, (2001b) 111–129.

Tordesillas, A. "Force chain buckling, unjamming transitions and shear banding in dense granular assemblies" Philosophical Magazine **87(**32) (2007) 4987-5016.

Vallance, J.W. and Savage, S.B., "Particle segregation in granular flows down chutes, in: A.D, Rosato, D. L Blackmore (eds.), IUTAM symposium on Segregation in granular Flows, Kluwer Academic Publisher, Norwell, U.S.A,(2000), pp. 31-51.

Rosato, A.D., Blackmore, D.L., Zhang, N. and Lan, Y., " A perspective on vibration- induced size segregation of granular materials". Chemical Engineering Science **57** (2002) 265-275

Rosato, A.D., Strandburg, K. J., Prinz, F.B., and Swendsen, R. H., "Why the Brazil nuts are on top: size segregation of particulate matter by shaking", Phys. Rev. Lett. **58**, (1987) 1038-1041.

Ulusoy, U., Yekeler, M., and Hicyilmaz, C., "Determination of the shape, morphological

and wettability properties of quartz and their correlations", Minerals Engg., 16, 2003,

951-964.

Van Tassel, P. R., Talbot J., Tarjus, G., and Viot, P. "A Distribution Function Analysis of the Structure of Depleted Particle Configurations," Phys. Rev. E **56**, (1997) 1299-1301. Walker, J., "When different powders are shaken they seem to have lives of their own" Scientific. American **247** (3) 166 (1982b) 206-216.

Walker, J., "Why do particles of sand and mud stick together when they are wet". Scientific American **246**, No 1 (1982a) 174-179

Walker, D.M., Blanchard M.H. "Pressures in experimental coal hoppers" Chem. Engrg. Sci, **22** (1967) 1713-1745

Wikipedia, the free enclopedia- granular convection. http://en.wikipedia.org/wiki/Brazil_nut_effect. Cited on 11/1/2012.

Wiliams, J.C., "The segregation of particulate materials". A review. Powder Technology **15**, (1976) 245- 251.

Williams, J.C., "The segregation of powders and granular materials". Fuel Society Journal, **14** (1963) 29-34

World Health Organization 46th Expert committee on "Specifications for Pharmaceutical Preparations". Document QAS/11.450 (2012)

Yan, H. and Barbosa-Canovas, G. V., “Compression characteristics of agglomerated food powders: Effect of agglomerate size and water activity” Food Science and Technology International, **3** (5) (1997) 351-359.

Yang S.C., “Density effect on mixing and segregation process in a vibrated binary granular mixture“, Powder Technology **164** (2006), 65-74.

Young, D.E., 1993, ‘focused Simulation”, available from International Safe Transit Association,1400 abbot Rd., Suite 160,E. Lansing, MI 48823-1900, www.ista.org.

USA Department of Agriculture, “Assessment of the Common Carrier Shipping Environment” FPL 22, 1979.

5.7.0 APPENDICES

5.7.1 Appendix 1: Shaker focused simulation program set up data

Test Type: Random

Test Name: Road simulation

Test Path: \\acfs5\empg\empgakr\Desktop\

Today's Date and Time: 03:50PM, Tuesday, April 03, 2012

Test

Test Title : Road simulation Test

Test Description : Kambaa to Mombasa RouteTest

Run ID 1

Run Name :Simulation

Run Increment : Query

Units

Displacement : in

Velocity : in/s

Acceleration : g

Run Notes

Enabled : No

Prompt1 : Load No:

Response1 : 1

Prompt2 : Rounds:

Response2 : 2

Prompt3 :

Response3 :

Prompt4 :

Response4 :

Prompt5 :

Response5 :

Prompt6 :

Response6 :

Prompt7 :

Response7 :

Prompt8 :

Response8 :

Comments :

Outputs

Drive Channel : 1

Max Volts : 2.000 V

Shaker : <Local>

Shaker Maximum Ratings

Model : Demo Shaker

Input Voltage : 5.000 V

Displacement : 0.500 / -0.500 in

Velocity : 70.000 in/s

Force : 333.333 lbf

Acceleration : 15.114 g

System Mass

DUT : 0.000 kg

Fixture : 0.000 kg

Armature : 10.000 kg

Slip Plate : 0.000 kg

Misc. : 0.000 kg

Inputs

Number of Active Channels: 1

Channel 1

Active : Yes

Type : Control

Name : Control

Sensitivity(mV/EU): 27.60

EU : g

Range(EU) : 36.23

ARF : OFF

Weight : 1.000

Coupling : ICP 4mp

Class : Manual

Serial # : N/A

Location : 1

Direction : +X

Control

Control Parameters

Multi-Channel Mode: Single

Sensitivity : 4.000

Startup Type : Pretest

Sigma Clip : 5.000

Min Freq. : 10.00 Hz

BandWidth : 1.000k Hz

Freqency Lines : 800

Resolution Lines : 1.250 Hz

Shutdown Time : 000:00:02

Startup Time : 000:00:02

Pretest

Signal Type : Uniform Random

Signal/Noise (dB) : 12.00

Safe Max Volts : 100.0m

Start Level(dB) : -12.00

Averages : 10

Check ICP : NO

Skip Stop Switch Test: NO

Pause At End : YES

Output Type : Continuous

Channels : Control Channel

Delay(sec) : 0.000

Linearity : 50.00

Reference

Profile

Accleration(rms) : 1.238 g

Accleration(peak) : 9.533 g

Velocity(peak) : 4.834 in/s

Displacement(peak): 26.82min

Spectrum Aborts

Frequency Lines : 4

No. of Repeats : 2

RMS Aborts

Abort Type : Auto

Abort Unit : %

RMS Low : 49.88

RMS High : 99.53

Reference Table

Point 1	10.0	6.00000	Slope	dB/Oct	-3.000	3.000	-6.000 6.000
Point 2	40.0	0.00250	Level	$(g)^2/Hz$	-3.000	3.000	-6.000 6.000
Point 3	350.0	0.00250	Level	$(g)^2/Hz$	-3.000	3.000	-6.000 6.000
Point 4	2000.0	-6.00000	Slope	dB/Oct	-3.000	3.000	-6.000 6.000

Measurement

Measurement Parameters

BandWidth : 1.000k Hz

Frequency Lines : 800

Resolution : 1.250 Hz

Means Avg Type : Stable

Frames : 60

Measurement DOF : 120

Reference Channel : 1

Functions

Gxx-Auto Spectrum : OFF

Gxy-Cross Spectrum: OFF

H(f)-FRF : OFF

Coh-Coherence : OFF

Measurement Schedule

Delay : 000:00:00

Period : 000:00:10

Run Schedule

Stage 1

Level : -12.00

Duration : 000:00:10

Lin Avg : 2

Exp Avg : 8.000

DOF : 60

Measure : Yes

Save : Yes

Abort : No

Stage 2

Level : -9.000

Duration : 000:00:10

Lin Avg : 3

Exp Avg : 8.000

DOF : 90

Measure : Yes

Save : Yes

Abort : No

Stage 3

Level : -6.000

Duration : 000:00:10

Lin Avg : 4

Exp Avg : 8.000

DOF : 120

Measure : Yes

Save : Yes

Abort : No

Stage 4

Level : -3.000

Duration : 000:00:10

Lin Avg : 4

Exp Avg : 8.000

DOF : 120

Measure : Yes

Save : Yes

Abort : No

Stage 5

Level : 0.000

Duration : 000:01:10

Lin Avg : 4

Exp Avg : 8.000

DOF : 120

Measure : Yes

Save : Yes

Abort : No

Save

End of Test: YES

End of Level: YES

Periodic: 000:01:00

End of Me

5.7.2 Appendix 2 Tri-axial truck transport transit measurement data

ôSaverXware Event PSD Export File

Generated From: C:\Users\user\Documents\Transit Data Kenya- Event Data Base.SXe

Event: Signal 1

Active Channel Code: 7

Freq (Hz)	CH1 PSD (G^2/Hz)	CH2 PSD (G^2/Hz)	CH3 PSD (G^2/Hz)
2.00E+00	1.59E-04	1.17E-04	4.47E-03
4.00E+00	7.34E-06	4.75E-05	3.90E-03
6.00E+00	3.92E-05	5.50E-06	5.85E-04
8.00E+00	3.33E-06	6.60E-05	4.49E-05
1.00E+01	3.01E-06	6.95E-05	4.49E-05
1.20E+01	2.09E-06	4.93E-06	5.15E-05
1.40E+01	6.51E-05	7.10E-06	9.52E-05
1.60E+01	5.18E-05	2.30E-05	7.59E-04
1.80E+01	2.62E-06	8.52E-06	7.09E-04
2.00E+01	1.69E-05	3.38E-07	3.33E-04
2.20E+01	2.92E-05	1.48E-05	1.87E-04
2.40E+01	8.24E-05	1.95E-05	2.56E-04
2.60E+01	2.20E-05	1.86E-06	7.56E-05
2.80E+01	6.01E-06	9.62E-07	1.30E-04
3.00E+01	2.03E-05	2.55E-06	2.89E-05
3.20E+01	2.02E-06	1.17E-06	2.71E-05
3.40E+01	6.14E-06	1.09E-05	8.43E-05
3.60E+01	3.95E-06	3.56E-05	1.04E-04
3.80E+01	2.46E-05	4.42E-05	5.66E-06
4.00E+01	8.19E-05	1.12E-05	4.23E-05
4.20E+01	2.31E-05	4.23E-06	4.91E-05
4.40E+01	8.97E-06	8.81E-06	5.84E-05
4.60E+01	8.15E-06	1.36E-05	5.63E-05
4.80E+01	2.05E-05	2.76E-05	6.71E-05
5.00E+01	2.29E-05	9.78E-06	1.75E-05
5.20E+01	6.22E-05	2.10E-05	5.55E-05
5.40E+01	4.39E-05	2.27E-05	3.79E-05
5.60E+01	1.39E-04	5.82E-05	8.48E-05
5.80E+01	1.53E-04	8.31E-05	1.30E-04
6.00E+01	5.90E-05	9.40E-05	6.43E-05
6.20E+01	1.27E-05	1.57E-04	2.66E-05
6.40E+01	2.58E-05	3.37E-04	2.38E-05
6.60E+01	6.43E-05	2.93E-04	2.57E-05
6.80E+01	6.21E-05	9.10E-05	1.07E-05
7.00E+01	5.65E-05	8.87E-06	4.29E-06
7.20E+01	2.83E-05	7.12E-06	8.04E-06
7.40E+01	2.57E-06	4.63E-06	4.61E-06
7.60E+01	7.38E-06	4.20E-07	1.28E-07
7.80E+01	1.06E-05	2.62E-06	6.66E-06

8.00E+01	5.27E-06	1.41E-05	8.35E-06
8.20E+01	2.58E-05	5.17E-06	4.35E-06
8.40E+01	1.13E-05	7.09E-07	4.13E-07
8.60E+01	1.39E-05	1.10E-06	1.53E-06
8.80E+01	9.19E-06	2.52E-07	2.31E-06
9.00E+01	2.23E-05	8.20E-07	1.08E-06
9.20E+01	2.01E-05	2.94E-06	1.31E-06
9.40E+01	2.00E-06	8.51E-06	2.79E-06
9.60E+01	9.26E-06	6.11E-06	2.50E-06
9.80E+01	6.07E-07	1.02E-05	3.90E-06
1.00E+02	1.19E-06	7.45E-06	1.81E-06
1.02E+02	1.23E-06	5.82E-06	8.14E-06
1.04E+02	3.90E-06	2.18E-06	5.92E-06
1.06E+02	2.60E-06	9.80E-07	3.22E-06
1.08E+02	4.13E-06	4.88E-06	2.13E-06
1.10E+02	2.88E-06	7.64E-06	2.41E-06
1.12E+02	5.31E-07	4.84E-06	2.24E-06
1.14E+02	9.05E-06	8.22E-06	6.71E-06
1.16E+02	3.57E-05	3.90E-06	4.00E-06
1.18E+02	4.62E-05	6.31E-06	1.98E-05
1.20E+02	1.00E-04	1.32E-05	3.28E-05
1.22E+02	6.18E-05	9.09E-06	3.73E-05
1.24E+02	2.57E-05	4.91E-06	2.41E-05
1.26E+02	1.07E-05	2.91E-06	6.12E-06
1.28E+02	2.74E-06	3.34E-07	5.70E-06
1.30E+02	8.51E-06	2.92E-06	3.60E-06
1.32E+02	2.48E-05	1.30E-05	1.34E-07
1.34E+02	4.77E-05	1.57E-05	6.79E-08
1.36E+02	6.18E-05	1.70E-05	2.00E-06
1.38E+02	2.59E-05	1.12E-05	3.61E-06
1.40E+02	4.24E-05	6.93E-06	6.13E-06
1.42E+02	6.67E-05	4.78E-06	9.79E-06
1.44E+02	8.19E-05	8.92E-07	2.96E-05
1.46E+02	1.34E-04	2.98E-06	5.58E-05
1.48E+02	1.20E-04	2.18E-06	7.17E-05
1.50E+02	6.97E-05	9.99E-07	1.03E-04
1.52E+02	6.27E-05	2.74E-06	9.95E-05
1.54E+02	3.92E-05	6.79E-07	7.95E-05
1.56E+02	7.01E-05	5.06E-07	8.27E-05
1.58E+02	1.00E-04	8.03E-06	8.12E-05
1.60E+02	6.35E-05	2.64E-05	6.80E-05
1.62E+02	1.37E-04	5.37E-05	7.32E-05
1.64E+02	1.71E-04	2.54E-05	7.15E-06
1.66E+02	1.27E-04	1.83E-05	4.40E-05
1.68E+02	2.42E-04	2.87E-05	7.31E-05

1.70E+02	1.17E-04	7.06E-06	3.48E-05
1.72E+02	5.12E-05	2.90E-06	7.93E-06
1.74E+02	2.53E-05	1.51E-06	2.04E-05
1.76E+02	2.45E-04	1.56E-05	4.01E-05
1.78E+02	1.46E-04	1.00E-05	9.88E-06
1.80E+02	1.01E-04	8.32E-07	9.10E-05
1.82E+02	2.85E-05	3.23E-06	8.31E-05
1.84E+02	6.02E-05	3.04E-06	1.27E-04
1.86E+02	9.80E-05	1.40E-05	2.88E-04
1.88E+02	2.24E-04	1.13E-05	2.28E-04
1.90E+02	2.98E-04	1.51E-05	1.12E-04
1.92E+02	8.28E-05	2.46E-05	4.88E-04
1.94E+02	1.57E-04	4.32E-05	3.51E-04
1.96E+02	2.16E-05	7.60E-06	4.09E-06
1.98E+02	1.27E-04	4.65E-07	3.06E-05
2.00E+02	6.70E-05	3.10E-06	3.27E-04
2.02E+02	1.35E-06	1.98E-06	2.60E-04
2.04E+02	1.49E-05	4.69E-07	6.53E-04
2.06E+02	2.86E-07	5.64E-06	1.22E-03
2.08E+02	1.00E-05	1.71E-05	8.86E-04
2.10E+02	1.16E-05	8.44E-06	4.69E-04
2.12E+02	1.01E-05	3.04E-06	4.36E-04
2.14E+02	1.68E-05	1.04E-05	4.89E-04
2.16E+02	2.36E-06	5.16E-06	1.85E-04
2.18E+02	7.49E-06	3.46E-07	3.45E-05
2.20E+02	4.25E-05	3.16E-06	3.53E-04
2.22E+02	2.64E-05	5.08E-06	2.43E-04
2.24E+02	1.96E-05	1.37E-06	2.71E-04
2.26E+02	9.14E-06	3.26E-06	1.33E-04
2.28E+02	4.64E-05	6.91E-06	4.23E-04
2.30E+02	5.07E-05	2.91E-06	5.42E-04
2.32E+02	6.99E-06	2.28E-06	2.12E-04
2.34E+02	1.43E-05	1.81E-06	1.22E-04
2.36E+02	1.26E-05	4.75E-08	5.72E-06
2.38E+02	2.09E-06	1.30E-06	4.79E-05
2.40E+02	2.55E-05	2.08E-06	3.24E-04
2.42E+02	4.08E-05	1.23E-06	6.46E-04
2.44E+02	3.96E-05	1.89E-06	1.05E-03
2.46E+02	1.95E-05	1.31E-06	7.55E-04
2.48E+02	3.55E-05	1.37E-06	1.70E-04
2.50E+02	4.76E-05	6.93E-07	7.97E-04
2.52E+02	2.60E-05	6.44E-07	9.22E-04
2.54E+02	3.80E-05	4.70E-06	1.15E-03
2.56E+02	2.42E-05	6.98E-06	9.76E-04
2.58E+02	1.35E-05	3.05E-06	6.48E-04

2.60E+02	1.11E-05	8.57E-07	6.11E-04
2.62E+02	6.08E-06	1.07E-06	5.76E-04
2.64E+02	2.16E-07	9.39E-07	3.23E-04
2.66E+02	7.27E-07	1.65E-06	1.07E-04
2.68E+02	3.70E-06	8.85E-07	6.01E-06
2.70E+02	5.73E-06	6.26E-07	5.75E-05
2.72E+02	7.31E-06	4.14E-07	2.96E-04
2.74E+02	4.91E-06	2.53E-08	3.85E-04
2.76E+02	1.78E-06	3.57E-07	3.68E-04
2.78E+02	1.88E-07	1.50E-06	2.67E-04
2.80E+02	2.98E-06	2.19E-06	1.08E-04
2.82E+02	2.90E-06	1.66E-06	9.77E-05
2.84E+02	1.53E-06	8.85E-07	1.48E-04
2.86E+02	1.06E-06	6.64E-07	1.45E-04
2.88E+02	5.19E-07	3.31E-07	1.12E-04
2.90E+02	1.52E-08	1.50E-07	7.64E-05
2.92E+02	3.60E-07	1.72E-07	4.21E-05
2.94E+02	1.24E-06	4.15E-08	2.13E-05
2.96E+02	1.73E-06	4.81E-08	2.64E-05
2.98E+02	1.31E-06	2.50E-07	1.97E-05
3.00E+02	2.70E-07	3.71E-07	1.82E-05
3.02E+02	1.87E-07	7.09E-08	7.46E-06
3.04E+02	1.91E-07	1.95E-07	4.20E-07
3.06E+02	1.60E-07	3.09E-07	2.32E-06
3.08E+02	5.87E-07	1.00E-07	3.98E-06
3.10E+02	1.57E-07	3.55E-08	2.42E-05
3.12E+02	2.02E-06	3.43E-08	2.25E-05
3.14E+02	2.27E-06	2.21E-07	2.97E-05
3.16E+02	6.64E-07	1.75E-07	3.07E-05
3.18E+02	1.72E-07	1.59E-07	1.83E-05
3.20E+02	5.64E-07	5.31E-08	1.32E-05
3.22E+02	8.44E-07	9.71E-08	1.53E-05
3.24E+02	8.93E-07	1.65E-07	1.71E-05
3.26E+02	7.08E-07	2.81E-07	9.72E-06
3.28E+02	7.48E-07	3.04E-07	1.41E-05
3.30E+02	1.07E-06	1.07E-07	1.76E-05
3.32E+02	7.77E-07	3.96E-08	1.67E-05
3.34E+02	9.58E-07	1.20E-07	2.29E-05
3.36E+02	6.87E-07	2.73E-07	1.16E-05
3.38E+02	1.75E-07	1.02E-07	2.38E-06
3.40E+02	6.35E-08	1.84E-08	2.16E-06
3.42E+02	4.84E-08	3.05E-08	6.82E-06
3.44E+02	1.55E-07	1.41E-08	8.93E-06
3.46E+02	2.55E-07	5.34E-08	1.15E-05
3.48E+02	2.47E-07	7.47E-08	9.57E-06

3.50E+02	2.45E-07	5.86E-08	7.32E-06
3.52E+02	4.51E-08	1.46E-08	4.64E-06
3.54E+02	4.24E-08	1.07E-08	5.23E-06
3.56E+02	2.30E-07	2.66E-08	5.43E-06
3.58E+02	4.31E-07	1.98E-08	4.30E-06
3.60E+02	5.35E-07	5.14E-09	3.87E-06
3.62E+02	4.96E-07	3.13E-09	3.06E-06
3.64E+02	1.53E-07	1.53E-08	9.78E-07
3.66E+02	1.63E-07	6.32E-08	1.84E-06
3.68E+02	4.45E-08	5.87E-08	3.28E-07
3.70E+02	1.14E-08	1.91E-08	1.76E-07
3.72E+02	2.70E-08	1.18E-08	1.45E-07
3.74E+02	9.33E-08	5.79E-08	1.83E-07
3.76E+02	1.30E-08	4.87E-08	6.57E-07
3.78E+02	1.82E-08	3.66E-08	5.49E-07
3.80E+02	2.80E-08	3.03E-08	3.75E-07
3.82E+02	7.91E-08	1.59E-08	2.82E-07
3.84E+02	6.26E-08	8.44E-08	1.05E-07
3.86E+02	9.97E-08	1.36E-07	1.24E-07
3.88E+02	1.14E-07	9.42E-08	2.06E-07
3.90E+02	1.02E-07	3.53E-08	9.35E-08
3.92E+02	3.98E-08	5.06E-08	2.20E-07
3.94E+02	4.71E-09	4.43E-08	6.74E-07
3.96E+02	4.72E-09	2.36E-08	6.70E-07
3.98E+02	5.64E-08	2.71E-08	2.53E-07
4.00E+02	1.61E-07	2.24E-08	1.79E-07
4.02E+02	1.67E-07	1.36E-08	3.59E-07
4.04E+02	1.28E-07	6.87E-09	3.23E-07
4.06E+02	1.36E-07	2.14E-08	2.39E-07
4.08E+02	8.73E-08	3.10E-08	1.97E-07
4.10E+02	4.26E-08	5.35E-08	2.17E-07
4.12E+02	2.38E-08	3.57E-08	3.11E-07
4.14E+02	8.31E-08	3.45E-09	2.66E-07
4.16E+02	9.11E-08	6.49E-09	1.80E-07
4.18E+02	1.16E-08	1.31E-08	4.27E-08
4.20E+02	3.29E-08	1.10E-08	1.65E-09
4.22E+02	4.41E-08	9.58E-09	1.54E-09
4.24E+02	3.94E-08	4.68E-09	2.28E-10
4.26E+02	3.97E-08	2.56E-09	1.89E-08
4.28E+02	5.65E-08	5.39E-09	8.04E-08
4.30E+02	8.53E-08	4.18E-09	1.01E-07
4.32E+02	3.32E-08	5.48E-09	4.24E-08
4.34E+02	4.17E-09	2.74E-09	4.34E-08
4.36E+02	6.52E-10	9.16E-10	4.52E-08
4.38E+02	7.30E-10	5.19E-10	2.80E-08

4.40E+02	5.31E-09	7.36E-10	7.08E-09
4.42E+02	1.70E-08	2.77E-09	8.73E-09
4.44E+02	7.19E-09	4.37E-09	5.53E-09
4.46E+02	2.77E-09	1.54E-09	2.49E-08
4.48E+02	8.54E-09	3.20E-10	3.50E-08
4.50E+02	6.68E-09	1.89E-10	1.66E-08
4.52E+02	1.03E-08	6.74E-10	3.24E-08
4.54E+02	2.56E-08	1.29E-09	2.50E-08
4.56E+02	2.85E-08	3.01E-09	1.19E-08
4.58E+02	3.57E-08	5.95E-10	9.11E-09
4.60E+02	2.04E-08	3.73E-10	2.45E-09
4.62E+02	3.66E-08	1.27E-09	3.16E-09
4.64E+02	4.82E-08	6.58E-09	1.86E-09
4.66E+02	2.34E-08	3.69E-09	2.05E-09
4.68E+02	3.45E-08	3.33E-09	1.82E-09
4.70E+02	1.93E-08	7.82E-10	1.82E-10
4.72E+02	4.93E-09	6.05E-10	2.05E-09
4.74E+02	6.39E-09	4.63E-09	1.05E-08
4.76E+02	1.92E-08	1.08E-08	1.35E-08
4.78E+02	8.74E-09	1.95E-09	3.78E-09
4.80E+02	2.49E-09	9.66E-10	9.95E-10
4.82E+02	8.92E-10	5.97E-10	1.95E-09
4.84E+02	3.81E-09	1.21E-09	3.69E-09
4.86E+02	4.04E-09	3.27E-09	1.74E-09
4.88E+02	2.61E-09	2.47E-09	4.21E-11
4.90E+02	1.34E-09	2.14E-09	2.39E-09
4.92E+02	9.43E-09	9.49E-10	1.43E-09
4.94E+02	1.09E-09	3.86E-09	2.23E-10
4.96E+02	1.85E-09	2.89E-09	1.49E-10
4.98E+02	5.88E-09	1.83E-09	1.52E-10

5.7.3 Appendix 3 Mean spectrum for truck transport in Kenya.

Frequency(Hz)	Kambaa route	Nyamache route	Michi route	Chebut route	Mean
1	0.009	-	0.009	-	0.009
2	0.03	0.09	0.06	0.003	0.04
3	0.03	0.04	0.06	0.005	0.03
4	0.001	0.02	0.02	0.0002	0.01
7	0.0003	0.008	0.002	0.0005	0.0002
20	0.003	0.003	0.008	0.0002	0.0004
100	0.00003	0.0009	0.00002	0.00002	0.00002

5.7.4 Appendix 4: Determination of angle of repose for various tea grades/fractions

Fraction size	**Tea pile Height (H)**	**Pile diameter (D)**	**Tanα =2H/D**	**α(^{0})**	**Angle of Repose**
2-1mm	60mm	172mm	0.6977	27.8	27.8
1mm-500µ	51mm	150mm	0.6800	29.3	29.3
500-250µ	45mm	148mm	0.6082	31.3	31.3
250-125µ	43mm	153mm	0.5621	34.2	34.2
125-63µ	33mm	125mm	0.5280	34.9	34.9

5.7.5 Appendix 5 Pre-calibrated gas pycnometer

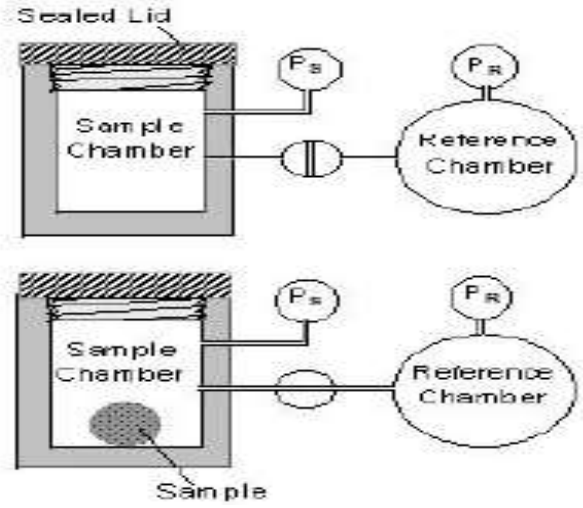

5.7.6 Appendix 6 Simulation Rig Design Parameters

1. Tea density determination

$Weight := 90.280gm$

$Volume := 0.200L$

Density

$$\rho := \frac{Weight}{Volume}$$

$$\rho = 451.4\frac{gm}{L}$$

2. Experimental Perspex tubes size and respective weight of tea determinations

Inner diameter:

$d_i := 25.4mm$

Outer diameter:

$d_o := 30mm$

Height of filled column of tea particles as a function of their weight:

$$h(w) := \frac{w}{\rho \cdot \frac{\pi \cdot d_i^2}{4}}$$

$h(10gm) = 43.72mm$

$h(20gm) = 87.44mm$

$h(30gm) = 131.16mm$

$h(40gm) = 174.88mm$

$h(50gm) = 218.6mm$

1. Static load steel rods size determination

Density of steel

$$\rho_s := 7850 \cdot 10^{-9}\frac{kg}{mm^3}$$

$$\rho_s = 7.85\times 10^{-3}\ \frac{gm}{mm^3}$$

Pressure on the tea particles

4 Determination of unit pressure on tea particles

$$p(w) := \frac{w\cdot g}{\frac{\pi\cdot d_i^{\,2}}{4}}$$

Height of steel rods and pressure on tea column

$$h_m(w) := \frac{w}{\rho_s\cdot\frac{\pi\cdot d_i^{\,2}}{4}}$$

$h_m(450gm) = 113.132mm$

$p(450gm) = 8.709\times 10^{3}\ Pa$

$h_m(360gm) = 90.506mm$

$p(360gm) = 6.967\times 10^{3}\ Pa$

$h_m(270gm) = 67.879mm$

$p(270gm) = 5.225\times 10^{3}\ Pa$

$h_m(180gm) = 45.253mm$

$p(180gm) = 3.484\times 10^{3}\ Pa$

$h_m(90gm) = 22.626mm$

$p(90gm) = 1.742\times 10^{3}\ Pa$

Height of longest tube

$$h_{lt} := h(50gm) + \frac{h_m(450gm)}{2}$$

$h_{lt} = 275.167mm$

5 Pressure on bottom bag tea particles in pallet

slength := 1120mm

swidth := 580mm

sheight := 205mm

vol10s := slength·swidth·sheight·10

$vol10s = 1.332 \times 10^{9}\ mm^{3}$

mass10s := vol10s·ρ

mass10s = 601.12kg

Pressure on the bottom layer of tea particles in the bottom sack (stacked 10 high)

$p_b := \frac{mass10s \cdot g}{slength \cdot swidth}$ $\qquad p_b = 9.075 \times 10^{3}\ Pa$

5.7.7 Appendix 7 Nyamache to Mombasa trip speed and location data

VEHICLE: KBJ 257T-OMOCHA ENT				VEHICLE HISTORY
TIME	LOCATION	STATUS	SPEED	COORDINATES
4/7/2011 4:55:14 PM	0.55KM South OF Nyamache		0	34.8208 -0.861302
4/7/2011 4:56:14 PM	0.51KM South OF Nyamache		24	34.8214 -0.860642
4/7/2011 4:58:15 PM	0.65KM North East OF Nyamache		43	34.8253 -0.851237
4/7/2011 5:00:16 PM	1.9KM North East OF Nyamache		57	34.8325 -0.839608
4/7/2011 5:03:16 PM	2.67KM South East OF Igare		22	34.8246 -0.824512
4/7/2011 5:04:16 PM	2.36KM South East OF Igare		32	34.8231 -0.821268
4/7/2011 5:05:17 PM	1.77KM South East OF Igare		57	34.8157 -0.820468
4/7/2011 5:07:17 PM	0.94KM South OF Igare		54	34.8031 -0.814205
4/7/2011 5:09:18 PM	0.2KM North West OF Igare		35	34.8046 -0.802885
4/7/2011 5:13:18 PM	2.38KM North East OF Igare		41	34.8223 -0.785747
4/7/2011 5:14:19 PM	3.22KM West OF Nyanturago		54	34.828 -0.780675
4/7/2011 5:18:20 PM	2.34KM South West OF Keumbu		35	34.8318 -0.757103
4/7/2011 5:19:21 PM	1.77KM South West OF Keumbu		52	34.8337 -0.750815
4/7/2011 5:20:20 PM	1.31KM South West OF Keumbu		28	34.8352 -0.745568
4/7/2011 5:23:21 PM	0.45KM South West OF Keumbu		24	34.8405 -0.7381
4/7/2011 5:24:21 PM	0.11KM North West OF Keumbu		35	34.843 -0.73455
4/7/2011 5:25:22 PM	0.17KM North East OF Keumbu		0	34.8453 -0.73409
4/7/2011 5:28:22 PM	0.32KM East OF Keumbu		0	34.8469 -0.734905

4/7/2011 5:34:24 PM	0.47KM East OF Keumbu		32	34.8483 -0.735482
4/7/2011 5:35:24 PM	1.15KM East OF Keumbu		50	34.8547 -0.73673
4/7/2011 5:39:25 PM	2.44KM West OF Burongo		19	34.8658 -0.74276
4/7/2011 5:43:26 PM	0.88KM West OF Burongo		46	34.8807 -0.74201
4/7/2011 5:44:27 PM	0.25KM South West OF Burongo		30	34.8872 -0.745997
4/7/2011 5:46:26 PM	0.47KM South East OF Burongo		13	34.8912 -0.748422
4/7/2011 5:49:28 PM	1.54KM West OF Matunwa		59	34.9046 -0.754055
4/7/2011 5:54:28 PM	1.59KM North West OF Keroka		35	34.9319 -0.76711
4/7/2011 5:59:30 PM	0.12KM South East OF Keroka		11	34.9459 -0.776732
4/7/2011 6:00:31 PM	0.3KM South East OF Keroka		11	34.947 -0.778355
4/7/2011 6:04:31 PM	1.27KM South East OF Keroka		41	34.9565 -0.780117
4/7/2011 6:05:31 PM	1.23KM South West OF Kijauri		61	34.9612 -0.776505
4/7/2011 6:08:32 PM	0.38KM South OF Kijauri		41	34.97 -0.77116
4/7/2011 6:10:33 PM	1.74KM East OF Kijauri		57	34.9856 -0.770493
4/7/2011 6:11:33 PM	2.09KM East OF Kijauri		46	34.9892 -0.767545
4/7/2011 6:14:19 PM	0.54KM West OF Menyenga		83	35.0126 -0.761305
4/7/2011 6:16:34 PM	1.14KM North OF Menyenga		48	35.0195 -0.749338
4/7/2011 6:19:34 PM	3.47KM North OF Menyenga		59	35.0349 -0.728705
4/7/2011 6:21:35 PM	5.98KM East OF Gesima		72	35.0447 -0.7117
4/7/2011 6:22:36 PM	6.33KM West OF Sotik		70	35.0504 -0.703632
4/7/2011 7:17:30 PM	4.04KM West OF Sotik		0	35.0711 -0.694035
4/7/2011 7:21:30 PM	2.1KM West OF Sotik		44	35.0892 -0.689175
4/7/2011 7:22:31 PM	1.77KM West OF Sotik		10	35.0927 -0.686315
4/7/2011 7:23:31 PM	1.24KM North West OF Sotik		59	35.0985 -0.684193
4/7/2011 7:28:32 PM	0.76KM North East OF Sotik		33	35.1157 -0.687045
4/7/2011 7:32:33 PM	2.63KM South OF Kiplanget		13	35.1365 -0.67636
4/7/2011 7:33:34 PM	2.61KM South OF Kiplanget		13	35.1384 -0.676047
4/7/2011 7:34:34 PM	2.69KM South OF Kiplanget		8	35.1392 -0.676915
4/7/2011 7:36:34 PM	2.41KM North West OF Yaganek		24	35.1407 -0.682707
4/7/2011 7:39:35 PM	0.94KM North West OF Yaganek		41	35.1437 -0.70253
4/7/2011 7:40:35 PM	0.37KM West OF Yaganek		43	35.1484 -0.706235
4/7/2011 7:45:30 PM	1.48KM South OF Yaganek		22	35.1581 -0.721472
4/7/2011 7:50:23 PM	3.82KM North West OF Kamusin		48	35.1842 -0.741895
4/7/2011 7:55:24 PM	1.67KM North OF Kamusin		17	35.2148 -0.750945
4/7/2011 7:56:24 PM	1.49KM North OF Kamusin		55	35.2174 -0.754113
4/7/2011 8:00:25 PM	2.37KM South OF Kiplelji		48	35.2445 -0.764643
4/7/2011 8:01:25 PM	2.65KM South OF Kiplelji		32	35.2495 -0.768563
4/7/2011 8:07:27 PM	3.8KM South West OF Chebunge		55	35.2889 -0.779665
4/7/2011 8:08:27 PM	3.48KM South West OF Chebunge		54	35.2959 -0.784145
4/7/2011 8:10:27 PM	3.18KM South West OF Chebunge		11	35.3026 -0.78638
4/7/2011 8:13:28 PM	2.34KM West OF Bomet		57	35.3212 -0.783383
4/7/2011 8:14:29 PM	1.37KM West OF Bomet		57	35.3305 -0.781187
4/7/2011 8:19:29 PM	0.16KM North East OF Bomet		6	35.3444 -0.78124
4/7/2011 8:20:30 PM	0.23KM South East OF Bomet		50	35.3452 -0.784035
4/7/2011 8:24:31 PM	2.81KM South OF Bomet		66	35.3391 -0.814025
4/7/2011 8:30:32 PM	3.65KM North West OF Longisa		19	35.3609 -0.840157
4/7/2011 8:31:33 PM	3.37KM North West OF Longisa		19	35.3638 -0.840437
4/7/2011 8:36:34 PM	0.88KM North West OF Longisa		26	35.3874 -0.851153
4/7/2011 8:37:34 PM	0.62KM North OF Longisa		26	35.3907 -0.853025
4/7/2011 8:38:34 PM	0.37KM North East OF Longisa		44	35.3935 -0.856965
4/7/2011 8:40:35 PM	0.55KM South East OF Longisa		61	35.3946 -0.864608
4/7/2011 8:41:35 PM	1KM South East OF Longisa		54	35.3965 -0.869257
4/7/2011 8:47:37 PM	1.61KM North West OF Mulot		57	35.4127 -0.919652
4/7/2011 9:00:03 PM	0.32KM South OF Mulot		0	35.4213 -0.93749
4/7/2011 9:02:24 PM	0.41KM South OF Mulot		0	35.4217 -0.938612
4/7/2011 9:03:25 PM	0.41KM South OF Mulot		2	35.4217 -0.938655
4/7/2011 9:07:26 PM	1.95KM South OF Mulot		46	35.4294 -0.954255
4/7/2011 9:08:25 PM	2.53KM South East OF Mulot		48	35.435 -0.958113
4/7/2011 9:13:27 PM	6.44KM South East OF Mulot		37	35.4767 -0.965595

VEHICLE: KBJ 257T-OMOCHA ENT				VEHICLE HISTORY
TIME	LOCATION	STATUS	SPEED	COORDINATES
4/7/2011 9:17:28 PM	5.41KM North OF Ngorengore		43	35.4965 -0.973188
4/7/2011 9:19:28 PM	5.26KM North OF Ngorengore		54	35.5127 -0.97654
4/7/2011 9:24:30 PM	7.26KM North East OF Ngorengore		76	35.5569 -0.98779
4/7/2011 9:25:30 PM	7.97KM North East OF Ngorengore		63	35.5666 -0.991295
4/7/2011 9:28:31 PM	7.78KM West OF Olulunga		61	35.5923 -0.993745
4/7/2011 9:29:31 PM	6.88KM West OF Olulunga		55	35.6004 -0.998613
4/7/2011 9:30:31 PM	5.94KM West OF Olulunga		68	35.6092 -1.00195
4/7/2011 9:35:32 PM	2.24KM South West OF Olulunga		48	35.6467 -1.0149
4/7/2011 9:36:33 PM	2.11KM South West OF Olulunga		11	35.6492 -1.01702
4/7/2011 9:41:34 PM	3.06KM South East OF Olulunga		74	35.687 -1.02554
4/7/2011 9:45:35 PM	6.07KM South East OF Olulunga		50	35.7144 -1.03792
4/7/2011 9:46:35 PM	6.62KM South East OF Olulunga		41	35.7189 -1.04098
4/7/2011 9:47:36 PM	7.35KM South East OF Olulunga		52	35.7252 -1.04464
4/7/2011 9:52:36 PM	7.88KM North OF Ewaso Ngiro		26	35.7511 -1.06399
4/7/2011 9:53:37 PM	7.47KM North OF Ewaso Ngiro		70	35.7584 -1.06783
4/7/2011 9:54:37 PM	7.14KM North OF Ewaso Ngiro		72	35.7687 -1.07189
4/7/2011 9:59:38 PM	6.37KM West OF Narok		59	35.8135 -1.08377
4/7/2011 10:00:38 PM	5.5KM West OF Narok		55	35.8218 -1.08917
4/7/2011 10:03:39 PM	3.15KM South West OF Narok		59	35.8466 -1.10035
4/7/2011 10:04:40 PM	2.25KM South West OF Narok		59	35.8559 -1.09962
4/7/2011 10:08:40 PM	1.07KM South OF Narok		24	35.8684 -1.09585
4/7/2011 10:09:41 PM	0.91KM South OF Narok		0	35.8692 -1.09429
4/7/2011 10:10:41 PM	0.91KM South OF Narok		0	35.8692 -1.09429
4/7/2011 10:15:43 PM	0.91KM South OF Narok		0	35.8691 -1.09427
4/8/2011 3:05:49 AM	0.86KM South OF Narok		0	35.8694 -1.09375
4/8/2011 3:07:50 AM	0.86KM South OF Narok		0	35.8694 -1.09379
4/8/2011 3:08:49 AM	0.63KM South OF Narok		28	35.8705 -1.09161
4/8/2011 3:11:50 AM	0.54KM South East OF Narok		21	35.8775 -1.08918
4/8/2011 3:13:51 AM	1.53KM South East OF Narok		39	35.8871 -1.0914
4/8/2011 3:19:52 AM	3.27KM South West OF Seyabeyi		68	35.9265 -1.09464
4/8/2011 3:20:52 AM	2.26KM South West OF Seyabeyi		74	35.9368 -1.09275
4/8/2011 3:23:54 AM	1.63KM South OF Seyabeyi		21	35.9605 -1.0932
4/8/2011 3:25:53 AM	2.71KM South East OF Seyabeyi		66	35.9684 -1.10179
4/8/2011 3:31:55 AM	6.27KM South East OF Seyabeyi		35	36.0017 -1.11797
4/8/2011 3:34:56 AM	6.14KM South East OF Seyabeyi		11	36.0063 -1.10502
4/8/2011 3:35:56 AM	6.32KM South East OF Seyabeyi		35	36.009 -1.10299
4/8/2011 3:36:56 AM	6.55KM South East OF Seyabeyi		0	36.0114 -1.10267
4/8/2011 3:39:02 AM	6.2KM West OF Ntulelei		85	36.0235 -1.10234
4/8/2011 3:40:58 AM	5.05KM West OF Ntulelei		68	36.0343 -1.10202
4/8/2011 3:46:59 AM	3.1KM South West OF Ntulelei		17	36.0539 -1.10948
4/8/2011 3:49:00 AM	2.58KM South West OF Ntulelei		17	36.0581 -1.10588
4/8/2011 3:53:00 AM	2.41KM West OF Ntulelei		6	36.0596 -1.10487
4/8/2011 3:54:00 AM	2.14KM West OF Ntulelei		33	36.0621 -1.10389
4/8/2011 3:59:01 AM	0.61KM North East OF Ntulelei		22	36.0867 -1.09567
4/8/2011 4:00:02 AM	0.97KM North East OF Ntulelei		0	36.0901 -1.09425
4/8/2011 4:06:04 AM	3.42KM East OF Ntulelei		30	36.1135 -1.09217
4/8/2011 4:07:41 AM	4.79KM East OF Ntulelei		81	36.1268 -1.09438
4/8/2011 4:08:26 AM	5.74KM East OF Ntulelei		81	36.1359 -1.09665
4/8/2011 4:09:57 AM	4.75KM South OF NairagieNgare		81	36.1514 -1.09854
4/8/2011 4:10:04 AM	4.7KM South OF NairagieNgare		72	36.1528 -1.09824
4/8/2011 4:12:04 AM	4.1KM South OF NairagieNgare		0	36.1618 -1.09182
4/8/2011 4:17:06 AM	6.08KM South OF NairagieNgare		50	36.1873 -1.10545
4/8/2011 4:18:06 AM	6.61KM South West OF Suswa		52	36.1952 -1.10524
4/8/2011 4:23:08 AM	2.9KM South West OF Suswa		33	36.2389 -1.10694
4/8/2011 4:24:08 AM	2.55KM South OF Suswa		76	36.2452 -1.10631
4/8/2011 4:26:08 AM	2.37KM South OF Suswa		63	36.2648 -1.10235
4/8/2011 4:29:09 AM	4.1KM South East OF Suswa		63	36.2912 -1.09006
4/8/2011 4:33:11 AM	7.49KM East OF Suswa		68	36.3225 -1.06054
4/8/2011 4:35:10 AM	5.34KM South West OF Akira		33	36.3328 -1.04954
4/8/2011 5:00:01 AM	5.69KM West OF Mai Mahiu		70	36.5367 -0.994263
4/8/2011 5:01:54 AM	4.22KM West OF Mai Mahiu		0	36.5507 -0.994898

VEHICLE: KBJ 257T-OMOCHA ENT				VEHICLE HISTORY
TIME	LOCATION	STATUS	SPEED	COORDINATES
4/8/2011 5:05:54 AM	1.64KM West OF Mai Mahiu		65	36.5746 -0.989137
4/8/2011 5:06:55 AM	0.84KM West OF Mai Mahiu		4	36.582 -0.986407
4/8/2011 5:08:55 AM	0.57KM North West OF Mai Mahiu		6	36.5858 -0.982445
4/8/2011 5:09:56 AM	0.35KM North West OF Mai Mahiu		17	36.5875 -0.983928
4/8/2011 5:11:57 AM	0.97KM South East OF Mai Mahiu		50	36.5975 -0.992982
4/8/2011 5:12:57 AM	1.37KM South East OF Mai Mahiu		22	36.6011 -0.994615
4/8/2011 5:16:57 AM	1.39KM West OF Kirenga		13	36.6018 -1.00955
4/8/2011 5:18:58 AM	1.5KM South West OF Kirenga		35	36.6012 -1.01464
4/8/2011 5:19:58 AM	1.48KM South West OF Kirenga		46	36.6032 -1.01954
4/8/2011 5:29:53 AM	3.24KM North West OF Murengeti		17	36.603 -1.05604
4/8/2011 5:31:00 AM	3.03KM West OF Murengeti		28	36.6038 -1.06014
4/8/2011 5:35:02 AM	2.56KM North OF ndiuini		6	36.6018 -1.07001
4/8/2011 5:40:03 AM	1.9KM East OF ndiuini		52	36.609 -1.10021
4/8/2011 5:41:03 AM	1.43KM North West OF Kamirithu		43	36.6125 -1.10739
4/8/2011 5:46:05 AM	0.98KM South East OF Kamirithu		61	36.6285 -1.12665
4/8/2011 5:50:05 AM	1.92KM South East OF Kamirithu		39	36.6352 -1.13391
4/8/2011 5:51:06 AM	1.17KM North OF Rironi		77	36.6371 -1.14346
4/8/2011 5:52:10 AM	0.66KM East OF Rironi		85	36.6391 -1.15612
4/8/2011 5:56:07 AM	0.48KM South East OF Muguga		52	36.65 -1.19182
4/8/2011 6:00:08 AM	0.9KM North OF Gataba1		52	36.6634 -1.22164
4/8/2011 6:02:09 AM	0.71KM South East OF Gataba1		48	36.6704 -1.23392
4/8/2011 6:07:10 AM	0.73KM South West OF Uthiru		52	36.7017 -1.25802
4/8/2011 6:08:10 AM	0.6KM South OF Uthiru		50	36.7099 -1.26016
4/8/2011 6:13:11 AM	1.03KM North East OF Kangemi		65	36.749 -1.26403
4/8/2011 6:14:11 AM	1.86KM North East OF Kangemi		59	36.7583 -1.2638
4/8/2011 6:18:13 AM	3.6KM North West OF NAIROBI		68	36.7939 -1.26062
4/8/2011 6:19:13 AM	2.88KM North West OF NAIROBI		19	36.8011 -1.26314
4/8/2011 6:21:14 AM	1.73KM North West OF NAIROBI		50	36.809 -1.27223
4/8/2011 6:28:15 AM	0.43KM South OF NAIROBI		0	36.8199 -1.2919
4/8/2011 6:29:16 AM	0.43KM South OF NAIROBI		0	36.82 -1.29187
4/8/2011 6:30:15 AM	0.43KM South OF NAIROBI		0	36.8199 -1.29189
4/8/2011 6:34:16 AM	1.34KM North East OF RiverCross Technologies		24	36.8253 -1.30211
4/8/2011 6:35:17 AM	1.25KM North East OF RiverCross Technologies		32	36.8271 -1.30604
4/8/2011 6:36:17 AM	1.39KM East OF RiverCross Technologies		61	36.8306 -1.31337
4/8/2011 6:40:18 AM	4.72KM South East OF RiverCross Technologies		66	36.8598 -1.33109
4/8/2011 6:41:18 AM	3.85KM South OF Doonholm		57	36.8689 -1.33004
4/8/2011 6:42:18 AM	3.36KM South OF Doonholm		68	36.878 -1.32881
4/8/2011 6:46:20 AM	3.6KM South OF Embakasi		50	36.9049 -1.34792
4/8/2011 6:47:19 AM	4.23KM South OF Embakasi		50	36.907 -1.35582
4/8/2011 6:50:20 AM	6.11KM North West OF Athi River		54	36.9236 -1.37518
4/8/2011 6:53:21 AM	4.16KM North West OF Athi River		33	36.9374 -1.39025
4/8/2011 6:54:22 AM	3.43KM North West OF Athi River		65	36.9418 -1.39723
4/8/2011 6:55:57 AM	2.14KM West OF Athi River		83	36.9499 -1.41221
4/8/2011 7:04:23 AM	3.2KM South East OF Athi River		21	36.991 -1.44353
4/8/2011 7:05:24 AM	3.24KM South East OF Athi River		2	36.9916 -1.44359
4/8/2011 7:10:25 AM	5.32KM South East OF Athi River		10	37.0066 -1.45901
4/8/2011 7:11:26 AM	5.61KM South East OF Athi River		26	37.009 -1.46067
4/8/2011 7:13:26 AM	6.42KM South East OF Athi River		30	37.016 -1.4651
4/8/2011 7:15:26 AM	7.83KM South East OF Athi River		32	37.0285 -1.47195
4/8/2011 7:16:27 AM	8.52KM South East OF Athi River		44	37.0346 -1.47527
4/8/2011 7:17:27 AM	9.36KM South East OF Athi River		63	37.042 -1.47926
4/8/2011 7:26:29 AM	10.2KM West OF Mathatani		52	37.0984 -1.51032
4/8/2011 7:27:30 AM	9.42KM West OF Mathatani		55	37.106 -1.51524
4/8/2011 7:28:30 AM	8.76KM West OF Mathatani		61	37.1126 -1.51951
4/8/2011 7:29:29 AM	8.12KM West OF Mathatani		44	37.1194 -1.52387
4/8/2011 7:33:31 AM	6.78KM South West OF Mathatani		61	37.1368 -1.53911
4/8/2011 7:34:31 AM	6.58KM South West OF Mathatani		57	37.1424 -1.54665
4/8/2011 7:38:32 AM	7.64KM South OF Mathatani		70	37.1572 -1.58077
4/8/2011 7:39:32 AM	8.16KM South OF Mathatani		68	37.1621 -1.59073
4/8/2011 7:40:32 AM	9.62KM West OF Kimutwa		66	37.1664 -1.59954
4/8/2011 7:44:34 AM	8.7KM South West OF Kimutwa		52	37.1823 -1.6324

VEHICLE: KBJ 257T-OMOCHA ENT				VEHICLE HISTORY
TIME	LOCATION	STATUS	SPEED	COORDINATES
4/8/2011 7:55:14 AM	7.88KM North East OF Konza		54	37.1961 -1.69316
4/8/2011 7:56:14 AM	7.61KM North East OF Konza		61	37.1966 -1.70156
4/8/2011 7:57:14 AM	6.72KM North West OF Kilima Kiu		50	37.197 -1.7101
4/8/2011 7:58:15 AM	6.24KM North West OF Kilima Kiu		57	37.1974 -1.71763
4/8/2011 7:59:15 AM	5.73KM North West OF Kilima Kiu		57	37.1978 -1.72632
4/8/2011 8:00:16 AM	5.23KM North West OF Kilima Kiu		61	37.1983 -1.73584
4/8/2011 8:01:15 AM	4.83KM North West OF Kilima Kiu		43	37.1994 -1.74345
4/8/2011 8:02:15 AM	4.28KM West OF Kilima Kiu		63	37.2023 -1.75192
4/8/2011 8:05:16 AM	3.37KM West OF Kilima Kiu		46	37.2099 -1.77347
4/8/2011 8:09:17 AM	3.74KM South West OF Kilima Kiu		57	37.2212 -1.80183
4/8/2011 8:10:17 AM	4.19KM South OF Kilima Kiu		46	37.223 -1.80909
4/8/2011 8:11:18 AM	4.21KM South OF Kilima Kiu		33	37.2277 -1.81199
4/8/2011 8:12:18 AM	4.05KM North West OF Salama		48	37.2335 -1.81403
4/8/2011 8:14:19 AM	2.32KM North West OF Salama		44	37.2433 -1.83008
4/8/2011 8:20:20 AM	1.71KM South OF Salama		55	37.2639 -1.86789
4/8/2011 8:22:21 AM	2.6KM South West OF Maiani		0	37.2654 -1.87822
4/8/2011 8:24:21 AM	2.6KM South West OF Maiani		0	37.2654 -1.87822
4/8/2011 8:25:22 AM	2.67KM South West OF Maiani		21	37.2654 -1.87924
4/8/2011 8:28:22 AM	2.52KM West OF Kiogwani		57	37.2731 -1.90011
4/8/2011 8:34:24 AM	3.54KM South OF Kiogwani		57	37.3024 -1.94542
4/8/2011 8:35:23 AM	4.18KM South OF Kiogwani		54	37.3066 -1.95183
4/8/2011 8:36:24 AM	4.94KM South OF Kiogwani		55	37.3123 -1.95892
4/8/2011 8:40:25 AM	4.72KM North West OF Sultan Hamud		65	37.3374 -1.98105
4/8/2011 8:41:25 AM	3.69KM North West OF Sultan Hamud		68	37.3459 -1.98718
4/8/2011 8:42:26 AM	2.81KM North West OF Sultan Hamud		52	37.3531 -1.99251
4/8/2011 8:45:26 AM	0.41KM North West OF Sultan Hamud		61	37.3692 -2.01205
4/8/2011 8:46:26 AM	0.28KM South East OF Sultan Hamud		19	37.3746 -2.01679
4/8/2011 8:47:27 AM	0.54KM South East OF Sultan Hamud		13	37.3765 -2.01858
4/8/2011 8:51:28 AM	2.73KM South East OF Sultan Hamud		54	37.3941 -2.03201
4/8/2011 8:52:27 AM	3.52KM South East OF Sultan Hamud		59	37.4005 -2.03665
4/8/2011 8:55:29 AM	4.9KM South West OF Ndauni		55	37.4214 -2.05179
4/8/2011 8:57:29 AM	4.13KM West OF Emali		63	37.4357 -2.06216
4/8/2011 9:02:30 AM	0.36KM South West OF Emali		21	37.4699 -2.07903
4/8/2011 9:06:32 AM	0.41KM South East OF Emali		0	37.4753 -2.08027
4/8/2011 9:47:34 AM	0.42KM South East OF Emali		0	37.4755 -2.08027
4/8/2011 9:47:58 AM	0.42KM South East OF Emali		0	37.4754 -2.08031
4/8/2011 9:49:59 AM	0.41KM South East OF Emali		0	37.4753 -2.08033
4/8/2011 9:50:59 AM	0.4KM South East OF Emali		0	37.4753 -2.08028
4/8/2011 9:53:00 AM	0.41KM South East OF Emali		0	37.4753 -2.08033
4/8/2011 9:54:00 AM	0.41KM South East OF Emali		0	37.4753 -2.08035
4/8/2011 9:54:59 AM	0.41KM South East OF Emali		0	37.4753 -2.08034
4/8/2011 9:56:00 AM	0.41KM South East OF Emali		0	37.4753 -2.0803
4/8/2011 10:02:43 AM	0.41KM South East OF Emali		0	37.4753 -2.08032
4/8/2011 10:03:43 AM	0.45KM South East OF Emali		4	37.4757 -2.08055
4/8/2011 10:18:18 AM	2.45KM South East OF Emali		61	37.4916 -2.09318
4/8/2011 10:19:18 AM	3.39KM South East OF Emali		57	37.5005 -2.09628
4/8/2011 10:22:18 AM	5.99KM South East OF Emali		68	37.5219 -2.1109
4/8/2011 10:23:18 AM	6.87KM South East OF Emali		54	37.5284 -2.11758
4/8/2011 10:24:19 AM	6.68KM North West OF Simba		63	37.5364 -2.12199
4/8/2011 10:26:20 AM	4.85KM North West OF Simba		59	37.5518 -2.13181
4/8/2011 10:28:20 AM	3.29KM North West OF Simba		48	37.5652 -2.13949
4/8/2011 10:31:20 AM	1.36KM West OF Simba		44	37.5814 -2.15136
4/8/2011 10:32:21 AM	0.99KM West OF Simba		13	37.585 -2.15395
4/8/2011 10:33:21 AM	0.78KM South West OF Simba		22	37.5873 -2.15563
4/8/2011 10:36:22 AM	0.69KM South OF Simba		15	37.5942 -2.16064
4/8/2011 10:39:22 AM	2.56KM South East OF Simba		65	37.6162 -2.16488
4/8/2011 10:42:23 AM	5.36KM South East OF Simba		59	37.6419 -2.17319
4/8/2011 10:43:24 AM	6.17KM South East OF Simba		57	37.6484 -2.17863
4/8/2011 10:46:24 AM	4.61KM North West OF Kiboko		41	37.6679 -2.19156
4/8/2011 10:48:25 AM	3.07KM West OF Kiboko		50	37.6809 -2.19993
4/8/2011 10:49:25 AM	2.28KM West OF Kiboko		63	37.6875 -2.20537

VEHICLE: KBJ 257T-OMOCHA ENT				VEHICLE HISTORY
TIME	LOCATION	STATUS	SPEED	COORDINATES
4/8/2011 10:50:25 AM	1.18KM West OF Kiboko		70	37.6976 -2.20806
4/8/2011 10:54:27 AM	1.23KM East OF Kiboko		33	37.7201 -2.21141
4/8/2011 10:55:26 AM	1.6KM East OF Kiboko		41	37.7235 -2.2123
4/8/2011 10:57:27 AM	3.25KM South East OF Kiboko		54	37.7381 -2.22055
4/8/2011 10:58:27 AM	3.51KM West OF Ikoyo		52	37.7457 -2.2248
4/8/2011 10:59:28 AM	2.66KM West OF Ikoyo		63	37.7534 -2.2287
4/8/2011 11:00:28 AM	1.92KM West OF Ikoyo		54	37.7605 -2.23456
4/8/2011 11:02:29 AM	1.27KM South OF Ikoyo		57	37.774 -2.24465
4/8/2011 11:04:28 AM	2.29KM South OF Ikoyo		59	37.7891 -2.25404
4/8/2011 11:06:29 AM	2.61KM North West OF Makindu		54	37.8032 -2.26384
4/8/2011 11:07:29 AM	1.89KM North West OF Makindu		50	37.8086 -2.26919
4/8/2011 11:08:30 AM	1.09KM North West OF Makindu		54	37.8145 -2.2754
4/8/2011 11:09:30 AM	0.82KM West OF Makindu		15	37.8167 -2.27769
4/8/2011 11:10:31 AM	0.58KM West OF Makindu		24	37.8187 -2.2799
4/8/2011 11:13:31 AM	0.39KM South West OF Makindu		11	37.821 -2.28213
4/8/2011 11:14:31 AM	0.39KM South OF Makindu		28	37.8236 -2.28447
4/8/2011 11:17:32 AM	1.87KM South East OF Makindu		44	37.835 -2.29721
4/8/2011 11:18:32 AM	2.47KM South East OF Makindu		50	37.8391 -2.30203
4/8/2011 11:19:33 AM	3.28KM South East OF Makindu		63	37.8455 -2.30762
4/8/2011 11:20:33 AM	4.16KM South East OF Makindu		54	37.8525 -2.31352
4/8/2011 11:21:33 AM	4.95KM South East OF Makindu		63	37.8588 -2.31872
4/8/2011 11:24:34 AM	2.92KM North West OF Mbuinzau		13	37.8764 -2.33264
4/8/2011 11:25:34 AM	2.59KM North West OF Mbuinzau		17	37.8789 -2.33501
4/8/2011 11:27:35 AM	1.49KM North West OF Mbuinzau		61	37.8866 -2.34391
4/8/2011 11:28:35 AM	0.72KM North West OF Mbuinzau		57	37.8894 -2.35284
4/8/2011 11:29:34 AM	0.4KM South West OF Mbuinzau		41	37.8915 -2.3609
4/8/2011 11:30:35 AM	0.55KM South OF Mbuinzau		6	37.8923 -2.36397
4/8/2011 11:31:35 AM	0.9KM South OF Mbuinzau		48	37.8937 -2.36866
4/8/2011 11:33:36 AM	1.97KM South OF Mbuinzau		10	37.9015 -2.37944
4/8/2011 11:34:36 AM	2.27KM South OF Mbuinzau		15	37.9036 -2.38221
4/8/2011 11:37:37 AM	4.88KM West OF Kibwezi		61	37.9178 -2.39849
4/8/2011 11:38:37 AM	3.97KM West OF Kibwezi		66	37.9259 -2.40508
4/8/2011 11:39:37 AM	3.63KM West OF Kibwezi		10	37.9291 -2.40714
4/8/2011 11:40:37 AM	3.35KM West OF Kibwezi		35	37.9319 -2.40837
4/8/2011 11:42:38 AM	1.82KM South West OF Kibwezi		59	37.9466 -2.41074
4/8/2011 11:44:39 AM	1.05KM South OF Kibwezi		55	37.9609 -2.41788
4/8/2011 11:46:39 AM	2.21KM South OF Kibwezi		32	37.9655 -2.43175
4/8/2011 11:47:39 AM	2.39KM South OF Kibwezi		24	37.9659 -2.43379
4/8/2011 11:48:39 AM	2.9KM South OF Kibwezi		50	37.9677 -2.43944
4/8/2011 11:49:40 AM	3.67KM South OF Kibwezi		48	37.9725 -2.44734
4/8/2011 11:50:40 AM	4.36KM South OF Kibwezi		61	37.9774 -2.45389
4/8/2011 11:52:41 AM	6.62KM West OF Masongaleni		54	37.9882 -2.46822
4/8/2011 11:53:41 AM	6.03KM West OF Masongaleni		68	37.9927 -2.47695
4/8/2011 11:56:41 AM	5.18KM West OF Masongaleni		37	38.0003 -2.48806
4/8/2011 11:57:42 AM	4.49KM West OF Masongaleni		68	38.0073 -2.49379
4/8/2011 11:58:42 AM	4.07KM South West OF Masongaleni		28	38.0131 -2.50185
4/8/2011 12:01:43 PM	3.99KM West OF Ngwata		48	38.0187 -2.51484
4/8/2011 12:02:43 PM	3.96KM West OF Ngwata		54	38.0191 -2.52317
4/8/2011 12:05:44 PM	3.3KM South West OF Ngwata		74	38.036 -2.54819
4/8/2011 12:07:44 PM	3.9KM South OF Ngwata		68	38.049 -2.56371
4/8/2011 12:11:46 PM	5.87KM West OF Darajani		24	38.0612 -2.58576
4/8/2011 12:12:45 PM	5.75KM West OF Darajani		59	38.0626 -2.59179
4/8/2011 12:15:46 PM	5.29KM South West OF Darajani		61	38.0723 -2.61346
4/8/2011 12:18:47 PM	5.67KM South West OF Darajani		35	38.0823 -2.63588
4/8/2011 12:19:48 PM	6.9KM West OF Kathekani		46	38.084 -2.64228
4/8/2011 12:20:47 PM	6.56KM South West OF Kathekani		52	38.0883 -2.64779
4/8/2011 12:21:47 PM	5.8KM South West OF Kathekani		68	38.0967 -2.65138
4/8/2011 12:22:48 PM	5.04KM South West OF Kathekani		59	38.1057 -2.65452
4/8/2011 12:23:48 PM	4.47KM South West OF Kathekani		63	38.1141 -2.65868
4/8/2011 12:26:49 PM	4KM South OF Kathekani		65	38.1385 -2.67274
4/8/2011 12:30:50 PM	2.07KM West OF Mtito Andei		21	38.1647 -2.69179

VEHICLE: KBJ 257T-OMOCHA ENT				VEHICLE HISTORY
TIME	LOCATION	STATUS	SPEED	COORDINATES
4/8/2011 12:31:50 PM	1.76KM West OF Mtito Andei		22	38.1674 -2.69421
4/8/2011 12:32:50 PM	1.2KM West OF Mtito Andei		59	38.1724 -2.6988
4/8/2011 12:35:51 PM	1.85KM South East OF Mtito Andei		50	38.1934 -2.71572
4/8/2011 12:36:52 PM	2.58KM South East OF Mtito Andei		54	38.1999 -2.72029
4/8/2011 12:38:52 PM	4.16KM South East OF Mtito Andei		50	38.2135 -2.72932
4/8/2011 12:39:52 PM	5.02KM South East OF Mtito Andei		57	38.2209 -2.73407
4/8/2011 12:40:52 PM	5.84KM South East OF Mtito Andei		55	38.2279 -2.73851
4/8/2011 12:43:53 PM	4.66KM North West OF Kenani		50	38.2503 -2.7538
4/8/2011 12:45:54 PM	2.99KM North West OF Kenani		57	38.2634 -2.76499
4/8/2011 12:48:54 PM	0.38KM North West OF Kenani		66	38.2811 -2.78622
4/8/2011 12:49:55 PM	0.55KM South OF Kenani		59	38.2866 -2.79453
4/8/2011 12:50:55 PM	1.42KM South East OF Kenani		63	38.2919 -2.80239
4/8/2011 12:51:55 PM	2.32KM South East OF Kenani		65	38.2973 -2.81048
4/8/2011 12:52:56 PM	3.08KM South East OF Kenani		57	38.302 -2.81734
4/8/2011 12:54:55 PM	4.84KM South East OF Kenani		55	38.3152 -2.83024
4/8/2011 12:55:56 PM	5.68KM South East OF Kenani		66	38.321 -2.83713
4/8/2011 12:59:57 PM	8.38KM North West OF Kyulu		55	38.3407 -2.86962
4/8/2011 1:04:58 PM	4.6KM North West OF Kyulu		54	38.3664 -2.90408
4/8/2011 1:05:58 PM	3.8KM West OF Kyulu		66	38.3727 -2.91024
4/8/2011 1:06:59 PM	2.97KM West OF Kyulu		57	38.3794 -2.91686
4/8/2011 1:10:00 PM	0.8KM South West OF Kyulu		48	38.4011 -2.9294
4/8/2011 1:11:00 PM	0.55KM South OF Kyulu		54	38.4088 -2.92938
4/8/2011 1:14:00 PM	3.02KM South East OF Kyulu		57	38.4248 -2.95091
4/8/2011 1:15:01 PM	3.89KM South East OF Kyulu		63	38.4308 -2.95806
4/8/2011 1:16:01 PM	3.78KM North West OF Tsavo		70	38.4387 -2.96446
4/8/2011 1:20:02 PM	1.02KM South West OF Tsavo		66	38.4591 -2.99404
4/8/2011 1:21:03 PM	0.75KM South OF Tsavo		50	38.4658 -2.99807
4/8/2011 1:25:03 PM	3.63KM South OF Tsavo		33	38.4809 -3.02927
4/8/2011 1:26:04 PM	4.04KM South OF Tsavo		30	38.4818 -3.03399
4/8/2011 1:31:04 PM	2.8KM North OF Manyani		33	38.4865 -3.05813
4/8/2011 1:36:06 PM	0.35KM South East OF Manyani		48	38.493 -3.09288
4/8/2011 1:37:07 PM	0.96KM South OF Manyani		57	38.494 -3.10093
4/8/2011 1:41:07 PM	3.83KM South OF Manyani		59	38.498 -3.1347
4/8/2011 1:42:07 PM	4.55KM South OF Manyani		54	38.4976 -3.14343
4/8/2011 1:43:08 PM	5.22KM South OF Manyani		59	38.4973 -3.1515
4/8/2011 1:47:08 PM	4.36KM North OF Ndi		59	38.4965 -3.18512
4/8/2011 1:51:10 PM	1.27KM North OF Ndi		57	38.5026 -3.22169
4/8/2011 1:54:11 PM	1.05KM South OF Ndi		54	38.5045 -3.24711
4/8/2011 1:55:11 PM	1.85KM South OF Ndi		63	38.5073 -3.25576
4/8/2011 1:56:11 PM	2.69KM South OF Ndi		66	38.5096 -3.26546
4/8/2011 2:01:12 PM	4.34KM East OF Ndome		63	38.5202 -3.31165
4/8/2011 2:02:13 PM	4.73KM South East OF Ndome		55	38.5222 -3.32009
4/8/2011 2:03:13 PM	5.25KM South East OF Ndome		52	38.5243 -3.32952
4/8/2011 2:04:12 PM	5.78KM South East OF Ndome		54	38.5265 -3.33757
4/8/2011 2:05:13 PM	5.4KM North West OF Voi		55	38.5286 -3.34518
4/8/2011 2:06:13 PM	4.66KM North West OF Voi		63	38.5312 -3.3543
4/8/2011 2:07:14 PM	4.04KM North West OF Voi		46	38.5335 -3.36228
4/8/2011 2:08:14 PM	3.44KM North West OF Voi		59	38.5359 -3.37065
4/8/2011 2:12:14 PM	1.94KM South West OF Voi		41	38.5467 -3.39873
4/8/2011 2:13:15 PM	1.78KM South West OF Voi		6	38.5487 -3.39983
4/8/2011 2:14:15 PM	1.77KM South West OF Voi		0	38.5489 -3.40004
4/8/2011 2:15:15 PM	1.77KM South West OF Voi		0	38.5489 -3.40005
4/8/2011 2:16:16 PM	1.77KM South West OF Voi		0	38.5489 -3.40006
4/8/2011 2:17:16 PM	1.73KM South West OF Voi		10	38.5493 -3.39997
4/8/2011 2:18:17 PM	1.6KM South West OF Voi		55	38.553 -3.40401
4/8/2011 2:20:17 PM	1.38KM South OF Voi		41	38.568 -3.40636
4/8/2011 2:21:18 PM	1.74KM South East OF Voi		65	38.5761 -3.40469
4/8/2011 2:22:17 PM	2.55KM South East OF Voi		55	38.5849 -3.40565
4/8/2011 2:23:17 PM	3.3KM South East OF Voi		44	38.5913 -3.40921
4/8/2011 2:24:18 PM	3.04KM West OF Ngutuni		63	38.5977 -3.41497
4/8/2011 2:25:18 PM	2.47KM West OF Ngutuni		52	38.6033 -3.42139

VEHICLE: KBJ 257T-OMOCHA ENT				VEHICLE HISTORY
TIME	LOCATION	STATUS	SPEED	COORDINATES
4/8/2011 2:26:18 PM	2.08KM South West OF Ngutuni		46	38.6085 -3.42728
4/8/2011 2:27:19 PM	1.91KM South West OF Ngutuni		35	38.6125 -3.4313
4/8/2011 2:28:19 PM	1.91KM South OF Ngutuni		57	38.6179 -3.4368
4/8/2011 2:29:20 PM	2.16KM South OF Ngutuni		50	38.6243 -3.44233
4/8/2011 2:30:19 PM	2.64KM South OF Ngutuni		57	38.6306 -3.44762
4/8/2011 2:33:20 PM	5.29KM South East OF Ngutuni		70	38.6564 -3.46663
4/8/2011 2:34:20 PM	6.25KM South East OF Ngutuni		63	38.6643 -3.47331
4/8/2011 2:35:21 PM	7.03KM South East OF Ngutuni		43	38.6698 -3.47957
4/8/2011 2:36:21 PM	7.65KM South East OF Ngutuni		39	38.6741 -3.48449
4/8/2011 2:39:21 PM	8.48KM North West OF Maungu		39	38.6861 -3.49779
4/8/2011 2:40:22 PM	7.8KM North West OF Maungu		57	38.6908 -3.50308
4/8/2011 2:41:22 PM	6.92KM North West OF Maungu		59	38.6971 -3.51003
4/8/2011 2:42:22 PM	6.11KM North West OF Maungu		61	38.7028 -3.51637
4/8/2011 2:43:23 PM	5.25KM North West OF Maungu		55	38.7088 -3.52337
4/8/2011 2:45:23 PM	3.6KM North West OF Maungu		55	38.72 -3.5375
4/8/2011 2:46:24 PM	2.81KM North West OF Maungu		57	38.7259 -3.54359
4/8/2011 2:47:23 PM	1.93KM North West OF Maungu		61	38.7334 -3.54828
4/8/2011 2:48:23 PM	1.02KM North West OF Maungu		52	38.7411 -3.55288
4/8/2011 2:50:24 PM	0.04KM North OF Maungu		32	38.7495 -3.55784
4/8/2011 2:51:25 PM	0.34KM South East OF Maungu		8	38.7527 -3.55949
4/8/2011 2:52:25 PM	0.63KM South East OF Maungu		15	38.7553 -3.56073
4/8/2011 2:53:25 PM	1.3KM South East OF Maungu		61	38.7611 -3.56388
4/8/2011 2:54:26 PM	2.28KM South East OF Maungu		63	38.7693 -3.56914
4/8/2011 2:55:26 PM	3.18KM South East OF Maungu		26	38.7769 -3.57371
4/8/2011 2:56:25 PM	3.85KM South East OF Maungu		57	38.7827 -3.57715
4/8/2011 2:58:26 PM	5.54KM South East OF Maungu		52	38.7969 -3.58612
4/8/2011 2:59:26 PM	6.29KM South East OF Maungu		48	38.8032 -3.59023
4/8/2011 3:00:27 PM	7.07KM South East OF Maungu		48	38.8098 -3.59429
4/8/2011 3:01:27 PM	7.83KM South East OF Maungu		48	38.8164 -3.59775
4/8/2011 3:02:28 PM	8.01KM South East OF Maungu		11	38.8179 -3.59856
4/8/2011 3:03:28 PM	7.72KM North West OF Buchuma		54	38.8227 -3.6011
4/8/2011 3:04:27 PM	6.9KM North West OF Buchuma		50	38.8299 -3.60489
4/8/2011 3:05:28 PM	6.04KM West OF Buchuma		63	38.8373 -3.60892
4/8/2011 3:06:28 PM	5.12KM West OF Buchuma		61	38.8452 -3.61394
4/8/2011 3:07:28 PM	4.23KM West OF Buchuma		48	38.8529 -3.6184
4/8/2011 3:08:29 PM	3.43KM West OF Buchuma		52	38.8598 -3.62238
4/8/2011 3:09:29 PM	3.25KM West OF Buchuma		0	38.8615 -3.62327
4/8/2011 3:10:29 PM	3.25KM West OF Buchuma		0	38.8615 -3.62326
4/8/2011 3:11:30 PM	3.12KM West OF Buchuma		26	38.8626 -3.62394
4/8/2011 3:12:30 PM	2.43KM West OF Buchuma		63	38.8687 -3.62744
4/8/2011 3:13:30 PM	1.59KM West OF Buchuma		54	38.8764 -3.63196
4/8/2011 3:14:30 PM	0.85KM South West OF Buchuma		59	38.8845 -3.63686
4/8/2011 3:15:30 PM	0.85KM South OF Buchuma		55	38.8923 -3.64166
4/8/2011 3:16:31 PM	1.58KM South East OF Buchuma		50	38.9001 -3.64667
4/8/2011 3:17:31 PM	2.41KM South East OF Buchuma		66	38.9077 -3.65149
4/8/2011 3:18:31 PM	3.35KM South East OF Buchuma		61	38.9162 -3.65597
4/8/2011 3:19:32 PM	3.79KM South East OF Buchuma		37	38.9202 -3.65806
4/8/2011 3:20:32 PM	4.6KM South East OF Buchuma		57	38.9274 -3.66196
4/8/2011 3:21:31 PM	5.43KM South East OF Buchuma		59	38.9345 -3.6662
4/8/2011 3:22:32 PM	6.27KM South East OF Buchuma		46	38.9416 -3.67051
4/8/2011 3:23:32 PM	6.92KM South East OF Buchuma		44	38.9472 -3.67386
4/8/2011 3:24:33 PM	7.82KM South East OF Buchuma		63	38.9549 -3.67849
4/8/2011 3:25:33 PM	8.63KM South East OF Buchuma		57	38.9619 -3.68243
4/8/2011 3:26:33 PM	8.91KM North West OF Makinnon Road		57	38.9699 -3.68695
4/8/2011 3:27:34 PM	7.99KM North West OF Makinnon Road		55	38.9777 -3.69181
4/8/2011 3:28:34 PM	7.08KM North West OF Makinnon Road		65	38.9856 -3.69609
4/8/2011 3:29:34 PM	6.03KM North West OF Makinnon Road		66	38.9946 -3.70121
4/8/2011 3:30:34 PM	5.14KM North West OF Makinnon Road		44	39.0022 -3.70572
4/8/2011 3:31:34 PM	4.33KM North West OF Makinnon Road		61	39.0092 -3.7098
4/8/2011 3:32:34 PM	3.74KM North West OF Makinnon Road		0	39.0142 -3.71276
4/8/2011 3:33:35 PM	3.62KM North West OF Makinnon Road		21	39.0153 -3.71338

VEHICLE: KBJ 257T-OMOCHA ENT				VEHICLE HISTORY
TIME	LOCATION	STATUS	SPEED	COORDINATES
4/8/2011 3:34:35 PM	3.07KM North West OF Makinnon Road		46	39.0199 -3.71605
4/8/2011 3:35:36 PM	2.3KM West OF Makinnon Road		55	39.0265 -3.71994
4/8/2011 3:36:36 PM	1.42KM West OF Makinnon Road		59	39.0341 -3.72456
4/8/2011 3:37:36 PM	0.6KM West OF Makinnon Road		57	39.0416 -3.7295
4/8/2011 3:38:37 PM	0.52KM South OF Makinnon Road		52	39.0486 -3.73409
4/8/2011 3:39:36 PM	1.2KM South East OF Makinnon Road		48	39.0555 -3.73792
4/8/2011 3:40:36 PM	2KM South East OF Makinnon Road		57	39.0626 -3.7419
4/8/2011 3:42:37 PM	3.69KM South East OF Makinnon Road		66	39.0799 -3.74311
4/8/2011 3:43:37 PM	4.61KM South East OF Makinnon Road		59	39.0893 -3.742
4/8/2011 3:44:38 PM	5.39KM West OF Taru		57	39.0979 -3.74351
4/8/2011 3:45:38 PM	4.47KM West OF Taru		65	39.1069 -3.74553
4/8/2011 3:46:39 PM	3.58KM South West OF Taru		52	39.1158 -3.74751
4/8/2011 3:48:38 PM	2.22KM South West OF Taru		65	39.131 -3.75088
4/8/2011 3:49:39 PM	1.63KM South OF Taru		52	39.1409 -3.75313
4/8/2011 3:59:41 PM	4.38KM West OF Samburu		70	39.2312 -3.76897
4/8/2011 4:02:42 PM	2.06KM South West OF Samburu		65	39.2533 -3.78754
4/8/2011 4:05:42 PM	1.65KM South OF Samburu		66	39.277 -3.79775
4/8/2011 4:06:43 PM	2.19KM South East OF Samburu		59	39.2874 -3.79613
4/8/2011 4:07:43 PM	2.87KM South East OF Samburu		68	39.2957 -3.79483
4/8/2011 4:09:44 PM	4.92KM South East OF Samburu		65	39.3167 -3.7929
4/8/2011 4:10:44 PM	5.83KM East OF Samburu		54	39.3257 -3.79137
4/8/2011 4:12:45 PM	7.48KM East OF Samburu		39	39.3412 -3.79346
4/8/2011 4:13:44 PM	8.13KM East OF Samburu		52	39.3478 -3.79054
4/8/2011 4:16:45 PM	10.6KM East OF Samburu		65	39.3712 -3.78961
4/8/2011 4:17:46 PM	9.69KM South West OF Mbongo		66	39.3802 -3.79103
4/8/2011 4:21:47 PM	9.07KM North West OF Mariakani		24	39.4035 -3.79914
4/8/2011 4:22:47 PM	8.51KM North West OF Mariakani		48	39.4081 -3.80253
4/8/2011 4:26:48 PM	5.43KM North West OF Mariakani		65	39.4304 -3.82633
4/8/2011 4:27:48 PM	4.64KM North West OF Mariakani		44	39.4359 -3.83299
4/8/2011 4:32:49 PM	1.71KM North West OF Mariakani		61	39.4588 -3.85322
4/8/2011 4:33:50 PM	0.9KM West OF Mariakani		39	39.4658 -3.85789
4/8/2011 4:34:50 PM	0.66KM West OF Mariakani		6	39.4678 -3.85925
4/8/2011 4:37:51 PM	0.27KM South OF Mariakani		37	39.4738 -3.86342
4/8/2011 4:39:51 PM	0.71KM South OF Mariakani		26	39.4772 -3.86757
4/8/2011 4:40:51 PM	1.35KM South East OF Mariakani		61	39.4817 -3.87303
4/8/2011 4:41:52 PM	2.23KM South East OF Mariakani		66	39.4877 -3.88034
4/8/2011 4:43:52 PM	3.88KM South East OF Mariakani		65	39.5008 -3.89172
4/8/2011 4:45:53 PM	5.45KM South East OF Mariakani		63	39.5099 -3.90652
4/8/2011 4:46:53 PM	5.7KM West OF Rabai		54	39.5171 -3.9118
4/8/2011 4:49:53 PM	4.18KM West OF Rabai		43	39.5296 -3.92305
4/8/2011 4:51:54 PM	2.7KM North West OF Mazeras		57	39.5366 -3.93664
4/8/2011 4:53:55 PM	1.2KM North West OF Mazeras		66	39.542 -3.95355
4/8/2011 4:57:55 PM	1.6KM South OF Mazeras		72	39.5501 -3.9836
4/8/2011 5:00:56 PM	3.9KM South East OF Mazeras		63	39.575 -3.99766
4/8/2011 5:01:57 PM	5.01KM West OF Changamwe		22	39.5787 -4.00545
4/8/2011 5:04:57 PM	3.78KM West OF Changamwe		8	39.59 -4.00883
4/8/2011 5:05:57 PM	3.63KM West OF Changamwe		4	39.5915 -4.00862
4/8/2011 5:06:58 PM	3.57KM West OF Changamwe		4	39.5921 -4.00855
4/8/2011 5:09:59 PM	3.37KM West OF Changamwe		0	39.5941 -4.00826
4/8/2011 5:11:59 PM	3.27KM West OF Changamwe		10	39.5952 -4.0081
4/8/2011 5:13:59 PM	3.13KM North West OF Changamwe		4	39.5966 -4.00814
4/8/2011 5:15:00 PM	3.1KM North West OF Changamwe		0	39.5969 -4.00822
4/8/2011 5:16:00 PM	3.1KM North West OF Changamwe		0	39.5969 -4.0082

5.7.8 Appendix 8: Nyamache to Mombasa Trip Summary report

TRIP REPORT

Unit Number : BT1899 **Vehicle:** KBJ 257T-OMOCHA

TRIP SUMMARY

Start Time	Start Location	End Time	Location
4/7/2011 12:01:54 AM	0.53KM South OF Nyamache	4/8/2011 11:55:44 PM	3.05KM North West OF Changamwe

Total Trip Time:	1.23:53:50	**Average Speed:**	24.71 KM/H
Total Mileage:	765.37 Km	**Max Speed:**	85 KM/H

STOPPAGE SUMMARY

Stop Time	Duration (dd:hh:mm)	Location
4/7/2011 12:01:54 AM	00:08:31	0.53KM South OF Nyamache
4/7/2011 9:56:20 AM	00:00:04	0.53KM South OF Nyamache
4/7/2011 10:02:27 AM	00:00:04	0.5KM South OF Nyamache
4/7/2011 10:07:28 AM	00:00:02	0.51KM South OF Nyamache
4/7/2011 10:10:29 AM	00:06:26	0.51KM South OF Nyamache
4/7/2011 4:39:10 PM	00:00:17	0.55KM South OF Nyamache
4/7/2011 5:25:22 PM	00:00:09	0.17KM North East OF Keumbu
4/7/2011 9:00:03 PM	00:00:03	0.32KM South OF Mulot
4/7/2011 10:09:41 PM	00:04:59	0.91KM South OF Narok
4/8/2011 6:28:15 AM	00:00:06	0.43KM South OF NAIROBI
4/8/2011 8:22:21 AM	00:00:03	2.6KM South West OF Maiani
4/8/2011 9:06:32 AM	00:00:57	0.41KM South East OF Emali
4/8/2011 2:14:15 PM	00:00:03	1.77KM South West OF Voi
4/8/2011 3:09:29 PM	00:00:02	3.25KM West OF Buchuma
4/8/2011 5:15:00 PM	00:00:16	3.1KM North West OF Changamwe
4/8/2011 5:32:29 PM	00:00:13	3.08KM North West OF Changamwe
4/8/2011 5:56:37 PM	00:05:43	3.05KM North West OF Changamwe

No. of Stops: 17 **Idle Time (hh:mm)** 1.04:00:42

5.7.9 Appendix 9 Analysis of angle of repose for commercial CTC tea grades

Grade	Tea pile Height (H)	Pile diameter (D)	Tanα =2H/D	α	Angle of Repose in degrees
FNGS1	**60mm**	**172mm**	**0.6977**	**0.6976**	**34.90**
Dust1	**55mm**	**165.5mm**	**0.6646**	**0.6646**	**33.61**
PD	**45mm**	**148mm**	**0.6082**	**0.6081**	**31.30**
PF1	**43mm**	**153mm**	**0.5621**	**0.5621**	**29.34**
BP1	**33mm**	**125mm**	**0.5280**	**0.5280**	**27.83**
Dust	**52mm**	**153mm**	**0.6797**	**0.6797**	**34.20**

5.7.10 Appendix 10 Regression analysis of correlation between movement by static load piston against tea compact density

Regression Statistics				
Multiple R	0.996587059			
R Square	0.993185767			
Adjusted R Square	0.991482209			
Standard Error	0.005495915			
Observations	6			
ANOVA				
	df	*SS*	*MS*	*F*
Regression	1	0.01760976	0.01761	583.0066273
Residual	4	0.00012082	3.02E-05	
Total	5	0.01773058		
	Coefficients	*Standard Error*	*t Stat*	*P-value*
Intercept	0.430420769	0.004877859	88.23968	9.88835E-08
Distance	0.010371494	0.000429541	24.14553	1.74524E-05